



HAL
open science

Bifunctional activation and heterolytic cleavage of ammonia and dihydrogen by silica-supported tantalum imido amido complexes and relevance to the dinitrogen cleavage mechanism by tantalum hydrides

Yasemin Kaya

► **To cite this version:**

Yasemin Kaya. Bifunctional activation and heterolytic cleavage of ammonia and dihydrogen by silica-supported tantalum imido amido complexes and relevance to the dinitrogen cleavage mechanism by tantalum hydrides. Organic chemistry. Université Claude Bernard - Lyon I, 2013. English. NNT : 2013LYO10054 . tel-01177064

HAL Id: tel-01177064

<https://theses.hal.science/tel-01177064>

Submitted on 16 Jul 2015

HAL is a multi-disciplinary open access archive for the deposit and dissemination of scientific research documents, whether they are published or not. The documents may come from teaching and research institutions in France or abroad, or from public or private research centers.

L'archive ouverte pluridisciplinaire **HAL**, est destinée au dépôt et à la diffusion de documents scientifiques de niveau recherche, publiés ou non, émanant des établissements d'enseignement et de recherche français ou étrangers, des laboratoires publics ou privés.

THESE

Présentée

devant l'UNIVERSITE CLAUDE BERNARD – LYON 1

ECOLE DOCTORALE de CHIMIE

Spécialité CHIMIE

Pour l'obtention du

DIPLOME DE DOCTORAT

(arrêté du 7 août 2006)

présentée et soutenue publiquement le

25 Mars 2013

par

Yasemin KAYA

Bifunctional activation and heterolytic cleavage of ammonia and dihydrogen by silica-supported tantalum imido amido complexes and relevance to the dinitrogen cleavage mechanism by tantalum hydrides.

Directeur de thèse :

Elsje Alessandra QUADRELLI

Jury :

M. Stéphane DANIELE- Université Claude Bernard Lyon 1

Mme. Moran FELLER- Rapporteur- Weizmann Institute of Science

M. George MARNELLOS- Rapporteur- University of Western Macedonia

Mme. E. Alessandra QUADRELLI- Centre National de la Recherche Scientifique

M. Alexander SOROKIN- Centre National de la Recherche Scientifique (Membre Invité)

*Bu tezi hayatım boyunca her zaman yanımda olan,
benden sevgi ve desteklerini esirgemeyen, bugünlere gelmemde büyük payı olan,
sevgili aileme adıyorum.*

Lyon 2013

UNIVERSITE CLAUDE BERNARD - LYON 1

Président de l'Université

M. François-Noël GILLY

Vice-président du Conseil d'Administration

M. le Professeur Hamda BEN HADID

Vice-président du Conseil des Etudes et de la Vie Universitaire

M. le Professeur Philippe LALLE

Vice-président du Conseil Scientifique

M. le Professeur Germain GILLET

Secrétaire Général

M. Alain HELLEU

COMPOSANTES SANTE

Faculté de Médecine Lyon Est – Claude Bernard

Directeur : M. le Professeur J. ETIENNE

Faculté de Médecine et de Maïeutique Lyon Sud – Charles Mérieux

Administrateur provisoire : M. le Professeur G. KIRKORIAN

UFR d'Odontologie

Directeur : M. le Professeur D. BOURGEOIS

Institut des Sciences Pharmaceutiques et Biologiques

Directeur : Mme la Professeure C. VINCIGUERRA.

Institut des Sciences et Techniques de la Réadaptation

Directeur : M. le Professeur Y. MATILLON

Département de formation et Centre de Recherche en Biologie Humaine

Directeur : M. le Professeur P. FARGE

COMPOSANTES ET DEPARTEMENTS DE SCIENCES ET TECHNOLOGIE

Faculté des Sciences et Technologies

Directeur : M. le Professeur F. De MARCHI

Département Biologie

Directeur : M. le Professeur F. FLEURY

Département Chimie Biochimie

Directeur : Mme le Professeur H. PARROT

Département GEP

Directeur : M. N. SIAUVE

Département Informatique

Directeur : M. le Professeur S. AKKOUCHE

Département Mathématiques

Directeur : M. le Professeur A. GOLDMAN

Département Mécanique

Directeur : M. le Professeur H. BEN HADID

Département Physique

Directeur : Mme S. FLECK

Département Sciences de la Terre

Directeur : Mme la Professeure I. DANIEL

UFR Sciences et Techniques des Activités Physiques et Sportives

Directeur : M. C. COLLIGNON

Observatoire de Lyon

Directeur : M. B. GUIDERDONI

Polytech Lyon

Directeur : M. P. FOURNIER

Ecole Supérieure de Chimie Physique Electronique

Directeur : M. G. PIGNAULT

Institut Universitaire de Technologie de Lyon 1

Directeur : M. C. VITON

Institut Universitaire de Formation des Maîtres

Directeur : M. R. BERNARD

Institut de Science Financière et d'Assurances

Directeur : Mme la Professeure V. MAUME DESCHAMPS

Acknowledgements

This thesis arose in part out of years of research that has been started long time ago before I joined to the group of Jean-Marie Basset at the “Laboratoire de la Chimie Organométallique de la Surface” (LCOMS) in *Ecole Supérieure de Chimie, Physique, Electronique* Lyon, France. By that time, I have worked with a great number of people whose contribution in assorted ways to the research and the making of the thesis deserved special mention. It is a pleasure to convey my gratitude to them all in my acknowledgment.

In the first place I would like to record my gratitude to Alessandra Quadrelli for her supervision, advice, and guidance from the early stage of this research as well as giving me different experiences throughout the work. Above all and the most needed, she provided me unflinching encouragement and support in various ways. Her truly scientist intuition has made her as a constant of ideas and passions in science, which exceptionally inspire and enrich me as a student, a researcher and a scientist. I am indebted to her more than she knows.

I gratefully acknowledge Mostafa Taoufik for his advice, supervision, and crucial contribution, which made him a backbone of this research and so to this thesis. His involvement with his originality has triggered and nourished me that I will benefit from.

Many thanks go in particularly to Kai Chung Szeto. I am thankful to him for his valuable advice, supervision in science discussions and furthermore, using his precious time to help me during the experimental procedures.

It is a pleasure to pay tribute also to our collaborators for DFT calculations. To Odile Eisenstein from *Institut Charles Gerhardt, Université Montpellier2*, France and Xavier Solans-Monfort from *Departament de Química, Universitat Autònoma de Barcelona*, Spain. I would like to thank them for their particular skills in calculations, their researches and efforts on our studies to help us in order to understand the mechanisms of our reactions.

To the role model of hard workers in the lab, Catherine Chow, I would like to thank her for being the first person who taught me how to work under high vacuum systems and helped me out in using many materials and machines in the very beginning of my studies. It is pleasure

to mention: Cherif Larabi and Nicolas Popoff who were always ready to lend a hand when I needed as well.

Collective and individual acknowledgments are also owed to my colleagues at LCOMS whose presence somehow perpetually refreshed, helpful, and memorable. Many thanks go in particular to Laurent Mathey, Reine El-Sayah, Pierre Laurent, Philippe Arquiliere, Hassan Sarrour and Piotr Putaj for giving me such a pleasant time while working together since I knew them in LCOMS. Special acknowledgements for those with whom I spent memorable moments also outside the lab: to Leila Moura and Inga Steinunn Helgadóttir for all the special, beautiful, unforgettable moments during our trips, parties, dinners wherever we were whatever we had together, to Lea for the sociability that she brings to our lives after work and of course to the new arrivals of the lab. Lots of thanks to Frederic, for supporting me during the hard times and being a super nice neighbor as well, to Stéphane, for opening a new window in my life with the modern technology and French grammar, to Iulia and Alina for showing a great passion of science and life from the beginning of their experiences in France.

I convey special acknowledgement to express my gratitude wholeheartedly to Hongpeng Jia who joined our group in the last year of my thesis; with whom I had the opportunity to work and discuss together the results in order to improve our studies furthermore.

I would like to thank everybody who was important to the successful realization of this thesis, in particular all the members of the LCOMS laboratory in CPE Lyon, as well as expressing my apology that I could not mention personally one by one.

My parents deserve special mention for their inseparable support and love. My Father, Aligül and My Mother, Zeynep in the first place are the people who put the foundation of my learning character, showing me the joy of intellectual pursuit ever since I was a child and they are the ones who sincerely raised me with their caring and gentle love. My sisters, Dilek and Hazal Işıl thanks for being supportive, caring siblings and extremely special people in my life. Words fail me to express my appreciation to my family whose dedication, love and persistent confidence in me, has taken the load off my shoulder in spite of the physically long distance between us. To them, I dedicated this thesis.

Finally, I wish to thank all my friends from all over the world for their support and love.

Abbreviations

Δ	Thermal treatment
δ	Chemical shift
δ_{A-B}	Bending frequencies of A-B bond
ν_{A-B}	Stretching frequencies of A-B bond
Å	Angström
atm	atmosphere (pressure)
BET	Brunauer- Emmett- Teller surface analysis
°C	Celsius degree
COMS	Surface organometallic chemistry (in french)
Cat.	Catalyst
CP	Cross-Polarization
Cp	Cyclopentadienyl groups, $\eta^5\text{-C}_5\text{H}_5$
Cp'	Methylcyclopentadienyl groups, $\eta^5\text{-C}_5\text{H}_4\text{Me}$
Cp*	Pentamethylcyclopentadienyl groups, $\eta^5\text{-C}_5\text{Me}_5$
DFT	Density Functional Theory
d	day
DQ	Double Quanta
dmpe	Dimethylphosphinethane, $\text{Me}_2\text{PCH}_2\text{-CH}_2\text{PMe}_2$
DRIFT	Diffuse Reflectance Infrared Fourier Transform
EPR	Electron Paramagnetic Resonance
Et	Ethyl groups, $-\text{CH}_2\text{-CH}_3$
Eq.	Equation
equiv.	Molar equivalent
EXAFS	Extended X-ray Absorption Fine Structure
F	Molar flow rate
GC	Gas Chromatography
GC/MS	Gas Chromatography coupled with Mass Spectrometry
g	gram (unit of mass)
h	hour
HETCOR	HETeronuclear CORrelation (^{13}C NMR)
HPDEC	High Power DECoupling (^{13}C NMR)

Hz	Hertz
I.R.	Infrared
K	Equilibrium constant of the reaction
k	Rate constant of the reaction
kcal	kilocalorie
kJ	kilojoule
J_{AB}	Scalar coupling constant between A and B nuclei
M	Metal
MAS	Magic Angle Spinning
Me	Methyl groups, $-\text{CH}_3$
MGE	Main Group Element
min	minute
mol	Mole
MS	Mass Spectroscopy
NMR	Nuclear Magnetic Resonance
<i>n</i> Bu	<i>n</i> -butyl groups, $-\text{CH}_2-(\text{CH}_2)_2-\text{CH}_3$
Np	Neopentyl groups, $-\text{CH}_2-\text{C}(\text{CH}_3)_3$
Np'	Neopentylidene groups, $=\text{CH}-\text{C}(\text{CH}_3)_3$
pKa	acid dissociation constant
pKb	base dissociation constant
ppm	part per million (10^{-6})
R	Ideal gas constant
RT	Room Temperature
s	second
S_{SPE}	surface specific area
SS	solid-state
SOMC	Surface Organometallic Chemistry
T	Temperature ($^{\circ}\text{C}$)
<i>t</i> Bu	tertiobutyl groups, $-\text{C}(\text{CH}_3)_3$
TM	Transition Metal
T.O.N.	Turn Over Number
TQ	Triple-quantum
1D, 2D	one, two dimensions

Nomenclature and classification of surface species

SiO_{2-T}	Silica partially dehydroxylated at $T^\circ\text{C}$
MCM-41_T	MCM-41 partially dehydroxylated at $T^\circ\text{C}$
1	The mixture of molecular complex $[(\equiv\text{SiO})_2\text{TaH}]$ and $[(\equiv\text{SiO})_2\text{TaH}_3]$
1a	The molecular complex $[(\equiv\text{SiO})_2\text{TaH}]$
1b	The molecular complex $[(\equiv\text{SiO})_2\text{TaH}_3]$
2	The molecular complex $[(\equiv\text{SiO})_2\text{Ta}(=\text{NH})(-\text{NH}_2)]$
2-d	The molecular complex $[(\equiv\text{SiO})_2\text{Ta}(=\text{ND})(-\text{ND}_2)]$
2.NH₃	The molecular complex $[(\equiv\text{SiO})_2\text{Ta}(=\text{NH})(-\text{NH}_2)(\text{NH}_3)]$
2.¹⁵NH₃	The ¹⁵ N labelled surface species $[(\equiv\text{SiO})_2\text{Ta}(=\text{15NH})(-\text{15NH}_2)]$
3	The molecular complex $[(\equiv\text{SiO})_3\text{Ta}]$

RESUMÉ DE LA THÈSE EN FRANÇAIS

L'activation de petites molécules azotées telles que l'azote et l'ammoniac a été développée dans notre laboratoire via la chimie organométallique de surface (COMS). Les recherches effectuées durant cette thèse ont permis d'établir la réactivité de complexe de tantale imido amido supporté sur silice, $[(\equiv\text{SiO})_2\text{Ta}(=\text{NH})(\text{NH}_2)]$ vis-à-vis de l'hydrogène et de l'ammoniac. Des étapes élémentaires de clivage hétérolytique de liaison H-H ou N-H ont été établies. En particulier, l'importance d'une molécule d'ammoniac dans la deuxième sphère de coordination (outer sphere assistance) du système s'est avérée cruciale pour la diminution des barrières d'énergie des états de transition pendant le transfert de protons. Les études ont été faites pour déterminer et expliquer le mécanisme de réduction de N_2 par les complexes d'hydrures de tantale. La compréhension du mécanisme a été établie grâce aux études avec N_2 , N_2H_4 et N_2H_2 pour trouver les intermédiaires de cette réduction suivis par *in-situ* infrarouge, RMN et l'analyse élémentaire, et à l'aide de calcul DFT. Un mécanisme de clivage de N_2 par des complexes dihydrogènes de Ta(V) est proposé. Enfin, la réactivité du complexe $[(\equiv\text{SiO})_2\text{Ta}(=\text{NH})(\text{NH}_2)]$ vers l'activation de liaison C-H de C_6H_6 , $\text{C}_6\text{H}_5\text{-CH}_3$, t-Bu-Ethylène et CH_4 a été étudié par la spectroscopie infrarouge.

TITRE EN ANGLAIS

Bifunctional activation and heterolytic cleavage of ammonia and dihydrogen by silica supported tantalum imido amido complexes and relevance to the dinitrogen cleavage mechanism by tantalum hydrides

RESUMÉ DE LA THÈSE EN ANGLAIS

The activation of small molecules such as nitrogen and ammonia was already developed in our laboratory using the surface organometallic chemistry (SOMC) approach. This thesis focused on understanding the reactivity of tantalum imido amido complex $[(\equiv\text{SiO})_2\text{Ta}(=\text{NH})(\text{NH}_2)]$, under hydrogen and/ or ammonia atmosphere. Heterolytic H-H and N-H cleavage across Ta-NH₂ and Ta=NH bonds appeared crucial. The assistance of an additional ammonia molecule in the outer sphere of the d⁰ tantalum(v) imido amido ammonia model complex in order to reduce the energy barriers of the transition states during proton transfer was also shown. Studies were done to identify the mechanism of N_2 reduction by tantalum hydride complexes. Studies with N_2 , N_2H_4 and N_2H_2 allowed identifying the intermediaries via *in situ* IR, NMR and elemental analysis. Combined with DFT calculations, these experiments led to the proposal of a novel mechanism for N_2 cleavage based on the central role of Ta(H₂) adducts. Finally, the reactivity of imido amido complex toward C-H bond activation was studied with C_6H_6 , $\text{C}_6\text{H}_5\text{-CH}_3$, t-Bu-Ethylene and CH_4 .

MOTS-CLÉS :

Tantale, imido, amido, hydrures, mécanisme, ammoniac, azote, coupure hétérolytique, activation bifonctionnelle, activation C-H, chimie organométallique de surface.

DISCIPLINE : Chimie

Ecole Supérieure de Chimie, Physique, Electronique de Lyon, C2PZ Laboratoire de Chimie Organométallique de Surface (LCOMS)- UMR 5265, 43 Bd du 11 Novembre 1918 69622 Villeurbanne cedex France

TABLE OF CONTENTS

CHAPTER I. Introduction	1
I. INTRODUCTION	3
II. PREPARATION OF WELL-DEFINED TANTALUM IMIDO AMIDO SURFACE ORGANOMETALLIC COMPLEX	4
II.1 The support	5
II.2 The preparation of well-defined tantalum imido amido complex	6
III. OVERVIEW OF CHAPTER I and OBJECTIVE OF MY THESIS	11
IV. REFERENCES	13
CHAPTER II. Activation of NH₃ and H₂: Mechanistic insight through bond activation reactions	17
I. INTRODUCTION	19
I.1 Introduction to ammonia and its properties	19
I.2 Activation of ammonia N-H bond	19
I.2.1. Ammonia Oxidative Addition by transition metal complexes:	20
I.2.2. Ammonia Oxidative addition “without transition metal complex”:	25
I.2.3. Ammonia activation by d ⁰ transition metal complexes:	26
I.3 Mechanistic understanding of ammonia activation.....	29
I.4 Overview of chapter II.....	34
II. RESULTS and DISCUSSIONS	35
II. 1. Reaction of [(≡SiO) ₂ Ta(=NH)(NH ₂)] with dihydrogen :.....	35
II. 2. Reaction of [(≡SiO) ₂ Ta(=NH)(NH ₂)] with ammonia :	39
II.2.1 Spectroscopic studies of NH ₃ activation on [(≡SiO) ₂ Ta(=NH)(NH ₂)], 2	39
II.2.2 Computational Studies of NH ₃ activation on cluster model 2q	43
II. 3. Mechanism of [(≡SiO) ₂ TaH _x (x: 1,3)] reaction with ammonia :	50
II.3.1 Spectroscopic studies of NH ₃ activation on [(≡SiO) ₂ TaH _x (x: 1,3)], 1.....	50
II.3.2 Computational Studies of NH ₃ activation on [(≡SiO) ₂ TaH _x (x: 1,3)], 1.....	53
III. CONCLUSION and PERSPECTIVES	56
IV. EXPERIMENTAL PART	57
V. REFERENCES	63
CHAPTER III. Mechanistic insight of dinitrogen activation reaction over silica supported tantalum hydrides	69
I. INTRODUCTION	71
I.1 Introduction to dinitrogen and its properties.....	71
I.2 Mechanistic understanding of dinitrogen activation	79
I.3 Overview of chapter III.....	81
II. RESULTS	83
II. 1 Reaction of [(≡SiO) ₂ TaH _x (x: 1, 3)] with dinitrogen	83
II.1.1 Reaction of [(≡SiO) ₂ TaH ₁]enriched 1 with N ₂	85
II.1.2 Reaction of [(≡SiO) ₂ TaH _x (x: 1, 3)] with ¹⁵ N ₂	87
II.1.3 Reaction of [(≡SiO) ₂ TaD _x (x: 1, 3)] with N ₂	90

II.2 Reaction of $[(\equiv\text{SiO})_2\text{TaH}_x (x: 1, 3)]$ with hydrazine	92
II.2.1 Reaction of $[(\equiv\text{SiO})_2\text{TaH}_x (x: 1, 3)]$ with N_2H_4	92
II.2.2 Reaction of $[(\equiv\text{SiO})_2\text{TaH}_x]$ with $^{15}\text{N}_2\text{H}_4$	97
II.3. Attempts to monitor reaction of $[(\equiv\text{SiO})_2\text{TaH}_x (x: 1, 3)]$ with diazene	99
III. DISCUSSION	102
IV. CONCLUSION and PERSPECTIVES	111
V. EXPERIMENTAL PART	112
VI. REFERENCES:.....	119
<i>CHAPTER IV. Attempts to use well-defined silica supported tantalum imido amido complex for C-H activation reactions</i>	<i>131</i>
I. INTRODUCTION	133
II. RESULTS and DISCUSSION	135
II.1. Reactivity of silica-supported $[(\equiv\text{SiO})_2\text{Ta}(=\text{NH})(\text{NH}_2)]$ and $[(\equiv\text{SiO})_2\text{TaH}_x (x:1, 3)]$ complexes with alkynes:	135
II.2. Well-defined $[(\equiv\text{SiO})_2\text{Ta}(=\text{NH})(\text{NH}_2)]$ complex in C-H activation reactions:	138
III. CONCLUSION and PERSPECTIVES	144
IV. EXPERIMENTAL PART.....	145
V. REFERENCES.....	147
<i>CHAPTER V. General Conclusions</i>	<i>151</i>
REFERENCES:.....	157
ANNEX	

CHAPTER I.
Introduction

I. INTRODUCTION

Introduction to the surface organometallic chemistry, SOMC

Surface organometallic chemistry (SOMC) is located at the interface between homogeneous and heterogeneous catalysis and represents a new approach to the development of well-defined heterogeneous catalyst which can be preferred industrially over their homogenous analogues for the ease of product separation and recycling. This approach consists in bringing the concepts and the tools of molecular chemistry to surface science and heterogeneous catalysis by studying specific characteristics of the structure and reactivity between the molecular intermediate and the surface (metallic) atoms.^[1-9]

The molecular definition of the surface species is confirmed by various physicochemical, spectroscopic and chemical analyses of the new species which allows the description of surface-grafted metal atoms in terms of coordination chemistry concepts (existence of metal ligand interactions, considering the surface as a rigid molecular ligand).^[5, 9] Transferring the concepts and tools of molecular organometallic chemistry to surfaces is the key concept of generating well-defined surface species by understanding the reaction of organometallic complexes with the support.

The major purpose of SOMC has been to design the coordination sphere that is expected to be able to carry out the desired catalytic heterogeneous reaction and to determine precisely the possible steps of the molecular mechanism occurring on the surface. However, the relationship between structure and activity remains difficult for such systems due to the low homogeneity of the surface structure and also the low concentration of active sites on the support. The work initially done by Basset and his group in our laboratory helped to develop new elements to address these issues and since well-defined “single-site” supported heterogeneous systems were prepared by SOMC, characterized by various physical-chemical tools and showed significant catalytic reactivities^[3-7], in established reactions such as olefin metathesis,^[10] olefin polymerization^[11] or even in original catalytic applications such as alkane cleavage by methane,^[12] alkane metathesis,^[13] coupling of methane to hydrogen and ethane,^[12] hydrogenolysis of polyolefins^[14] and alkanes,^[15] direct transformation of ethylene into propylene.^[16]

The studies of Basset et al. on SOMC attracted considerable attention in the literature showing an alternative approach to heterogeneous catalysis, a crucial field in addressing current economic and environmental issues for the production of industrially relevant molecules such as agrochemicals, petrochemicals, pharmaceuticals, polymers, basic chemicals.

The objective of this thesis focuses on SOMC approach applied to the synthesis and the reactivities of metal-nitrogen bond from N_2 and NH_3 that mainly relies on the preparation of well-defined tantalum(V) imido amido surface species, their characterization by various spectroscopic techniques, the study of their reactivity and the elucidation of the elementary reaction steps involved in the mechanism. The key surface species of this thesis is the recently developed silica-grafted tantalum imido amido complex $[(\equiv SiO)_2Ta(=NH)(NH_2)]$, **2** by our team through the reaction of well-established silica supported tantalum hydride complex $[(\equiv SiO)_2Ta-H_x (x:1,3)]$, **1**^[17] with either N-H bond cleavage of ammonia^[18] and/ or very robust $N\equiv N$ cleavage of dinitrogen.^[19]

This chapter will describe such state of art: the preparation and characterization of well-defined silica supported tantalum complex **2** by activating ammonia and dinitrogen over silica supported tantalum hydrides via surface organometallic chemistry. The general layout will be given in conclusion of this chapter.

II. PREPARATION OF WELL-DEFINED TANTALUM IMIDO AMIDO SURFACE ORGANOMETALLIC COMPLEX

The development of single-site heterogeneous catalysts has been the main aim of SOMC approach^[20] which is based on the application of molecular organometallic chemistry principles to the development of well-defined surface-grafted metallic complexes particularly allyl derivatives of group 4-8 transition metals on different types of oxide supports.^[16, 21] In the following section, the preparation of well-defined silica supported imido amido tantalum surface complex from the reaction of tantalum hydrides either with ammonia or dinitrogen and hydrogen will be represented. To start, brief information about the choice of the support will be described.

II.1 The support

The support is a key component in surface organometallic chemistry in order to control the reactivity (selection and concentration of reactive functional groups) and the structure of the organometallic complexes. The recent synthesis and investigation of a new family of silica-based mesoporous materials designated as M41-S have attracted great interest because of their potential for applications in catalysis, separation and absorption for very bulky molecules.^[22, 23] MCM-41 is the best studied member of the M41-S family, first synthesized by Mobil Company researchers in early 90s,^[24, 25] characterized by a uniform hexagonal array of mesoporous and used in many applications as heterogenous catalysis, catalyst support and absorbent.^[26, 27]

MCM-41 has a very large void fraction due to the presence of mesopores and concomitantly a rather low density. This material therefore is more promising as a support with the advantages of large surface area for catalytic reagents and adjustable pore size distribution for shape selective reactions over conventional supports. The large surface area (S_{SPE} : $1000 \text{ m}^2\text{g}^{-1}$) is five times greater than that of silica Aerosil Degussa (S_{SPE} : $200 \text{ m}^2\text{g}^{-1}$), therefore provides three times more surface silanols, $[\equiv\text{SiOH}]$, the grafting sites of a silica surface.

In this study, we have used MCM-41 mesoporous silica supplied by the Laboratoire des Materiaux Mineraux, E.N.S. de Chimie Mulhouse, France which was prepared according to a classical literature method.^[27] The study of dehydroxylated MCM-41 at $500 \text{ }^\circ\text{C}$ has already been reported in our laboratory and showed the formation of mostly isolated surface silanols which leads to monografted tantalum species.^[17] The surface silanols of this material were monitored by IR, ^1H and ^{29}Si solid-state NMR, in addition to the measurement of their density at the surface of MCM-41₅₀₀ under a reaction of MeMgBr (in Et₂O) by GC. The values are reported in Table 1 including the structure parameters determined by X-ray diffraction and nitrogen adsorption methods for calcinated MCM-41 at 500°C .

Table 1

	Unit cell d (Å)*	Pore diameter pd (Å)	Wall thickness (Å)**	S _{SPE} BET (m ² .g ⁻¹)	OH/nm ² mmol/g
(MCM-41) ₅₀₀	42.0	28.5	13.5	1060 ± 1	1.7 (3.01)

* determined as $d_{100}/\sin 60$.

** determined as the difference of the unit cell parameter and the pore diameter.

The dehydroxylation process was particularly followed by IR spectroscopy on a MCM-41 pellet for our reactions; the spectrum showed a single sharp peak at 3747 cm⁻¹ corresponding to the $\nu(\text{O-H})$ band of free silanols. In the region of 2100-1500 cm⁻¹, weak but large band involving combinations and harmonics of ($\equiv\text{Si-O-Si}\equiv$) vibrations was observed as reported in the literature.^[28, 29]

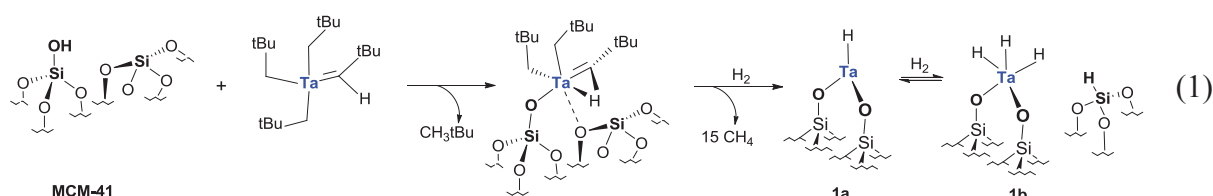
II.2 The preparation of well-defined tantalum imido amido complex

The strategy adopted in our laboratory to prepare the well-defined organometallic complexes performs first a sylanolysis reaction of a metal-carbon bond of an organometallic alkyl precursor (MR_n) by surface silanols ($[\equiv\text{Si-OH}]$) in order to lead to the formation of the grafted siloxy species, $[(\equiv\text{SiO})_x \text{M}_{R-x}]$. This behavior of $[\equiv\text{Si-OH}]$ is found quite similar to the "-OH" of alcohols/ silanols in the molecular chemistry.^[30]

According to the technique based on SOMC approach, the reaction of molecular peralkyl complexes with reactive surface silanol groups of a silica surface affords well-defined supported organometallic species which can undergo further hydrogenolysis to lead to silica-supported transition metal hydrides with examples of Ti,^[31] Zr,^[32] Hf,^[33] and Ta^[34, 35] being already reported in our laboratory.

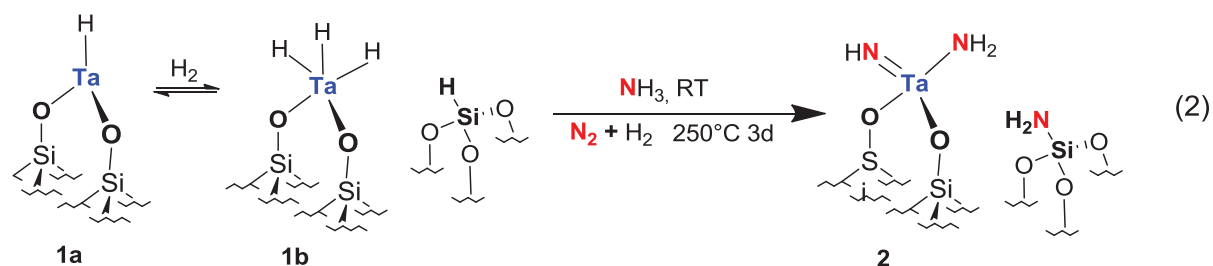
The starting tantalum hydrides are the key complexes of this thesis which were first prepared by Basset et al. in 1996 from the grafting reaction of molecular tantalum alkyl-alkyldene complex, $[\text{Ta}(\text{CH}_2\text{C}(\text{CH}_3)_3)_3(=\text{CHC}(\text{CH}_3)_3)]$ on the dehydroxylated aerosol silica at 700 °C, following an hydrogen treatment at 150 °C for 12 hours.^[35] The recent studies on the same

reaction with MCM-41 (dehydroxylated at 500 °C) have shown the formation of same surface species with an increase of tantalum loading from 5 %_{wt} to 15 %_{wt} on MCM-41 surface.^[17] As shown in Equation 1, hydrogenolysis reaction leads to the transformation of neopentyl and neopentyldine ligands into methane as well as the formation of a mixture of tantalum hydrides.



The silica-supported tantalum hydrides, **1** mainly consist in a mixture of monohydride Ta(III) species, $[(\equiv\text{SiO})_2\text{TaH}]$, **1a** and of tris-hydride Ta(V) species, $[(\equiv\text{SiO})_2\text{TaH}_3]$, **1b** whose relative ratio on the surface is influenced by dihydrogen presence and thermal treatment. These hydrides have already proven their reactivity in the catalytic transformation of alkanes (e.g. alkane metathesis) by C-H and C-C bond cleavage as previously mentioned.^[12-13, 33]

The capacity of isolated Ta hydrides is unique in the context of surface science to activate ammonia and dinitrogen. Eq. 2 represents the formation of well-defined imido amido complex from the reaction of ammonia as well as dinitrogen over tantalum hydride mixture.



The reaction of tantalum hydrides with ammonia at room temperature was the first report on direct metal imido amido formation via surface organometallic chemistry. This report added to the very few literature precedents available at the time on well-defined molecular solution organometallic complexes capable of cleaving N-H bonds of ammonia to yield either an amido^[36-40] or an imido^[41] complex.

The reaction of tantalum hydrides with ammonia in order to obtain complex **2** occurs at room temperature in excess of ammonia (min. 4 fold) followed by 4 hours of vacuum treatment at 150 °C to remove the unreacted ammonia from the system. The well-defined imido amido surface complex $[(\equiv\text{SiO})_2\text{Ta}(=\text{NH})(\text{NH}_2)]$ is in equilibrium with its ammonia adduct **2**. NH_3 . Surface silylamidos, $[\equiv\text{SiNH}_2]$ are also formed and measured (2.7 N/ Ta ratio) by elemental analysis showing a good agreement with the formulated imido amido and the silylamido products.^[18]

The surface complexes have been characterized by *in situ* IR, NMR and EXAFS studies (Chart 1). Particularly, the proton TQ solid-state NMR experiments that had never been applied to surface science before our study have allowed the discrimination of NH, NH₂, and NH₃ groups on the surface complexes **2** and **2**. NH_3 .^[18]

¹ H NMR (ppm)	¹⁵ N NMR (ppm)		EXAFS*
9.0 ^{a,b}	Ta=NH	-70	Ta=NH
4.0 ^b	Ta-NH ₂	-260	Ta-NH ₂
2.4	Ta(NH ₃)	-340	Ta(NH ₃)
2.4	(NH ₃) _{phys}	-385 ^{c,d}	(NH ₃) _{phys}
1.1	Si-NH ₂	-400 ^c	Si-NH ₂

^a no autocorrelation was observed for this resonance under 1H DQ MAS conditions

^b no autocorrelation was observed for this resonance under 1H TQ MAS conditions

^c observed also by independent addition of ¹⁵NH₃ on pure highly dehydroxylated silica

^d decreases under vacuum

* All EXAFS values correspond to the distance from Ta in Å.

Chart 1: The structure of well-defined silica supported tantalum imido amido complex.

Even more surprisingly, the same starting hydrides, **1a** and **1b** showed the unique ability to cleave the very robust N≡N bond of dinitrogen stoichiometrically in the presence of hydrogen (1:1) at 250 °C to form the same tantalum imido amido species. The products of this reaction have been successfully characterized at that time by IR spectroscopy, 2D HETCOR and DQ NMR spectroscopy, EXAFS and elemental analysis.^[19]

No solution or surface molecular system has so far achieved all the tantalum hydride properties simultaneously (i.e., well-defined isolated Ta^{III/V} atoms, three or five coordinate, d² or d⁰ low electron configuration, stable up to 250 °C), which probably contributes to the

capacity reported for cleaving the $\text{N}\equiv\text{N}$ bond on an isolated metal atom with dihydrogen rather than with the judicious alternate additions of protons and electron sources as in other examples in the literature (see Chapter III for detailed information). Therefore, the singularity of this process is not only due to the role of tantalum hydrides as monometallic species to split N_2 but also the presence of molecular dihydrogen as the reducing agent in the system.

The modeling studies were carried out by *Xavier Solans-Monfort* at Universitat Autònoma de Barcelona and *Odile Eisenstein* at Institut Charles Gerhardt, Université Montpellier 2 for the first time, to perform the theoretical modeling of this reaction. The studies were also consisted in density and geometry optimizations based on DFT calculations using either periodic or cluster model, **2q**.

This model has been very similar and equal to those used in previous studies for modeling silica-supported transition metal hydride. The reliability of the presentation has been verified by comparing the structures and energetics of all minima obtained with the periodic calculations, using C_{100} as model for silica.^[19]

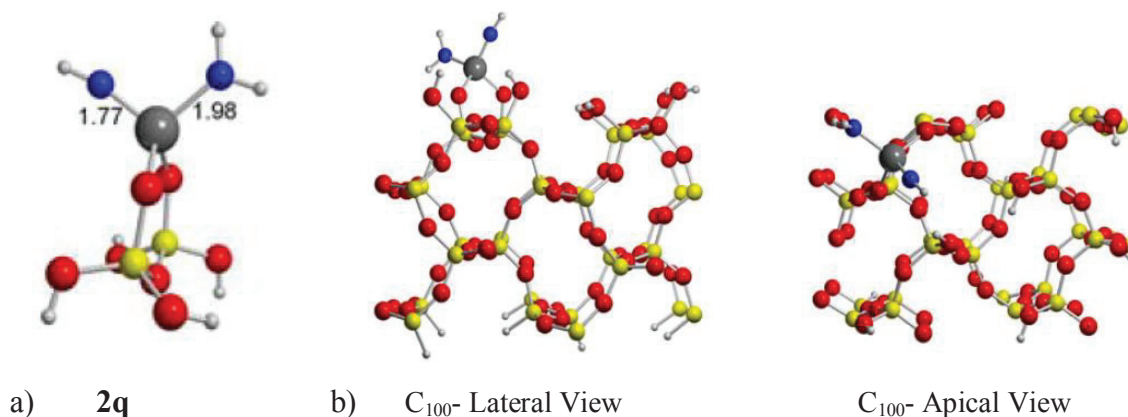


Figure 1: Silica grafted complex **2** models: a) **2q** cluster model and b) C_{100} period model with lateral and apical views.

Figure 1 presents the **2q** cluster model for silica grafted tantalum imido amido complex (left) and the C_{100} period model (right). DFT studies on the cluster model give identical geometrical structures of grafted species to those obtained with calculations within the periodic boundary condition, both calculations close to the structure obtained from EXAFS measurement. The

calculations show that both synthetic routes for $[(\equiv\text{SiO})_2\text{Ta}(=\text{NH})(\text{NH}_2)]$, **2q** are extremely exothermic. The details of this study will be given briefly later.

The studies on the reactivity of silica-grafted tantalum hydrides to yield well-defined tantalum imido amido species from either ammonia or dinitrogen and hydrogen by our group thus appeared model in the literature. Therefore, the next step was to understand the mechanistic insight of the bond cleavage mechanisms of these reactions (N-H bond of ammonia at room temperature and $\text{N}\equiv\text{N}$ bond cleavage in the presence of H_2 at 250 °C); in addition to study the reactivity of well-defined $[(\equiv\text{SiO})_2\text{Ta}(=\text{NH})(\text{NH}_2)]$ complex. These have been the starting points of my thesis, the objectives will be detailed in the following part.

III. OVERVIEW OF CHAPTER I AND OBJECTIVE OF MY THESIS

In this chapter, the reported unique reactivity of tantalum hydrides developed by SOMC approach to cleave the N–H bond of ammonia and the N≡N triple bond of dinitrogen have been outlined.

The room temperature cleavage of ammonia N-H bond achieved by tantalum hydride surface complexes by SOMC was a fairly rare occurrence. The cleavage of robust N≡N bond in N₂ occurs in an unprecedented manner on a monometallic tantalum center with H₂ as a reducing agent.

Therefore, searching the reactivity of the well-defined imido amido complex was the next step of our group; at first the reaction of D₂ at moderate temperatures with highly electropositive tantalum complex **2** was studied (see next chapter).

Chapter II will initially give a brief literature report on the ammonia activation by different systems and some selected examples on the possible reaction mechanisms. Our experimental and computational studies on the reactivity of complex **2** with H₂ and NH₃ to split H-H and N-H bonds heterolytically through its Ta=NH and Ta-NH₂ bonds will be explained. The importance of the additional ammonia molecule in the system will be also highlighted.

Chapter III will first describe the coordination and activation of dinitrogen molecule in heterogeneous, biochemical and organometallic systems with the possible dissociation pathways in the literature. Experimental studies during my thesis on dinitrogen coordination / cleavage over tantalum hydrides with N₂, N₂H₄ and N₂H₂ in order to find out the intermediates of the reaction mechanism will be given in this section. The methods mainly by *in situ* IR, NMR and elemental analysis will be used to explain the results in addition to DFT calculations done by our co-workers.

Finally, the fourth chapter will deal with the catalytic reactivity of complex **2** towards CH bond activation of benzene, toluene, t-Bu-ethylene and methane.

In the last chapter, a general conclusion and the perspectives of the thesis will be established.

IV. REFERENCES

- [1] M. Agnelli, P. Louessard, A. El Mansour, J.-P. Candy, J.-P. Bournonville, J.-M. Basset, *Catal. Today* **1989**, *6*, 63.
- [2] J.-M. Basset, J.-P. Candy, A. Choplin, C. Santini, A. Theolier, *Catal. Today* **1989**, *6*, 1.
- [3] a) B. Didillon, C. Houtman, T. Shay, J. -P. Candy, J.-M. Basset, *J. Am. Chem. Soc.* **1993**, *115*, 9380; b) J. Thiovolle- Cazat, C. Copéret, S. Soignier, M. Taoufik, J.-M. Basset, *NATO Sci. Ser., II* **2005**, 191, 107.
- [4] a) J.-P. Candy, B. Didillon, E. L. Smith, T. B. Shay, J.-M. Basset, *J. Mol. Catal.* **1994**, *86*, 179; b) C. Copéret, O. Maury, J. Thiovolle- Cazat, J.-M. Basset, *Angew. Chem. Int. Ed.* **2001**, *40*, 2331.
- [5] S. L. Scott, J.-M. Basset, *J. Mol. Cat.* **1994**, *86*, 5.
- [6] P. Lesage, O. Clause, P. Moral, B. Didillon, J.-P. Candy, J.-M. Basset, *J. Catal.* **1995**, *155*, 238.
- [7] F. Humblot, D. Didillon, F. Lepeltier, J.-P. Candy, J. Corker, O. Clause, F. Bayard, J.-M. Basset, *J. Am. Chem. Soc.* **1998**, *120*, 137.
- [8] J.-M. Basset, D. Roberto, R. Ugo, *Modern Surface Organometallic Chemistry*, Wiley, **2009** ISBN : 978 3 527 31972 5.
- [9] D. Roberto, E. Cariati, M. Pizzotti, R. Psaro, *J. Mol. Catal. A: Chemical* **1996**, *111*, 97.
- [10] F. Quignard, C. Lecuyer, A. Choplin, D. Olivier, J.-M. Basset, *J. Mol. Catal.* **1992**, *74*, 353.
- [11] M. Chabanas, A. Baudouin, C. Copéret, J.-M. Basset, *J. Am. Chem. Soc.* **2001**, *123*, 2062.
- [12] D. Soulivong, S. Norsic, M. Taoufik, C. Copéret, J. Thivolle-Cazat, S. Chakka, J.-M. Basset, *J. Am. Chem. Soc.* **2008**, *130*, 5044.
- [13] a) V. Vidal, A. Theolier, J. Thivolle-Cazat, J.-M. Basset, *Science* **1997**, *276*, 99; b) Maury, O., L. Lefort, *Stud. Surf. Sci. Catal.* **2000**, *130*, 917; c) J.-M. Basset, C. Copéret, D. Soulivong, M. Taoufik J. Thivolle-Cazat, *Angew. Chem. Int. Ed.* **2006**, *45*, 6082.
- [14] V. Dufaud, J.-M. Basset, *Angew. Chem. Int. Ed.* **1998**, *37*, 806.
- [15] a) C. Lecuyer, F. Quignard, A. Choplin, D. Olivier, J.-M. Basset, *Angew. Chem. Int. Ed.* **1991**, *103*, 1692; b) J. M. Basset, C. Copéret, L. Lefort, B.-M. Maunders, O.

- Maury, E. Le Roux, G. Saggio, S. Soignier, D. Soulivong, G. J. Sunley, M. Taoufik, J. Thivolle- Cazat, *J. Am. Chem. Soc.* **2005**, *127*, 8604.
- [16] M. Taoufik, R. E. Le Roux, J. Thivolle- Cazat, J.-M. Basset, *Angew. Chem., Int. Ed.* **2007**, *46*, 7202.
- [17] S. Soignier, M. Taoufik, E. Le Roux, G. Saggio, C. Dablemont, A. Baudouin, F. Lefebvre, A. De Mallmann, J. Thivolle-Cazat, J.-M. Basset, G. Sunley, B.-M. Maunders, *Organometallics* **2006**, *25*, 1569.
- [18] P. Avenier, A. Lesage, M. Taoufik, A. Baudouin, A. De Mallmann, S. Fiddy, M. Vautier, L. Veyre, J.-M. Basset, L. Emsley, E. A. Quadrelli, *J. Am. Chem. Soc.* **2007**, *129*, 176.
- [19] P. Avenier, M. Taoufik, A. Lesage, X. Solans-Monfort, A. Baudouin, A. de Mallmann, L. Veyre, J.-M. Basset, O. Eisenstein, L. Emsley, E. A. Quadrelli, *Science* **2007**, *317*, 1056.
- [20] C. Copéret, M. Chabanas, R. P. Saint-Arroman, J.-M. Basset, *Angew. Chem. Int. Ed.* **2003**, *42*, 156.
- [21] R. R. Schrock, J. D. Fellmann, *J. Am. Chem. Soc.* **1978**, *100*, 3359.
- [22] J. C. Vartuli, K. D. Schmitt, C. T. Kresge, W. J. Roth, M. E. Leonowicz, S. B. McCullen, S. D. Hellring, J. S. Beck, J. L. Schlenker, D. H. Olson, E. W. Sheppard, *Chem. Mater.* **1994**, *6*, 2317.
- [23] F. Hoffmann, M. Cornelius, J. Morell, M. Froeba, *Angew. Chem., Int. Ed.* **2006**, *45*, 3216.
- [24] J. S. Beck, J. C. Vartuli, W. J. Roth, M. E. Leonowicz, C. T. Kresge, K. D. Schmitt, C. T. W. Chu, D. H. Olson, E. W. Sheppard, S. B. McCullen, S. D. Hellring, *J. Am. Chem. Soc.* **1992**, *114*, 10834.
- [25] P. Behrens, *Adv. Mater.* **1993**, *5*, 127.
- [26] H. Kosslick, G. Lischke, H. Landmesser, B. Parlitz, W. Storek, R. Fricke, *J. Catal.* **1998**, *176*, 102.
- [27] C. Y. Chen, H. X. Li, M. E. Davis, *Microporous Mater.* **1993**, *2*, 17.
- [28] B. A. Morrow, J. L. G. Fierro, *Studies in Surface Science and Catalysis*, **1990**, *57*, 161.
- [29] B. A. Morrow, I. A. Cody, *J. Phys. Chem.* **1976**, *80*, 1995.
- [30] M. Chabanas, E. A. Quadrelli, B. Fenet, C. Copéret, J. Thivolle- Cazat, J.-M. Basset, A. Lesage, L. Emsley, *Angew. Chem. Int. Ed.* **2001**, *40*, 4493.
- [31] C. Rosier, G. P. Niccolai, J.-M. Basset, *J. Am. Chem. Soc.* **1997**, *119*, 12408.

- [32] C. Corker, F. Lefebvre, C. Lecuyer, V. Dufaud, F. Quignard, A. Choplin, J. Evans, J. M. Basset, *Science* **1996**, *271*, 966.
- [33] a) F. Lefebvre, J. Thivolle-Cazat, V. Dufaud, G. P. Nicolai, J.-M. Basset, *Appl. Catal.* **1999**, *182*, 1; b) C. Thieuleux, C. Copéret, V. Dufaud, C. Marangelli, E. Kuntz, J.-M. Basset, *J. Mol. Catal.* **2004**, *213*, 47; c) S. Schinzel, H. Chermette, C. Copéret, J.-M. Basset, *J. Am. Chem. Soc.* **2008**, *130*, 7984.
- [34] V. Dufaud, G. P. Nicolai, J. Thivolle-Cazat, J.-M. Basset, *J. Am. Chem. Soc.* **1995**, *117*, 4288.
- [35] V. Vidal, A. Theolier, J. Thivolle-Cazat, J.-M. Basset, J. Corker, *J. Am. Chem. Soc.* **1996**, *118*, 4595.
- [36] J. Zhao, A. S. Goldman, J. F. Hartwig, *Science* **2005**, *307*, 1080.
- [37] G. L. Hillhouse, J. E. Bercaw, *J. Am. Chem. Soc.* **1984**, *106*, 5472.
- [38] G. Parkin, A. van Asselt, D. J. Leathy, L. Whinnery, N. G. Hua, R. W. Quan, L. M. Henling, W. P. Schaefer, B. D. Santarsiero, J. E. Bercaw, *Inorg. Chem* **1992**, *31*, 82.
- [39] A. L. Casalnuovo, J. C. Calabrese, D. Milstein, *Inorg. Chem.* **1987**, *26*, 971.
- [40] E. G. Bryan, B. F. G. Johnson, J. Lewis, *J. Chem. Soc., Dalton. Trans.* **1977**, 1328.
- [41] J. S. Freundlich, R. R. Schrock, W. M. Davis, *J. Am. Chem. Soc.* **1996**, *118*, 3643.

CHAPTER II.

Activation of NH_3 and H_2 :

Mechanistic insight through bond activation reactions

I. INTRODUCTION

I.1 Introduction to ammonia and its properties

Ammonia is one of the most highly produced chemicals in the world (around 150 million tons per year) and has widespread use in many sectors.^[1-5] Being an important source of nitrogen for living systems it contributes significantly to the nutritional needs of organisms by serving as a precursor to food and fertilizers. It is directly or indirectly a building block for the synthesis of many nitrogen-containing pharmaceuticals, therefore it has large applications in the production of fertilizers, chemicals, precursors, cleaners, vehicle fuel as well as explosives. The activation of ammonia has therefore attracted increasing interest over the years.

According to its structure, ammonia consists of one nitrogen atom covalently bonded to three hydrogen atoms. The nitrogen atom in the molecule has a lone electron pair, which makes NH_3 a moderate base ($\text{pK}_b \approx 9.2$ (H_2O)). The lone pair of electrons on the nitrogen induces the 107° H...N...H bond angle and ensuing triangular pyramid shape gives a dipole moment to the molecule by making it polar. Ammonia is very weak acid ($\text{pK}_a \approx 38$ (H_2O)) and the N-H bond enthalpy is calculated as 107 kcal/ mol.^[5, 6]

These characterizations combined with ammonia's toxicity, danger and corrosiveness mostly explain the paucity of mild route for direct ammonia transformation to added-value products. Chapter IV will report more detailed discussion for full catalytic transformation of ammonia to amine and will focus on the preliminary transition metal activation of ammonia.

I.2 Activation of ammonia N-H bond

The interaction of the ammonia N-H bond with transition metal centers as well as with main group element atoms is of great importance in many fields such as catalysis, surface science, and material synthesis. However the main hurdle for this activation by the transition metal is

to generate Lewis acid-base adducts, like “Werner’s complexes” with ammonia due to its electrophilicity.^[4, 8-12]

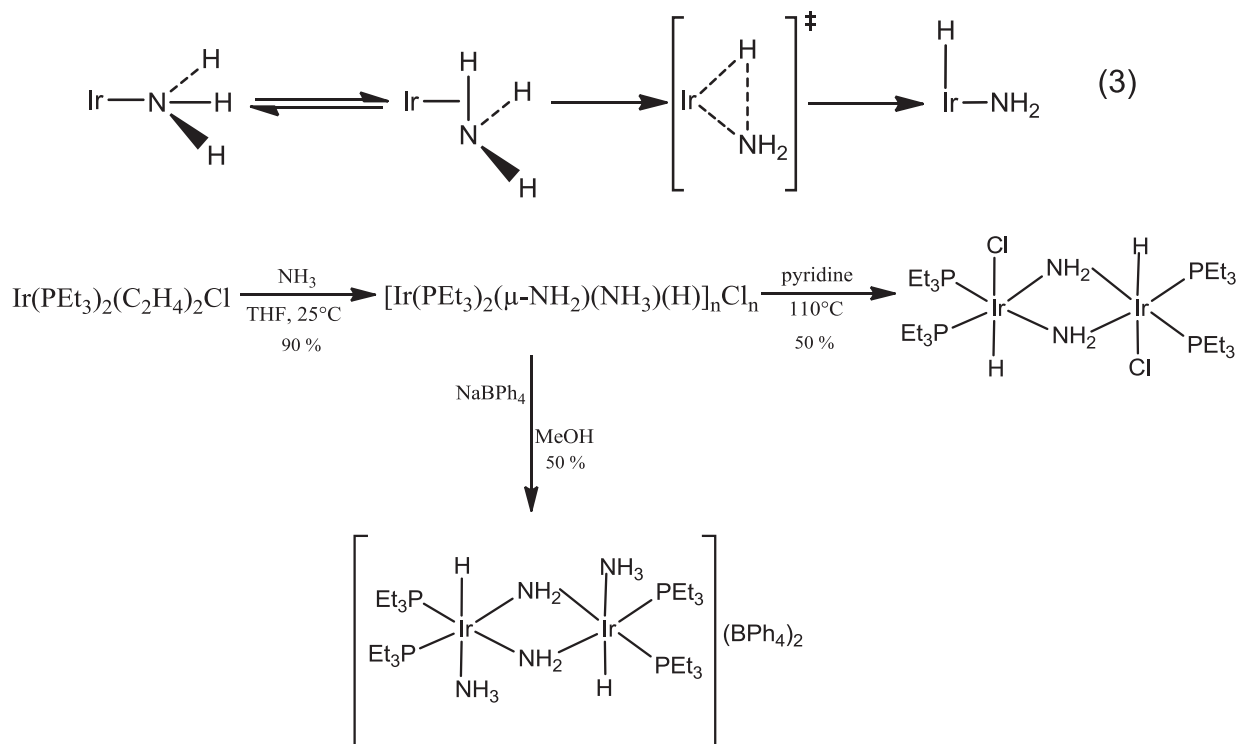
This chapter will start with the significant results and challenging studies on ammonia N-H bond activation in addition to the mechanistic insights in the literature and will continue with the description of our results concerning this bond cleavage.

I.2.1. Ammonia oxidative addition by transition metal complexes:

Transition-metal complexes may react with many other small molecules by inserting into generally unreactive X-H bonds. This process, termed oxidative addition, is useful for chemical synthesis by enabling the catalysis of reactions of H₂ (hydrogenation), H-SiR₃ (hydrosilation), H-BR₂ (hydroboration), C-H (hydroarylation, alkane dehydrogenation) that yield products ranging from chemical feedstocks to pharmaceuticals.^[13] Oxidative addition of the ammonia N-H bond can similarly be regarded as a model reaction for the development of new catalytic reaction cycles which involve the N-H bond cleavage of NH₃ by insertion of a transition metal as a key-step. Even though ammonia activation by transition metal complexes has difficulties, there are some well-defined examples that have been reported:

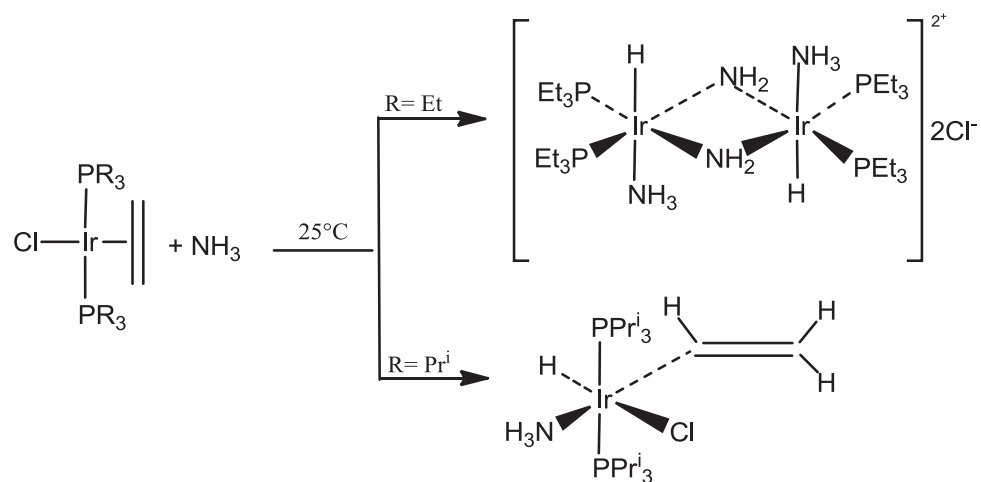
The study of Casalnuovo and Milstein in 1987^[14] on ammonia activation over late-transition-metal iridium (I) complex [Ir(PEt₃)₂(C₂H₄)Cl] led to the bimetallic amido-hydride complex including isolation, structural characterization, and reactivity of the product as given in Scheme 1, while Eq. 3 describes the oxidative addition of ammonia N-H bond over starting Ir(PEt₃)₂Cl species.

This reaction was crucial as it described for the first time the ammonia activation by electron-rich, low-valent, sterically unhindered transition metal complex and cleaving the N-H bond of ammonia by oxidative addition.



Scheme 1

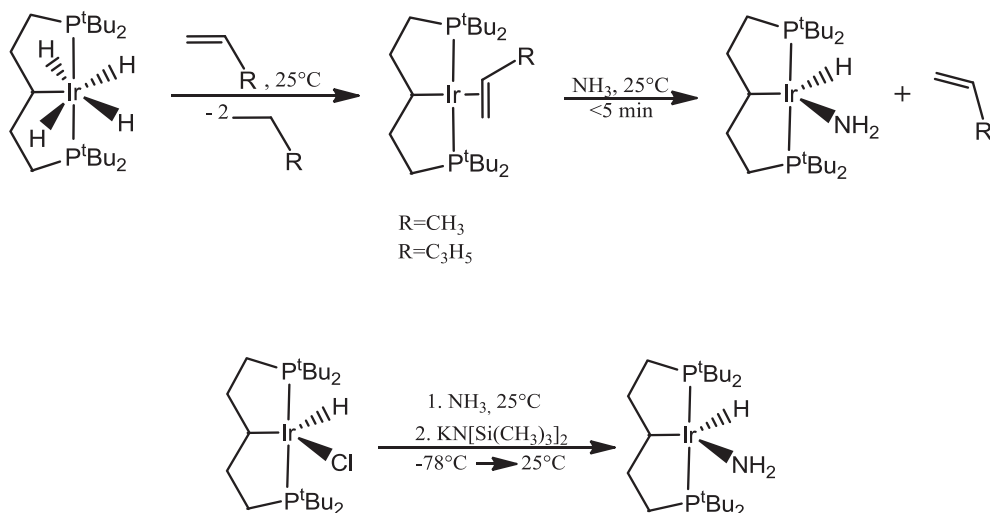
Further work of the group with the same iridium complex demonstrated the effect of different ligands for ammonia N-H bond activation as shown in the Scheme 2 below ^[15]



Scheme 2

Using the ligands with different size in this reaction showed that the influence was not only on the reaction rate, as is well known, but also on the direction of reactivity as surprisingly C-H activation took place rather than N-H, leading to the hydrido vinyl compound in case of $\text{R}=\text{Pr}^i$.

The next challenging result of the transition metal complexes for the development of ammonia activation came from Hartwig and his group who reported the first stable terminal amido complex (Scheme 3).^[16]



Scheme 3

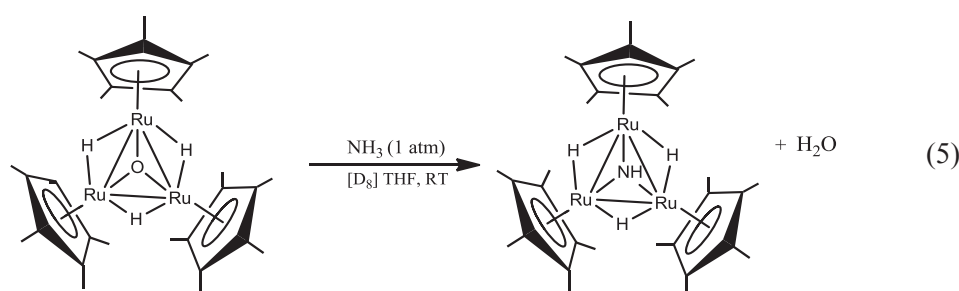
Insertion of an iridium center with a tridentate pincer ligand into the N-H bond rapidly cleaved ammonia at room temperature in a homolytic way and obtained mononuclear iridium hydrido amido by oxidative addition.

The oxidative addition tends to be favoured by increasing electron density at the metal center. Therefore, a pincer ligand with an aliphatic backbone was preferred for this study in order to donate more electron than an aromatic ligand.^[16-18] The activation of ammonia N-H bond has been explained by using electron-rich iridium complex, which helped the coordinated ammonia to transfer the electron density over the metal center as well as the π -bonding between the electron pair on nitrogen and the LUMO on the metal and form a stable monomeric amido hydride complex.

Studies are ongoing in this field while one of the most representative example has been reported by Turculet^[19] showing the N-H bond oxidative addition for both ammonia and aniline by Iridium complexes supported by silyl pincer ligands (Eq.4).

The dinuclear Ir complex reacts with excess NH₃ at -50 °C to give not only mono- and dicationic complexes but also, the first amido-olefin complex. N-H activation under such exceptionally mild conditions is of interest for the catalytic functionalization of olefins with NH₃.

There have been several examples with binuclear metal complexes in the literature to activate ammonia, while the first example of the double activation (trinuclear oxidative addition) was reported by Suzuki with a polyhydride ruthenium complex which formed μ₃- imido cluster via ammonia (Eq.5).^[21]



A new mode of ammonia activation was later described by Ozerov and co-workers by a dimeric Pd pincer complex via a binuclear oxidative addition to give amido-hydrido Pd monomers (Eq. 6).^[22]



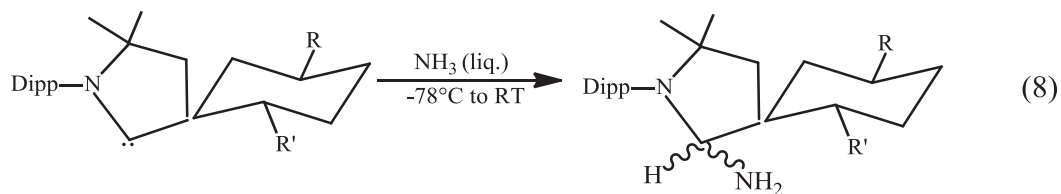
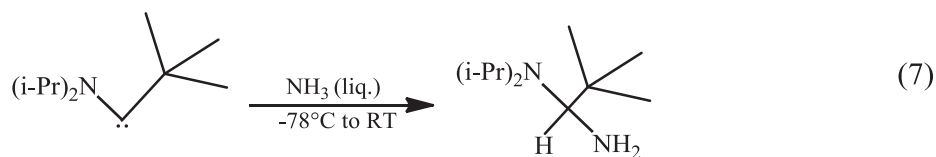
PNP = 2,6-bis-(di-*t*-butylphosphinomethyl)pyridine

This initial example showed the cooperation of two metal centers to split NH₃ into terminal M-H and M-NH₂ (for conversion of NH₃ to bridging amido and imido ligands see reference^[8]). The described system is elegant, because of comprising a well-defined, tunable ligand with a highly reactive metal-metal bond as central feature in the bimetallic complex.

I.2.2. Ammonia oxidative addition “without transition metal complex”:

Metal-free ammonia N–H activation using main-group based systems has recently enjoyed much attention and progress: Bertrand et al. demonstrated the first example of the NH_3 (and H_2) oxidative addition by cyclic (alkyl)(amino)carbenes.^[23]

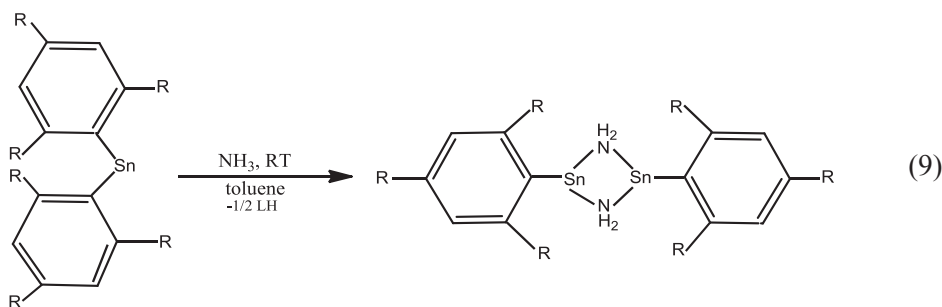
The group has reported the homolytic cleavage of ammonia by nucleophilic activation under very mild conditions at a stable single carbene center (mono (amino) carbenes) (Eq. 7 and 8).



Dipp: 2, 6-*i*-Pr₂C₆H₃ R=R'=H; R= Me, R'=*i*-Pr

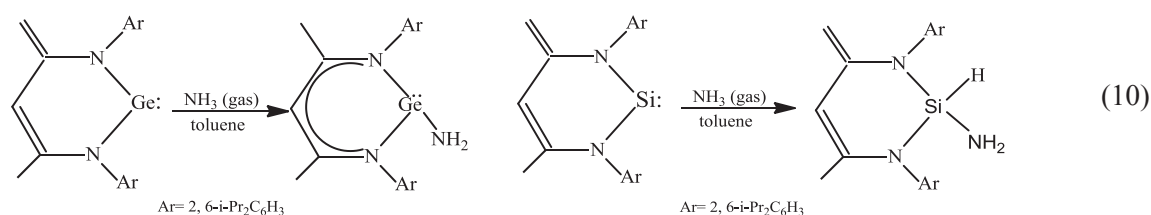
Because of the strong nucleophilic character of carbenes, no “Werner-like” adducts were formed, and hence N–H bond cleavage occurred smoothly.

Power and co-workers subsequently described the activation of ammonia by the heavier group 14 element (Poor metal/ carbene analogue) SnAr^*_2 [$\text{Ar}^* = \text{C}_6\text{H}_3\text{-2,6}(\text{C}_6\text{H}_2\text{-2,4,6-Me}_3)_2$].^[24]



Related to this study (Eq 9), two-coordinate distannyll complexes were exhibited similar reactivity under mild conditions, leading to the formation of dimeric bridging amido tin-species, concomitant with arene elimination.

The quantitative reaction of ammonia with the carbene analogue poor metal, germylene has been recently reported by the group of Roesky leading N-H bond cleavage at room temperature.^[25, 26]



This reaction generated a terminal GeNH₂ group at mild conditions and oxidative addition to the final complex which demonstrated an important example of sustainable chemistry. The oxidative addition of ammonia at the silicon (II) center of a silylene in order to form Si(H)NH₂ has been recently published by the same group.^[26]

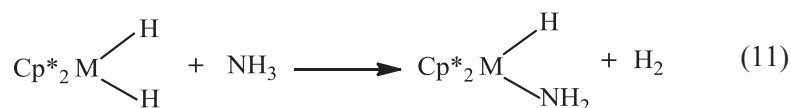
1.2.3. Ammonia activation by d⁰ transition metal complexes:

Even though most of the studies on ammonia activation are based on transition metals and/ or carbenes/ carbene analogues, one of the earliest examples for N-H bond cleavage has been reported by Bercaw in 1984 on d⁰ complexes.^[27] The purpose of the group at that time was to investigate the interactions between 4B transition metals (mainly Zr and Hf) in their high oxidation states and hard ligands in order to study their reactions for water and ammonia splitting.

The activation of NH₃ by d⁰ complexes has been studied about three decades ago by various groups, showing that both monomeric and dimeric early transition metals can activate N–H bonds of ammonia.^[8-10, 27] However, these systems were not always well-defined and final products were not fully characterized in some cases. The activation was also not specific that the cleavage of N–H bonds leads to inter alia bridging nitrido-complexes. Some complexes containing a d⁰ metal center, such as [Cp*₂MH₂] (M=Zr, Hf; Cp* =

pentamethylcyclopentadiene),^[27] $[\text{Cp}^*_2\text{ScR}]^{[9]}$ and $\text{Ta}(=\text{CH-tBu})(-\text{CH}_2\text{tBu})_3^{[8]}$ activated ammonia to generate stable amido and nitrido complexes.

The group of Bercaw was interested in the chemistry of the group 4B metals in their higher oxidation states that were dominated by the propensity of these metals to form extremely strong bonds with “hard” ligands such as O, N, F and Cl donors (Eq.11).

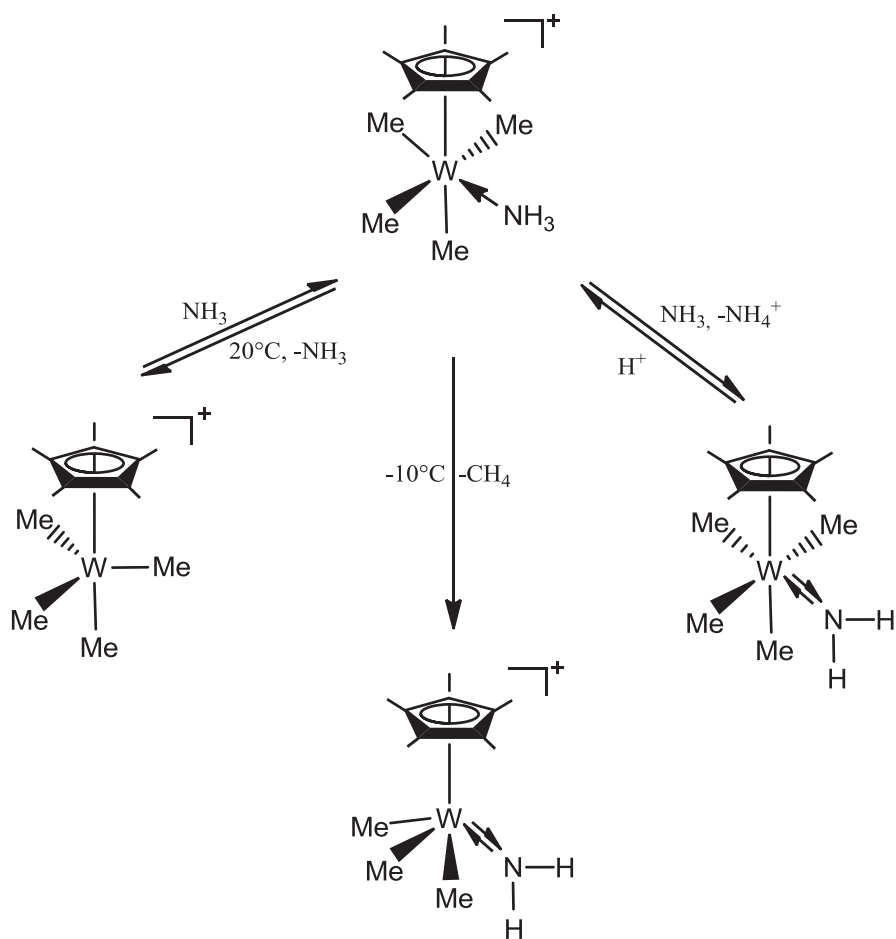


M = Zr, Hf

They reported the deprotonative activation of ammonia and related amines with Zr and Hf metal-complexes where the oxidation degree of the metal remained same at the end of the reaction.^[27] As already mentioned above, despite the significant results for ammonia activation on d^0 metal centers Zr and Hf, there was no additional investigation in order to understand the route of the N-H cleavage reaction on these complexes.

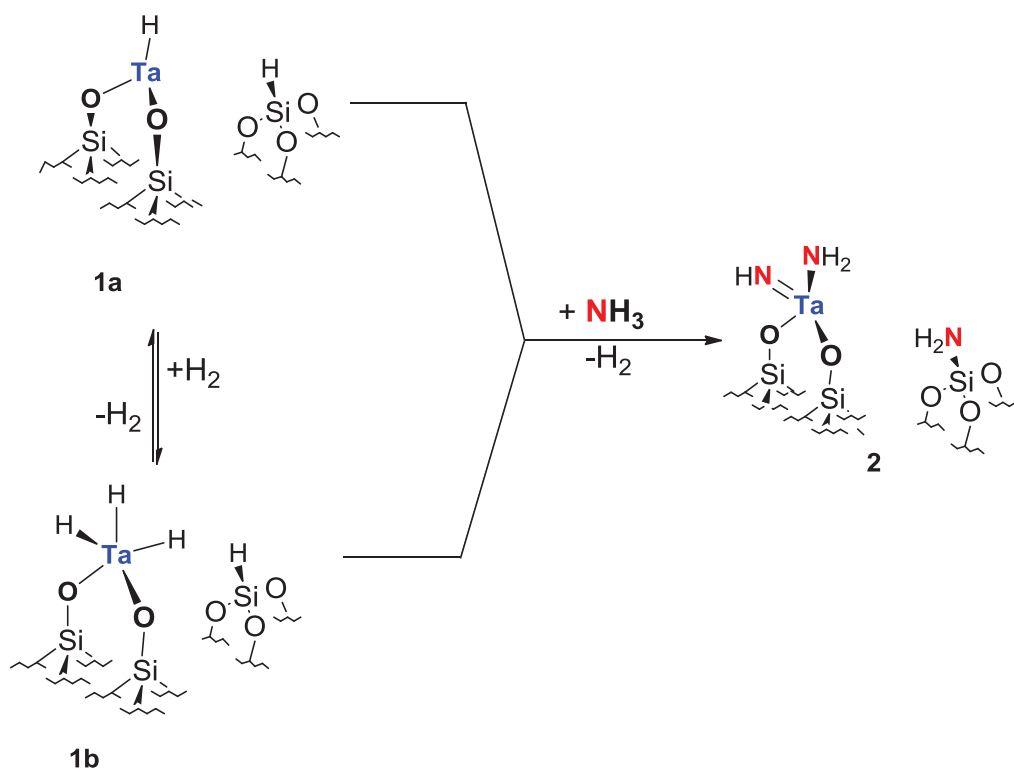
The work of Schrock published in 1991 supported Bercaw’s studies for ammonia N-H bond cleavage by high oxidation state transition metal complexes.^[30] According to his work, ammonia coordinated reversibly to a d^0 tungsten complex which was afterwards deprotonated below room temperature to amido product (Scheme 5). Good yields of the product (~ 85%) were obtained if a large excess of ammonia was added to the starting methyl W(II) complex in solution at room temperature.^[30]

Complexes that contain the $\text{Cp}^*\text{M-Me}_4$ core were well-suited for multiple bonding by ammonia to amido ligands as in the scheme 5. These complexes provided an important pathway for the development of ammonia usage in catalytic reactions.



Scheme 5

Our group presented the first evidence of surface organometallic chemistry (SOMC) of well-defined metal imido amido species from the reaction of ammonia in 2007. A mixture of the silica-supported tantalum hydrides, $[(\equiv\text{SiO})_2\text{TaH}]$, **1a** (d^2) and $[(\equiv\text{SiO})_2\text{TaH}_3]$, **1b**, (d^0) converted completely into Ta(V) amido imido species $[(\equiv\text{SiO})_2\text{Ta}(=\text{NH})(\text{NH}_2)]$, **2** (d^0) in the presence of ammonia at room temperature.^[33] The characterizations by various methods such as EXAFS, *in situ* IR and NMR spectroscopies confirmed the cleavage of ammonia N-H bond as well as the formation of well-defined imido amido complex.



Scheme 6

The same well-defined imido amido complex were also yielded from the reaction of the starting hydrides with dinitrogen by our group,^[34] however in this chapter, we will only focus on the ammonia activation and talk about dinitrogen activation later on. Further studies on the reactivity and the mechanism of this imido-amido complex will be presented in different parts and chapters of this thesis as the recent advancements are very important for the emergence of N-based chemistry.

The following part of this chapter will describe the mechanistic insight of ammonia activation in the literature.

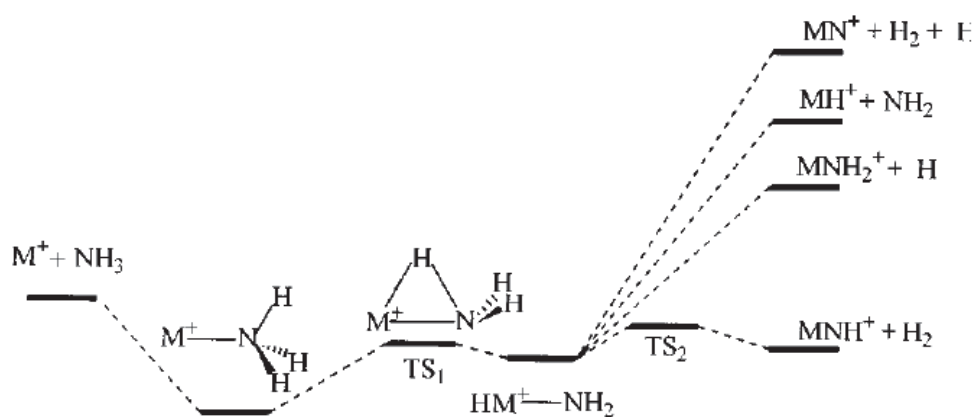
I.3 Mechanistic understanding of ammonia activation

Ammonia activation has attracted significant attention and has been studied by various groups as shown above, however in many cases there have been no detailed mechanistic studies. To obtain a deep knowledge of the reaction mechanisms and to understand the origin of the

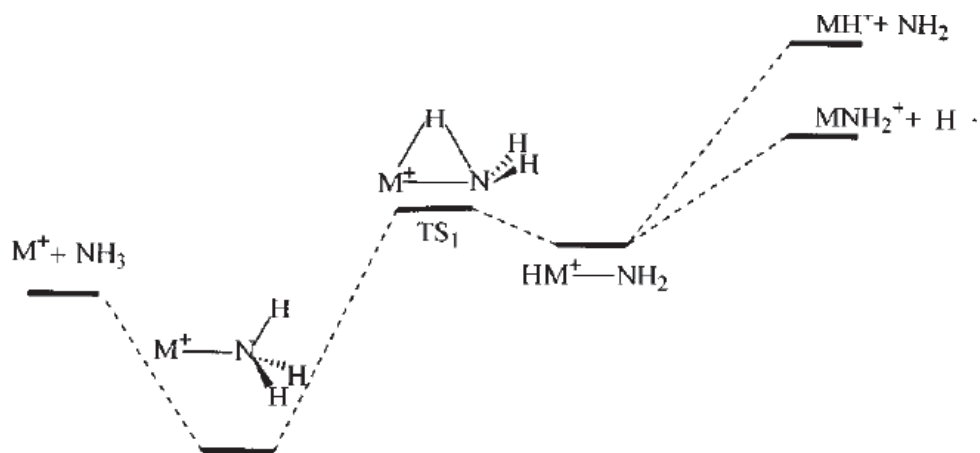
their reaction mechanisms.^[39-41] In the first stage of these reactions, M(I) and NH₃ were expected to form a stable ion-dipole complex MNH₃⁺ which was observed in the late transition metal cations (Co, Ni, Cu),^[41] but not in the early transition metal cations (Sc, Ti, V).^[40]

Scheme 8 illustrates the mechanisms for early and late transition metals with the reaction of ammonia.

(a) Early Transition Metal Cation



(b) Late Transition Metal Cation



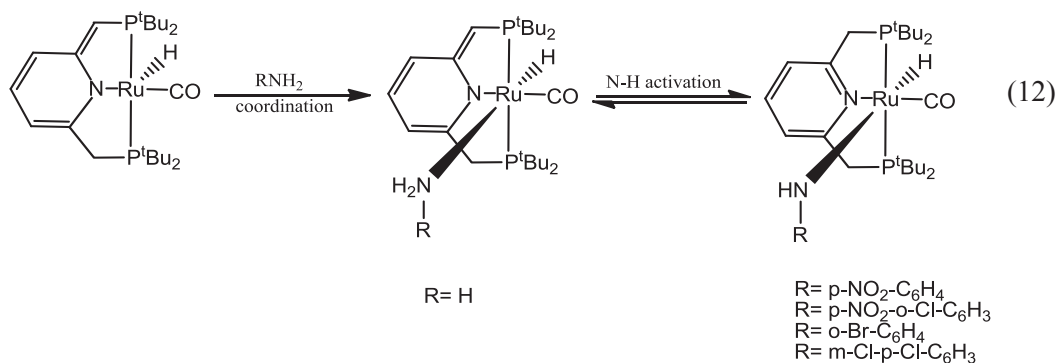
Scheme 8

For all the transition metal cations, MNH_2^+ and MH^+ were observed in the endothermic reactions. The analysis after the dehydrogenation of ammonia for these metals showed the stability of $H-M^+-NH_2$ intermediate for both low- and high-spin states. In all cases, the low spin state was more stable due to the two covalent σ -bond formations while the electrostatic interaction between metal and H as well as NH_2 stabilized the high spin complexes. Gas-phase experiments such in these cases are of importance in catalytic processes as they have considerable insight into the mechanism of the activation of stable molecules by transition metals. Various theoretical studies help to improve the understanding of the reaction mechanism by different evaluations.

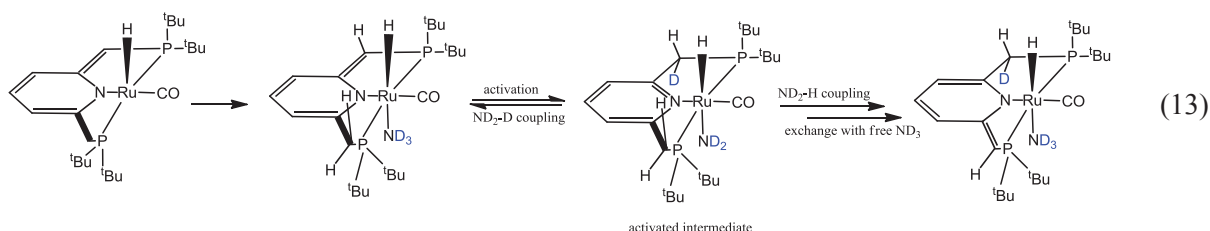
The investigations of ammonia N-H bond cleavage mechanism performed by Chen and his group later on dealt with the reaction of early transition metal atoms (Sc, Ti, V) with ammonia in solid argon matrix.^[29] This formed the stable MNH_3 complexes spontaneously on annealing, which then turned into intermediate $HMNH_2$ after the insertion of metal atom in N-H bond by photomerization, upon different UV-Visible photolysis (exothermic). The reactions of middle transition metals (Mn, Fe, Ni) were compared and it was found that they favor MNH_2 molecules energetically. The metal atoms in this study were produced by pulsed laser ablation of pure metal targets. This work has a great importance due to the various reaction intermediates and products which have been identified by isotopic substitutions (infrared absorption spectroscopy), in addition to the understanding of the reaction mechanism by density functional theory calculations on ammonia N-H bond activation.

Very few groups compared the activation of ammonia with methane in order to have a mechanistic insight for the reaction of N-H bond cleavage, Sakaki was one of them publishing his work^[51] relying on the DFT and other theoretical calculations by Ti-imido complex to show the differences in the C-H σ -bond activation between early and late transition metal complexes, and to clarify the essential role of the orbital interaction in the C-H σ -bond activation by this complex. A theoretical prediction of ammonia has been presented that Ti-imido and Ti-alkylidyne complexes applied to the heterolytic N-H σ -bond activation. The typical coordination bond was found to be stronger and larger than that methane C-H bond due to the coordination of ammonia center “by charge transfer of lone pairs” to the empty d orbital of Ti center. The results also confirmed the activation of C-H of methane and N-H bonds of ammonia by Ti-imido complex in a heterolytic way.

Milstein and his group recently represented a novel approach that has been never reported up to that date involving the reversible ammonia activation via metal-ligand cooperation.^[53] The study included the reaction of ammonia with a dearomatized (PNP)Ru complex at room temperature with no change in the formal oxidation state of the metal.

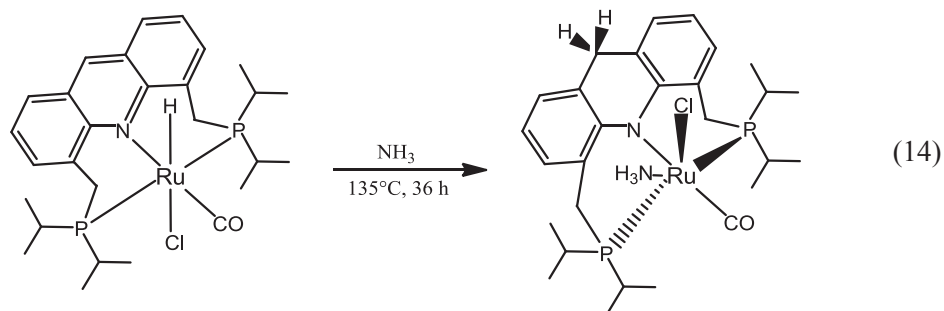


N-H bond cleavage in this system was *reversible*, suggesting that the barrier for N-H bond activation was low enough for the reaction to occur rapidly at room temperature and that product amines could be eliminated in potential catalytic cycles based on such systems.



To probe the possibility of ammonia activation, starting Ru(II) hydride complex was reacted with an excess of ND₃ and selectively obtained the deuterated amino adduct after addition. The reaction was highly stereospecific that the activation process occurs on only one face of the ligand and in an intramolecular manner with one coordinated molecule of ND₃. The reverse reaction affected only the (endo)hydrogen on the same face as the coordinated ND₃ moiety.

Further studies of the same group with the acridine based ruthenium complex, (A-PNP)RuHCl(CO) showed a unique and an unprecedented mode of metal-ligand cooperation involving a “long-range” interaction of acridine central ring and the metal for ammonia activation.^[54]



Ammonia reaction with (A-PNP)RuHCl(CO) led to the hydride transfer from the Ru center to **C9** position of the complex by forming an unusual coordination of the dearomatized A-PNP ligand. The implications of this novel mode of metal-ligand cooperation for catalytic design as well as for improvement of the mechanistic insight have been currently working by the same group.

I.4 Overview of chapter II

The examples given above show the literature precedents of ammonia activation by different processes as well as the proposed mechanisms for some cases. Our group has already reported their work on activation of ammonia N-H bond at room temperature by silica grafted tantalum hydrides and obtained the first evidence of surface organometallic chemistry of well-defined metal imido amido species ($[(\equiv\text{SiO})_2\text{Ta}(=\text{NH})(\text{NH}_2)]$) from the reaction of ammonia as mentioned before.^[33]

This chapter aims at describing the recent studies on the reactivity of this well-defined surface complex $[(\equiv\text{SiO})_2\text{Ta}(=\text{NH})(\text{NH}_2)]$ with dihydrogen and ammonia in along with the connected studies on the possible mechanism of these reactions. The investigations on the mechanistic insight of H-H and ammonia N-H bond activation at room temperature by tantalum hydrides will be explained according Density Functional Theory calculations and infrared spectroscopy studies.

II. RESULTS AND DISCUSSIONS

II. 1. Reaction of $[(\equiv\text{SiO})_2\text{Ta}(=\text{NH})(\text{NH}_2)]$ with dihydrogen :

The reactions of well-defined tantalum imido amido complex in the presence of H_2 (and D_2) have been studied stepwise recently by *in situ* IR spectroscopy and modeled by DFT Calculations to propose an exchange mechanism for this reaction.^[55] Brief information on these results will be given here in order to understand the further work done during my thesis on the analogues studies of complex **2** with ammonia with the analysis of *in situ* IR, solid-state NMR spectroscopies and DFT Calculations.

The reaction of silica supported surface $\text{Ta}^{(\text{V})}$ complex $[(\equiv\text{SiO})_2\text{Ta}(=\text{NH})(\text{NH}_2)]$, **2** with D_2 at 60 °C for 3 hours leads to the formation of fully labeled $[(\equiv\text{SiO})_2\text{Ta}(=\text{ND})(\text{ND}_2)]$, **2-d** complex. Figure 2 shows the observed IR spectra of the starting tantalum hydrides **1** (a); their reaction with dinitrogen and dihydrogen at 250 °C for 2 days in order to obtain well-defined tantalum imido amido complex (b) and in the last spectrum after the addition of D_2 at 60 °C for 3 hours to yield the deuterated complex (c) monitored by *in situ* infrared spectroscopy.

The typical mode of residual unreacted surface silanols of the starting silica is found at 3740 cm^{-1} . Residual surface alkyls are in the $\nu(\text{CH}_x)$ region between 3000-2800 cm^{-1} . The most intense and diagnostic band displaying $\nu(\text{TaH}_x)$ is around 1850 cm^{-1} (Figure 2-a). The decrease of $\nu(\text{TaH}_x)$ peak and appearance of the new peaks in N-H region (3530-3330 cm^{-1}) corresponding to the stretching modes ($\nu(\text{NH}_x)$) of the tantalum imido amido complex are at 3500, 3462 and 3374 cm^{-1} in addition to the bending modes at 1551 and 1521 cm^{-1} for $\delta(\text{NH}_2)$ as already described elsewhere (Figure 2-b).^[33] Addition of a large excess of D_2 to the reaction vessel with respect to the grafted tantalum shows H/ D exchange of the complex and leads to the deuterated complex $[(\equiv\text{SiO})_2\text{Ta}(=\text{ND})(\text{ND}_2)]$, **2-d**. The exchange reaction occurs already at room temperature but is accelerated by heating at 60 °C (Figure 2-c). All the observed isotopic shifts are in good agreement with literature precedents of the **2-d** complex presenting the bands at 2760 cm^{-1} for the deuterated residual silanols $\nu(\text{Si-OD})$ and at 2600, 2580, 2522 and 2475 cm^{-1} for $[(\equiv\text{SiO})_2\text{Ta}(=\text{ND})(\text{ND}_2)]$ species.^[33]

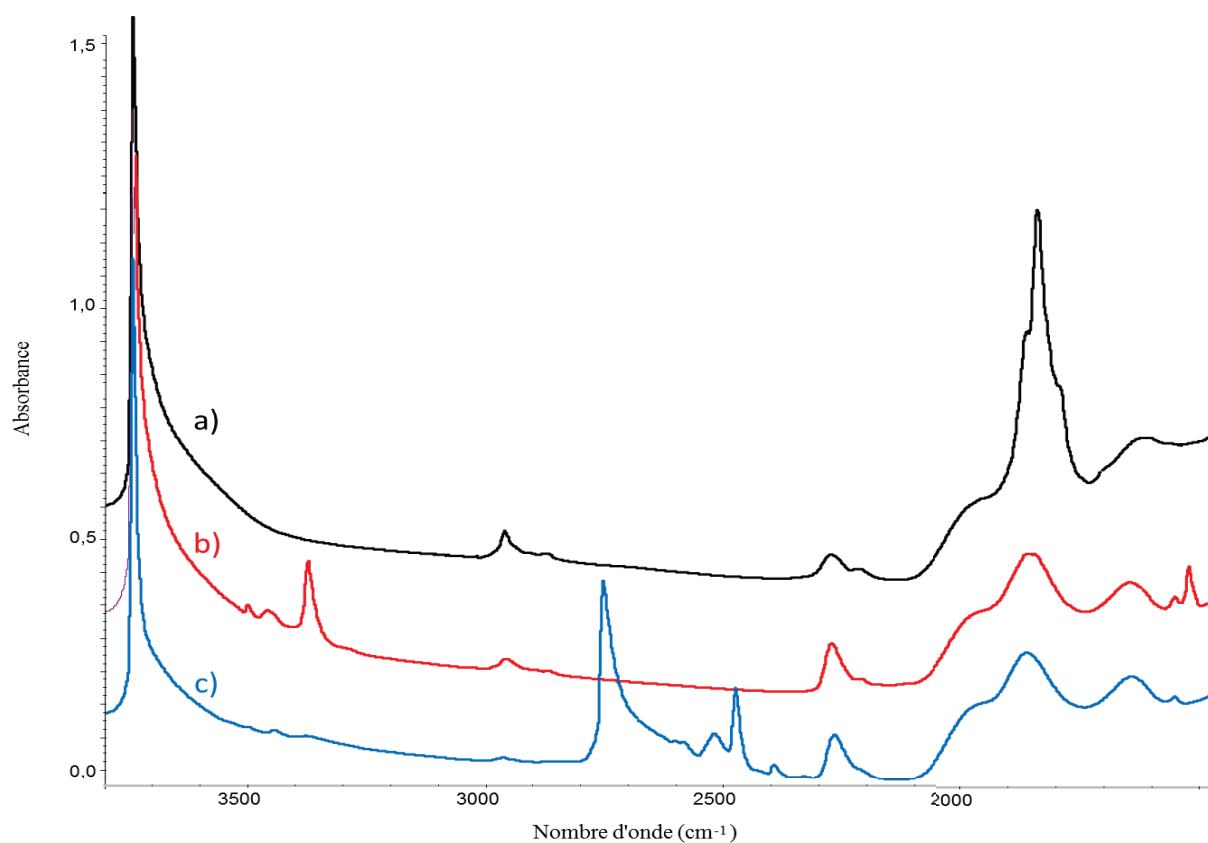


Figure 2: IR spectra of (a) starting silica grafted $[(\equiv\text{SiO})_2\text{TaH}_x \text{ (x:1,3)}]$; (b) $[(\equiv\text{SiO})_2\text{Ta(=NH)(NH}_2)]$ obtained by addition of N_2 and H_2 at $250\text{ }^\circ\text{C}$ in 2 days; (c) after addition of D_2 (550 Torr, 3 hours at $60\text{ }^\circ\text{C}$) to previous sample leading to the fully deuterated complex **2-d**.

Table 2 displays the observed and calculated IR frequencies (cm^{-1}) upon exposure of silica-supported tantalum hydrides **1** to N_2 and H_2 leading complex **2** at $250\text{ }^\circ\text{C}$ 2 days and after H/D exchange yielding respectively to the deuterated compound, **2-d**.

Table 2: Observed and calculated IR frequencies (cm⁻¹) for complex **2 (from N₂ and H₂ at 250 °C) and **2-d**.**

Starting frequencies for 2 (cm ⁻¹)	Observed shifted frequencies in 2-d by D ₂ addition ^b , (cm ⁻¹)	Expected shifted frequencies ^a (cm ⁻¹)	Proposed assignment
3500	2597	2556	vTa(NH ₂)
3462	2578	2528	vTa(=NH)
3449	2525	2519	vSi(NH ₂)
3374	2474	2468	vTa(NH ₂)
3293	2422	2405	vTa(NH ₃)
1606	— ^c	1173 ^c	vTa(NH ₃)
1551	— ^c	1132 ^c	δSi(NH ₂)
1521	— ^c	1110 ^c	δTa(NH ₂)

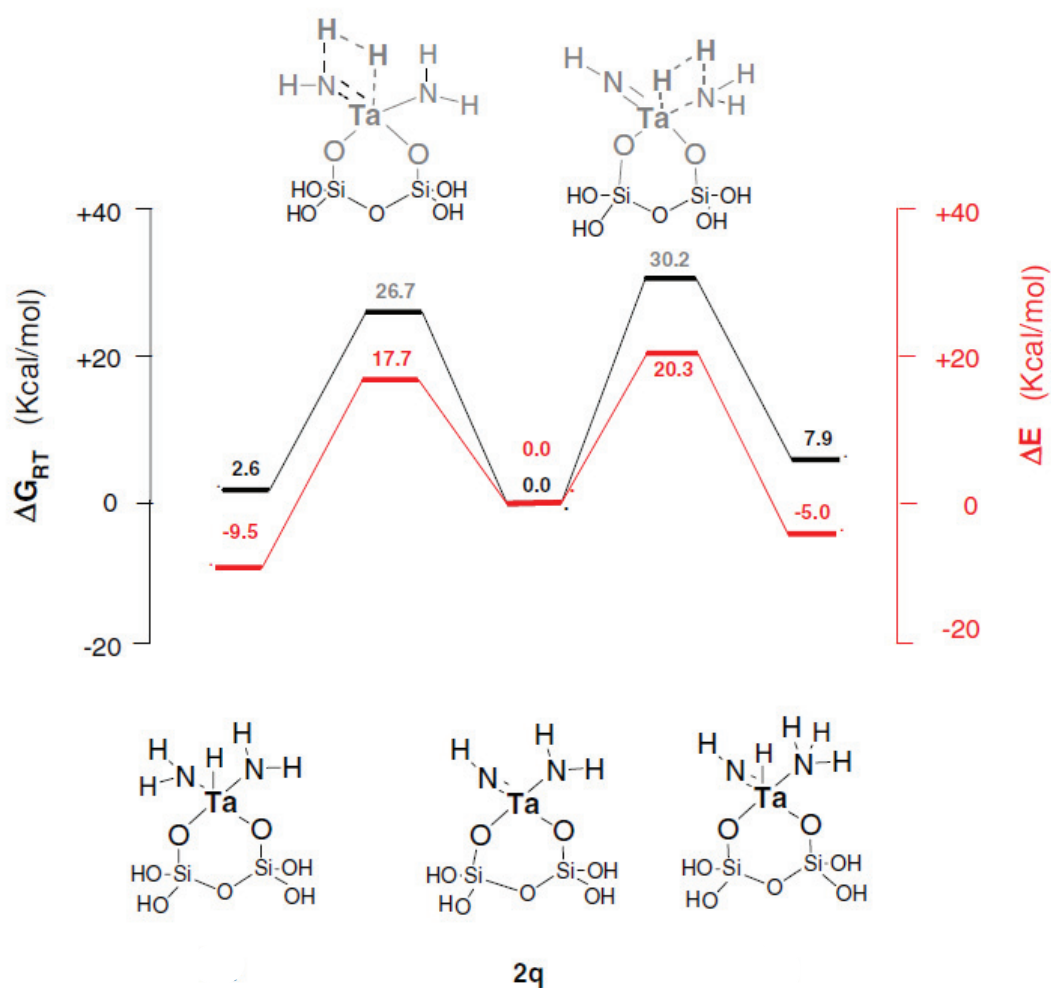
^a Using the spring model and the reduced mass approximation

^b Obtained by the reaction of D₂ at 60 °C on [(≡SiO)₂Ta(=NH)(NH₂)]

^c The band cannot be observed in the accessible spectral window of silica.

DFT studies on **2q** model, [(-SiO)₂Ta(=NH)(NH₂)] show the energetically preferred pathways for the reaction of H₂ involving heterolytic cleavage of this molecule, with the transfer of the hydride to the metal and concomitant protonation of the imido and amido ligands (Scheme 9).

The resulting two products are [(-SiO)₂TaH(NH₂)₂] and [(-SiO)₂TaH(NH)(NH₃)]. The transition states show the addition of the two hydrogen atoms to **2q** by heterolytic splitting of H₂ where a proton transfer between an hydride, close to Ta, and a negatively charged N atom occurs. The reverse reaction of α-H dihydrogen elimination from the amido in the bisamidohydride or ammonia in the imidoamidohydride leads to the regeneration of the starting imido amido complex **2q**. If this sequence of steps occurs with D₂, it scrambles H/D and forms **2-d**, as observed experimentally. A very similar mechanism has been already proposed for some other molecular d⁰ early-transition metal or lanthanide complexes and more recently for analogous d⁰ silica supported metal hydrides.^[56, 57] The two processes are exoenergetic (see Scheme 9): the bisamidohydride and imidoamidohydride are, respectively, -9.5 and -5.0 kcal mol⁻¹ more stable than the starting imido amido complex **2q**, showing that the loss of a H–H σ-bond and a π-Ta-N interaction is outweighed by the formation of a N–H and a Ta–H σ-bonds.



Scheme 9: Potential (black) and Gibbs free (red) energies of the reaction for H₂ with **2q** leading to the heterolytic splitting of H₂ on either imido or amido bond.

The two processes present moderate energy barriers (ΔE^\ddagger are 17.7 and 20.3 kcal mol⁻¹ and ΔG^\ddagger are 26.7 and 30.2 kcal mol⁻¹) in agreement with the need of heating to experimentally observe the full H/D exchange (*vide supra*). In the two accessible pathways for the heterolytic splitting of H₂, attack to the imido group appears easier than attack on the amido group, both from a kinetic and a thermodynamic point of view, but the difference does not seem very pronounced. The impossibility of oxidative addition of H₂ to the tantalum center, which is formally a d⁰ center, has finally been checked computationally.

II. 2. Reaction of $[(\equiv\text{SiO})_2\text{Ta}(=\text{NH})(\text{NH}_2)]$ with ammonia :

II.2.1 Spectroscopic studies of NH_3 activation on $[(\equiv\text{SiO})_2\text{Ta}(=\text{NH})(\text{NH}_2)]$, **2**

The reaction of ammonia was monitored by *in situ* IR spectroscopy in order to explore its reaction with the surface imido amido tantalum(v) complex, **2** on a self-supporting pellet as given in Figure 3 below:

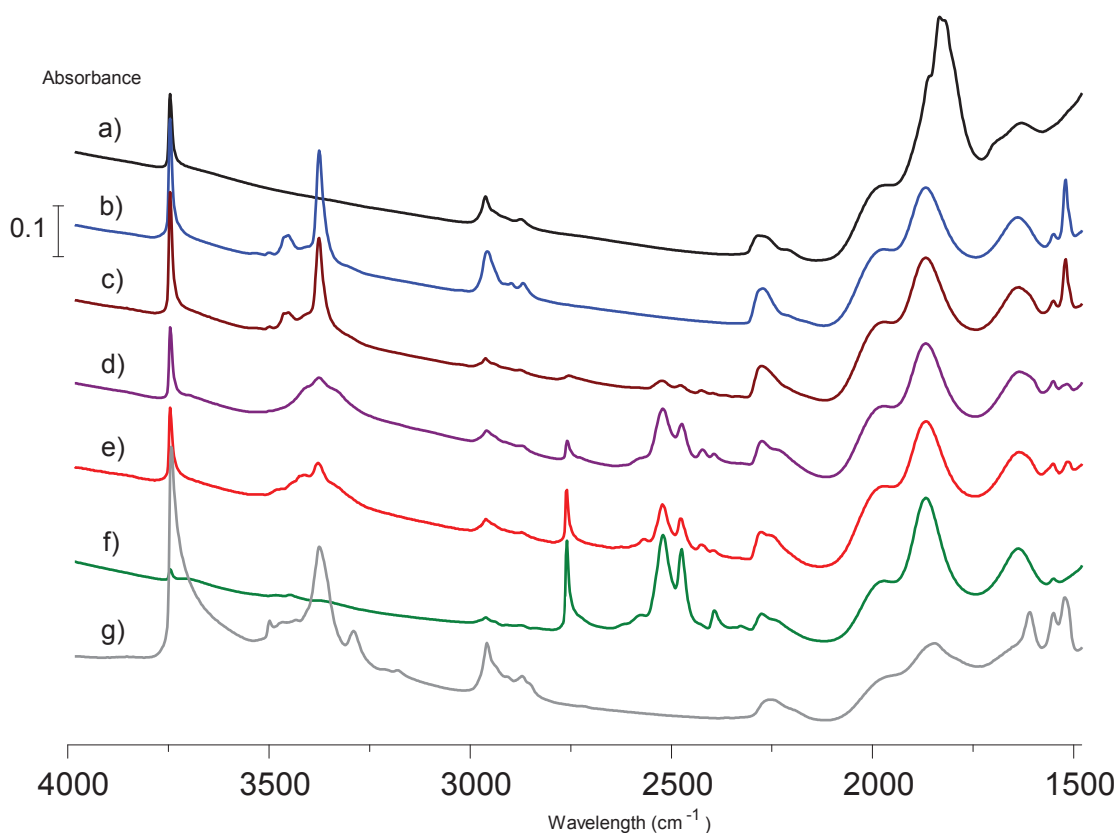


Figure 3: IR spectra of a) starting tantalum hydrides, $[(\equiv\text{SiO})_2\text{TaH}]$, **1a** and $[(\equiv\text{SiO})_2\text{TaH}_3]$, **1b**; b) $[(\equiv\text{SiO})_2\text{Ta}(=\text{NH})(-\text{NH}_2)]$, **2**, resulting after reaction of **1a** and **1b**, with N_2 and H_2 at 250°C , (1:1, $P_{\text{tot}} = 550$ torr, 72h); c) addition of ND_3 (1 Torr, RT, 5 min) to previous sample d) further addition of ND_3 (5 torr, RT, 5 min), e) heating at 150°C during 2 days, f) addition of ND_3 (200 torr, RT, 5 min) – spectrum collected while condensing the gas phase-, and, for comparison, (g) $[(\equiv\text{SiO})_2\text{Ta}(=\text{NH})(-\text{NH}_2)]$, **2**, and $\mathbf{2}\cdot\text{NH}_3$, obtained independently from reaction of another self-supporting pellet of $[(\equiv\text{SiO})_2\text{TaH}]$, **1a**, and $[(\equiv\text{SiO})_2\text{TaH}_3]$, **1b**, with NH_3 (5 Torr, RT, 10 min).

The spectrum of $[(\equiv\text{SiO})_2\text{Ta}(=\text{NH})(\text{NH}_2)]$, **2**, obtained from dinitrogen and dihydrogen from starting dihydrides shows very little deuteration under ND_3 atmosphere (1 Torr, *ca.* 1 eq. NH_3/Ta), as shown in the $\nu(\text{ND}_x)$ area of spectrum c in Figure 4. Addition of 4 eq. ND_3 immediately shows the broadening and overall intensity decrease of $\nu(\text{NH}_x)$ bands (spectrum d). The presence of new bands in the $\nu(\text{ND}_x)$ region, in agreement with the previous assignments for $[(\equiv\text{SiO})_2\text{Ta}(=\text{ND})(-\text{ND}_2)]$, **2-d**, $[(\equiv\text{SiO})_2\text{Ta}(=\text{ND})(-\text{ND}_2)(\text{ND}_3)]$, **2-d·ND₃**, $[\equiv\text{Si-ND}_3]$ and possibly mixed H/D amido amino compounds.^[33] As already observed for the direct reaction of the starting tantalum hydrides with ND_3 ,^[33] the NH_x/ND_x exchange is also accompanied by deuteration of residual surface silanols $[\equiv\text{SiOH}]$, and appearance of the $\nu(\text{OD})$ stretching mode at 2759 cm^{-1} . Treatment at $150\text{ }^\circ\text{C}$ and evacuation of the gas phase does not induce further substantial changes in the extent of deuteration (spectrum e). Addition of very large excess of ND_3 (200 Torr, 200 eq.) is necessary to achieve complete deuteration of all the NH_x bond (see spectrum f, recorded while condensing the gas phase in a cold spot to remove excess physisorbed ammonia to reduce extensive broadening of the peaks). For comparison, the spectrum of fully protonated $[(\equiv\text{SiO})_2\text{Ta}(=\text{NH})(-\text{NH}_2)]$, **2**, $[(\equiv\text{SiO})_2\text{Ta}(=\text{NH})(-\text{NH}_2)(\text{NH}_3)]$, **2·NH₃**, obtained directly from Ta(III) and Ta(V) hydrides $[(\equiv\text{SiO})_2\text{TaH}]$ and $[(\equiv\text{SiO})_2\text{TaH}_3]$ with reaction with regular NH_3 at room temperature is also reported (spectrum g).

A complementary IR monitoring experiment was performed by addition of NH_3 to a deuterium containing sample of $[(\equiv\text{SiO})_2\text{Ta}(=\text{ND})(-\text{ND}_2)]$, **2-d**, and showed the expected reverse isotopic shifts; that is: decrease of the $\nu(\text{ND}_x)$ and increase of the $\nu(\text{NH}_x)$ with appearance of $\delta(\text{NH}_2)$ and $\delta(\text{NH}_3)$ (Figure 4). Details of the experiments will be given in the experimental section.

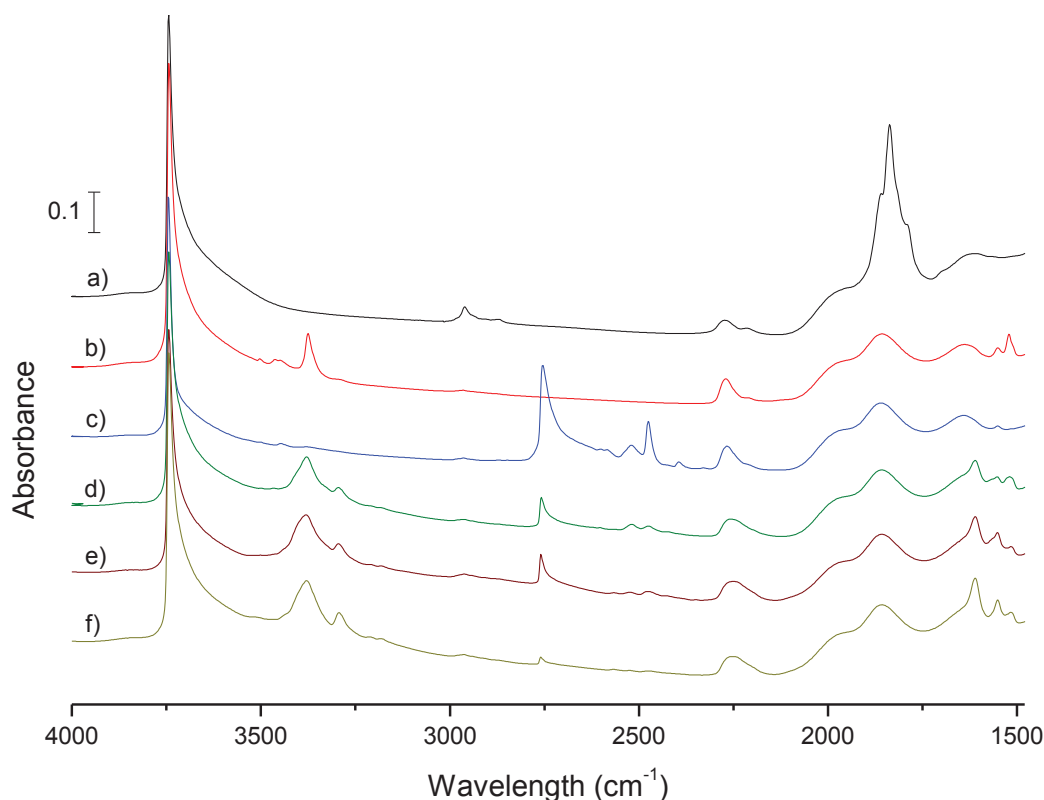


Figure 4: IR spectra of a) tantalum hydrides **1** ; b) addition of N₂/H₂ (1/1) (P_{tot} = 550 torr, 250°C, 72h) ; c) addition of large excess of D₂ (P = 550 torr, 150°C, 12h) ; d) addition of dry ammonia (5 torr) ; e) thermal treatment at 150°C ; f) second addition of dry ammonia (5 torr) condensed to the sample order by cooling the reactor in liquid nitrogen.

In order to study the reactivity of ammonia with the imido and amido bonds of [(≡SiO)₂Ta(=NH)(-NH₂)], **2**, we investigated by MAS solid-state nitrogen NMR spectroscopy a sample obtained by condensing ¹⁵NH₃ (*ca.* 3 equivalents per tantalum) stoichiometrically on loose powder of **2** prepared from ¹⁴N₂ and H₂, and hence with no starting coordinated ammonia on the tantalum. The gas-solid reaction is carried out at room temperature (4h). As shown in Figure 6, the ¹⁵N CP MAS NMR of the resulting product displays multiple ¹⁵N resonances which indicate that reactions other than simple NH₃ coordination and physisorption have occurred. In particular, the spectrum displays, beside both tantalum-coordinated and physisorbed ammonia (at -350 and -390 ppm respectively), intense ¹⁵N resonances attributed to [(≡SiO)₂Ta(=¹⁵NH)(-¹⁵NH₂)], **2***, **2*·NH₃** and [≡Si-¹⁵NH₂] (at -83, -273 and -400 ppm, respectively).^[34] The presence of [≡Si-¹⁵NH₂] is consistent with the known Ta-assisted reaction of surface silanes [≡SiH], coproduct of **1a** and **1b**,^[58] with ammonia. The

intensity of 2^* resonances indicates that extensive activation of ^{15}N -H bonds of ammonia has occurred, to lead to 2^* or mixed $^{14}\text{N}/^{15}\text{N}$ analogues. For comparison, the spectra of the ^{15}N -labelled sample 2^* obtained from the reaction of $[(\equiv\text{SiO})_2\text{TaH}]$, **1a**, and $[(\equiv\text{SiO})_2\text{TaH}_3]$, **1b**, with $^{15}\text{N}_2$ and with $^{15}\text{NH}_3$ recorded under similar acquisition conditions are also reported below.

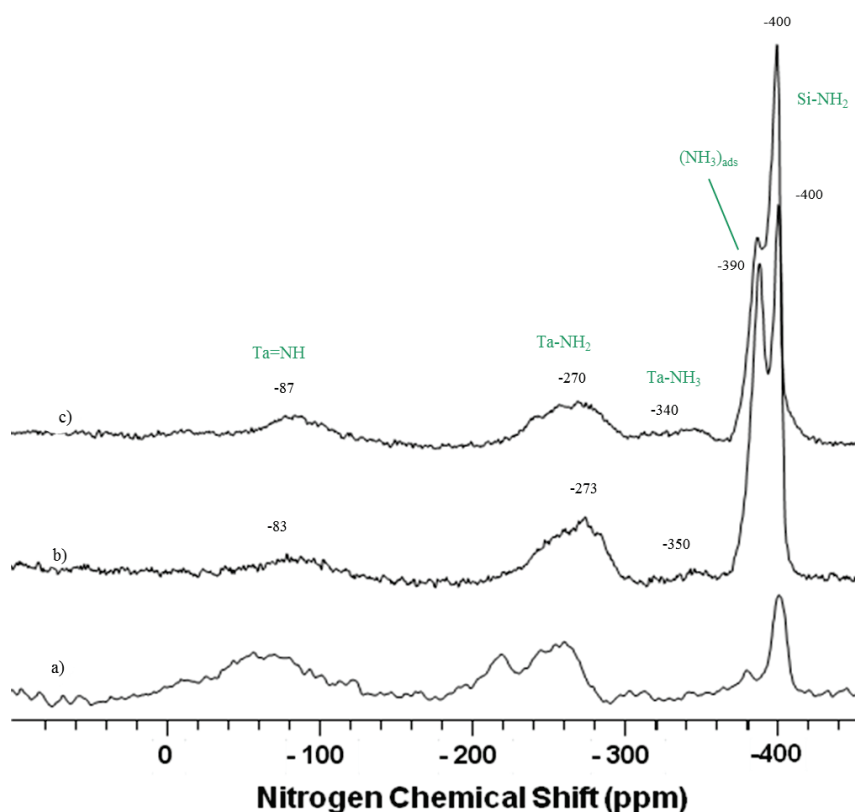


Figure 5: ^{15}N CP MAS NMR spectra (a) ^{15}N labelled sample $[(\equiv\text{SiO})_2\text{Ta}(=^{15}\text{NH})(-^{15}\text{NH}_2)]$, 2^* , obtained directly from reaction of tantalum hydrides, **1**, with $^{15}\text{N}_2$ and H_2 at $250\text{ }^\circ\text{C}$ [NS = 50000, d1 = 4 sec, p15 = 5 msec, LB = 300 Hz]; (b) the product resulting from the room temperature reaction of $^{15}\text{NH}_3$ with $[(\equiv\text{SiO})_2\text{Ta}(=\text{NH})(-\text{NH}_2)]$, **2**, previously obtained from $^{14}\text{N}_2$ and H_2 [NS = 2100, d1 = 1 sec, p15 = 5 msec, LB = 50 Hz]; and (c) the product obtained after direct ammonia $^{15}\text{NH}_3$ addition to of **1a** and **1b** hydrides [NS = 4000, d1 = 16 sec, p15 = 5 msec, LB = 50 Hz].

The NMR and IR results reported above show that ammonia N-H bond is activated at room temperature by the grafted tantalum complex **2**, leading to proton exchanges between all the available N-H bonds of the surface species.

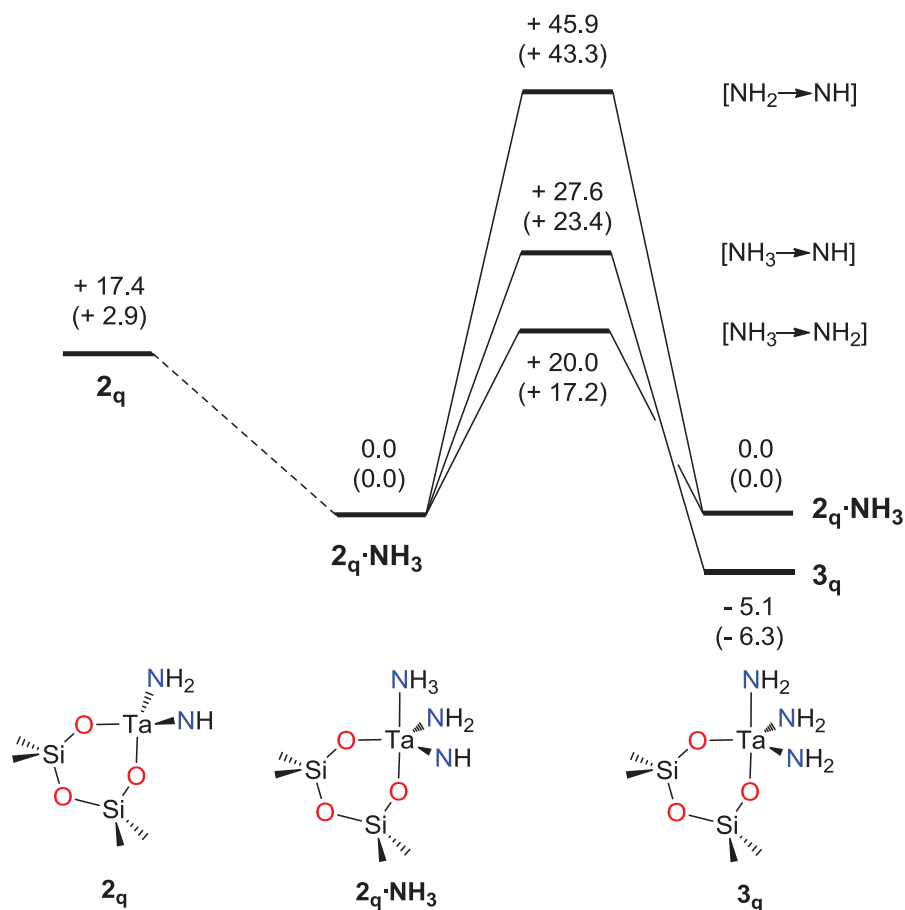
II.2.2 Computational and Experimental Studies of NH₃ activation on Complex 2

a) H₂ scrambling in [(≡SiO)₂Ta(=NH)(-NH₂)(NH₃)]

DFT (B3PW91) calculations have been performed by *Odile Eisenstein* and *Xavier Solans-Monfort* on the previously mentioned **2_q** model complex (-SiO)₂Ta(=NH)(-NH₂) in order to investigate an energetically feasible reaction mechanism for ammonia N-H cleavage by [(≡SiO)₂Ta(=NH)(-NH₂)], **2**. The addition of a NH₃ molecule leading to **2_q·NH₃** is exoenergetic ($\Delta E = -17.4 \text{ kcal mol}^{-1}$) and it makes the process favorable and changes the Ta coordination. Therefore, present calculations agree with the experimental simultaneous detection of **2** and **2·NH₃** when NH₃ is present in the system.

As already seen for H-H heterolytic splitting by (-SiO)₂Ta(=NH)(-NH₂), **2_q**,^[55] scheme 10 show that intramolecular H-transfer from the amido ligand to imido NH ligand needs a very high energy barrier (47.8 kcal mol⁻¹). This suggests the process forbidden at room temperature. Therefore, the mechanism for the observed H/D scrambling implicates coordinated ND₃ and either of the other two ligands. Scheme 10 summarizes the relative computed energies of all considered paths for H-transfer from coordinated ammonia of **2_q·NH₃**, considered as the zero energy level, and the relative transition states.

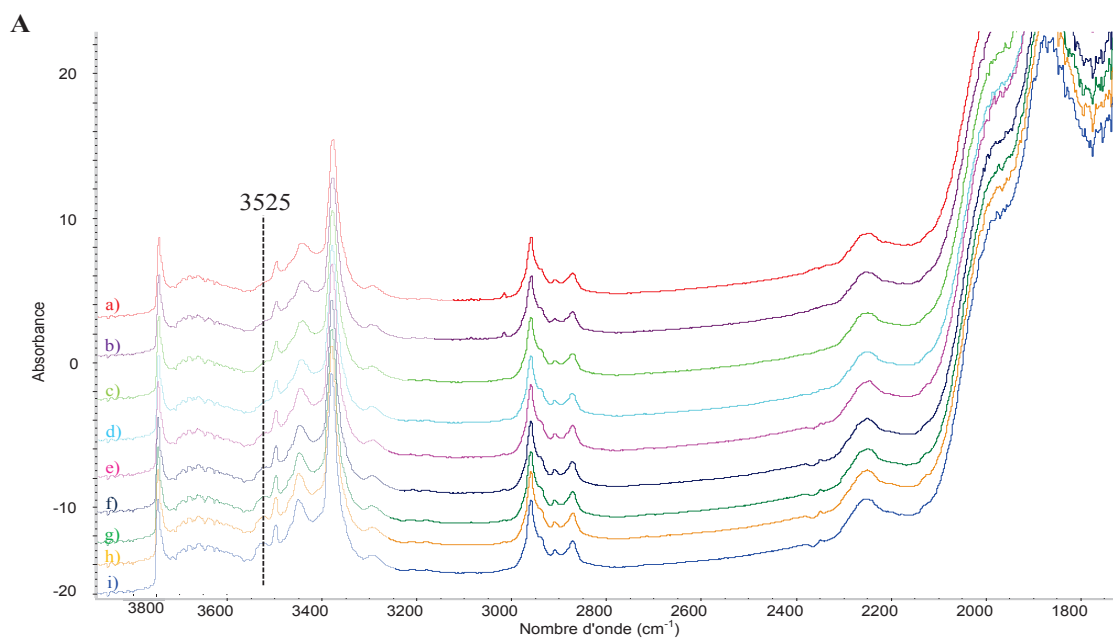
The H-transfer between NH₃ and NH₂ leads to an equivalent **2_q·NH₃** species through an energy barrier of 20.0 kcal mol⁻¹. The H-transfer between NH₃ and NH leads to the tautomer tris-amino complex (SiO)₂Ta(-NH₂)₃ (**3_q**) with slightly higher energy barrier ($\Delta E^\ddagger = 27.6 \text{ kcal mol}^{-1}$). Trisamino complex **3_q** is computed 5.1 kcal mol⁻¹ lower in energy than **2_q·NH₃** which is consistent with the formation of three σ -bonds.



Scheme 10: Potential energies and Gibbs energies in parenthesis (kcal mol^{-1}) for the H-transfer paths for $(-SiO)_2Ta(=NH)(-NH_2)(NH_3)$, $2q \cdot NH_3$: i) from the amido to the imido ligands, $[NH_2 \rightarrow NH]$, ii) from the coordinated ammonia to the imido ligand $[NH_3 \rightarrow NH]$, and iii) from coordinated the ammonia to the amido ligand, $[NH_3 \rightarrow NH_2]$. The first and last transfers regenerate $2q \cdot NH_3$. The second transfer gives a tautomer $(-SiO)_2Ta(-NH_2)_3$, $3q$.

b) Observation of tris-amido tantalum complex $[(\equiv SiO)_2Ta(-NH_2)_3]$, **3**

The tris-amido complex $[(\equiv SiO)_2Ta(-NH_2)_3]$, **3** was experimentally observed by IR spectroscopy through the utilization of a high pressure reaction chamber IR DRIFT with low/high temperature controller (see Annex of Chapter II).



B

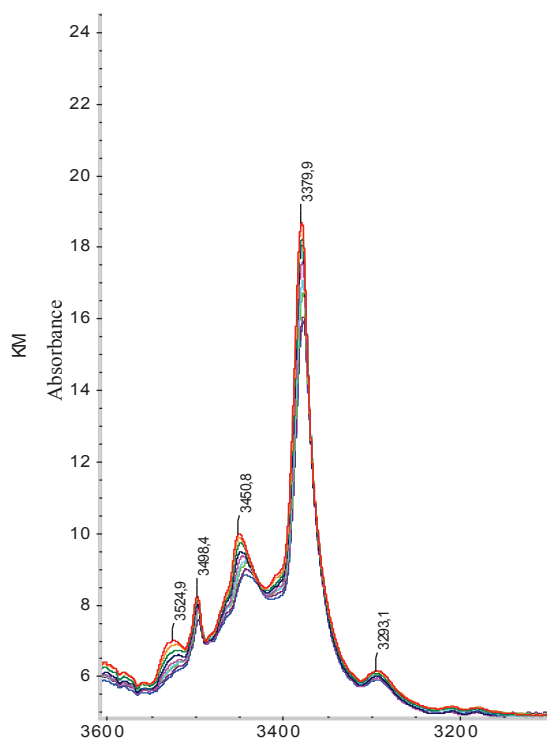


Figure 6: **A-** Spectra of the tantalum imido amido complex under argon at different temperatures: a) starting from room temperature; b) after 5h at room temperature; c) cooling to 0 °C; d) -25 °C; e) -50 °C; f) -80 °C; g) -100 °C; h) -125 °C; i) -150 °C; **B-** $\nu(\text{NH}_x)$ region between 3550- 3200 cm^{-1} .

The stepwise monitoring of *in situ* infrared spectroscopy shows that complex **2** can survive under argon at room temperature and even after cooling at low temperatures $T \text{ } ^\circ\text{C} > -150 \text{ } ^\circ\text{C}$ in the reaction chamber for praying mantis. The appearance of a new peak around 3525 cm^{-1} is observed at $-150 \text{ } ^\circ\text{C}$ (Fig. 6-B); while other peaks in NH region increased their intensity.

Figure 7 below compares the IR spectrum of silica- supported $[(\equiv\text{SiO})_2\text{Ta}(=\text{NH})(-\text{NH}_2)(\text{NH}_3)]$ complex at room temperature and at -150°C under argon.

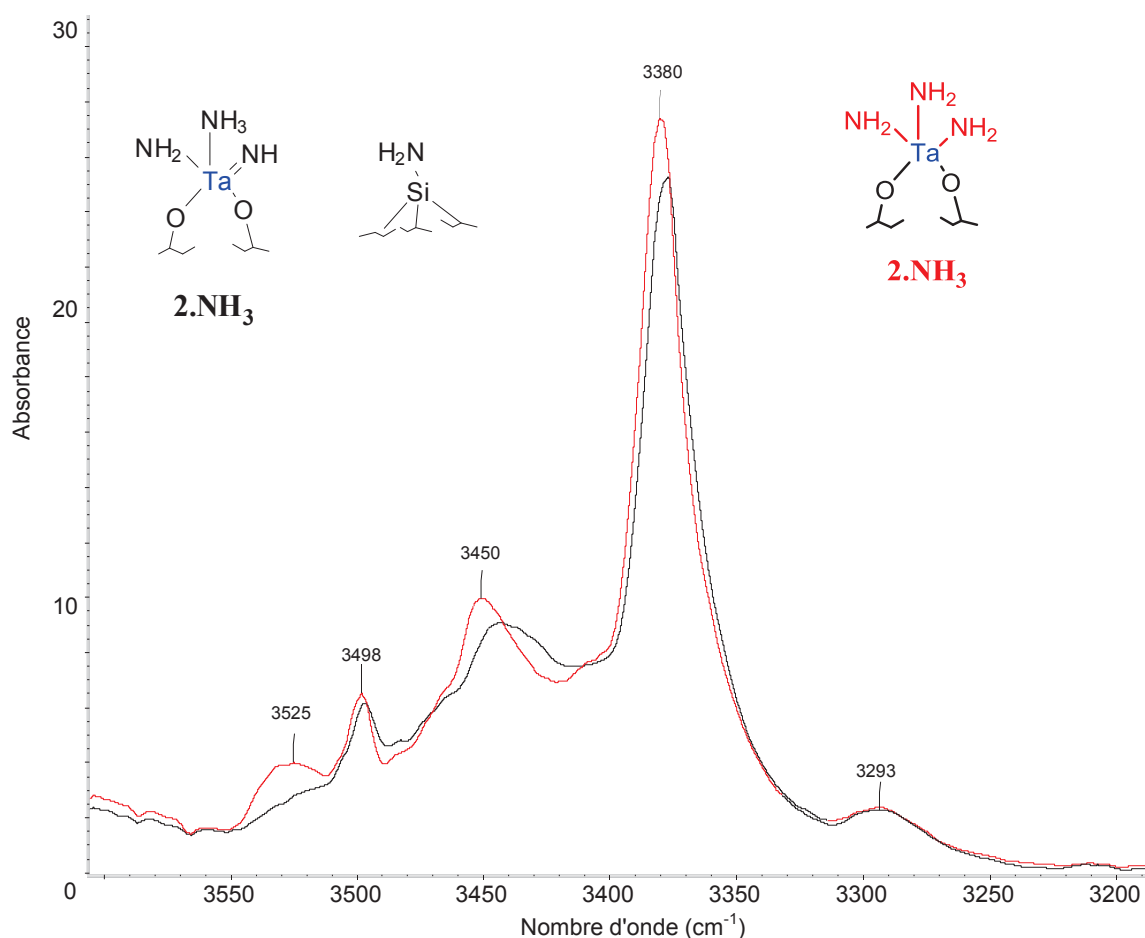


Figure 7: Zoom of the NH region ($3600\text{-}3200 \text{ cm}^{-1}$): $[(\equiv\text{SiO})_2\text{Ta}(=\text{NH})(-\text{NH}_2)(\text{NH}_3)]$ at room temperature under argon (black) and the same complex cooled at -150°C (red) under argon.

The spectra above compare the starting silica supported tantalum imido amido complex under argon at room temperature and after its treatment at $-150 \text{ } ^\circ\text{C}$ on the reaction chamber as described before. The new peak at 3525 cm^{-1} is observed starting from $-25 \text{ } ^\circ\text{C}$. Its intensity increased by decreasing the temperature and reached to a maximum value at $-150 \text{ } ^\circ\text{C}$. The peaks in NH region ($3498, 3451, 3380 \text{ cm}^{-1}$) are also increased by lowering the temperature.

This study appears to corroborate experimentally the existence of, $[(-\text{SiO})_2\text{Ta}(-\text{NH}_2)_3]$, **3**, a tris-amido tautomer, whose analogue **3q** has already been proposed by based DFT calculations.

Values from Scaled DFT calculations and *in situ* IR spectroscopy attributed to the silica supported tantalum tris-amido complex are given in Table 3.

Table 3: $\nu(\text{NH}_2)$ stretching frequencies of the model **3q** and experimentally observed peaks attributed to $[(\equiv\text{SiO})_2\text{Ta}(-\text{NH}_2)_3]$, **3**.

DFT (Scaled)	EXPERIMENTAL
[Intensity]	[Intensity]
NH ₂	NH ₂
3534, 3533	3525
[20, 15]	[35]
3492, 3425	3498
[18, 29]	[18]
3422, 3395	3450, 3380
[45, 46]	[74, 46]

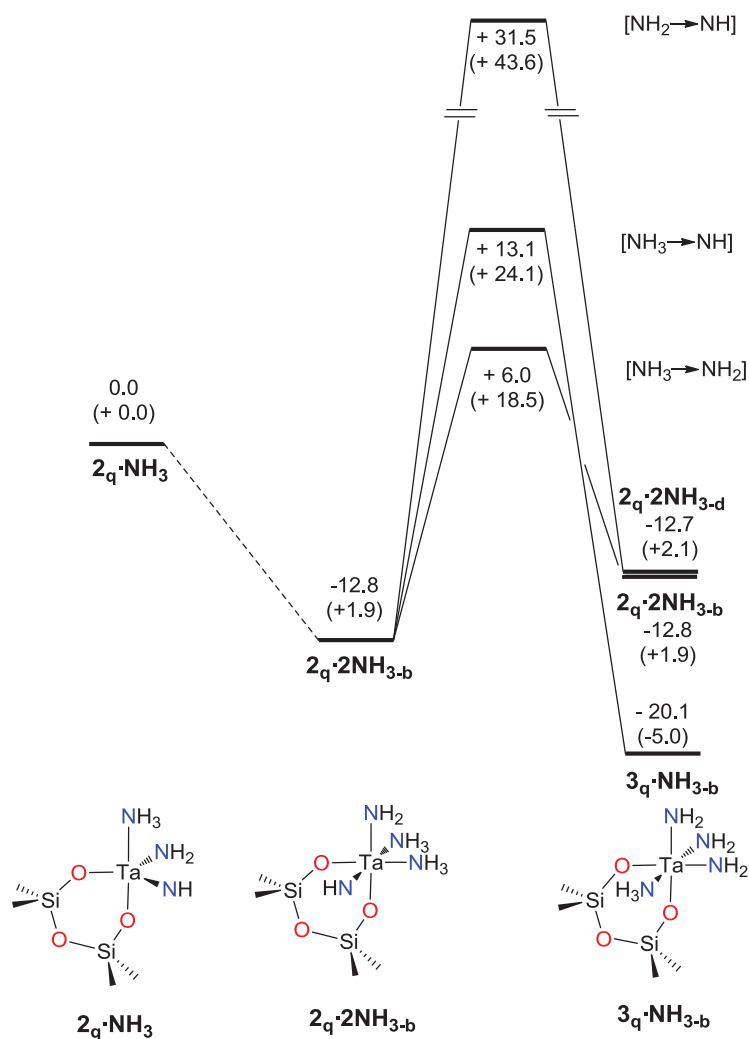
The higher complexity of the IR spectrum obtained after reaction of **1** with NH_3 compared with the IR spectrum obtained after reaction of **1** with $\text{N}_2 + \text{H}_2$, where no ammonia coordination is present (see Fig. 4, spectrum b and g) is consistent with this co-presence of tautomers **2**· NH_3 and **3**. Therefore, the comparison of the spectroscopic data and density functional theory calculations show a significant analogy to confirm the existence of tantalum tris-amido complex, $[(\equiv\text{SiO})_2\text{Ta}(-\text{NH}_2)_3]$, **3**.

c) The role of additional ammonia molecules on $[(\equiv\text{SiO})_2\text{Ta}(=\text{NH})(-\text{NH}_2)(\text{NH})_3]$

DFT calculations showed that ammonia can coordinate to the electron-poor metal center to form a bis-ammonia Ta^{V} amido imido complex. Coordination of one molecule of NH_3 to **2q**· NH_3 yields **2q**·**2NH₃** with an accesible energy under excess of NH_3 .

Three processes have been studied for **2q**· NH_3 ($[\text{NH}_2 \rightarrow \text{NH}]$, $[\text{NH}_3 \rightarrow \text{NH}_2]$ and $[\text{NH}_3 \rightarrow \text{NH}]$). The relative energies (E, G) of intermediates and transition states involved in the H transfer

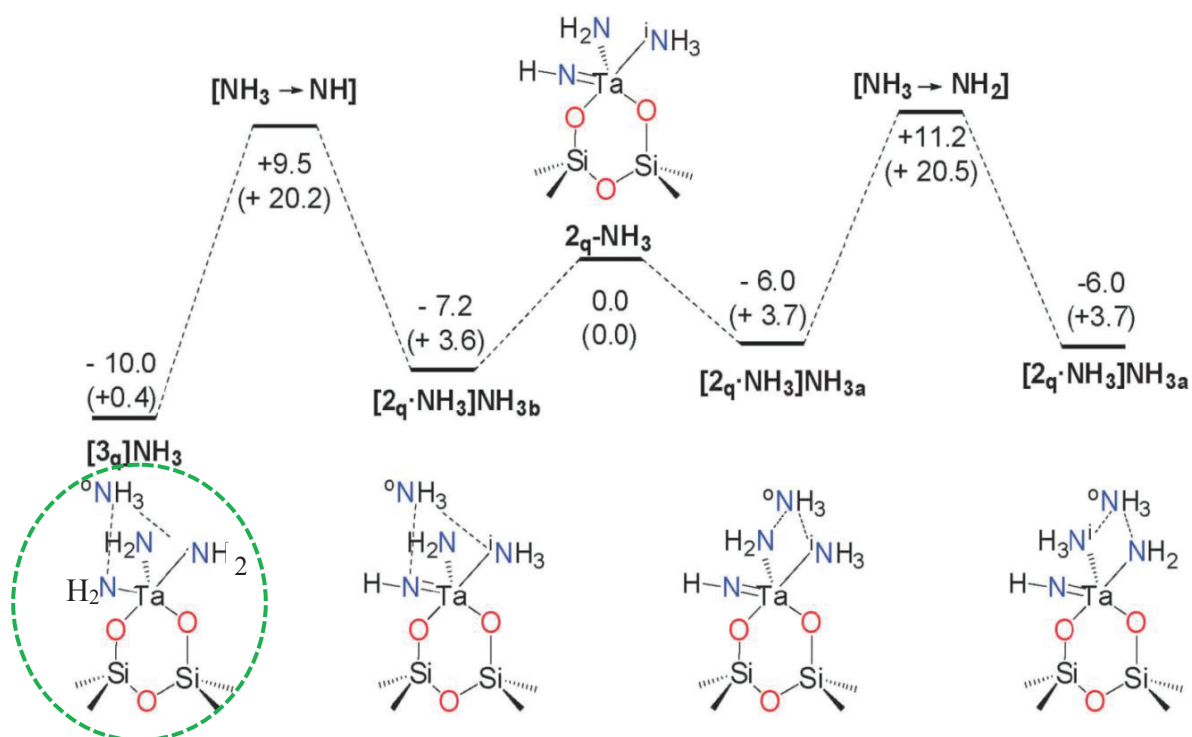
reactions starting from $2q \cdot 2NH_3$ are shown in Scheme 11. Noteworthy, the barriers are 18.8 kcal mol⁻¹ and 25.9 kcal mol⁻¹ for the $[NH_3 \rightarrow NH_2]$ and the $[NH_3 \rightarrow NH]$ H transfers, respectively, which indicates a decrease of the energy barrier by about 1-2 kcal mol⁻¹ when adding a second NH₃ molecule. Thus, the coordination of one additional ammonia molecule to the tantalum metal in the inner sphere does not significantly facilitate the H transfer.



Scheme 11: Potential energies and Gibbs energies in parenthesis (kcal mol⁻¹) for the H-transfer paths for $2q \cdot 2NH_3-b$ isomer: i) from the amido to the imido ligands $[NH_2 \rightarrow NH]$, ii) from the coordinated ammonia to the imido ligand $[NH_3 \rightarrow NH]$, and iii) from the coordinated ammonia to the amido ligand, $[NH_3 \rightarrow NH_2]$.

The calculations have been done also for two additional ammonia molecules. In this case, ammonia interacts with the ligands by H bonding without coordinating to the tantalum atom. The resulting effect on the proton transfer is representative of an “outer sphere assistance”.

The outer sphere ammonia, named $^o\text{NH}_3$, interacts with one of the hydrogens of the coordinated ammonia, named $^i\text{NH}_3$ and points one of its hydrogen towards either the amido or the imido ligand (Scheme 12). Overall, while the energy barrier for ammonia-amido exchange is only slightly lowered by the presence of an outer sphere ammonia, the energy barrier for the H transfer to the imido group is significantly lowered.



Scheme 12: Potential energies and Gibbs energies in parenthesis (kcal mol^{-1}) for the outer sphere assisted H-transfer paths for $2q \cdot \text{NH}_3$: i) from the coordinated ammonia to the imido ligand $[\text{NH}_3 \rightarrow \text{NH}]$, and ii) from the coordinated ammonia to the amido ligand, $[\text{NH}_3 \rightarrow \text{NH}_2]$. The complex containing the circle around is important as it shows the stronger donor imido group in apical position and stabilizes more the square pyramid geometry than the amido group.

In summary, it has been showed by experimental results that silica-supported Ta^{V} imido amido complex **2** coordinates ammonia and a dynamic exchange occurs between the various N bonded ligands which can be accounted by H transfers which exchange the ammonia, amido and imido groups. DFT Calculations supported by experimental evidence for the expected intermediate $[(\equiv\text{SiO})_2\text{Ta}(-\text{NH}_2)_3]$ showed that these H transfers are only energetically feasible when the proton donor is the coordinated ammonia and the proton

acceptor is the amido or the imido ligands. Moreover, additional NH₃ molecules assisting these processes decrease the energy barrier leading ammonia splitting a facile process.

II. 3. Mechanism of [(≡SiO)₂TaH_x (x: 1,3)] reaction with ammonia :

As discussed in the introduction, the reactivity of the surface Ta hydrides towards ammonia is rather singular in organometallic chemistry. The silica-supported tantalum hydride mixture [(≡SiO)₂TaH_x (x:1,3)], **1** is reacted stepwise with ammonia at room temperature to be able to see the intermediates during the reaction and to understand the mechanism of the N-H bond activation.

II.3.1 Spectroscopic studies of NH₃ activation on [(≡SiO)₂TaH_x (x: 1,3)], **1**

Figure 8 shows the evolution on IR spectra of silica-supported tantalum hydride pellet with successive addition of ammonia. Peaks at 3393, 3290, and 1610 cm⁻¹ appear and increase in intensity with each addition of NH₃; these are consistent with the presence of physisorbed ammonia on the pellet. Although subtracted spectra also reveal the consumption of the Ta-H band centered at 1830 cm⁻¹, only small increases in the bands corresponding to the imido amido species are seen until the final addition of (excess) NH₃. At this point the characteristic peak attributed to Ta-NH₂ at 1520 cm⁻¹ appears clearly, and the removal of coordinated ammonia under dynamic vacuum at 150 °C reveals that the Ta hydrides have been completely consumed and that the imido amido species has been formed (peaks at 3495, 3445, and 3375 cm⁻¹ in the ν(NH) region; 1520 cm⁻¹ in the δ(NH₂) region).

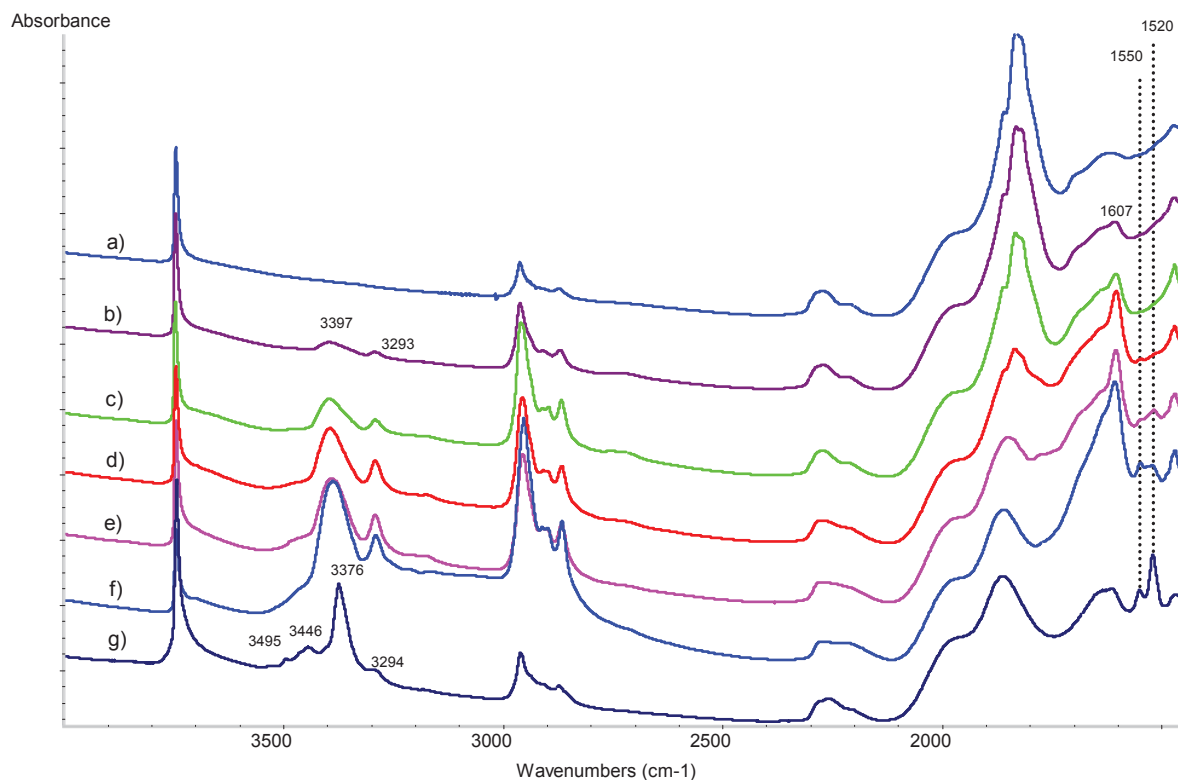


Figure 8: IR spectra: (a) Starting Ta hydrides; (b) after the first addition of NH_3 ; (c) after the second addition of NH_3 ; (d) after the third addition of NH_3 ; (e) after the fourth addition of NH_3 ; (f) after the final addition of NH_3 ; (g) after removal of coordinated NH_3 .

Subtractions between successive additions of NH_3 reveal that the initial decrease in the Ta-H peak is primarily observed at 1834 cm^{-1} ; these would therefore seem to be the most reactive hydrides assigned to the monohydride species. This species would therefore seem to be the most reactive towards coordinating ammonia (a proposition supported by DFT calculations; *vide infra*), though not necessarily towards cleaving N-H bonds. It is only in later additions that the hydrides at 1816 cm^{-1} appear to be consumed, while the hydrides at 1860 cm^{-1} seem to be consumed at a consistent rate throughout the course of the additions.

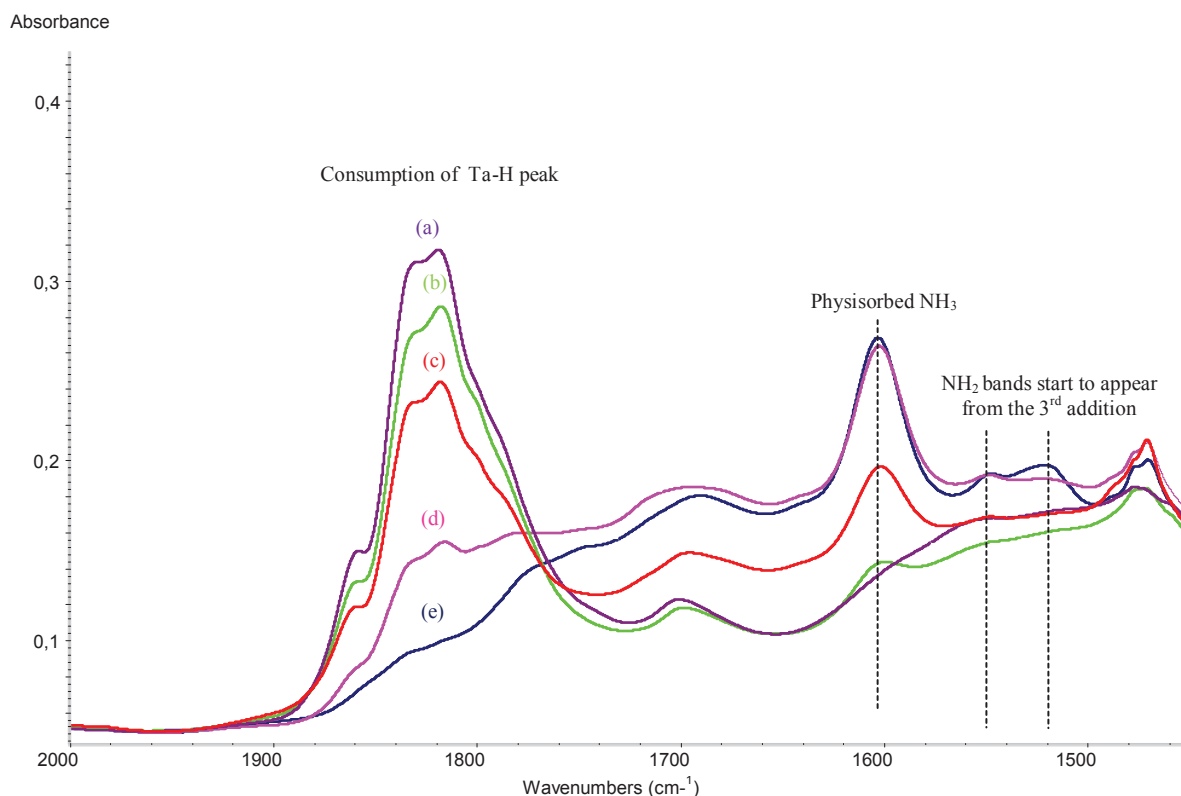


Figure 9: Zoom (2000-1450 cm⁻¹) on the $\nu(\text{TaH})$ and $\delta(\text{NH}_2)$ regions in the IR spectra of the pellet. (a): starting Ta hydrides; (b): after first NH_3 addition; (c): after second NH_3 addition; (d): after third NH_3 addition; (e): after fourth NH_3 addition

No increases in the expected region of $\nu(\text{TaH}_x)$ bands are observed during the course of the reaction (Figure 9). Thus, any hydride intermediates formed are either IR-invisible or do not display bands significantly different from the starting Ta hydrides. The gas phase was analyzed by GC before the final (excess) addition of ammonia. The chromatogram did show the presence of other gases (so H_2 evolution remains a possibility), although analysis is complicated by the fact that H_2 , neopentane, and ammonia may all be present in the gas phase. Quantification of the amount of H_2 evolved would not be reliable due to the small quantities detected.

In the following figure the differences of the peaks can be seen for the NH region between 3500 and 3250 cm⁻¹.

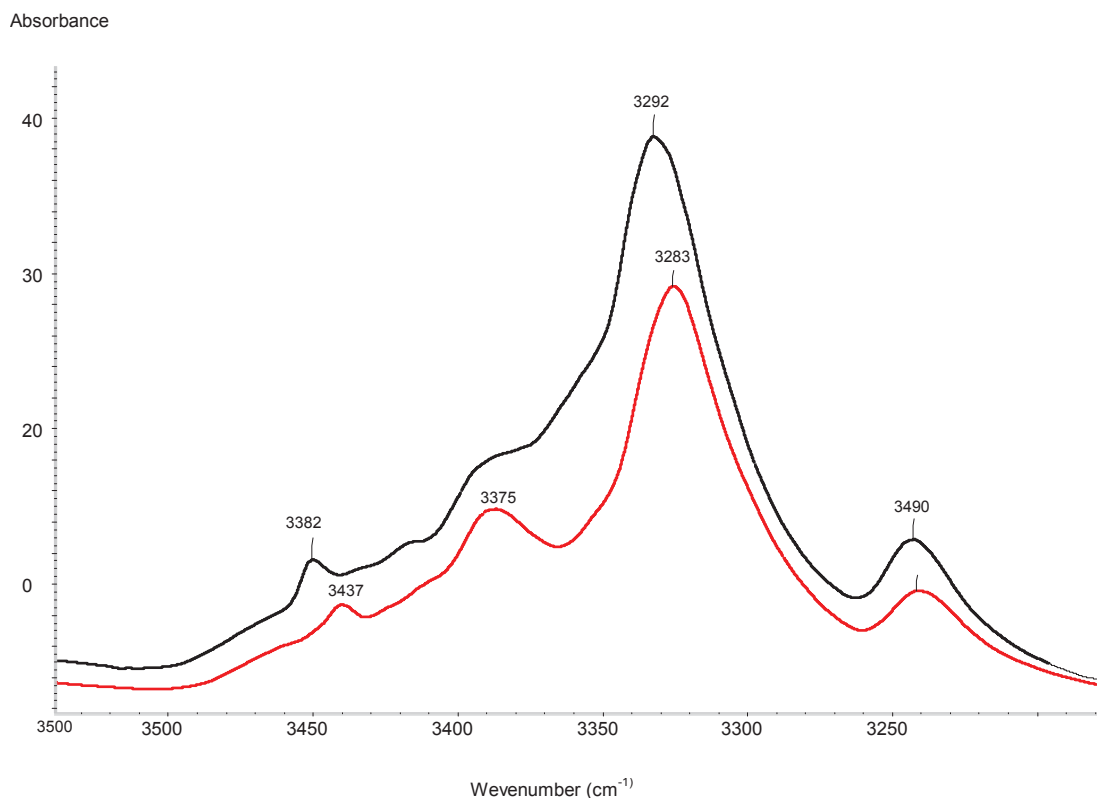
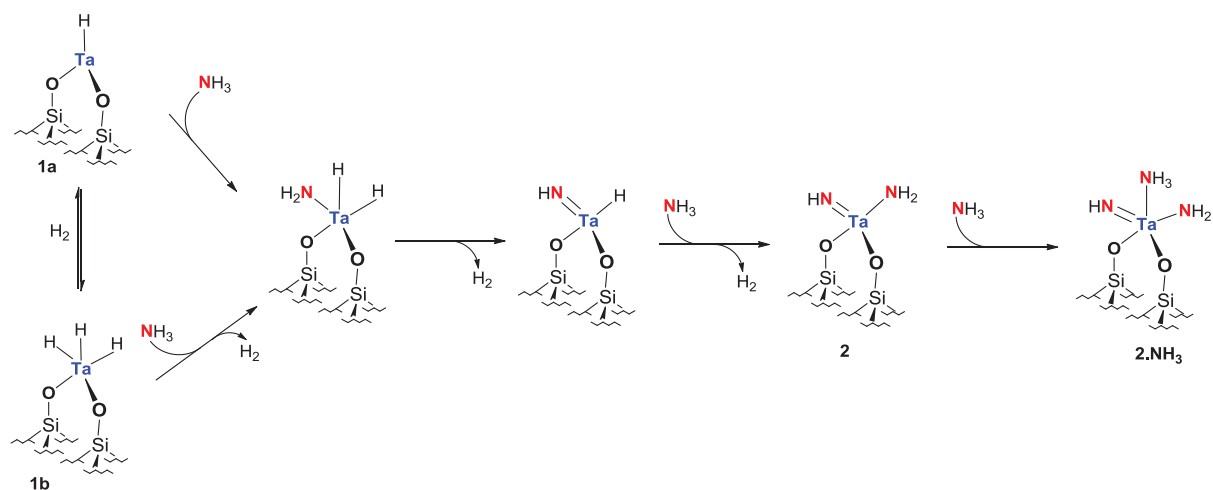


Figure 10: The zoomed NH region 3500-3250 cm⁻¹ showing the shift for the reaction of tantalum hydrides with labeled ¹⁵NH₃ ammonia (red line) comparing to the tantalum imido amido complex (black line).

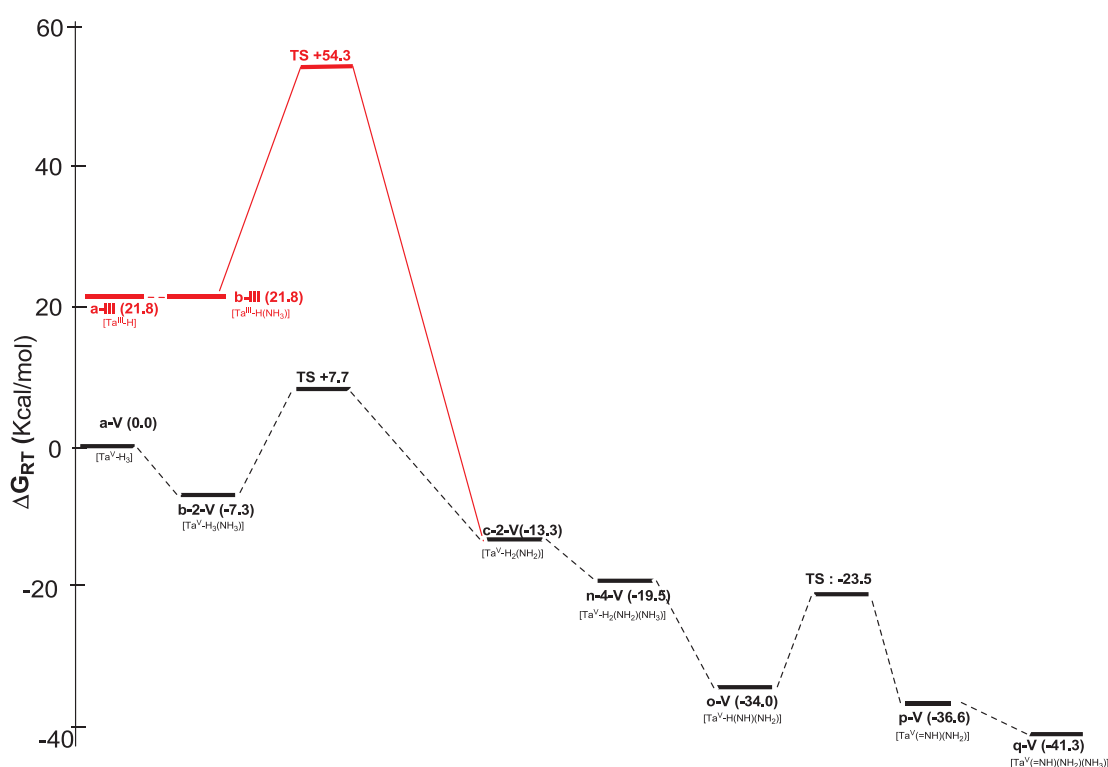
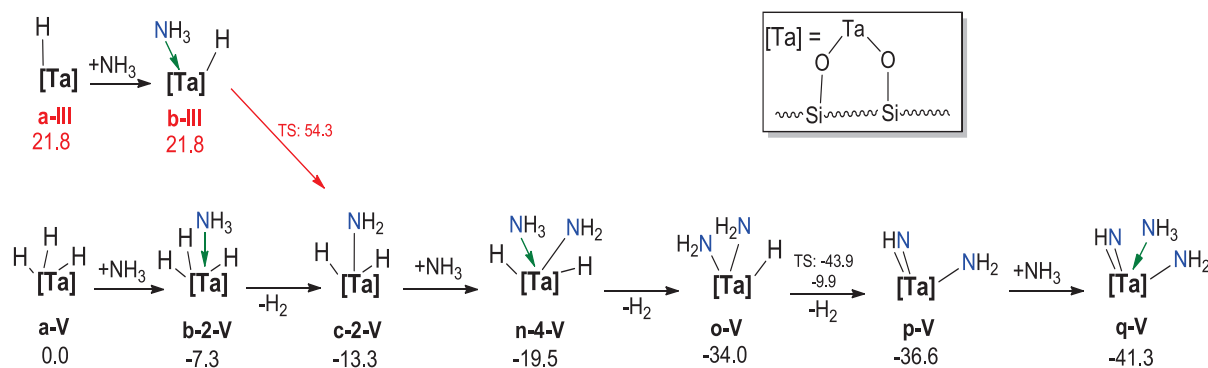
II.3.2 Computational Studies of NH₃ activation on [(≡SiO)₂TaH_x (x: 1,3)], 1

In 2007, our group reported the activation of ammonia by tantalum hydrides which gave the well-defined silica supported imido amido tantalum complexes that has been characterized by various methods such as *in situ* IR, solid state NMR and EXAFS.^[33] These analyses were not enough to understand the mechanism of the reaction; nevertheless, a route for this reaction was proposed according to the analogy to the methane activation with the same complex **1** (Scheme 13).



Scheme 13: Proposed elementary steps for the formation of well-defined tantalum imido amido complex in 2007 by our group.

Preliminary DFT calculations performed on the usual model system **2q** (Scheme 14) shows that coordination of ammonia to tantalum monohydrides doesn't change the energy level, while it is exothermic (-7.3 kcal/mol) in the case of tantalum trishydrides. Different steps corresponding to H₂ reductive coupling (i.e. the reverse step of H₂ heterolytic splitting that discussed earlier) and addition of stoichiometric ammonia gives the final imido amido complex [(≡SiO)₂Ta(=NH)(NH₂)], **2** while the excess of NH₃ gives the coordinated ammonia to the complex **2** as [(≡SiO)₂Ta(=NH)(NH₂)(NH₃)], **2.NH₃**. The fact that no IR bands attributable to NH₂ moieties are observed until the later additions of ammonia supports the hypothesis that the reaction proceeds through a pre-coordination of ammonia, whose N-H bonds are subsequently cleaved to form the imido amido species.



Scheme 14: DFT calculations of ΔG , free energy: red, for TaH₁ species and black, for TaH₃ species for the formation of the imido amido species from the reaction of Ta hydrides with ammonia.

Comparing the latest DFT calculations which have been done by *Xavier Solans-Monfort* to the proposed mechanism in 2007, we can see the details of the intermediates with precise energy levels and transition states during the reaction together with the steps of ammonia addition and dihydrogen dissociation in this system. Thus, a new route has been suggested which also fits well with the results observed by *in situ* infrared data. Nevertheless, no proposal is available for the reaction of ammonia with the tantalum monohydride. Therefore, more work is necessary to access the full mechanism.

III. CONCLUSION AND PERSPECTIVES

The present chapter has shown the reactivity properties of the well-defined silica supported tantalum imido amido complex **2** toward dihydrogen and ammonia. The first reactivity assay of **2** on dihydrogen demonstrates the easy D/H scrambling of both imido and amido ligands with mild heating by in-situ IR spectroscopy, while DFT calculations describes this N-based ligand deuteration via successive H₂ heterolytic cleavage either to the imido or to the amido ligands.

In the second part of our studies, ammonia reaction with the well-defined complex **2** was studied at room temperature with excess ammonia, but needed 150 °C heating when added stoichiometrically. DFT calculations on the model complex shows that the proton transfer from the coordinated ammonia to the adjacent basic ligated amido or imido N center has relatively high energy barrier even if it is thermodynamically accessible. These barriers can be lowered by an external (non-coordinated) ammonia molecule which transfers the proton more easily by the heterolytic cleavage of ammonia N-H bond through addition to a polar metal-N bond. Experimentally, we also observed the presence of tantalum tris-amido species [(≡SiO)₂Ta(NH₂)₃] by comparison of IR spectroscopy of the low temperature spectrum with the calculated DFT peaks for this intermediate.

The last results explained in this chapter give a possible route for the mechanism of the formation of well-defined imido amido complex from the reaction of tantalum trishydride and ammonia that imply once more bifunctional heterolytic elementary steps.

In conclusion, these results present the possible stoichiometric and catalytic activation of N–H bond by using ammonia as a precursor, which is important for N1 chemistry. It also highlights the kinetic difficulties of intramolecular proton transfers and the need of assistance by an outside molecule which makes the proton transfer an intermolecular process. The emergence of surface organometallic chemistry dealing with transition-metal imido amido species from ammonia can be contribute to the emergence of N1-based chemistry and catalysis from ammonia as feedstock in the future given the central role played by transition metal imido and amido moieties as key catalytic intermediates in N-transfer homogenous reaction.

IV. EXPERIMENTAL PART

General Procedure:

All experiments were carried out by using standard air-free methodology in an argon-filled Vacuum Atmospheres glovebox, on a Schlenk line, or in a Schlenk-type apparatus interfaced to a high-vacuum line (10^{-5} Torr). $[\text{Ta}(\text{CH}_2\text{C}(\text{CH}_3)_3)_3(=\text{CHC}(\text{CH}_3)_3)]$ was prepared by the reaction of TaCl_5 (Strem) with $t\text{Bu-CH}_2\text{MgCl}$ according to literature procedure.^[60] $\text{Bu-CH}_2\text{MgCl}$ was prepared from $t\text{BuCH}_2\text{MgCl}$ (98%, Aldrich, used as received) and Mg turnings (Lancaster). MCM-41 mesoporous silica was supplied by the Laboratoire des Matériaux Minéraux, E.N.S. de Chimie Mulhouse, 3 rue Alfred Werner, 68093 Mulhouse Cédex, France. It was prepared according to literature method.^[61] Its BET surface area, determined by nitrogen adsorption at 77K, is $1060 \text{ m}^2/\text{g}$ with a mean pore diameter of 28 \AA (BJH method). The wall thickness was found to be 14 \AA by subtraction of the pore diameter from the unit cell parameter deduced from X-ray powder diffraction data. MCM-41 supported tantalum hydrides $[(\equiv\text{SiO})_2\text{TaH}]$, **1a**, and $[(\equiv\text{SiO})_2\text{TaH}_3]$, **1b**, were prepared by impregnation in pentane or by sublimation for *in situ* IR monitoring as previously reported by the reaction of $[\text{Ta}(\text{CH}_2t\text{Bu})_3(=\text{CH}t\text{Bu})]$ with MCM-41 previously dehydroxylated at 500°C , followed by hydrogenolysis (550 Torr, 12h, 150°C). Pentane was distilled on NaK alloy followed by degassing through freeze-pump-thaw cycles.

Gas-phase analysis of alkanes: Gas phase analysis was performed on a Hewlett-Packard 5890 series II gas chromatograph equipped with a flame ionisation detector and an $\text{Al}_2\text{O}_3/\text{KCl}$ on fused silica column (50m X 0.32 mm). Dihydrogen gas phase analysis was performed on a Intersmat-IGC 120-MB gas chromatograph equipped with a catharometer.

Infrared spectra were recorded on a Nicolet 550-FT spectrometer by using an infrared cell equipped with CaF_2 windows, allowing *in situ* monitoring under controlled atmosphere. Typically 36 scans were accumulated for each spectrum (resolution, 2 cm^{-1}).

Infrared spectra for reaction chamber experiments were recorded on a Nicolet 6700 FT-IR Spectrometer by using a high pressure reaction chamber with ZnSe windows (WMD-U23), allowing *in situ* monitoring under controlled atmosphere and high pressure and a metallic part on the reaction chamber to cool the system by adding liquid nitrogen. The spectrometer is equipped with Harrick temperature controller (220/ 240 V) that provides accurate temperature

between -200 °C and +1250 °C and Edwards 1.5 Vacuum Pump with two stage rotary vane pump. Typically 64 scans were accumulated for each spectrum (resolution: 4 cm⁻¹).

High temperature and pressure reaction chamber experiments were performed by reaction chambers that are well suited for studies under carefully controlled temperatures and pressures: Made of chemically resistant 316 stainless steel, readily adapted for operation up to 3.44MPa (25.8 ktorr) with an optional high-pressure dome, WID-U43 (4mm thick) and three ZnSe windows.

NMR Spectroscopy. All the NMR spectra were obtained on a Bruker 500 MHz wide bore spectrometer using a double resonance 4 mm MAS probe at the Laboratoire de Chimie Organometallique de Surface in Ecole Supérieure de Chimie Physique Electronique de Lyon. The samples were introduced under Argon in a zirconia rotor, which was then tightly closed. The spinning frequency was set to 10 kHz for all the NMR experiments. The one-dimensional (1D) ¹⁵N spectra were obtained from crosspolarization (CP) from protons using an adiabatic ramped CP to optimize the magnetization transfer efficiency.

Preparation and reactivity of surface complexes:

*Hydrogenolysis of [(≡SiO)Ta(CH₂C(CH₃)₃)₂(=CHC(CH₃)₃)]: Preparation of [(≡SiO)₂TaH] and [(≡SiO)₂TaH₃], **1**:*

Loose powder of [(≡SiO)₂Ta(=CH*t*Bu)(CH₂*t*Bu)₂] (400mg, 0.26 mmol Ta) was twice treated at 150°C with anhydrous hydrogen (550 torr, 15 mmol, 60 equivalent / Ta) for 15 h. Gas chromatography analysis indicated the formation of 13±2 CH₄ coming from the Hydrogenolysis of 2,2-dimethylpropane, CMe₄ (2.6±0.4 CMe₄/Ta, expected 3). The gas evolved during the reaction was removed under vacuum and the final hydrides [(≡SiO)₂TaH], **1a**, and [(≡SiO)₂TaH₃], **1b**, were recovered as a brown powder. As already reported, some surface alkyl groups (<0.1 C/Ta) resist hydrogenolysis. Elemental Analysis: Ta 15.91%wt C 0.67%wt. Solid state ¹H MAS NMR = 29.5, 26.8, 23.2, 18.0, 13.0 (Ta(**H**)_x), 4.3, 4.0 (Si**H** and Si**H**₂), 1.8 (Si**OH**), 0.8 (C**H**_n) ppm. IR spectra were recorded at each step of the preparation. IR: 3747 (ν_{OH}), 3270-2850 (ν_{CH}), 2270 (ν_{SiH}), 2220 (ν_{SiH₂}), 2100-1600 (δ_{Si-O-Si}), 1890-1700 (ν_{TaH}), 1467 w, 1362 (δ_{CH}) cm⁻¹.

Since such surface alkyls also resist all the further treatments with ammonia described below, no mention will be made to them except in the IR data below and in the discussion of the TQ $^1\text{H-NMR}$ spectrum in the main text. Likewise, some surface silanols from the starting MCM-41 do not undergo reaction with tantalum. Since they remain unchanged throughout the syntheses with ammonia, they will not be further mentioned except in the IR data below and in the $^1\text{H-NMR}$ section of the main text.

*In-situ IR study of the reaction of $[(\equiv\text{SiO})_2\text{TaH}_x(x=1,3)]$, **1** with ammonia:*

A disk of $[(\equiv\text{SiO})_2\text{TaH}]$ and $[(\equiv\text{SiO})_2\text{TaH}_3]$, **1**, (25 mg, 0.025 mmol Ta), prepared as previously reported, was treated by condensing ammonia (4 -5 Torr in a glass T) onto a pellet of tantalum hydride. Removal of excess coordinated ammonia was achieved by heating at 150 °C under dynamic vacuum for 3-4 hours. IR spectra were recorded at each step of the preparation. Similar experiments were carried out with $^{15}\text{NH}_3$ (17 torr, 12 equivalent) leading to $[(\equiv\text{SiO})_2\text{Ta}(=^{15}\text{NH})(^{15}\text{NH}_2)]$, **2***

Selected IR frequencies for the reaction with NH_3 : 3747 (ν_{OH}), 3502 ($\nu_{\text{Ta-N-H}}$), 3461 ($\nu_{\text{N-H}}$), 3377 ($\nu_{\text{Ta-N-H}}$), 3290 (ν_{NH_3}), 3270-2850 (ν_{CH}), 2270 (ν_{SiH}), 2220 (ν_{SiH_2}), 2100-1600 ($\delta_{\text{Si-O-Si}}$), 1890-1700 (ν_{TaH}), 1607(δ_{TaNH_2}), 1550 (δ_{SiNH_2}), 1520 (δ_{TaNH_2}) cm^{-1} .

Selected IR frequencies for the reaction with $^{15}\text{NH}_3$: 3490w ($\nu_{\text{Ta-N-H}}$), 3454w ($\nu_{\text{N-H}}$), 3372w ($\nu_{\text{Ta-N-H}}$), 3289w (ν_{NH_3}), 1602w (δ_{TaNH_2}), 1546w (δ_{SiNH_2}), 1516w (δ_{TaNH_2}) cm^{-1} .

*Reaction of $[(\equiv\text{SiO})_2\text{TaH}_x(x=1,3)]$, **1** with ammonia:*

Excess of ammonia (70 Torr, 15 mmol, 30 equivalents per Ta) was added on $[(\equiv\text{SiO})_2\text{TaH}]$ and $[(\equiv\text{SiO})_2\text{TaH}_3]$, **1**, (75 mg, 0.06 mmol) at room temperature. Gas phase analysis indicated an evolution of 0.3 H_2/Ta . After 2 h at room temperature, the powder was heated for 4 h at 150 °C in order to remove the excess of ammonia. 0.7 H_2/Ta were evolved. This sample was used for NMR experiments. $[(\equiv\text{SiO})_2\text{Ta}(=^{15}\text{NH})(^{15}\text{NH}_2)]$, **2**, was prepared identically using $^{15}\text{NH}_3$. Elemental analysis: Ta 15,7 %_{wt}; N 1,34 %_{wt}.

Presence of $[(\equiv\text{SiO})_2\text{Ta}(\text{NH}_2)_3]$ trisamido species in the reaction chamber:

The Low/ High temperature reaction chamber for praying mantis was filled with the powder of tantalum imido amido species from ammonia. After controlling the survival of these species under argon at room temperature in the instrument, the dewar was filled with liquid nitrogen in order to cool the sample till -150 °C. The appearance of a new peak at 3525 cm^{-1}

was observed from -25 °C and increased its intensity by cooling. The rest of the peaks in NH region remained same except increased their intensity as well.

Selected IR frequencies for the reaction with NH₃: 3747 (ν_{OH}), 3525 (ν_{Ta-N-H}), 3502 (ν_{Ta-N-H}), 3461 (ν_{N-H}), 3377 (ν_{Ta-N-H}), 3290 (ν_{NH₃}), 3270-2850 (ν_{CH}), 2270 (ν_{SiH}), 2220 (ν_{SiH₂}), 2100-1600 (δ_{Si-O-Si}), 1890-1700 (ν_{TaH}), 1607(δ_{TaNH₂}), 1550 (δ_{SiNH₂}), 1520 (δ_{TaNH₂}) cm⁻¹.

*IR Monitoring of the H/D Exchange on [(≡SiO)₂Ta(=¹⁵NH)(¹⁵NH₂)], **2**, **2.NH₃** and [≡Si-NH₂] with D₂:*

A disk of **2**, **2.NH₃** and [≡Si-NH₂] was prepared as described above. The excess ammonia in the gas phase was removed under vacuum, and a large excess of deuterium (570 Torr, 60 equiv per tantalum) was added in the cell at room temperature overnight and heated at 60 °C for 3 h.

Selected IR frequencies: 3502 (ν_{TaNH}), 3461 (ν_{NH}), 3377 (ν_{TaNH}), 3290 (ν_{NH₃}) and 2587 (ν_{N₂D}), 2473 (ν_{N₂D}), 2424 (ν_{N₂D}), 2398 (ν_{N₂D₃}), 1605 (δ_{NH₃}), 1550 (δ_{SiNH₂}), 1520 (δ_{TaNH₂}) cm⁻¹.

Reaction of [(≡SiO)Ta(=NH)(-NH₂)] with ¹⁵NH₃ for NMR monitoring experiment:

Dry ammonia ¹⁵NH₃ (9 torr) was introduced in a glass vessel (195 ml) previously loaded with **2** (45 mg, Ta = 15 %w) prepared as previously described from N₂ and H₂ over [(≡SiO)₂TaH], **1a**, and [(≡SiO)₂TaH₃], **1b**.^[59] The gas phase was condensed over the powder by cooling the reactor in liquid nitrogen and allowed to react at room temperature for 5 hours. The reactor was then put under vacuum during 2h and, after transfer in a glove box under argon atmosphere, the sample was loaded into the NMR rotor.

Reaction of [(≡SiO)Ta(=NH)(-NH₂)] with ND₃ for the in situ IR monitoring experiment:

A disk of [(≡SiO)₂TaH], **1a**, and [(≡SiO)₂TaH₃], **1b**, (15 mg, 0,012 mmol Ta) was treated under an isobar mixture of dinitrogen and dihydrogen (P_{tot} = 550 torr, 30 equivalents each per tantalum) at 250°C for 72 hours. [(≡SiO)₂TaH], **1a**, and [(≡SiO)₂TaH₃], **1b**, is convert to [(≡SiO)₂Ta(=NH)(-NH₂)], **2**. Selected IR frequencies (cm⁻¹): 3500, (ν_{NH}), 3450 (ν_{NH}), 3373 (ν_{NH}), 1521 (δ_{NH₂}).

Two aliquots of deuterated ammonia were successively added (1 torr and 5 torr, respectively) to the reactor and the IR evolution was monitored after each addition. After a thermal treatment

at 150°C during 50h a further spectrum was acquired. A large excess of ND₃ (200 torr, 200 eq per Ta) was finally added and the spectrum recorded after 5 min at room temperature.

Selected IR frequencies (cm⁻¹) : 2760 (ν_{OD}), 2600(ν_{SiND₂}), 2580(ν_{TaND₂}), 2520 (ν_{TaND₂} + ν_{SiND₂}), 2474 (ν_{TaND₂}), 2393 (ν_{TaND₃}).

Models and Computational details

(see the publication for details: Solans- Monfort X, *Inorganic Chemistry*, 51, 7237 (2012))

Calculation of [(=SiO)Ta(=NH)(-NH₂)] with H₂:

Cluster calculations have been carried out with the Gaussian03^[61] package using two different density functionals: B3PW91^[62,63], and PBEPBE^[64]. The first is thought to reproduce better the global process while the second is used to compare with the periodic model. Silicon and tantalum have been represented with the quasi-relativistic effective core pseudopotentials (RECP) of the Stuttgart group, and the associated basis sets augmented with a polarization function^[65-68]. All other atoms (O, N and H) have been represented by Dunning's correlation consistent aug-cc-pVDZ^[69]. All optimizations were performed without any geometry constraint and the nature of the extrema has been checked by analytical frequency calculations. In addition, the Intrinsic Reaction Coordinate (IRC) procedure has been used to ensure that the minima connected by each transition state. The discussion of the results is based on the electronic energies E without any ZPE corrections and Gibb's free energies at 298.15 K and 1 atm. The G values are computed assuming an ideal gas, unscaled harmonic vibrational frequencies and the rigid rotor approximation. Periodic calculations have been performed with the VASP package^[70,71] using the projector augmentedwave (PAW)^[72,73] formalism and the PBEPBE density functional^[64]. The energy cut-off has been fixed to 400 eV and we have used the Monkhorst-Pack sampling of the Brillouin zone with a (2,2,1) mesh. These parameters are the same as those used in our previous work and they have been shown to be accurate enough for describing silica supported systems^[34, 74-75]. Comparison between 2T PBEPBE cluster calculations and those performed with the periodic C₍₁₀₀₎ reveals that the cluster size has very little influence on the geometry of all computed minima. The largest M-L bond distance variation, which is in any case lower than 0.05 Å, is found for the weaker Ta-NH₃ bond in 4q. All other distances are within 0.02 Å. The thermodynamics is the same for the cluster and periodic calculations. The more visible difference is the increased stability of system **4q** by 4 kcal mol⁻¹ because of some interaction between the protons of NH₃ and surface oxygen.

Calculation of $[(\equiv\text{SiO})\text{Ta}(=\text{NH})(-\text{NH}_2)]$ with NH_3 :

The MCM-41 surface has been modeled using a hexatetrahedral 6T cluster (T stands for SiO_4 4 tetrahedral units) represented in Figure. $[\{(\mu\text{-O})[(\text{H}_3\text{SiO})_2\text{SiO}]_2\}\text{Ta}]$ —noted $(-\text{SiO})_2\text{Ta}$ hereafter—to model the silica-supported tantalum species. A simpler cluster model has been used with success in previous related work. This simpler cluster model has given geometrical structures of grafted species identical to those obtained with calculations within the periodic boundary condition, both calculations giving results close to the structure obtained from EXAFS measurement. In this work, the cluster has been enlarged by replacing the pendant OH groups of the surface model by OSiH_3 to avoid some of the artifacts associated with the interaction of NH_3 with the OH bonds.

The tantalum cation is covalently bonded to two vicinal oxygen surface atoms leading to a non-constrained 6 membered ring. Similar surface models have been shown to give results equivalent to those obtained with periodic calculations.^[34] All calculations have been carried out with Gaussian03 package^[61] using B3PW9116 hybrid density functional^[62,63]. Silicon and tantalum are represented with the quasi-relativistic effective core pseudopotentials (RECP) of the Stuttgart group, and the associated basis sets augmented with a polarization function.^[65-69] The other atoms (O, N and H) are represented by Dunning's correlation consistent aug-cc-pVDZ.^[70] All optimizations were performed without any geometry constraint and the nature of the extrema was checked by analytical frequency calculations. The discussion of the results is based on either electronic energies E without any ZPE corrections or Gibbs energies at 298.15 K and 1 atm.

V. REFERENCES

- [1] S. T. Oyama, *The Chemistry of Transition Metal Carbides and Nitrides*, **1996**, ISBN: 07514 03652, 1.
- [2] S. A. Macgregor, *Organometallics* **2001**, 20, 1860.
- [3] T. E. Mueller, M. Beller, *Chem. Rev.* **1998**, 98, 675.
- [4] D. M. Roundhill, *Chem. Rev.* **1992**, 92, 1.
- [5] S. A. Lawrence, *Amine: Synthesis, Properties and Applications*, Cambridge University Press **2004**, ISBN 0 5221 78284 8.
- [6] D. F. McMillen, D. M. Golden, *Annu. Rev. Phys. Chem.* **1982**, 33, 493.
- [7] G. B. Kauffman, *ACS Symp. Ser.* **1994**, 565, 3.
- [8] M. M. Banaszak Holl, P. T. Wolczanski, G. D. Van Duyne, *J. Am. Chem. Soc.* **1990**, 112, 7989.
- [9] J. E. Bercaw, D. L. Davies, P. T. Wolczanski, *Organometallics* **1986**, 5, 443.
- [10] J. N. Armor, *Inorg. Chem.* **1978**, 17, 203.
- [11] D. Conner, K. N. Jayaprakash, T. R. Cundari, T. B. Gunnoe, *Organometallics* **2004**, 23, 2724.
- [12] M. V. Ovchinnikov, E. LeBlanc, I. A. Guzei, R. J. Angelici, *J. Am. Chem. Soc.* **2001**, 123, 11494.
- [13] S. Murai, *Activation of unreactive bonds and organic synthesis*, Springer, **1999**, ISBN: 3-540-64862-3.
- [14] A. L. Casalnuovo, J. C. Calabrese, D. Milstein, *Inorg. Chem.* **1987**, 26, 971.
- [15] M. Schulz, D. Milstein, *J. Chem. Soc., Chem. Commun.* **1993**, 318.
- [16] J. Zhao, A. S. Goldman, J. F. Hartwig, *Science* **2005**, 307, 1080.
- [17] M. Kanzelberger, X. Zhang, T. J. Emge, A. S. Goldman, J. Zhao, C. Incarvito, J. F. Hartwig, *J. Am. Chem. Soc.* **2003**, 125, 13644.
- [18] J. Zhou, J. F. Hartwig, *Angew. Chem. Int. Ed.* **2008**, 47, 5783.
- [19] E. Morgan, D. F. MacLean, R. McDonald, L. Turculet, *J. Am. Chem. Soc.* **2009**, 131, 14234.
- [20] R. Koelliker, D. Milstein, *Angew. Chem.* **1991**, 103, 724.
- [21] Y. Nakajima, H. Kameo, H. Suzuki, *Angew. Chem., Int. Ed.* **2006**, 45, 950.
- [22] C. M. Fafard, D. Adhikari, B. M. Foxman, D. J. Mindiola, O. V. Ozerov, *J. Am. Chem. Soc.* **2007**, 129, 10318.

- [23] G. D. Frey, V. Lavallo, B. Donnadiou, W. W. Schoeller, G. Bertrand, *Science* **2007**, *316*, 439.
- [24] Y. Peng, B. D. Ellis, X. Wang, P. P. Power, *J. Am. Chem. Soc.* **2008**, *130*, 12268.
- [25] A. Jana, I. Objartel, H. W. Roesky, D. Stalke, *Inorg. Chem.* **2009**, *48*, 798.
- [26] A. Jana, C. Schulzke, H. W. Roesky, *J. Am. Chem. Soc.* **2009**, *131*, 4600.
- [27] G. L. Hillhouse, J. E. Bercaw, *J. Am. Chem. Soc.* **1984**, *106*, 5472.
- [28] Y. Nakao, T. Taketsugu, K. Hirao, *J. Chem. Phys.* **1999**, *110*, 10863.
- [29] M. Chen, H. Lu, J. Dong, L. Miao, M. Zhou, *J. Phys. Chem. A* **2002**, *106*, 11456.
- [30] T. E. Glassman, M. G. Vale, R. R. Schrock, *Organometallics* **1991**, *10*, 4046.
- [31] J. R. Fulton, S. Sklenak, M. W. Bouwkamp, R. G. Bergman, *J. Am. Chem. Soc.* **2002**, *124*, 4722.
- [32] D. J. Fox, R. G. Bergman, *J. Am. Chem. Soc.* **2003**, *125*, 8984.
- [33] P. Avenier, A. Lesage, M. Taoufik, A. Baudouin, A. De Mallmann, S. Fiddy, M. Vautier, L. Veyre, J.-M. Basset, L. Emsley, E. A. Quadrelli, *J. Am. Chem. Soc.* **2007**, *129*, 176.
- [34] P. Avenier, M. Taoufik, A. Lesage, X. Solans-Monfort, A. Baudouin, A. de Mallmann, L. Veyre, J. M. Basset, O. Eisenstein, L. Emsley, E. A. Quadrelli, *Science* **2007**, *317*, 1056.
- [35] R. H. Crabtree, *Selective Hydrocarbon Activation: Principles and Progress*, *VCH Publishers* **1990**, 1-18.
- [36] R. H. Crabtree, *The Organometallic Chemistry of Transition Metals*, *Wiley* **2009**, ISBN : 978- 0- 470- 25762- 3.
- [37] M. R. A. Blomberg, P. E. M. Siegbahn, M. Svensson, *Inorg. Chem.* **1993**, *32*, 4218.
- [38] P. E. M. Siegbahn, M. R. A. Blomberg, M. Svensson, *J. Am. Chem. Soc.* **1993**, *115*, 4191.
- [39] D. E. Clemmer, L. S. Sunderlin, P. B. Armentrout, *J. Phys. Chem.* **1990**, *94*, 208.
- [40] D. E. Clemmer, P. B. Armentrout, *J. Am. Chem. Soc.* **1989**, *111*, 8280.
- [41] L. S. Sunderlin, P. B. Armentrout, *J. Am. Chem. Soc.* **1989**, *111*, 3845.
- [42] D. E. Clemmer, P. B. Armentrout, *J. Phys. Chem.* **1991**, *95*, 3084.
- [43] P. A. M. Van Koppen, J. Brodbelt-Lustig, M. T. Bowers, D. V. Dearden, J. L. Beauchamp, E. R. Fisher, P. B. Armentrout, *J. Am. Chem. Soc.* **1991**, *113*, 2359.
- [44] E. R. Fisher, P. B. Armentrout, *J. Am. Chem. Soc.* **1992**, *114*, 2039.
- [45] Y.-M. Chen, D. E. Clemmer, P. B. Armentrout, *J. Am. Chem. Soc.* **1994**, *116*, 7815.

- [46] P. A. M. van Koppen, M. T. Bowers, E. R. Fisher, P. B. Armentrout, *J. Am. Chem. Soc.* **1994**, *116*, 3780.
- [47] S. Goebel, C. L. Haynes, F. A. Khan, P. B. Armentrout, *J. Am. Chem. Soc.* **1995**, *117*, 6994.
- [48] D. Walter, P. B. Armentrout, *J. Am. Chem. Soc.* **1998**, *120*, 3176.
- [49] J. F. Hartwig, *Acc. Chem. Res.* **1998**, *31*, 852.
- [50] T. Braun, *Angew. Chem. Int. Ed.* **2005**, *44*, 5012.
- [51] N. Ochi, Y. Nakao, H. Sato, S. Sakaki, *J. Am. Chem. Soc.* **2007**, *129*, 8615.
- [52] M. A. Salomon, A.-K. Jungton, T. Braun, *Dalton Trans.* **2009**, 7669.
- [53] E. Khaskin, M. A. Iron, L. J. W. Shimon, J. Zhang, D. Milstein, *J. Am. Chem. Soc.* **2010**, *132*, 8542.
- [54] C. Gunanathan, B. Gnanaprakasam, M. A. Iron, L. J. W. Shimon, D. Milstein, *J. Am. Chem. Soc.* **2010**, *132*, 14763.
- [55] P. Avenier, X. Solans-Monfort, L. Veyre, F. Renili, J.-M. Basset, O. Eisenstein, M. Taoufik, E. A. Quadrelli, *Top. Catal.* **2009**, *52*, 1482.
- [56] C. Copéret, A. Grouiller, J.-M. Basset, H. Chermette, *Chem. Phys. Chem.* **2003**, *4*, 608.
- [57] A. Poater, X. Solans-Monfort, E. Clot, C. Copéret, O. Eisenstein, *Dalton Transactions* **2006**, 3077.
- [58] S. Soignier, M. Taoufik, E. Le Roux, G. Saggio, C. Dablemont, A. Baudouin, F. Lefebvre, A. De Mallmann, J. Thivolle-Cazat, J.-M. Basset, G. Sunley, B. M. Maunders, *Organometallics* **2006**, *25*, 1569.
- [59] R. R. Schrock, J. D. Fellmann, *J. Am. Chem. Soc.* **1978**, *100*, 3359.
- [60] C. Y. Chen, H. X. Li, M. E. Davis, *Microporous Mater.* **1993**, *2*, 17.
- [61] M. J. Frisch, G. W. Trucks, H. B. Schlegel, G. E. Scuseria, M. A. Robb, J. R. Cheeseman, J. A. Jr Montgomery, K.N. Kudin, J. C. Burant, J. M. Millam, S. S. Iyengar, J. Tomasi, V. Barone, B. Mennucci, M. Cossi, G. Scalmani, N. Rega, G. A. Petersson, H. Nakatsuji, M. Hada, M. Ehara, K. Toyota, R. Fukuda, J. Hasegawa, M. Ishida, T. Nakajima, Y. Honda, O. Kitao, H. Nakai, M. Klene, X. Li, J. E. Knox, H. P. Hratchian, J. B. Cross, C. Adamo, J. Jaramillo, R. Gomperts, R. E. Stratmann, O. Yazyev, A. J. Austin, R. Cammi, C. Pomelli, J. W. Ochterski, P. Y. Ayala, K. Morokuma, G. A. Voth, P. Salvador, J. J. Dannenberg, V. G. Zakrzewski, S. Dapprich, A. D. Daniels, M. C. Strain, O. Farkas, D. K. Malick, A. D. Rabuck, K. Raghavachari, J. B. Foresman, J. V. Ortiz, Q. Cui, A. G. Baboul, S. Clifford, J. Cioslowski, B. B.

- Stefanov, G. Liu, A. Liashenko, P. Piskorz, I. Komaromi, R. L. Martin, D. J. Fox, T. Keith, M. A. Al-Laham, C. Y. Peng, A. Nanayakkara, M. Challacombe, P. M. W. Gill, B. Johnson, W. Chen, M. W. Wong, C. Gonzalez, J. A. Pople, Rev. B.04 ed. **2003**, Gaussian Inc.
- [62] A. D. Becke, *J. Chem. Phys.* **2003**, 98, 5648.
- [63] J. P. Perdew, Y. Wang, *Phys. Rev.* **1992**, 45, 3244.
- [64] J. P. Perdew, K. Burke, M. Ernzerhof, *Phys. Rev. Lett.* **1996**, 77, 3865.
- [65] D. Andrae, U. Haubermann, M. Dolg, H. Stoll, H. Preub, *Theor. Chim. Acta.* **1990** 77, 123.
- [66] A. Bergner, M. Dolg, W. Kuchle, H. Stoll, H. Preub, *Mol. Phys.* **1993**, 80, 1431.
- [67] A. W. Ehlers, M. Bohme, S. Dapprich, A. Gobbi, A. Hollwarth, V. Jonas, K. F. Kohler, R. Stegmann, A. Veldkamp, G. Frenking, *Chem. Phys. Lett.* **1993**, 208, 111.
- [68] A. Hollwarth, M. Bohme, S. Dapprich, A. W. Ehlers, A. Gobbi, V. Jonas, K. F. Kohler, R. Stegmann, A. Veldkamp, A. Frenking, *Chem. Phys. Lett.* **1993**, 208, 237.
- [69] R. A. Kendall, T. H. Jr Dunning, R. J. Harrison, *J. Chem. Phys.* **1992**, 96, 6796.
- [70] G. Kresse, J. Furthmuller, *Phys. Rev. B.* **1996**, 54, 1169.
- [71] G. Kresse, J. Furthmuller, *Comput. Mater. Sci.* **1996**, 6, 15.
- [72] P. E. Blochl *Phys. Rev. B.* **1994**, 50, 17953.
- [73] G. Kresse, D. Joubert, *Phys. Rev. B.* **1999**, 59, 1758.
- [74] X. Solans-Monfort, J.-S. Filhol, C. Copéret, O. Eisenstein, *New J. Chem.* **2006**, 30, 842.
- [75] F. Blanc, J.-M. Basset, C. Copéret, A. Sinha, Z. J. Tonzetich, R. R. Schrock, X. Solans-Monfort, E. Clot, O. Eisenstein, A. Lesage, L. Emsley, *J. Am. Chem. Soc.* **2008**, 130, 5886.

CHAPTER III.

Mechanistic insight of dinitrogen activation reaction
over silica supported tantalum hydrides

I. INTRODUCTION

I.1 Introduction to dinitrogen and its properties

Nitrogen is among the most important element in functional group chemistry, being of vital biological, synthetic and industrial importance. Its derivatives find uses as intermediates in a variety of applications including pharmaceuticals, agricultural chemicals, rubber chemicals, water treatment chemicals and solvents.^[1]

Its ultimate source is atmospheric dinitrogen (N₂). However, this inert molecule must first be ‘fixed’ in order to have a more useful form. The inertness of dinitrogen molecule is not just due to its triple bond strength, but also due to a number of factors such as the lack of a dipole moment, high ionization potential (15.058 eV), high endothermic electron affinity, high bond dissociation enthalpy (225 kcal mol⁻¹) and large gap between the highest occupied molecular orbital (HOMO) and the lowest unoccupied molecular orbital (LUMO) (Table 4). This large HOMO/ LUMO gap of dinitrogen is in part responsible for the inertness of this molecule because it gives rise to resistance in electron transfer in the redox process and Lewis acid-base reactions.^[2, 3]

Table 4: Dinitrogen characteristics are given below.

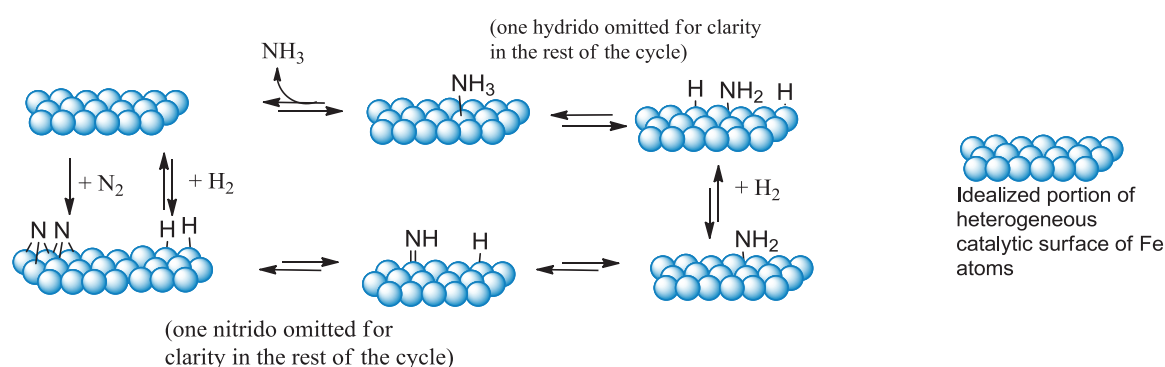
Physico-chemical characteristics of N₂ molecule	
Interatomic distance	1.095 Å
Ionization potential	15.058 eV
N≡N bond dissociation enthalpy	225 kcal.mol ⁻¹
Vibration frequency (gas)	2231 cm ⁻¹
Electron affinity	-1.8 eV
Proton affinity	5.12 cV
Solubility:	
In water	1.7 x 10 ⁻² cm ³ .cm ⁻³
In benzene	1.11 x 10 ⁻¹ cm ³ .cm ⁻³

Development of a chemical N₂-fixing system converting a quite inert N₂ molecule into nitrogenous compounds under mild conditions is a challenging topic in chemistry. We will describe herein the crucial examples in the literature for dinitrogen coordination and cleavage.

N₂ cleavage is a key process that is performed naturally in biological systems at atmospheric pressure and ambient temperature by nitrogenase enzymes containing the “FeMoco” (iron molybdenum cofactor) as given below in Equation 15.^[4-12]



In non-biological chemistry, the reduction of N₂ to ammonia in mild conditions is a major challenge. The need for an industrial source of fixed nitrogen became apparent in the early 20th century as natural sources of nitrogen compounds, used largely for the production of fertilizers, were becoming depleted. A number of different processes were developed. Only Haber-Bosch process is still in use among them to synthesize over 150 million tons/year of ammonia requiring temperatures above 400 °C and pressures of between 200-300 atmospheres. It is thus one of the most important discoveries in industrial catalysis.



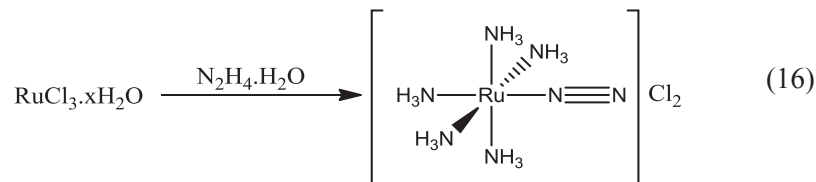
Scheme 15

The simplified proposed reaction mechanism for catalytic ammonia synthesis in heterogeneous catalysis by surface science studies on Haber-Bosh model systems can be seen in Scheme 15.^[13-15]

Despite the remarkable success of these two catalytic processes, in the case of nitrogenases its structure is still not well-defined and the reaction mechanism is unclear even after various researches over a period of more than forty years^[9] and for Haber-Bosch process, it needs a high activation barrier, high pressures and temperature in addition to the very costly massive utilization of H₂ with only 15% yield.^[3, 4, 17]

The studies for the development of dinitrogen reduction to ammonia by transition metal complexes are abundant in the literature and several reviews have been published.^[2, 16-18]

Dinitrogen coordination chemistry began with the discovery of [Ru(NH₃)₅N₂]²⁺ complex by Allen and Senoff in 1965 which was prepared by treating ruthenium chloride with hydrazine and gave clues of the possible role of the metal in the nitrogenase system.^[19]



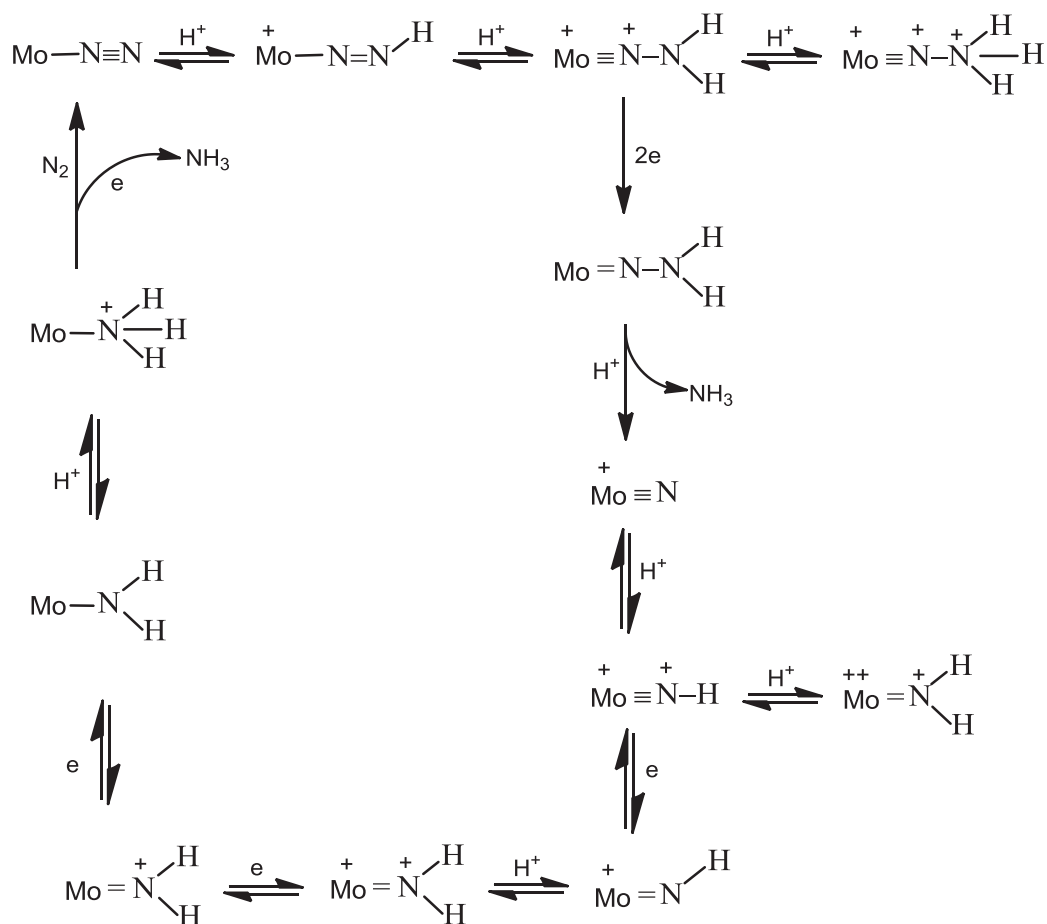
The binding mode of N₂ unit to one or more metal centers plays a significant role in the extent of dinitrogen activation. In this complex, dinitrogen is coordinated to the metal by the lone pair of one nitrogen atom, a coordination mode called end-on type. This mode is the most common bonding mode for transition metal dinitrogen complexes.^[20] Therefore, the coordination mode of dinitrogen is considered as a prerequisite for the level of its activation and reduction (Table 5).^[21] The side-on coordination implies a participation of the triple bond. These two types are used to describe nitrogen coordination on one or more metals. Coordination of dinitrogen on a metal center corresponds to N-N bond activation by π -backbonding. The strength of this activation is different for each coordination type and the N-N bond representation differs depending on this strength, as shown in Table 5 below.

Table 5: Dinitrogen coordination types with one or two metal in the complex.

<u>weak activation</u>		<u>strong activation</u>
	<i>side-on mononuclear</i>	
	<i>end-on mononuclear</i>	
	<i>end-on dinuclear</i>	
	<i>side-on dinuclear</i>	
	<i>end-on side-on dinuclear</i>	

While several reductions of dinitrogen with reducing agents such as acids^[22, 23] or silanes^[24] are reported to activate dinitrogen, we will describe herein N₂ reduction with dihydrogen, since its activation with [(≡SiO)₂TaH], **1a**, and [(≡SiO)₂TaH₃], **1b**, in presence of H₂ is the focus of our study.

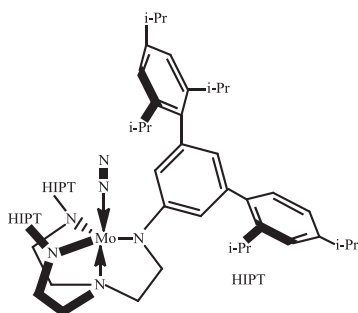
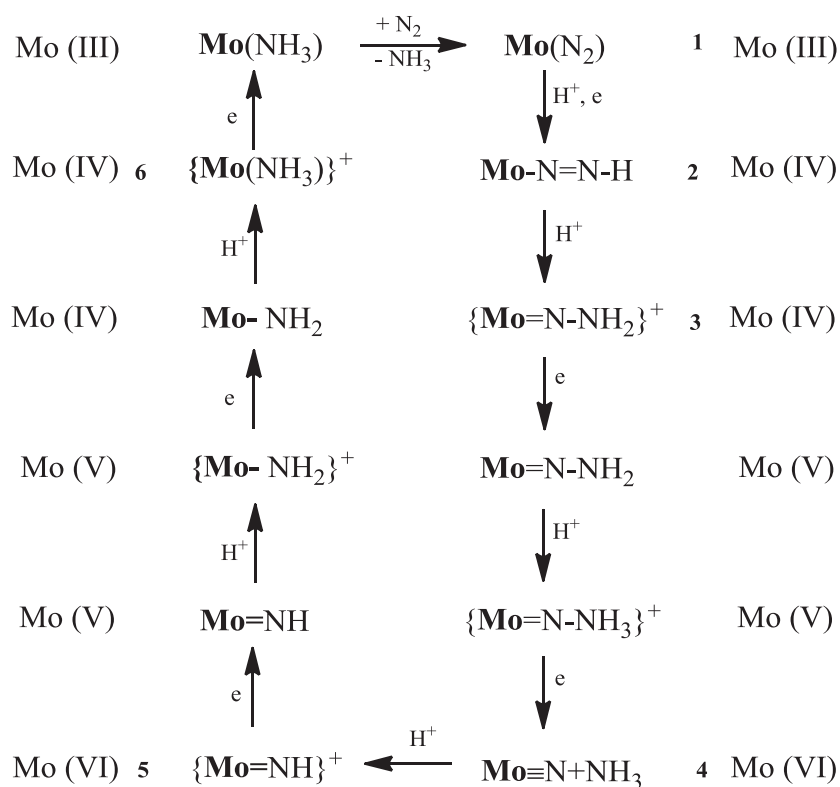
Chirik and co-workers have reported a significant molecular system, *i.e.* excluding Haber-Bosch, that produced, albeit sub-stoichiometrically, ammonia from N₂ and H₂ (Scheme 16).^[25] The protonation of dinuclear N₂ complex, [(Cp₂N₂)Zr]₂(μ₂,η²,η²-N₂) with 1-4 atmospheres of H₂ produced homogenously both N-H and zirconium hydride bonds. Subsequent protonation ultimately yielded ammonia.



Scheme 17

This chart describes the Chatt cycle with the information on electron and proton transfer pathways of hydrazides and imides and related organo-N species. The cycle operated between Mo^0 and Mo^{IV} oxidation levels and referred specifically to the protonation of coordinated molybdenum- and also tungsten-dinitrogen complexes and represented an enormous amount of work in attempts to the model nitrogenase.

In 2003, Yandulov and Schrock showed how N_2 could be catalytically converted to NH_3 in presence of $\text{Mo}[(\text{HIPTN})_3\text{N}]$, ($\text{HIPTN} = \{3,5-(2,4,6\text{-}i\text{Pr}_3\text{C}_6\text{H}_2)_2\text{C}_6\text{H}_3\}\text{NCH}_2\text{CH}_2$) using consecutive addition of protons from a lutidium salt and electrons from hexamethyldecachromocene (Scheme 18).^[23, 32-35] Today, this is one of the very rare well-defined monometallic system that is able to catalyze the conversion of N_2 and H_2 to NH_3 . But overall efficiencies and turn over numbers are still limited despite enormous studies in the field of homogenous N_2 activation by transition metals.



Mo = Mo[(HIPTN)₃N] complex

HIPT: (hexa-iso-propyl-terphenyl) \rightarrow 3,5-(2,4,6-*i*-Pr₃C₆H₂)₂C₆H₃.

Scheme 18: Proposed intermediates in the reduction of dinitrogen at a [HIPTN₃N]Mo (**Mo**) center through the stepwise addition of protons and electrons.

In addition to these landmarks results, considerable amount of work was carried out to better understand the factors that could be important in the dinitrogen activation such as electrochemical^[36-39] or photochemical processes^[40, 41] used as energy sources to achieve N₂ and H₂ to ammonia conversion. The first example of ammonia formation from dinitrogen and dihydrogen under mild conditions was reported by Hidai and Nishibayashi (Scheme 19).^[42]

Many research groups have focused their attention on the N₂ coordination and cleavage. In this way, bare metals in matrice-isolation conditions have been found to cleave N₂.^[44-46] In addition, a larger palette of experimental conditions have been now used to cleave the dinitrogen bond in either di- or polymetallic complexes of N₂ even though ammonia is not the final product of reaction.^[47-56] Although molecular dihydrogen is rarely used as the source for protons and electrons, Tyler et al. represented the formation of a mixture ammonia and N₂H₄ from N₂ in presence of Fe(II) complex with H₂ at room temperature and atmospheric pressure.^[57, 58] On the other hand, the functionalization of dinitrogen has also been achieved in several cases either with hydrogen, silane, borane, or even CO usually via the coordination of N₂ to a dinuclear complex.^[59-66]

A significant example shown by us and co-workers in 2007 was the stoichiometric reaction of N₂ and H₂ with silica-supported tantalum hydrides complexes [(≡SiO)₂TaH], **1a** and [(≡SiO)₂TaH₃], **1b** forming the amido-imido complex [(≡SiO)₂Ta(NH)(NH₂)], **2** at 250 °C.^[67] The low pressures of N₂ and H₂ without the need of an additional reagent were reported in this unique example offered by surface organometallic chemistry (SOMC). The singularity of this process is that tantalum hydrides act as monometallic species capable of splitting N₂ with molecular dihydrogen as the reducing agent. *In situ* IR monitoring of N₂ addition to the hydride mixture followed by H₂ exposure, and heating allowed observing two intermediates, I₁ and I₂. I₁ is characterized by $\nu = 2280 \text{ cm}^{-1}$ upon addition of N₂ in addition I₂ is characterized by $\nu = 3400 \text{ cm}^{-1}$ forming upon heating. Addition of H₂ and heating above 200 °C were necessary to observe the full conversion to the final product. The focus of this chapter will be the latest results on the mechanistic insight of dinitrogen activation via SOMC and assigning the two intermediates I₁ and I₂.

I.2 Mechanistic understanding of dinitrogen activation

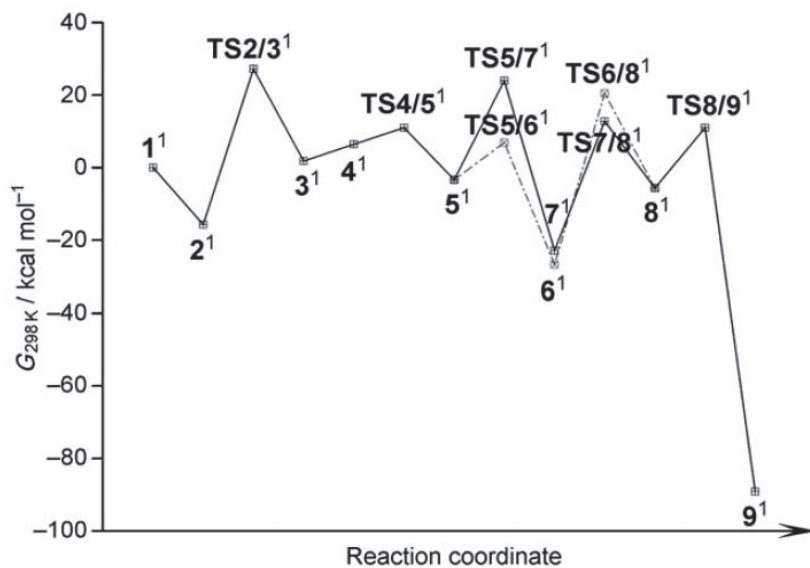
In parallel to the experimental literature reports above, a large number of theoretical studies have been carried out to understand the mechanism of the dinitrogen coordination as well as its activation. Several of these examples have centered their efforts on understanding the catalytic processes leading to the formation of ammonia. The heterogeneous activation of N₂ has been studied by several authors. According to their DFT calculations, dinitrogen cleavage is usually the rate determining step and it occurs most likely at step sites of the surface.^[69-72]

Various studies have been described the different aspects involved in catalytic reaction of ammonia from N_2 and H_2 was able to predict catalysis and understand ammonia synthesis from first-principles calculations in atomic-scale directly by the application of various levels of quantum-mechanics-based electronic structure calculation.

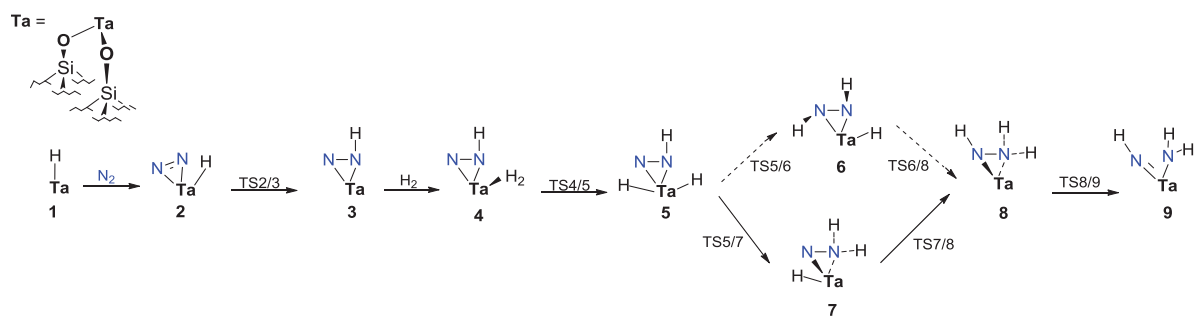
Theoretical studies have also attracted considerable attention on the mechanistic insight of the reaction of molybdenum complex reported by Yandulov and Schrock in 2003. Calculations using small and larger models of the real systems reproduced reasonably well the experimental results validating Scheme 18 reported above.^[73,75,78,81,83] The processes involving N_2 activation and cleavage by polymetallic species without forming NH_3 have also attracted the attention of theoretical chemists.^[83-98] Activation of the dinitrogen is usually accomplished when N_2 is side-on coordinated and/or bridged between two metal centers.

Finally, the reactivity of silica supported tantalum hydrides $[(\equiv SiO)_2TaH]$, **1a** and $[(\equiv SiO)_2TaH_3]$, **1b** with N_2 and H_2 has also been studied through DFT calculations as shown in Scheme 20 below by another group in 2008.^[99]

The authors proposed a mechanism consisting in three successive hydride transfers, with unusual high energy barriers, which are barely compatible with the high temperature during the experiment.



Structure proposed by Li and Li in 2008



Scheme 20: Gibbs energy profile for the reduction of dinitrogen by H_2 at a single surface Ta^{III} center and the schematic structures of all stationary points for the reduction of N_2 proposed by Li and Li in 2008.

I.3 Overview of chapter III

In the introduction of this chapter, the remarkable examples in the literature for dinitrogen coordination and cleavage by transition metal complexes mainly in the presence of H_2 have been shown.

The aim of the following part is to present the latest investigations on the mechanistic insight through the stoichiometric $\text{N}\equiv\text{N}$ bond splitting by silica supported tantalum hydrides, $[(\equiv\text{SiO})_2\text{TaH}_x$ ($x: 1,3$), **1**. The results will be mainly given according to the *in situ* infrared

spectroscopy and Density Functional Theory (DFT) calculations. Solid state NMR and elemental analysis will be also reported for some experiments. DFT calculations by our co-workers *Odile Eisenstein* from *Institute Charles Gerhardt Montpellier* and *Xavier Solans-Monfort* from *Universitat Autònoma de Barcelona* will be presented. In addition to this, differences between the recent mechanism and the previously proposed mechanism by Li & Li in 2008 ^[99] will be subsequently described in the discussion part.

II. RESULTS

The reaction of tantalum hydrides with N_2 and H_2 has been already reported to give well defined $[(\equiv SiO)_2Ta(=NH)(NH_2)]$ complex by cleaving $N\equiv N$ bond at $250^\circ C$ in 3 days.^[67] In this part, experimental studies in order to find the intermediates and proposed an overall mechanism of this reaction will be given.

II. 1 Reaction of $[(\equiv SiO)_2TaH_x (x: 1, 3)]$ with dinitrogen

Figure 11 shows the subtracted infrared spectra of tantalum hydride mixture before dinitrogen addition at room temperature. The peak at 2280 cm^{-1} , distinctive of the first observed intermediate I_1 , is observed at room temperature after stepwise addition of N_2 to a sample of silica-supported $[(\equiv SiO)_2TaH_x (x: 1, 3)]$ complex, **1**.

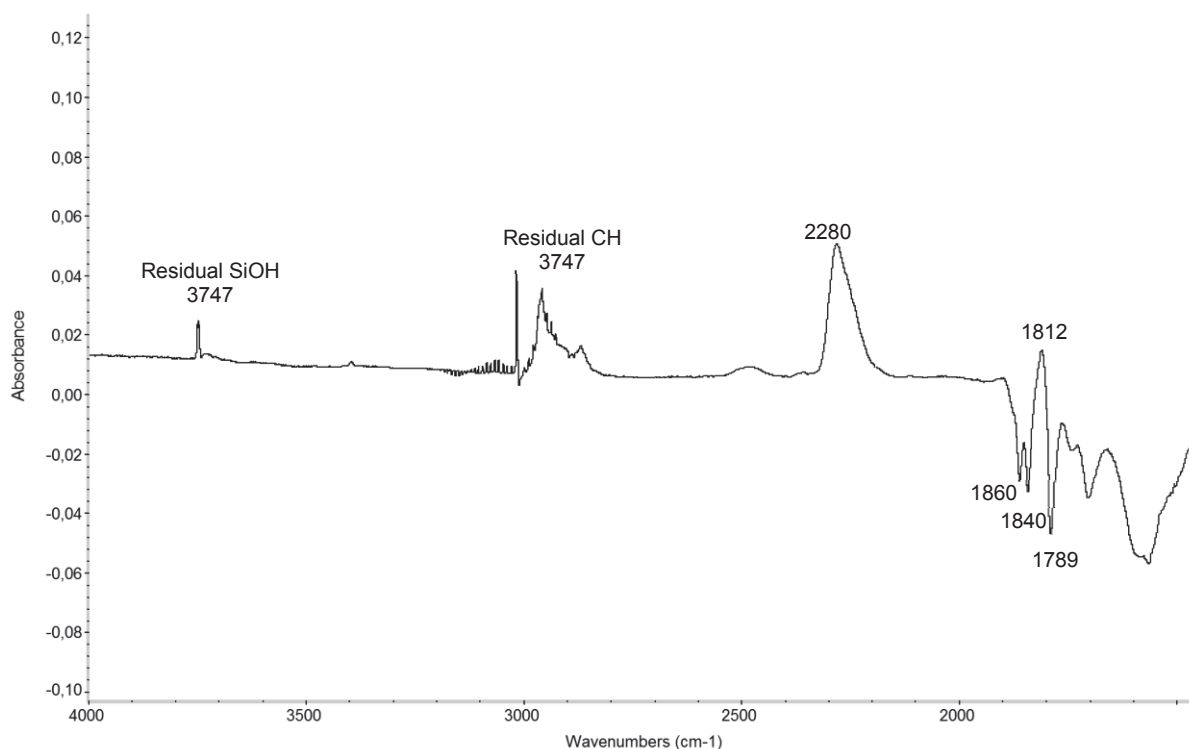


Figure 11: Subtracted spectrum: Before and after addition of N_2 on $[(\equiv SiO)_2TaH_x]$ at room temperature.

Although the peak at 2280 cm^{-1} overlaps with the peaks assigned to the surface silanes, subtracted spectra shows a clear increase in this region (cf. $\nu(\text{NN})$ of free dinitrogen at 2331 cm^{-1}). This coordination is reversible; upon application of vacuum, the band at 2280 cm^{-1} disappears. Decreases in Ta-H bands are also observed at 1860 , 1840 , and 1789 cm^{-1} . Conversely, an increase in the band at 1812 cm^{-1} is seen. If heated to $250\text{ }^\circ\text{C}$, these species evolve to the intermediate, I_2 which gives a band in the IR spectrum at 3400 cm^{-1} , attributable to a $\nu(\text{NH})$ stretch, presumably TaN_2H_x , and not present in the final product (Figure 12).

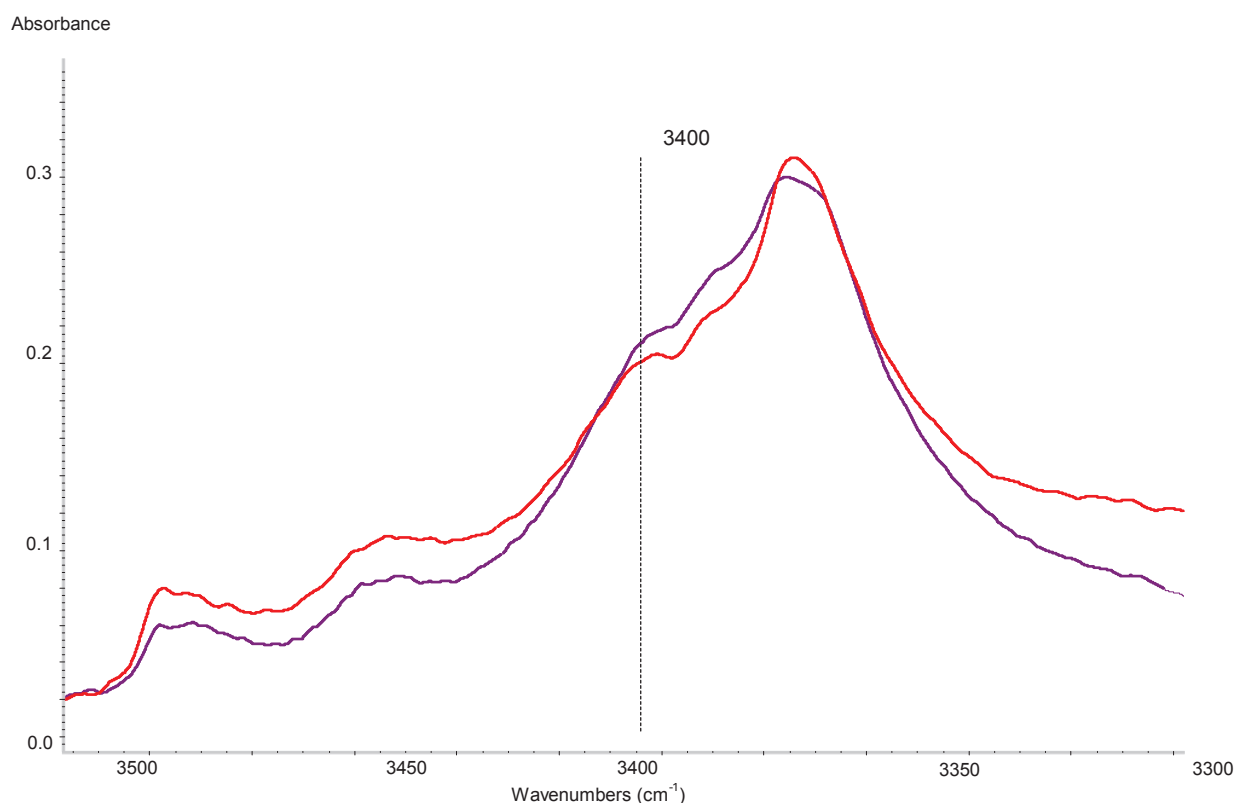
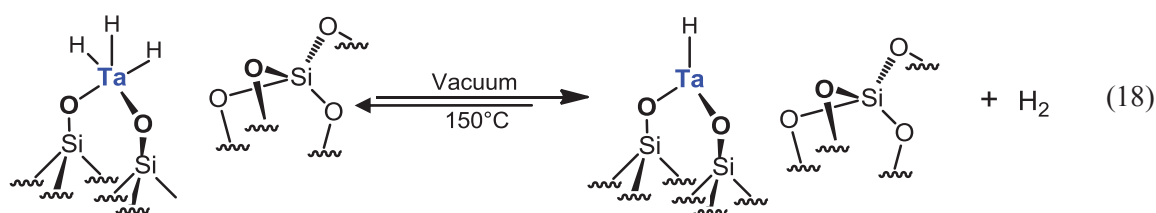


Figure 12: IR spectra of the enlarged region $3550\text{--}3300\text{ cm}^{-1}$ for two distinct experiments of the reaction of silica supported tantalum hydrides with the addition of N_2 at $250\text{ }^\circ\text{C}$ for 4h.

The other emerging bands observed in the spectra of Figure 12 are a $\nu(\text{NH}_x)$ of the final $[(\equiv\text{SiO})_2\text{Ta}(=\text{NH})(\text{NH}_2)]$. Addition of H_2 reforms some $[(\equiv\text{SiO})_2\text{TaH}_x$ (x : 1, 3)] and leads to final imido amido product only after heating at $250\text{ }^\circ\text{C}$ for 3 days as reported previously. ^[67]

II.1.1 Reaction of $[(\equiv\text{SiO})_2\text{TaH}_x]$ enriched **1** with N_2

Heating the complex $[(\equiv\text{SiO})_2\text{TaH}_x]$ ($x: 1, 3$), **1** at $150\text{ }^\circ\text{C}$ under vacuum for 4 hours leads to a decrease in the intensity of the $\nu(\text{TaH}_x)$ bands observed by *in situ* IR spectroscopy. Treating the hydrides in this manner leads to a decrease of tantalum trishydride species and increase the monohydride species which will be called as $[(\equiv\text{SiO})_2\text{TaH}_1]$ enriched **1** as already established in the literature (see Eq. 18 and Annex of Chapter III for further information)



Similarly to the behavior observed for the tantalum hydride mixture, an increase in the band at 2280 cm^{-1} is observed at room temperature upon addition of N_2 to this TaH_1 enriched complex. On the contrary, no increase is observed for this complex at 1812 cm^{-1} .

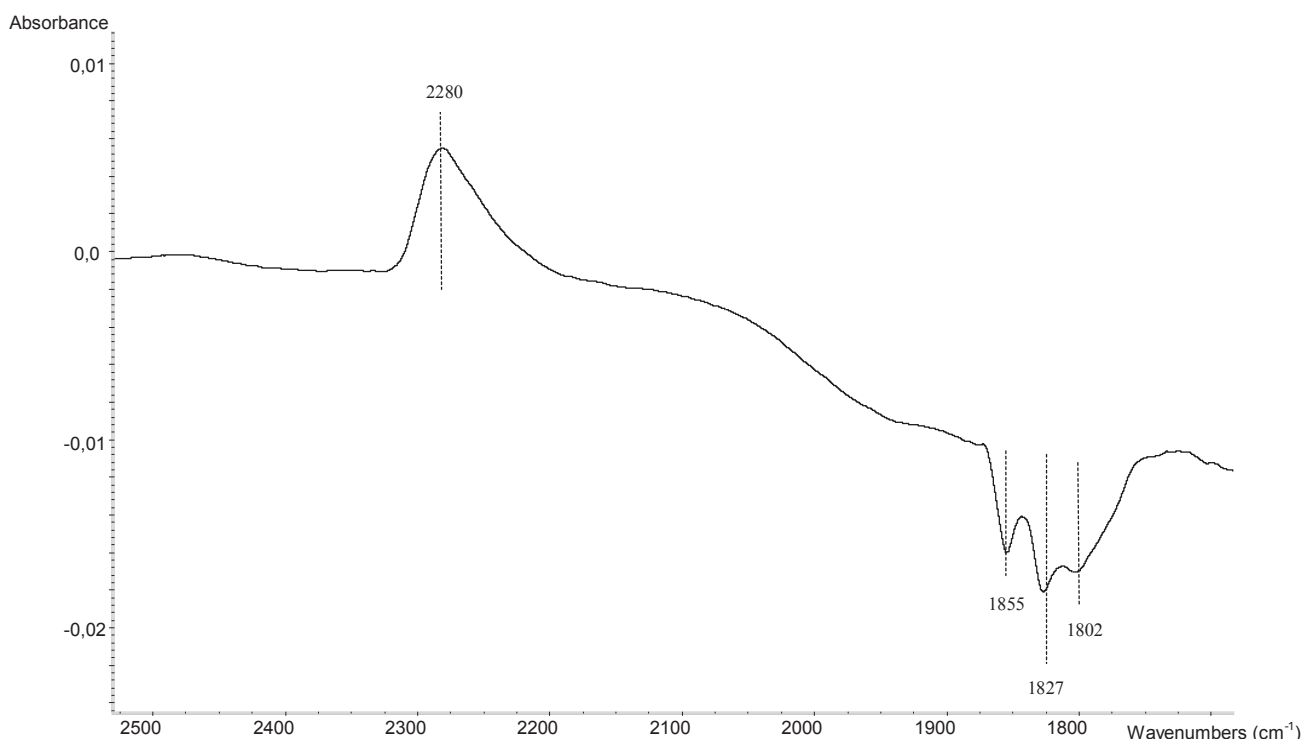


Figure 13: Enlarged spectrum of $2550\text{-}1700\text{ cm}^{-1}$ region showing the subtracted result of dinitrogen addition to **1a** at room temperature: Dotted lines, $\nu(\text{TaN}_2)$ of intermediate species at 2280 cm^{-1} and decreasing $\nu(\text{TaH})$ of starting complexes tantalum monohydride.

Upon heating to 250 °C for 3 h, a weak band at 3372 cm⁻¹ and a small peak around 1520 cm⁻¹ appear. At no point the intermediate band at 3400 cm⁻¹ is observed (Figure 14 and Figure 15). Suggesting the formation of intermediate I₂ is less extensive from the [(≡SiO)₂TaH₁] enriched starting hydrides **1** than for the regular starting tantalum hydride [(≡SiO)₂TaH_x (x: 1, 3)] .

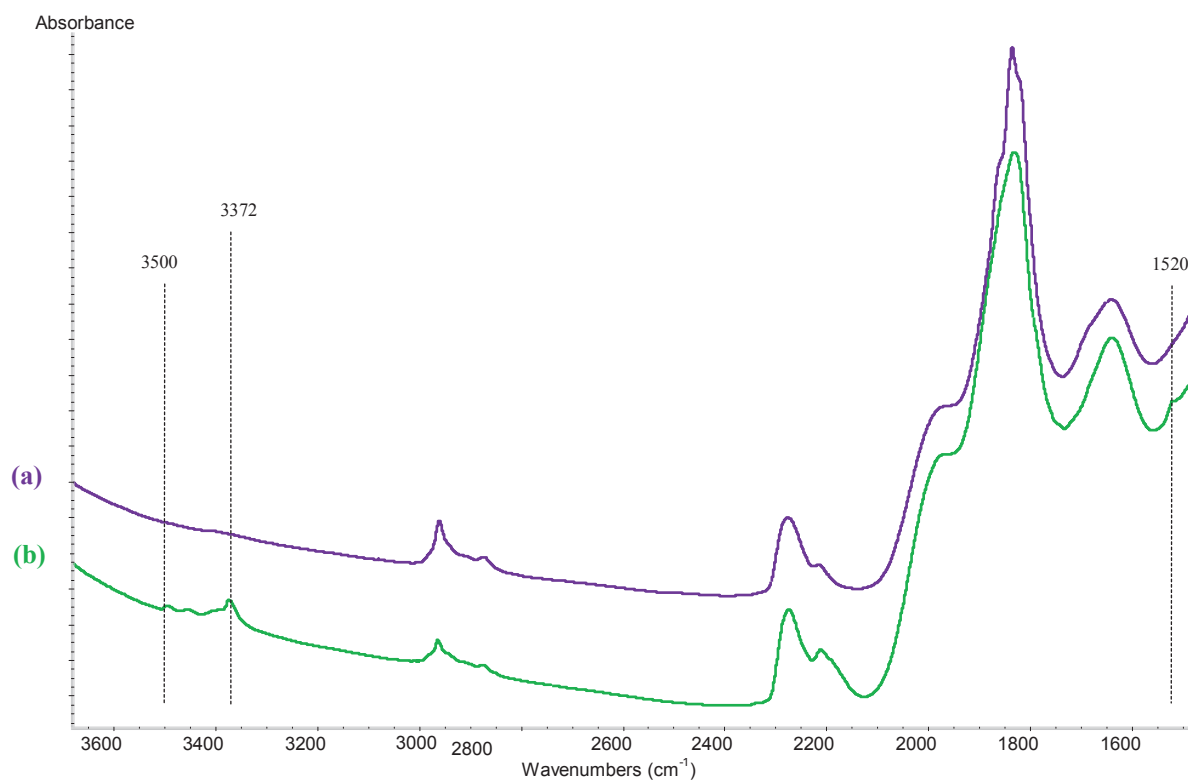


Figure 14: The spectra of tantalum monohydride enriched **1** after dinitrogen addition: (a) at room temperature; (b) after heating at 250 °C for 3 hours.

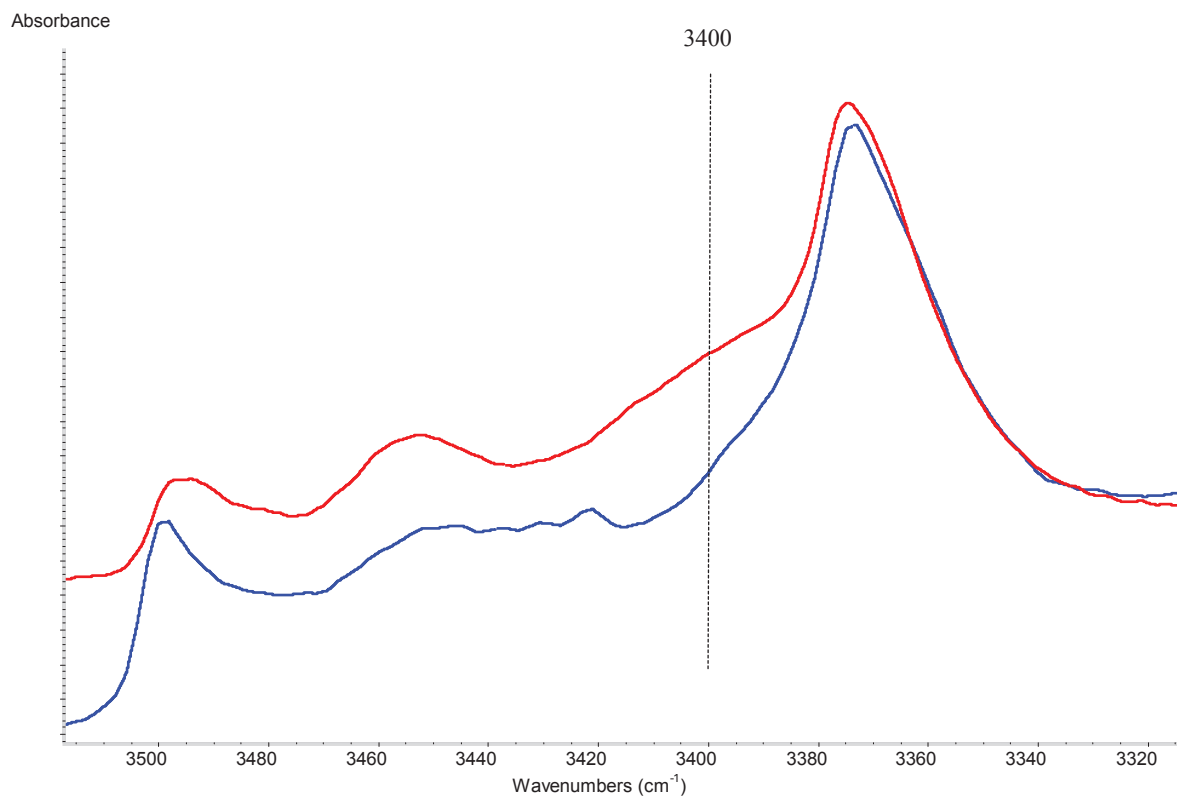


Figure 15: Enlarged spectra of the region 3550- 3300 cm^{-1} : Comparison of two repeated examples for the addition of dinitrogen to the silica supported tantalum monohydride enriched complex **1** at 250 $^{\circ}\text{C}$, 1 Night.

Elemental analysis of the solid obtained after addition of N_2 to both the hydride mixture **1** and the mono-hydride enriched **1** at 250 $^{\circ}\text{C}$, show substantial amount of nitrogen (N/Ta by e.a.= *ca.*0.96 and 0.95, respectively, very similar to final N/ Ta ratio= 1.1 in $[(\equiv\text{SiO})_2\text{Ta}(=\text{NH})(\text{NH}_2)]$).

II.1.2 Reaction of $[(\equiv\text{SiO})_2\text{TaH}_x$ (x: 1, 3)] with $^{15}\text{N}_2$

Tantalum hydride mixture is reacted with labelled dinitrogen at room temperature and subsequently treated under vacuum for 10 minutes. *In situ* IR and solid state NMR spectroscopies are used in order to monitor the product. Following figures represent these results.

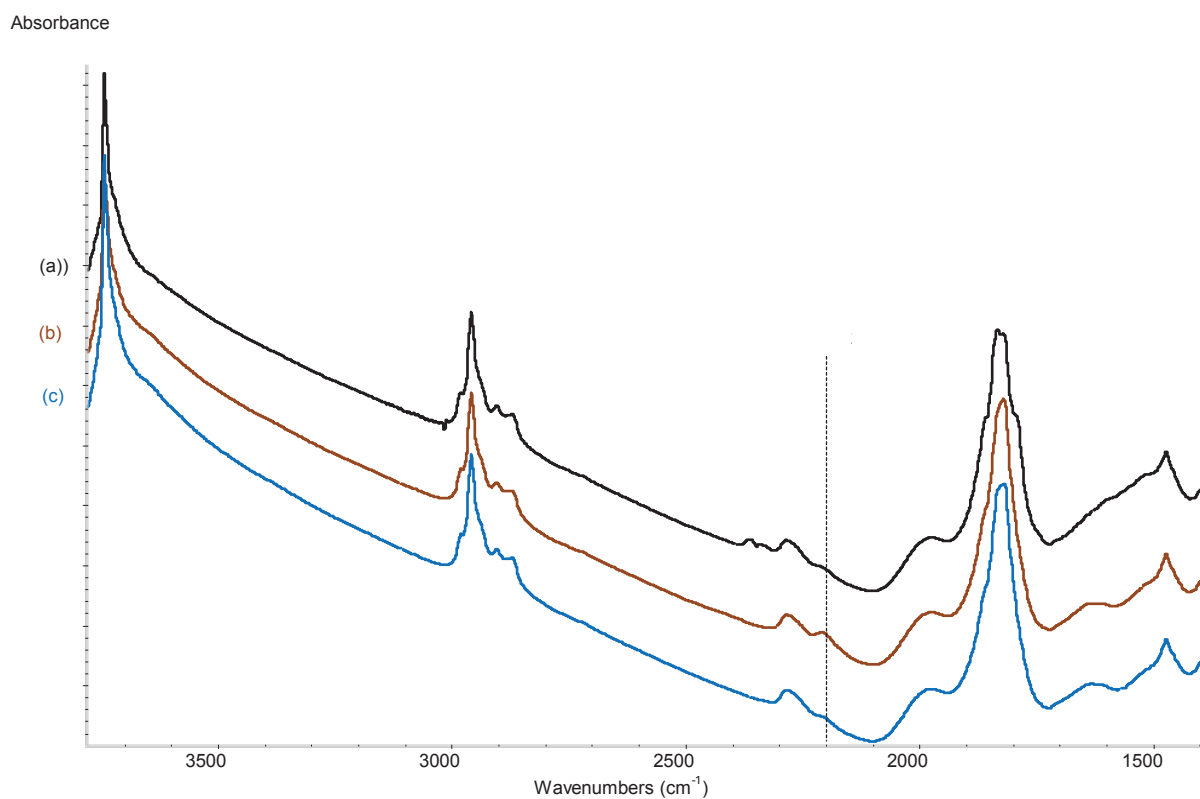


Figure 16: Reaction of $^{15}\text{N}_2$ with tantalum hydrides: (a) starting tantalum hydrides; (b) $^{15}\text{N}_2$ addition at room temperature; (c) vacuum treatment to the sample.

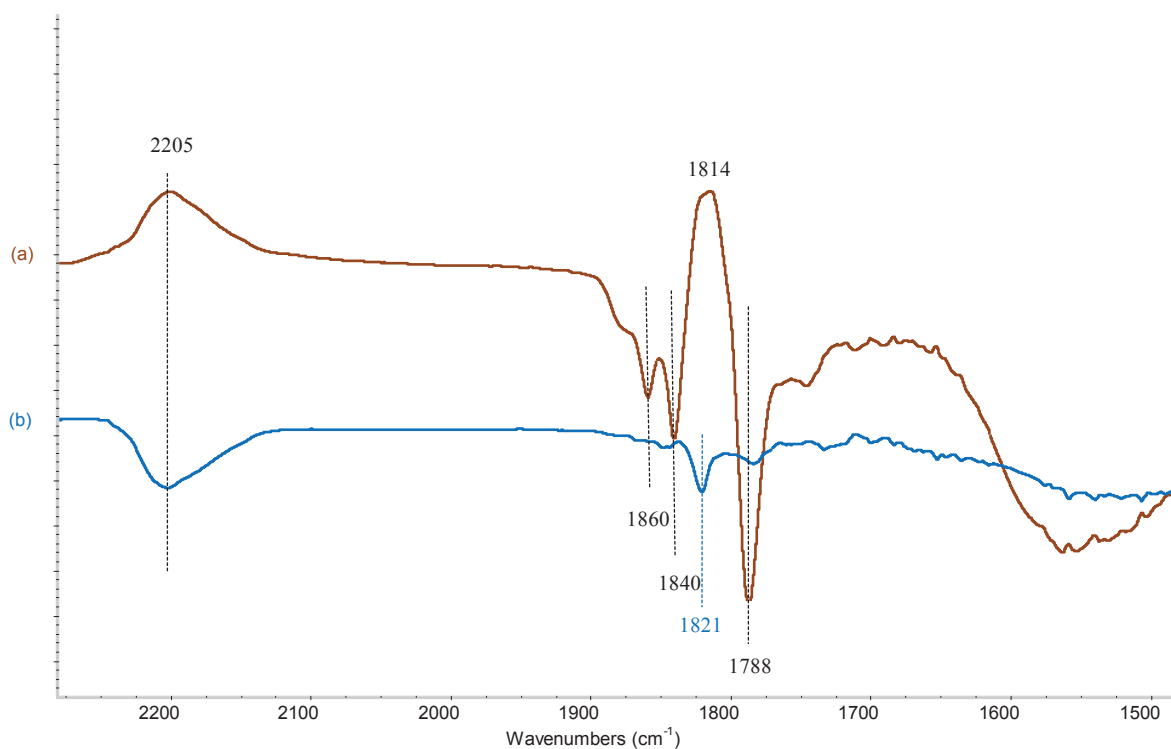


Figure 17: Enlarged region of $2250\text{-}1500\text{ cm}^{-1}$ for the subtraction of the spectra: (a) $^{15}\text{N}_2$ addition to the starting tantalum hydrides; (b) after the vacuum treatment to the sample.

An expected shift around 75 cm^{-1} for $^{14}\text{N}_2$ - $^{15}\text{N}_2$ substitution in $\nu(\text{N}_2)$ end-on type bonding is observed after the reaction with labelled dinitrogen which gives the peak of coordinated dinitrogen at 2205 cm^{-1} on the tantalum hydride complex **1**. There is no shift for the rest of the peaks in the region of 1900 - 1750 cm^{-1} .

Ongoing solid state ^{15}N CP MAS NMR measurements of this sample are being performed from the reaction of $^{15}\text{N}_2$ with $[(\equiv\text{SiO})_2\text{TaD}_x]$ followed by vacuum treatment (That is when there is no residual $\nu(^{15}\text{N}_2)$ is observed by in situ IR spectroscopy). The preliminary results show the presence of $^{15}\text{N}_2$ peak around 18 ppm, probably suggesting nitrogen containing tantalum compound (Figure 18) which is substantially different from the $^{15}\text{N}_2$ NMR resonances of previously observed in a system (viz. -400 ppm for NH_3 adduct, -270 ppm for tantalum amido species and -100 ppm for tantalum imido species (See Figure 5 in Chapter II).

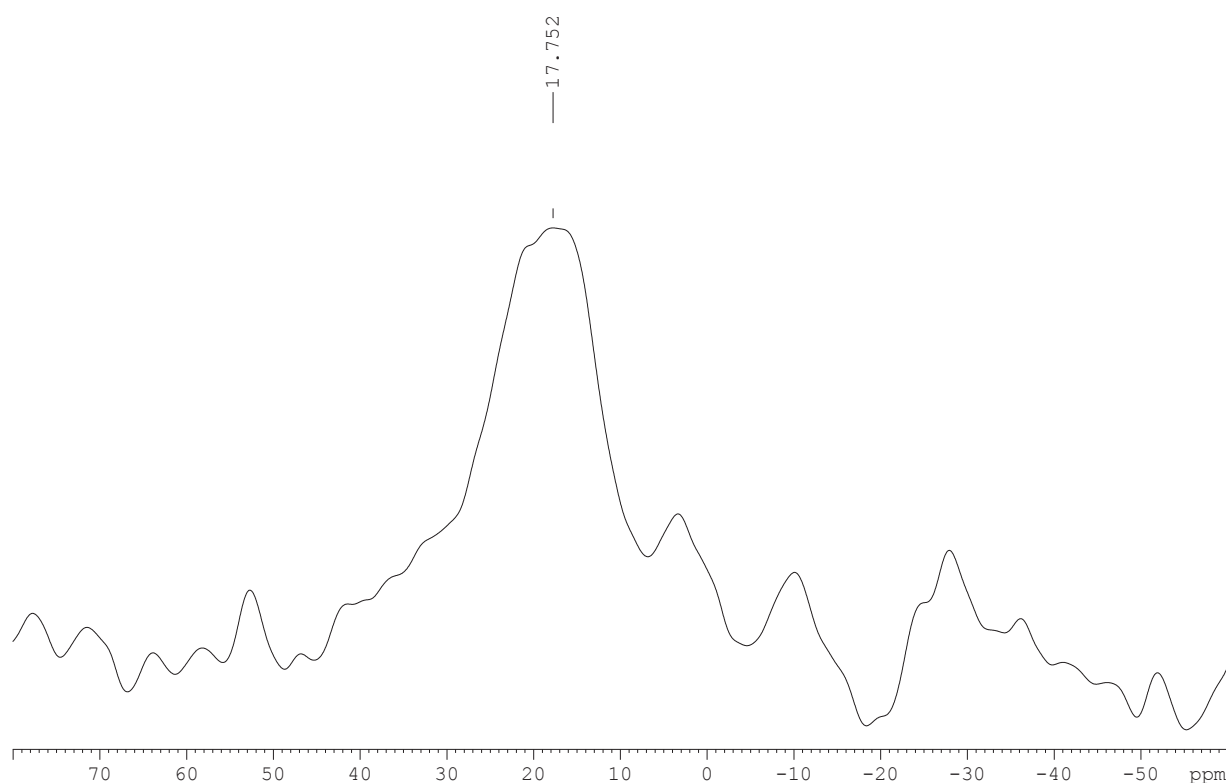


Figure 18: Enlarged region of 70-(-50) ppm from the results of ^{15}N CP MAS NMR spectrum of the $^{15}\text{N}_2$ labelled $[(\equiv\text{SiO})_2\text{TaD}_x (x: 1, 3)]$ at room temperature followed by 15 min of vacuum treatment. [NS: d: secp15: mgHz LB: Hz]

II.1.3 Reaction of $[(\equiv\text{SiO})_2\text{TaD}_x (x: 1, 3)]$ with N_2

$[(\equiv\text{SiO})_2\text{TaD}_x (x: 1, 3)]$ complex is prepared from the reaction of D_2 (600 Torr) either with tantalum grafted species or with tantalum hydrides at $150\text{ }^\circ\text{C}$ overnight. The goal was to avoid the characteristic peak of $\nu(\text{Ta-H})$ at 1834 cm^{-1} which overlaps with the peaks in $1900\text{-}1800\text{ cm}^{-1}$ region (corresponding possibly to different coordination modes of dinitrogen to the complex). As expected, there is no peak at 1834 cm^{-1} corresponding $\nu(\text{Ta-H})$ but at 2760 cm^{-1} for the deuterated residual silanols $\nu(\text{Si-OD})$ (Figure 19-a).

Figure 19 shows the steps of N_2 addition and vacuum treatment to the deuterated tantalum species. The reaction of dinitrogen over tantalum deuterated species at room temperature gives a peak at 2280 cm^{-1} as previously observed in other experiments. After each N_2 addition, the vacuum is applied to the system and the results are monitored by *in situ* infrared spectroscopy showing the reversible coordination of N_2 .

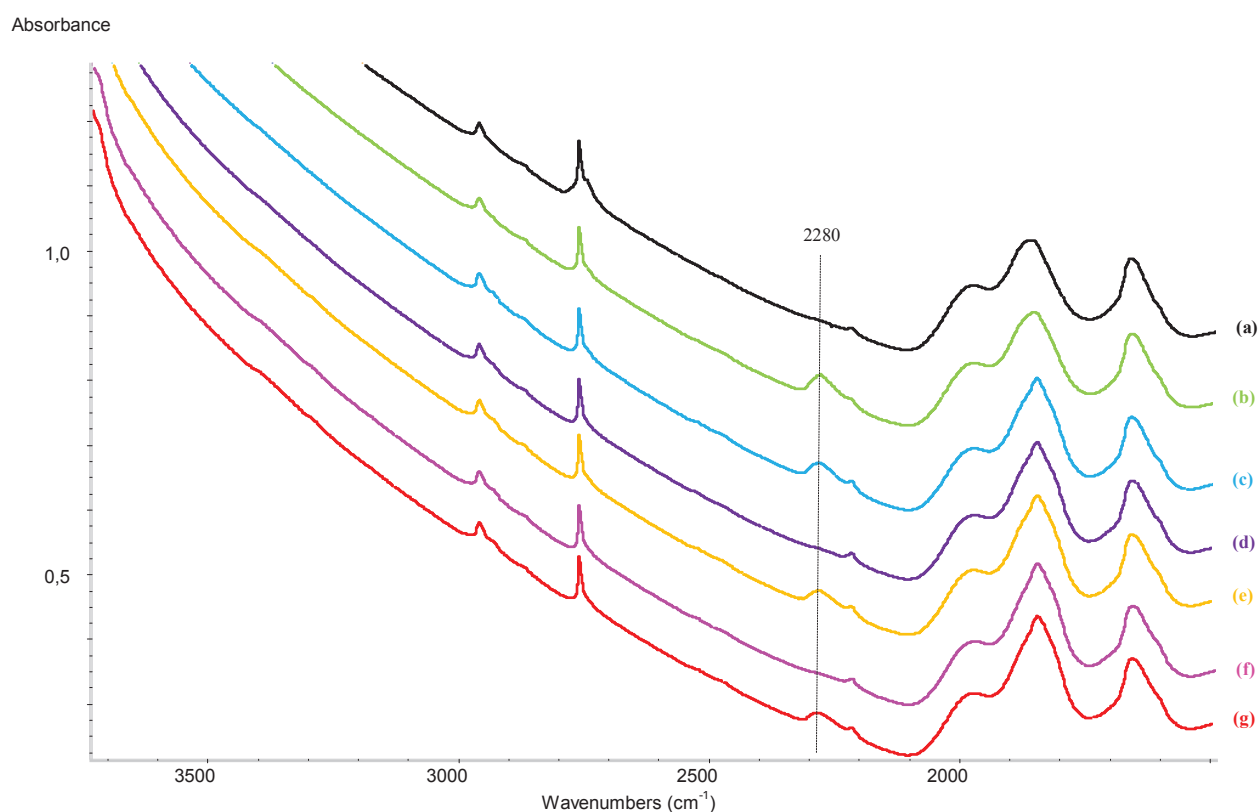


Figure 19: The spectra of (a) starting deuterated tantalum complex; (b) N_2 addition at room temperature (RT); (c) after 1 Night at RT; (d) 1st vacuum treatment to the sample; (e) 2nd N_2 addition at RT; (f) 2nd vacuum treatment; (g) last dinitrogen addition to the system.

Subtractions of the spectra for each step show the appearance of the peak at 2280 cm^{-1} for every dinitrogen addition with the decreases at 1850, 1825 and 1807 cm^{-1} and under vacuum treatment, the peak at 2280 cm^{-1} disappears with the decreases of the peaks at 1837 and 1820 cm^{-1} (Figure 20).

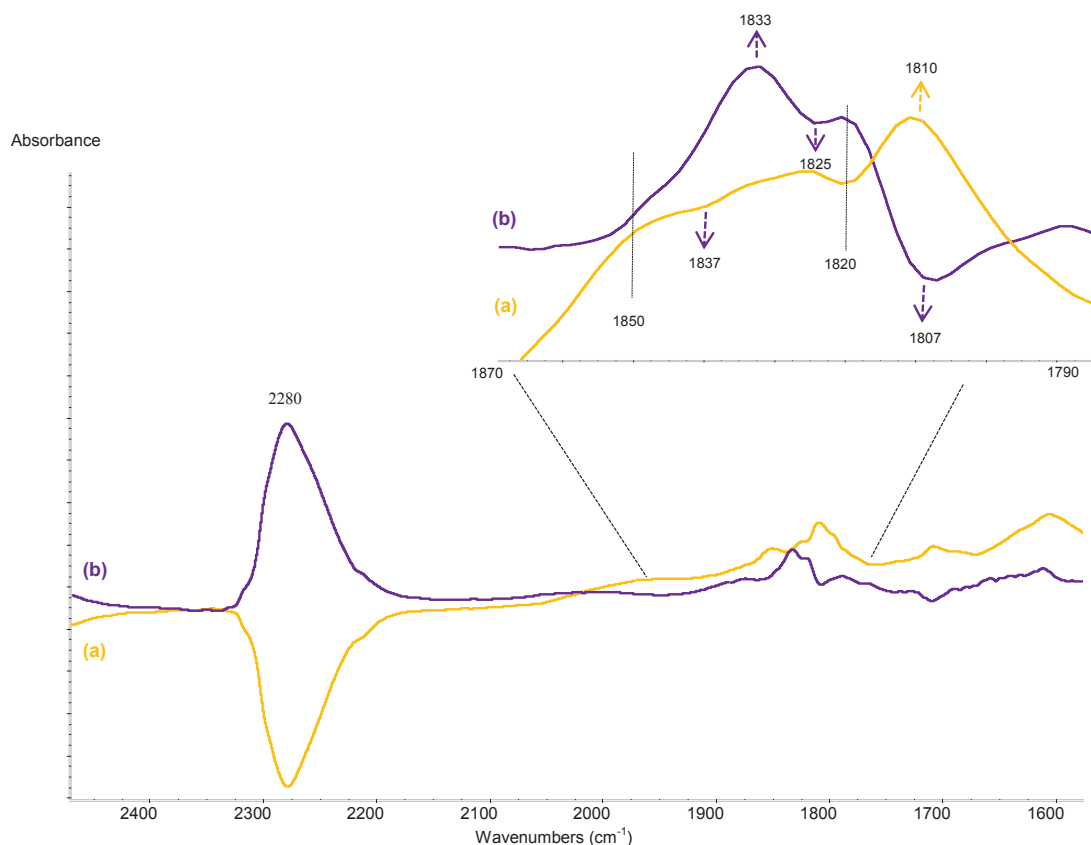


Figure 20: The subtracted spectra of starting deuterated tantalum complex with N_2 at room temperature; (a) vacuum treatment to the sample; (b) 2nd N_2 addition at RT.

If N_2 is replaced by $^{15}\text{N}_2$, the already observed shifted peak at 2205 cm^{-1} appears, but no isotopically shifted band appears in the 1900- 1800 cm^{-1} region. Therefore, there is no IR evidence for a second N_2 adduct with respect to the ones reported in Figure 20.

Collectively, the above experiments with N_2 and $^{15}\text{N}_2$ on the starting hydrides suggest the involvement of at least two dinitrogen adducts: one which is IR active ($\nu(\text{N}_2) = 2280 \text{ cm}^{-1}$) and loses N_2 under vacuum, the other one is IR silent but NMR active even after vacuum treatment.

II.2 Reaction of $[(\equiv\text{SiO})_2\text{TaH}_x (x: 1, 3)]$ with hydrazine

In order to have reduced intermediate (*hydrazido and diazenido*) species in the reduction of dinitrogen and to understand its mechanism by *in situ* analysis, the molecules with lower NH bond order “hydrazine, N_2H_4 and diazene, N_2H_2 ” are used over tantalum hydride complexes. Hydrazine is prepared from the monohydrated hydrazine over KOH stirred one night under argon as explained in the literature.^[100]

II.2.1 Reaction of $[(\equiv\text{SiO})_2\text{TaH}_x (x: 1, 3)]$ with N_2H_4

Upon addition of hydrazine to $[(\equiv\text{SiO})_2\text{TaH}_x (x: 1, 3)]$ complex at room temperature, complete consumption of the $\nu(\text{Ta-H})$ band is observed. The new bands corresponding to hydrazine ($\nu(\text{NH})$: 3359, 3283, 3190 cm^{-1} ; $\delta(\text{NH}_2)$: 1605 cm^{-1}) are distinct from hydrazine physisorbed on silica ($\nu(\text{NH})$: 3362, 3290, 3197 cm^{-1} ; $\delta(\text{NH}_2)$: 1612 cm^{-1}). At the same time, no increase in the characteristic $\delta(\text{NH}_2)$ bands at 1520 cm^{-1} for $\delta(\text{Ta-NH}_2)$ and 1550 cm^{-1} for $\delta(\text{Si-NH}_2)$ observed (Figure 21 and 22).

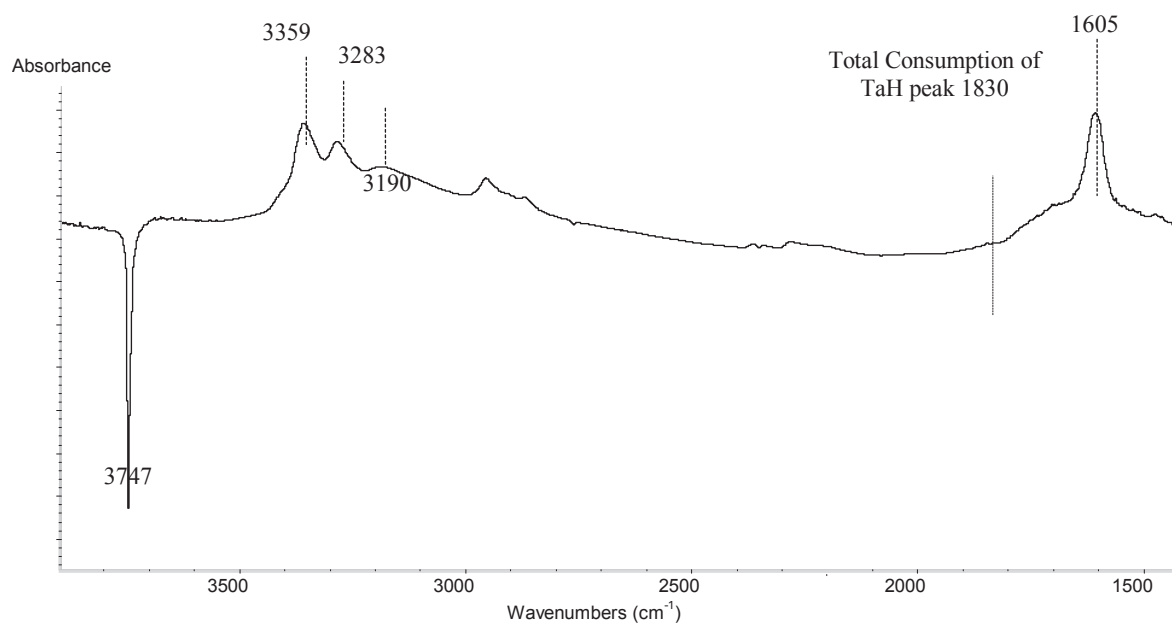


Figure 21: Subtracted spectrum of $[(\equiv\text{SiO})_2\text{TaH}_x (x: 1, 3)]$ immediately after addition of hydrazine at RT.

Unlike ammonia, the activation of hydrazine does not proceed at room temperature. However, hydrazine is fairly strongly coordinated, as placing the system under high vacuum (10^{-5} torr) is insufficient to remove it. Different experiments show that an excess of hydrazine is needed to consume the total of tantalum hydrides and new peaks at N-H region appear from 100 °C.

Figure 22 represents the reaction of hydrazine with complex **1** immediately at room temperature and the new peaks corresponding physisorbed hydrazine on the sample at 3362, 3290, 3197 and 1612 cm^{-1} (Fig.22.a-b). After heating the sample at 100 °C, we observe the appearance of new peaks at 3494, 3458, 3374 and 3294 cm^{-1} corresponding to the coordinated hydrazine (Fig.22.c).

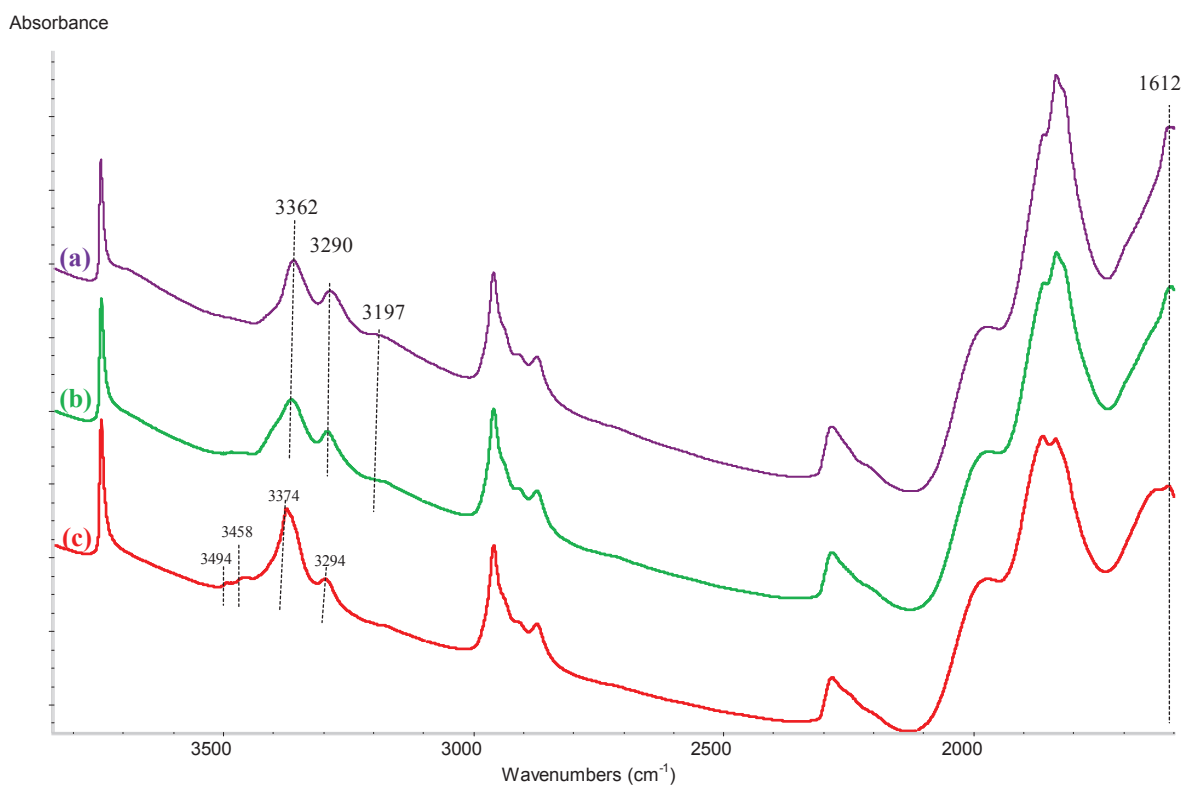


Figure 22: Spectra presenting the reaction of hydrazine over $[(\equiv\text{SiO})_2\text{TaH}_x]$ species; (a) immediately after addition at RT, (b) after 1h at RT and the physisorbed hydrazine is collected in a cold finger, (c) at 100 °C for 1 hour under static vacuum.

A similar reaction is observed by addition of hydrazine onto complex $[(\equiv\text{SiO})_2\text{TaH}_1]$ enriched **1** (Figure 23)

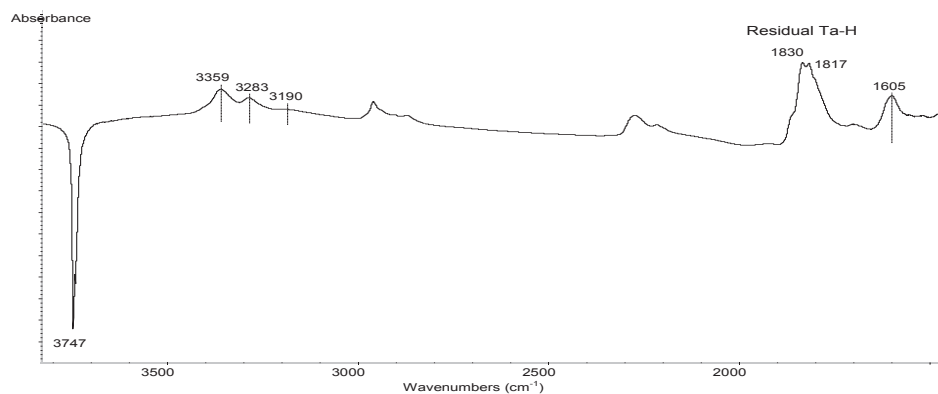


Figure 23: MCM-41-subtracted spectrum of $[(=SiO)_2TaH_1]$ immediately after addition of hydrazine at room temperature.

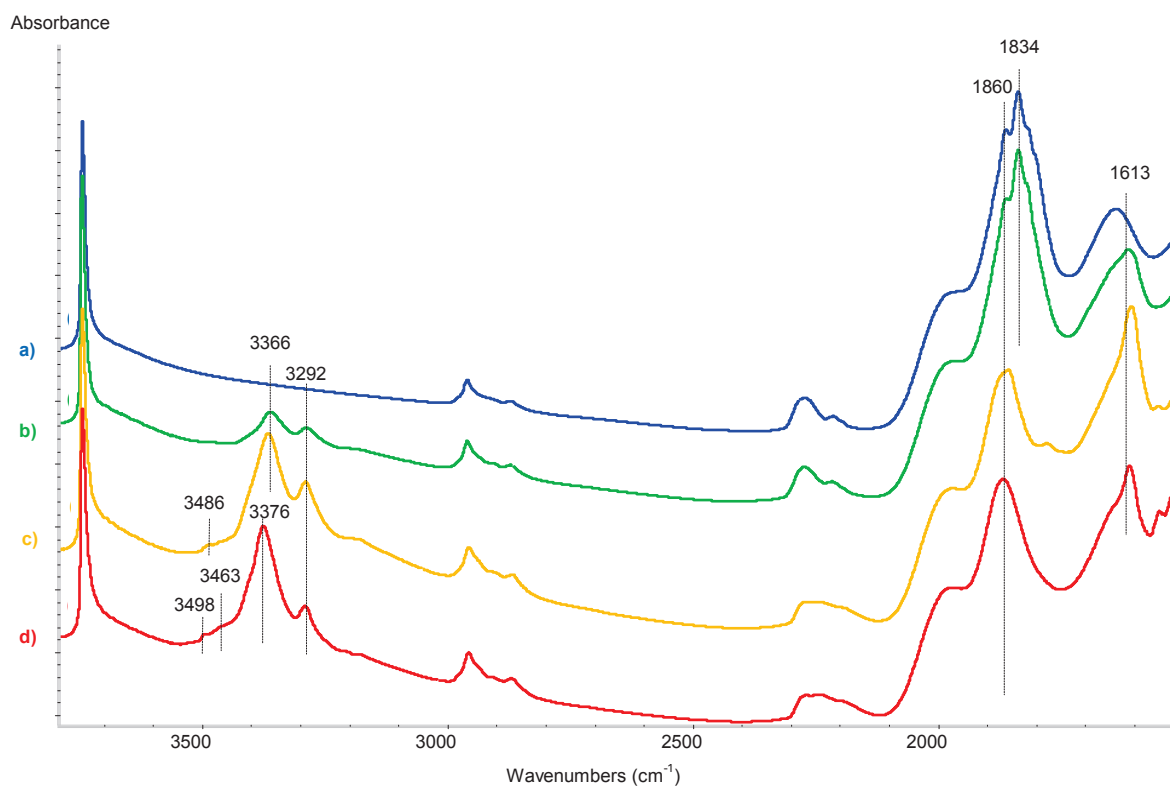


Figure 24: Spectra of (a) starting tantalum monohydride enriched **1**, (b) addition of hydrazine at room temperature to TaH_1 enriched **1** complex, (c) hydrazine in excess at room temperature for one night (d) after heating the system at 80 °C for 8h.

Small increases in the band corresponding to $\delta(\text{Ta-NH}_2)$ are observed after second addition of hydrazine in addition to the storage at room temperature overnight (Figure 24-c) and $\nu(\text{NH})$ bands more or less identical to the experiment with TaH_x . Finally, the last spectrum corresponds to the sample with the new peaks at 3498, 3463, 3376 and 3292 cm^{-1} after heating at 80 °C for 8 h.

In the experiment of TaH_1 enriched **1** with hydrazine, H_2 is added afterwards to the reaction in order to determine if regenerating the trishydride species and if the addition of a reducing atmosphere would lead to formation of the final imido amido product (Figure 25).

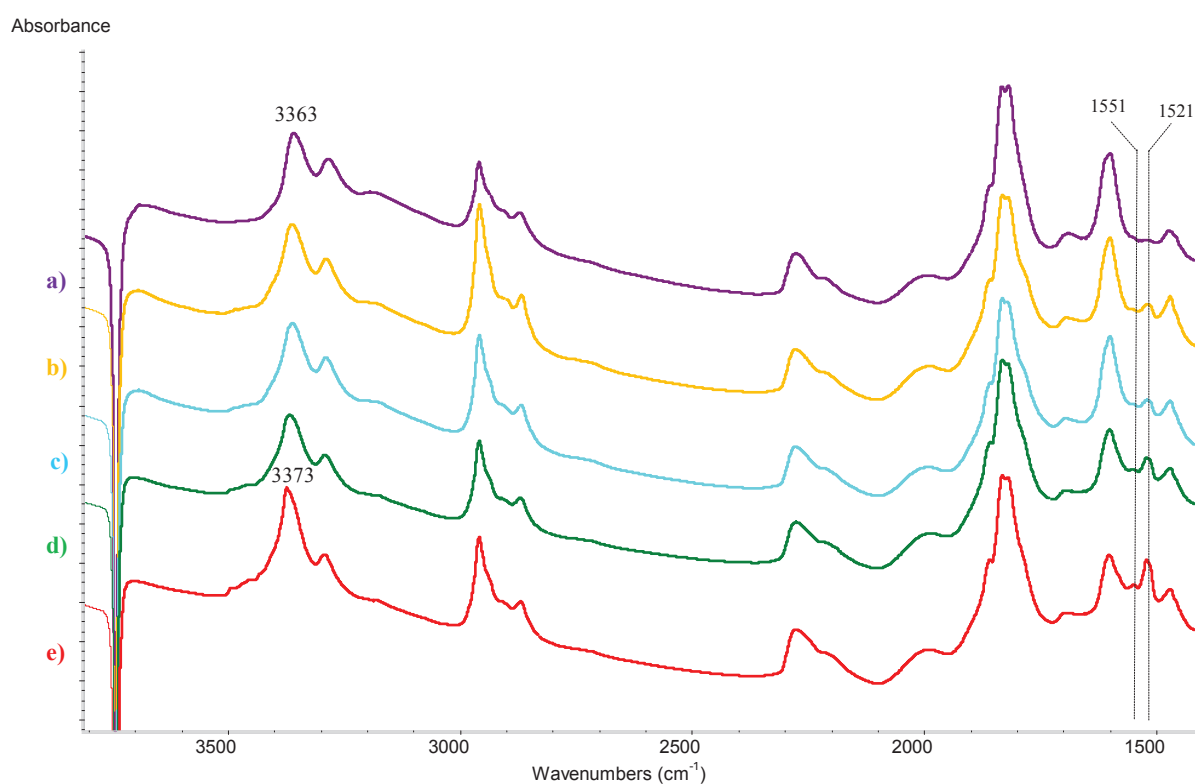


Figure 25: Subtracted spectra for the evolution of (a) TaH_1 enriched **1** with N_2H_4 , (b) immediately after addition of H_2 ; (c): after 2 h at RT; (d) heating at 80 °C for 1h; (e) 100 °C for 1h.

Although regeneration of the Ta-H band is observed, there are no bands increasing in the $\delta(\text{NH}_2)$ region. Heating till 100 °C is necessary to observe increases in the peaks at 3495, 3463, 3452, 3434, 3375 and 3295 cm^{-1} corresponding to the final silica grafted tantalum imido amido complex (Figure 26).

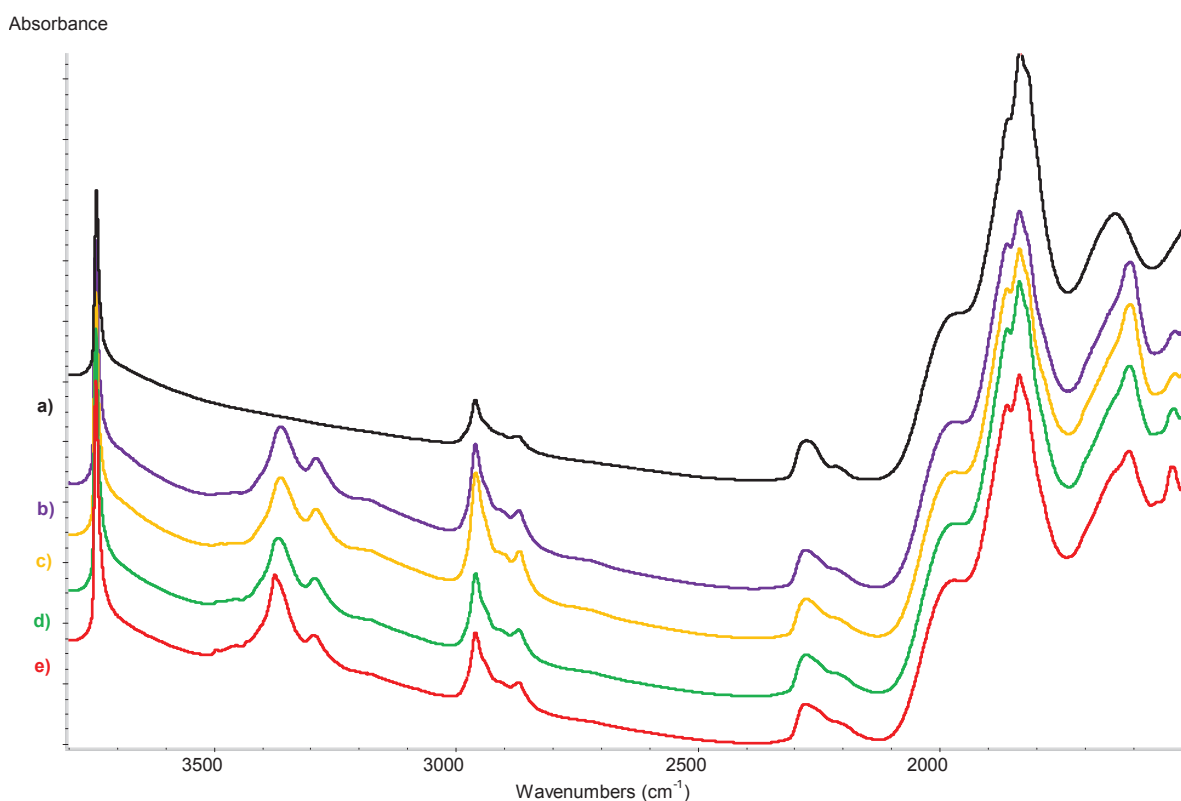


Figure 26: Evolution of (a) tantalum monohydride enriched **1** species; (b) hydrazine addition at room temperature; (c) under H₂ at RT; (d) heating at 80°C for 1h; (e) 100°C for 1h.

We observed by blank experiments on hydrazine over a calcinated silica pellet at different temperatures, that no spontaneous decomposition of N₂H₄ occurs below 150 °C on silica, suggesting that our observed reactivity of N₂H₄ on **1** is due to N₂H₄ coordination chemistry on tantalum. The spectra of N₂H₄ on silica are given below in Figure 27:

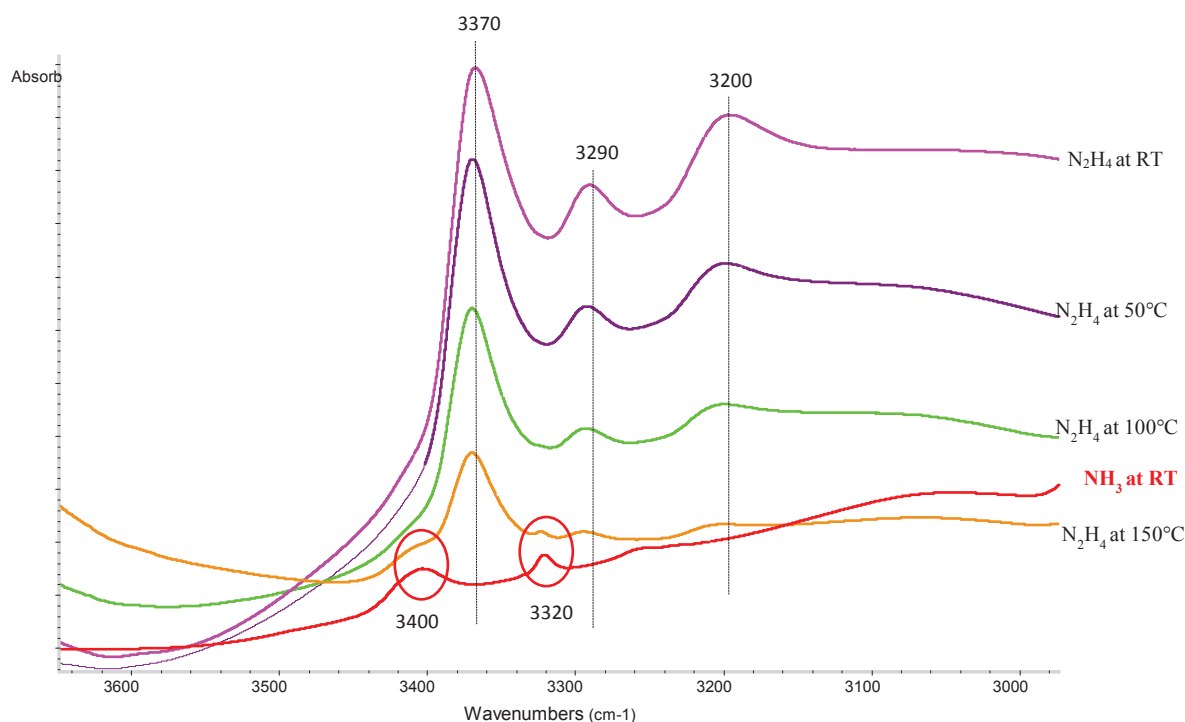


Figure 27: The evolution of the pellet silica in the presence of hydrazine at different temperatures and the comparison with ammonia at room temperature.

The IR spectrum of ammonia on silica is characterized by two signals in the region of the NH bands at 3400 and 3320 cm^{-1} (red spectrum). IR Spectrum of hydrazine physisorbed on silica at room temperature shows three signals distinct from those of ammonia (3370, 3290 and 3200 cm^{-1}). Thermal treatment at 50 °C and 100 °C does not seem to lead to decomposition of hydrazine to ammonia. Nevertheless, after 1h at 150 °C, two characteristic signals of ammonia at 3400 and 3200 cm^{-1} are weakly visible. This indicates the presence of a very small amount of ammonia while hydrazine majority presents on the pellet, peak at 3370 cm^{-1} .

II.2.2 Reaction of $[(\equiv\text{SiO})_2\text{TaH}_x]$ with $^{15}\text{N}_2\text{H}_4$

Analogously to the previous experiments, labelled hydrazine was added to the reactor containing a pellet of $[(\equiv\text{SiO})_2\text{TaH}_x]$. Bands in the $\nu(\text{NH})$ and $\delta(\text{NH}_2)$ region confirmed the presence of ^{15}N -hydrazine on the pellet with an expected redshift of 8 cm^{-1} ($\nu(\text{NH})$: 3348, 3278, 3189 cm^{-1} ; $\delta(\text{NH}_2)$: 1608 cm^{-1}). For each addition, slight perturbations in the intensity of the Ta-H band are observed, but no true consumption is observed until the pellet is heated at 100°C (Figure 28).

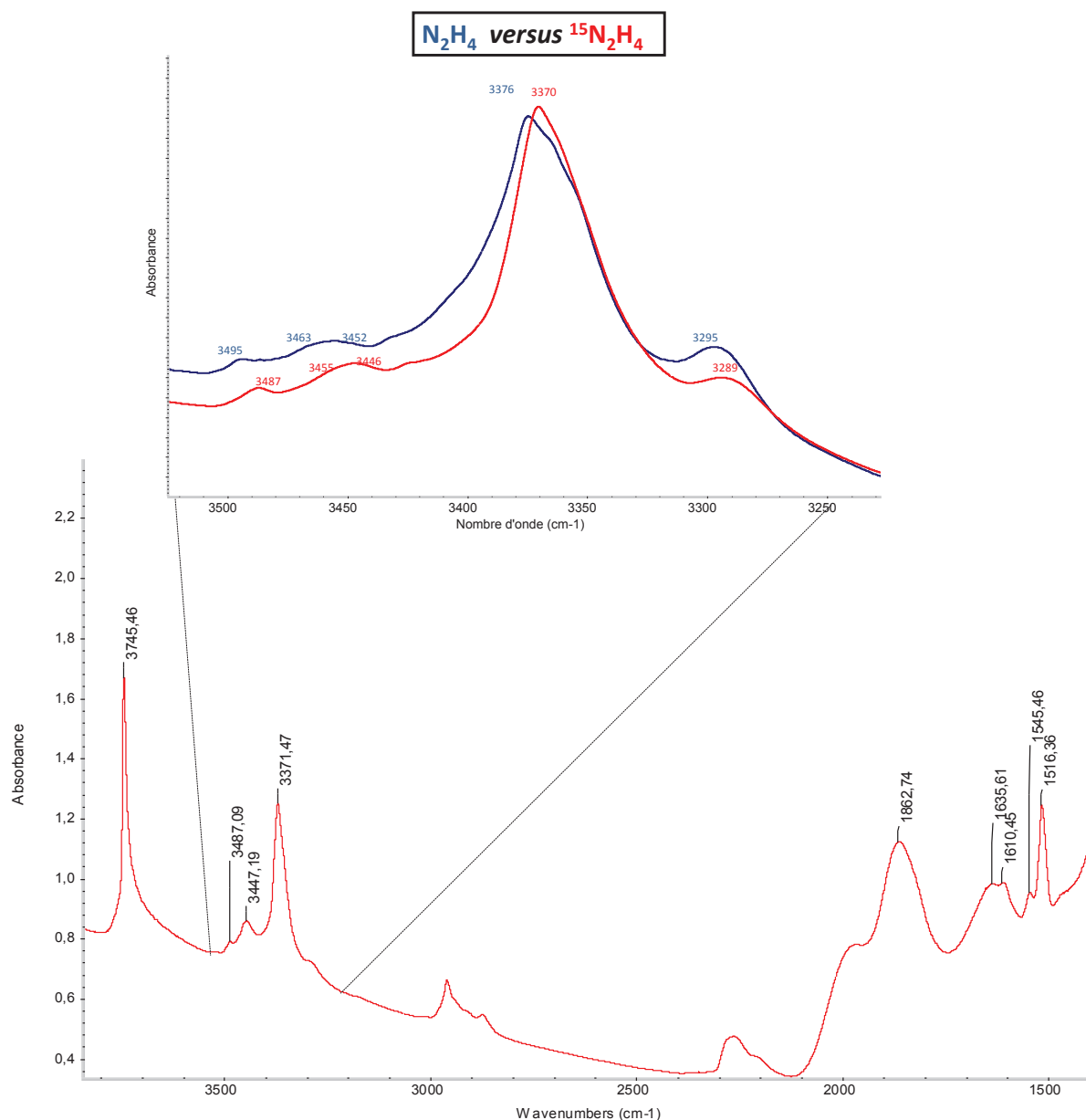


Figure 28: IR spectrum of the final product: $^{15}\text{N}_2\text{H}_4$ over TaH_x at $100\text{ }^\circ\text{C}$ 2h. Enlarged spectra comparing the values for the reaction of tantalum hydrides with normal (blue line) and labeled hydrazine (red line) for the N-H region ($3550\text{-}3250\text{ cm}^{-1}$).

Heating the sample at $100\text{ }^\circ\text{C}$ for 2 h gave the peaks at 1516 and 1545 cm^{-1} leading the $\text{Ta-}^{15}\text{NH}_2$ and $\text{Si-}^{15}\text{NH}_2$ respectively. Both the shape of the peaks and the isotopic shifts in the $\nu(\text{NH})$ regions are similar to those for the imido amido species synthesized from reaction of TaH_x with $^{15}\text{NH}_3$ (from hydrazine: $3487, 3447, 3371, 3289\text{ cm}^{-1}$; $1545, 1516\text{ cm}^{-1}$; from ammonia: $3490, 3454, 3372, 3289\text{ cm}^{-1}$; $1546, 1516\text{ cm}^{-1}$).

In summary the reaction with hydrazine shows that hydrazine on complex **1** does not lead to the formation of the previously observed intermediate I_2 , since no band at 3400 cm^{-1} is

observed and that the evolution of the hydrazine to complex **1** in the system to obtain the final imido amido **2** occurs below 100°C while temperatures above 100°C transforms I₂ to final complex **2**.

II.3. Attempts to monitor reaction of $[(\equiv\text{SiO})_2\text{TaH}_x (x: 1, 3)]$ with diazene

Diazene is difficult to use in reactions due to its easily decomposition to N₂ and H₂, hydrazine and H₂ and NH₃. Several studies have been reported in order to obtain N₂H₂ under specific conditions (metastable phase gas pressure less than 10⁻³ Torr.). The method for our experiment has been detailed in the experimental section.

Figure 29 shows the addition of diazene to the silica supported tantalum hydride mixture at room temperature.

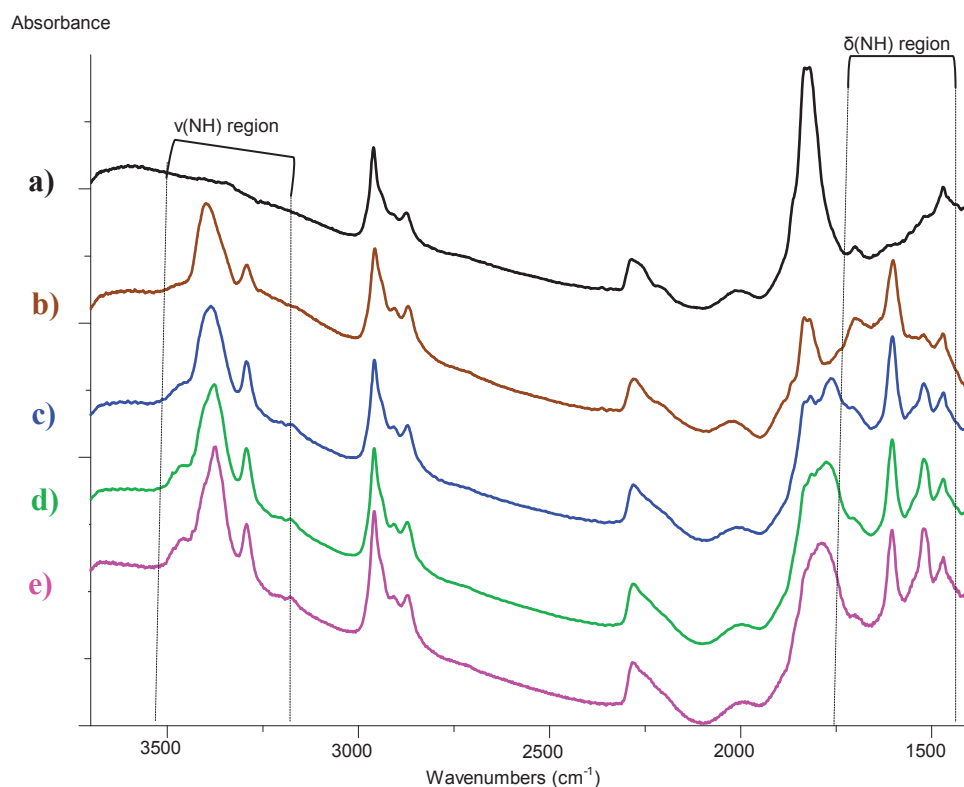


Figure 29: Reaction of diazene on (a) the starting tantalum hydride mixture, (b) addition of N₂H₂ at room temperature, (c) excess of N₂H₂ on the sample, (d) 2h at RT, (e) after 1N at RT.

This reaction leads to an intermediate displaying $\nu(\text{NH}) = 3400 \text{ cm}^{-1}$ which was also observed by *in situ* IR spectroscopy when diazene is contacted with tris hydride enriched material $[(\equiv\text{SiO})\text{TaH}_3]$.

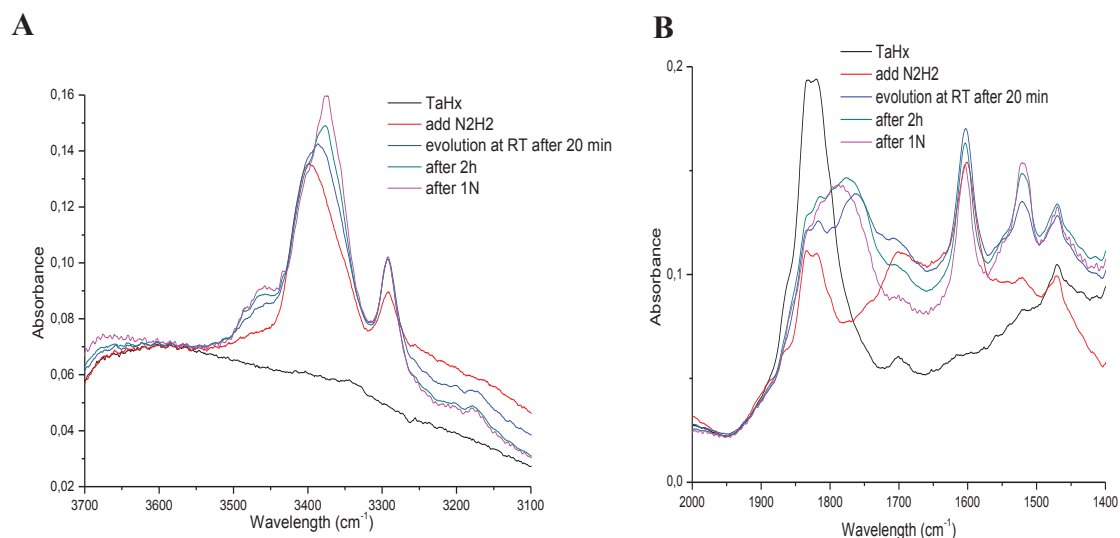


Figure 30: Enlarged spectra for the evolution of diazene addition to the $[(\equiv\text{SiO})_2\text{TaH}_x]$ ($x: 1, 3$) complex at room temperature (Regions: **A**- 3700- 3100 cm^{-1} ; **B**- 2000-1400 cm^{-1}).

Since diazene is known to undergo decomposition to, *inter alia*, NH_3 , at moderate temperatures (80- 100 $^\circ\text{C}$), we cannot say if the peaks corresponding $[(\equiv\text{SiO})_2\text{Ta}(\text{=NH})(\text{NH}_2)]$ are due to genuine reactivity of $[(\equiv\text{SiO})_2\text{Ta-H}(\text{HN-NH})]$ at high temperatures or parasite reaction with decomposition product NH_3 .

The blank tests on N_2H_4 on calcinated MCM-41 confirmed the presence of ammonia from the first moment of pellet exposure to the diazene vapour by decomposition at room temperature (Figure 31).

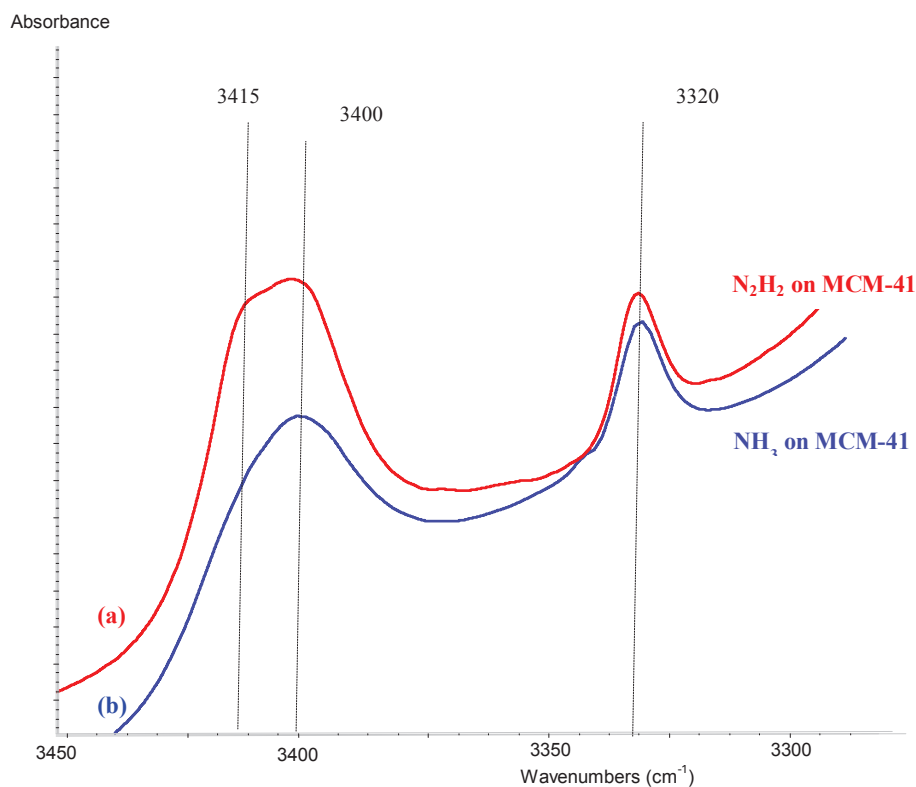


Figure 31: Comparison of the spectra of (a) diazene and (b) ammonia addition on calcinated MCM-41₅₀₀ at room temperature.

Even after various experiments have been carried out on tantalum hydrides with diazene, it is not possible to obtain straightforward data on these reactions. While diazene exposure to **1** leads to the observation of a peak at 3400 cm⁻¹, corresponding I₂, existence of a similar band in the spectra of physisorbed diazene as well as physisorbed ammonia, adventitiously present in N₂H₂, doesn't allow to assert that intermediate I₂ is certainly appeared by reaction of N₂H₂ with tantalum hydrides, **1**. Therefore, the results are not able to be used to infer information on the mechanism of dinitrogen cleavage by H₂ on TaH_x as diazene is coproduced with traces of ammonia already at room temperature.

III. DISCUSSION

The reactions of tantalum hydride mixture and monohydride enriched **1** complex with dinitrogen ($^{14}\text{N}_2$ and $^{15}\text{N}_2$), hydrazine ($^{15}\text{N}_2\text{H}_4$ and $^{15}\text{N}_2\text{H}_4$) and diazene were studied by *in situ* IR, solid state NMR as well as elemental analysis. Recent DFT calculations with **2q** cluster model by our co-workers *Odile Eisenstein* and *Xavier Solans-Monfort* for the reaction of tantalum hydrides with dinitrogen in the absence and presence of dihydrogen at room temperature and at 250 °C were also reported concomitantly. Here, we will propose and discuss stepwise succession of elementary steps for our observed dinitrogen cleavage and link them to these calculations and experimental studies described above.

Step1:

Formation of N_2 adducts $(\equiv\text{SiO})_2\text{TaH}_x(-\text{N}_2)$ *x*: 1, 3

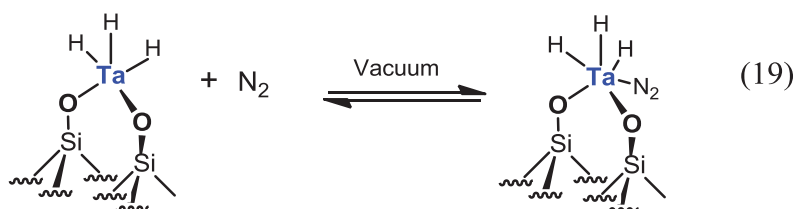
As previously described in the introduction part, dinitrogen coordinates to the transition metal center(s) via several modes. N_2 activation mostly correlates with its coordination mode in addition to the elongation of $\text{N}\equiv\text{N}$ bond. During our experiments, we observed a peak at 2280 cm^{-1} (a red shift of 50 cm^{-1} comparing to the free $\nu(\text{NN})$) by *in situ* IR spectroscopy from the reaction of tantalum hydride complexes (**1**, monohydride enriched **1** and **1-d**) with dinitrogen at room temperature which disappeared under vacuum and that is isotopically shifted to 2205 cm^{-1} when $^{15}\text{N}_2$ is used instead of $^{14}\text{N}_2$ (Figure 16).

The most commonly observed coordination in the literature for mononuclear transition metal dinitrogen complexes has been reported as end-on (η^1) bonding which is characterized by a NN distance not significantly elongated with respect to the free $\text{N}\equiv\text{N}$ distance (1.12 Å vs. 1.097 Å).^[16, 30, 101-104] This bonding of dinitrogen can be described in a similar manner to the isoelectronic CO, involving σ -donation from N_2 moiety to the metal and same backdonation to N_2 antibonding orbital depending on the backbonding capacity of the metal.^[105-108] The end-on coordinated dinitrogen can be therefore described as particularly weakly activated in our case.

DFT calculations have been done for our experiment on a model that has already been used in our previous studies (see the experimental section) and described the pathways of dinitrogen

coordination in more details. The results^[68] give a calculated red shift of 16 cm⁻¹ with respect to the free N₂ upon end-on coordination of N₂ to the trishydride.

While end-on coordination of N₂ to the tantalum monohydride is calculated to give a red shift of 405 cm⁻¹, side-on coordination of dinitrogen on the same species was reported to shift around 700 cm⁻¹. Our experimentally observed weak red shift (-80 cm⁻¹) with respect to free N₂ is compatible with first adduct and intermediate I₁ is therefore assigned to [(≡SiO)₂TaH₃(-N₂)]. The weak activation is consistent with the reversibility of dinitrogen coordination (see Eq. 19). The d⁰ configuration of [(≡SiO)₂TaH₃], which prevents substantial backdonation is in full agreement with the observed weak activation.



The experiments of N₂ (and ¹⁵N₂) coordination on [(≡SiO)₂TaD_x] (Figure 19) allowed to explore the eventual formation of N₂ adducts in the 1900- 1800 cm⁻¹ region that is the expected region suggested by DFT calculation for end-on adducts on the monohydride. Such exploration is not possible in the experiments with [(≡SiO)₂TaH_x (x: 1, 3)], as it would overshadow the putative ν(N₂) for (≡SiO)₂TaH_x(-N₂). The lack of peaks around 1900 cm⁻¹ upon N₂ addition to [(≡SiO)₂TaD_x] that fail to shift by about 90 cm⁻¹ when ¹⁵N₂ is used instead of ¹⁴N₂ suggest that such adduct (≡SiO)₂TaH_x(-N₂) is not present in our system. The peaks that we observe are possible due to traces of residual [(≡SiO)₂TaH_x (x: 1, 3)] present in our [(≡SiO)₂TaD_x] sample.

Formation of side-on N₂ complexes (≡SiO)₂TaH_x(η²-N₂) x: 1, 3

Surprisingly, studies by solid state ¹⁵N CP- MAS NMR and elemental analysis of the isolated hydride sample exposed to ¹⁵N₂ and heated under vacuum (therefore without (≡SiO)₂TaH_x(-N₂) species, see Eq.19) display ¹⁵N resonances and contain substantial amount of nitrogen (e.a. N/ Ta by e.a.=0.95).

One possible exciting explanation could be the formation of the side on adduct $[(\equiv\text{SiO})_2\text{TaH}(\eta^2\text{-N}_2)]$, that calculation suggested thermodynamically stable and kinetically accessible for our system.

There has been no example in the literature for the mononuclear side-on bonding mode structurally characterized in the solid state as this bounding considered less favorable for the late transition metal^[105] except for, possibly zirconium (III) system $\text{Cp}_2\text{Zr}(\text{CH}_2\text{CMe}_3)(\eta^2\text{-N}_2)$ with the spectroscopic evidence of side-on N_2 bonding in 1978.^[109] Contrarily to the mononuclear complexes, dinitrogen can coordinate to the dinuclear transition metal complexes in multiple ways (as shown in Table 5) and prefers most commonly the side-on bonding due to the σ donation from the occupied orbitals of N_2 to the metal and a σ^* back-donation from the metal to the empty σ^* orbitals of the N_2 . For this reason, in principle, side-on coordination is only possible for late transition metals which have doubly occupied σ orbitals. Furthermore, this strong back-donation from the transition metal center(s) to the σ^* antibonding orbitals of N-N leads to a more significant elongation and activation of the $\text{N}\equiv\text{N}$ bond.

It has been also reported that group 4 transition metals generally form dinuclear complexes containing a dinitrogen ligand between two metal centers (bridging), commonly in a $\mu\text{-}\eta^1:\eta^1$ geometry. In addition, the activation of coordinated dinitrogen shows an increase by going to the left in the d-block.^[62] The first structurally characterized dinitrogen complex was reported in 1988 producing a dinuclear samarocene complex $((\eta^2\text{-C}_5\text{Me}_5)_2\text{Sm})_2(\mu\text{-}\eta^2:\eta^2\text{-N}_2)$ with the side-on $\text{N}\equiv\text{N}$ bond length of 1.088 Å, hardly changed from the bond length of free N_2 .^[110] A similar observation was made later with the tris(amido)amine complex of U(III) where the side $\text{N}\equiv\text{N}$ bond distance was 1.109 Å.^[111] Both of these species showed to lose dinitrogen readily under vacuum as described for our reactions whereas none of them are monometallic as in our case.

The calculations show that for tantalum monohydride species, side-on coordination is more favorable in terms of stability due to the significant backdonation from d^2 Ta center and also direct side-on coordination of N_2 to the TaH_1 . The distance of side-on $\text{N}=\text{N}$ bounding is calculated as 1.21 Å for both TaH_1 and TaH_3 complexes while this coordination to the tantalum trishydride lead to the reductive coupling of dihydrogen molecule. The fact of

having longer N=N bond distances in our case than the examples given above might be due to a stronger coordination of dinitrogen over monometallic tantalum center.^[16, 24, 28, 63, 104, 112-117]

The computational results of the side-on coupling dinitrogen coordination in our case have been given larger red shifts ($\Delta\nu < -750 \text{ cm}^{-1}$) which are in principle silent in the infrared spectroscopy. That was most probably the reason of not being able to observe the peaks for side-on dinitrogen coordination of tantalum complexes during our experiments. Studies are ongoing to attempt RAMAN, EXAFS measurements as well as solid state NMR experiments on our samples.

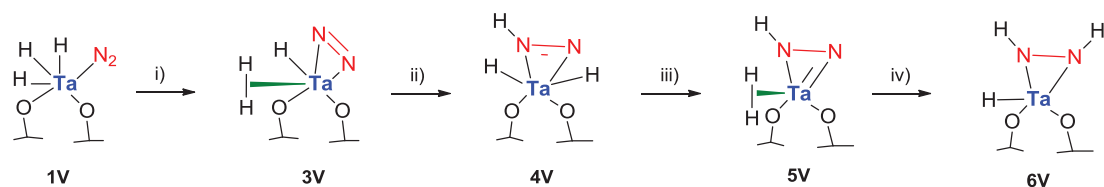
Step 2:

Formation of side-on H_2 complex $(\equiv\text{SiO})_2\text{Ta}(-H_2)(\eta^2-N_2H)$:

The reaction of dinitrogen to the complex **1** and $[(\equiv\text{SiO})_2\text{TaH}_1]$ enriched **1** is later studied at 250 °C by *in-situ* IR and elemental analysis. Although the elemental analyses of both compounds are quite similar; a band at 3400 cm^{-1} is observed for **1** corresponding to TaN_2H_x stretching frequency but not for the tantalum monohydride enriched **1**.

These results could be better understood with the help of the DFT calculations. The calculated unscaled $\nu(\text{NH})$ frequencies in $\text{TaH}_2(\text{N}_2\text{H})$ are between 3566 and 3468 cm^{-1} , which are close to the band observed around 3400 cm^{-1} . Noteworthy, calculations suggest that such complex can be obtained from trishydride complex by:

- i) dihydride reductive coupling to the metal center leading $[(\equiv\text{SiO})_2\text{TaH}(\eta^2-H_2)(\eta^2-N_2)]$ as a key intermediate of the reaction mechanism,
- ii) proton transfer from coordinated dihydrogen to the coordinated N_2 (to yield $[(\equiv\text{SiO})_2\text{TaH}_2(\text{NNH})]$, called **3V** (see scheme 21),
- iii) a further reductive coupling of the dihydride to a dihydrogen,
- iv) followed by another proton transfer to $[(\equiv\text{SiO})_2\text{TaH}(\text{N}_2\text{H}_2)]$ (see scheme 21),



Scheme 21

The scheme 21 presents such proposed elementary steps for the transfer of $[(\equiv\text{SiO})_2\text{TaH}_3(\text{N}_2)]$ (intermediate I_1) into $[(\equiv\text{SiO})_2\text{TaH}(\text{N}_2\text{H}_2)]$ (intermediate I_2).

Calculations show that the rate determining step for this succession of elementary steps is first the reductive coupling of dihydrogen (step i, $\Delta G_{523\text{K}}^\ddagger = 40.5$ kcal/ mol), all the successive step being substantially lower in energy. Conversely, the final diazenido adduct $[(\equiv\text{SiO})_2\text{TaH}(\text{N}_2\text{H}_2)]$, **6V** is not expected to further evolve (calculated ΔG^\ddagger for the next possible step, i.e. third hydride transfer to $[(\equiv\text{SiO})_2\text{Ta}(\text{NH}_2\text{-NH})]$ (**6V** \rightarrow **8V**) is almost 50 kcal/ mol) Therefore we assign such intermediate to the observed I_2 . The fact that such intermediate, observed by $(\text{NH}) = 3400$ cm^{-1} , doesn't appear as strongly when monohydride enriched sample; has been also understood due to the DFT proposal of the energy barriers.

While the succession of steps i)- iv) is quite original in N_2 chemistry, each separate step has relevant precedents in the literature. H_2 coordination to a transition metal complex was first discovered and well-established about 30 years ago in the stable $\text{W}(\text{CO})_3(\text{PiPr}_3)_2(\text{H}_2)$ complex by Kubas where the distance of H-H bond was 0.89 Å vs. 0.75 Å in free H_2 .^[118] This distance for our side-on H_2 tantalum complex, $(\equiv\text{SiO})_2\text{Ta}(\eta^2\text{-H}_2)(\eta^2\text{-N}_2\text{H})$ has been calculated around 0.79 Å similarly to the literature data.

Various examples have been reported in the literature for side-on H_2 binding to a transition metal center and it has been described that this dihydrogen molecule might undergo either an oxidative addition by the back donation from the metal center into the σ^* orbital of the H_2 ligand where the H-H bond split homolytically or alternatively, if there is a suitable base present, the dihydrogen split heterolytically to give a six-coordinate metal hydride product and a protonated base (increased σ donation from H_2 to the electrophilic metal center). This is an important reaction in dihydrogen chemistry since H_2 is not an acid ($\text{pK}_a \sim 35$) while

dihydrogen complexes can be very acidic with pKa values of less than 0.^[119-122] In the context of N₂ chemistry, Hidai had already shown that metal coordinated H₂ can protonate a metal-coordinated N₂ (see scheme 19). The heterolytic addition of hydrogen across a metal–nitrogen bond was first investigated systematically by Fryzuk and coworkers.^[123, 124] In the meantime, this reaction has been recognized as a key step in the very efficient catalytic hydrogenation of unsaturated substrates RR₁C=X, especially of ketones (X=O), which became known as metal–ligand bifunctional catalysis through the work of Morris and Nobel-laureate Noyori.^[125-134]

In our case, DFT calculations suggests that for (\equiv SiO)₂Ta(η^2 -H₂)(η^2 -N₂H) complex, there are two different types of hydrogen: weakly bonded H₂ to the Ta center has an acidic character while directly bonded hydrogen is a hydride. Side-on coordinated dinitrogen, [N₂]²⁻ therefore prefers to react with the electron poor hydrogen of the coordinated H₂ in order to yield [(\equiv SiO)₂TaH₂(N₂H)] complex by H⁺...H⁻ heterolytic cleavage of dihydrogen molecule. On the other hand, for side-on TaH₁, hydride transfer to the dinitrogen ligand is highly endoergic for the transition state that it is disfavored. Therefore, even we heat this monohydride complex at high temperatures during our experiment; we don't observe the peak at 3400 cm⁻¹ corresponding to the formation of [TaH₂(N₂)H] unless adding H₂ to the system.

Furthermore, our independent experiments with hydrazine and diazene on the starting tantalum hydrides allow us to exclude the assignments of intermediate I₂ to an hydrazine species. Since the hydrazine adduct easily evolves to final [(\equiv SiO)₂Ta(=NH)(-NH₂)] (Fig. 26) while I₂ is observed at temperatures above 100 °C. Diazene experiments, although not fully conclusive, do not play the signature peak of the assignment of I₂ as a diazenido adduct.

It has been already reported in the literature that partially reduced dinitrogen ligands such as aryldiazenido, hydrazine or diazene have fundamental importance not only for possible relevance to inorganic and bioinorganic N₂-reduction processes but also for organic chemistry.^[29, 103, 138-140] Despite their potentially interesting developments, the chemistry of transition metal complexes with these ligands has developed in the past 25 years^[103, 141-150] containing rare examples of stable hydrazine and diazene complexes because of their reactivity and lifetime of minutes at low temperatures.^[148, 151-154]

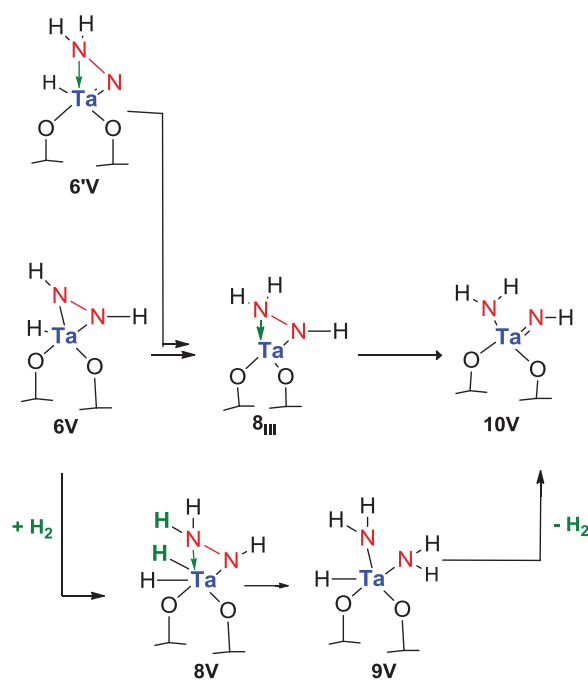
Step 3:

Reaction of $(\equiv\text{SiO})_2\text{TaH}(\text{N}_2\text{H}_2)$ in absence and in presence of additional H_2

Formation of the final complex $(\equiv\text{SiO})_2\text{Ta}(\text{=NH})(\text{NH}_2)$:

The necessity of H_2 addition to the system in order to complete the cleavage of the robust $\text{N}\equiv\text{N}$ dinitrogen bond to obtain final imido amido tantalum compound from intermediate I_2 has already been reported in Science 2007 by our group. It has been also showed that heating at 250 °C for 3 days is important for this reaction over supported tantalum hydrides to have a yield around 95 %.^[67]

DFT calculations confirm that direct hydride transfer from I_2 to yield the hydrazido adduct is too demanding energetically ($\Delta G_{523\text{K}}^\ddagger = 49$ kcal/ mol). Involvement of an extra H_2 molecule does provide a lower energy path (scheme 22). Heterolytic addition of H_2 to the complex **6V** is energetically easier via proton transfer to $[\text{N}_2\text{H}_2]^{2-}$ ligand (**TS(6V-8V)**) which avoids 50 kcal/ mol high energy barrier. Such step is then followed by an easier hydride transfer to the empty σ^* orbital of the $[\text{NH}_2\text{NH}]^-$ ligand (**TS(8V-9V)**) $\Delta G_{523\text{K}}^\ddagger = 47.3$ kcal/ mol), cleaves N-N bond by yielding bisamido Ta^{V} $[(\equiv\text{SiO})_2\text{TaH}(\text{NH}_2)_2]$ complex (**9V**). Heterolytic coupling of H_2 follows this step in order to form the final imido amido complex (**10V**).



Scheme 22

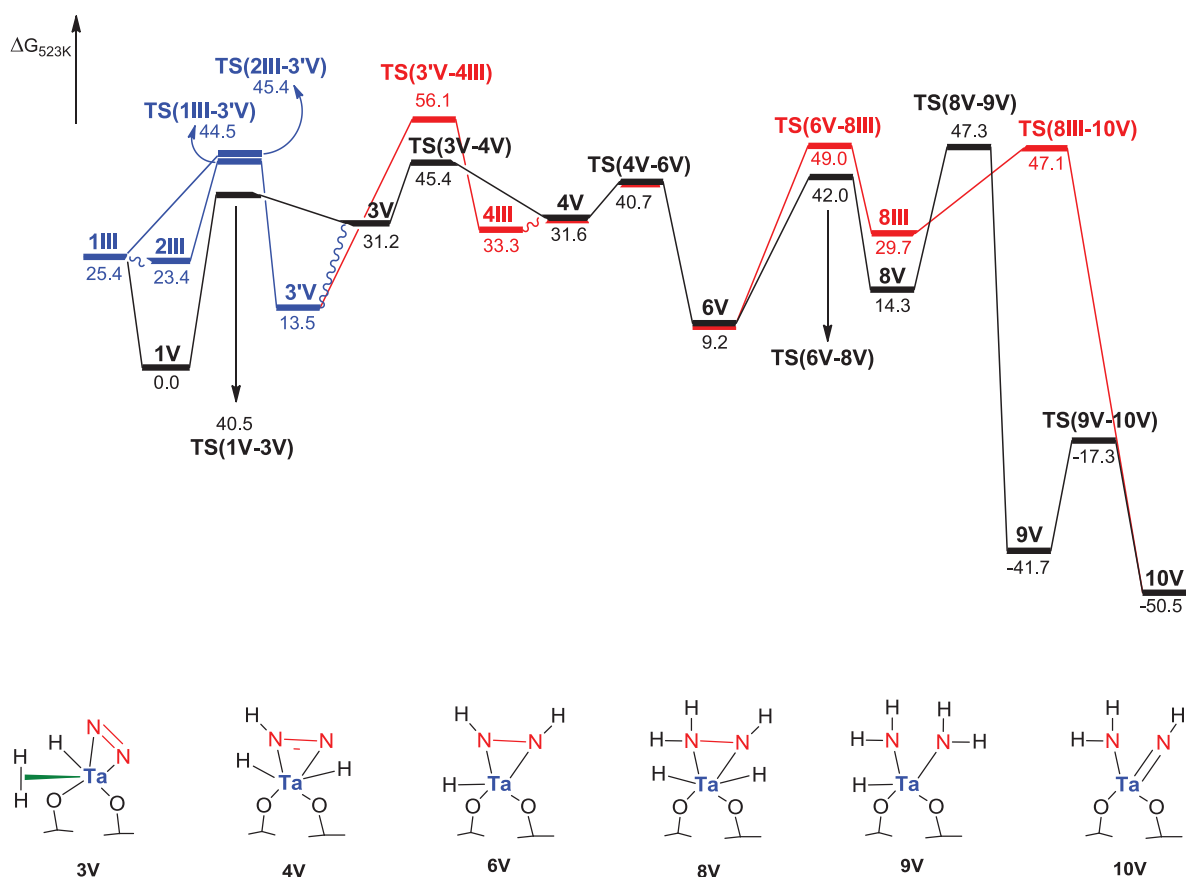
According to the calculations, overall H₂ appears to facilitate the last phases of N-N cleavage without itself being consumed. H₂ addition also allows the conversion of the inert TaHN₂ into dihydrogen complex [(≡SiO)₂TaH(H₂)(N₂)] or its follow up intermediate [(≡SiO)₂TaH₂(N₂H)] which can thus follow the mechanism just outlined for the trishydride.

A hydride is transferred to the σ* NN orbital of [NH₂NH]⁺ ligand by dihydrogen heterolytic cleavage. This interaction has high energy barriers for the transition state but preferred thermodynamically to cleave N≡N bond via H⁻ transfer. Therefore, high temperature and long reaction time to complete the reaction even after addition of dihydrogen to the system could be understood due to the calculations. It is also showed that in the absence of dihydrogen, reaction should stop at the formation of [(≡SiO)₂TaH(N₂H₂)] complex even heating at 250 °C (Figure14). This intermediate is already observed by in-situ IR spectroscopy at 3400 cm⁻¹ for [(≡SiO)₂TaH_x] species with N₂ at the same temperature (Figure 12).

Overall view of proposed mechanism

The pathway emerging from our calculations is given in Scheme 23 with the sequence of elementary steps that yield the formation of well-defined imido amido tantalum complex from the initial silica grafted tantalum trishydride mixture, N₂ and H₂ (blue and black lines). The previously proposed pathway of Li & Li has also been given in order to compare the energies and the intermediates of their calculations (red line).

Calculations of our co-workers have been showed the end-on bonding of N₂ to the tantalum trishydride complex leads a very weakly activated dinitrogen ligand by a kinetically easier step. The transition states of the pathway proposed in this study (black curve, Scheme 23) are lower in Gibbs energy than those proposed by Li and Li (red curve). The difference in Gibbs energy between the two highest transition structures is ~ 9 kcal mol⁻¹.



Scheme 23: Gibbs energy profiles (in kcal/ mol) for the reaction of N_2 and H_2 with monohydride enriched **1** (**1III**) and tantalum trishydride (**1V**) in order to yield $[(\equiv\text{SiO})_2\text{Ta}(=\text{NH})(\text{NH}_2)]$ complex at 523 K. The green line between metal and ligand represents a ligand-to-metal donor-acceptor bond.

Even though the temperature used in the experiment is high (250 °C), this difference in energy between the two highest transition states is significant due to the hydride transfer to a formally doubly charged ligand. The succession of proton and hydride transfers occurs twice in the whole reaction. In both cases, the proton originates from H_2 , which is made acidic by being coordinated to the metal or by heterolytic addition of H_2 to a Ta-N polar bond. In the second case, H_2 is heterolytically added before being eliminated in a heterolytic manner. By leading to lower energy barriers and by being fully recovered, H_2 appears as a co-catalyst in the final steps of the reaction. Therefore, molecular hydrogen has been used as the source of protons and electrons due to the ability of the metal and ligands in this system to promote its heterolytic cleavage provided that an empty coordination site at the metal is available to host the hydride.

IV. CONCLUSION AND PERSPECTIVES

Elucidation of mechanistic understanding that can support the design of transition-metal-based catalysts for the direct conversion of N_2 and H_2 to ammonia at, or near, ambient temperatures still presents important experimental and theoretical challenges now into the 21st century. Indeed, although important advances toward this goal have been made, the number of well-defined inorganic and organometallic complexes that can ligate N_2 in such a fashion that ultimately leads to facile $N\equiv N$ bond cleavage and N-atom functionalization remains extremely small.

We reported herein experimental and computational results for the reactions of tantalum hydride mixture and monohydride enriched **1** with N_2 at room temperature and at 250 °C in the absence/ presence of the dihydrogen molecule. The different reactivities of these complexes through dinitrogen coordination/ activation were monitored mainly by *in situ* IR spectroscopy. SS NMR and elemental analysis have also been used for certain experiments to characterize the type of different bonding modes of dinitrogen to the samples.

The mechanistic insight of dinitrogen reduction at a monometallic tantalum center has been finally determined with the help of various experimental and computational studies differing from other examples in the literature that use specific proton and electron sources. Heterolytic cleavage of additional dihydrogen to system acts as a co-catalyst for our example. Furthermore, the obtained results may also be helpful to understand dinitrogen activation at mononuclear surface centers which have similar reactivities to tantalum metal (such as niobium, vanadium etc.) in order to explain the binding types of dinitrogen and the pathways of the reaction mechanism.

V. EXPERIMENTAL PART

General Procedure:

All experiments were carried out by using standard air-free methodology in an argon-filled Vacuum Atmospheres glovebox, on a Schlenk line, or in a Schlenk-type apparatus interfaced to a high-vacuum line (10^{-5} Torr). $[\text{Ta}(\text{CH}_2\text{C}(\text{CH}_3)_3)_3(=\text{CHC}(\text{CH}_3)_3)]$ was prepared by the reaction of TaCl_5 (Strem) with $t\text{Bu-CH}_2\text{MgCl}$ according to literature procedure.^[158] $\text{Bu-CH}_2\text{MgCl}$ was prepared from $t\text{BuCH}_2\text{MgCl}$ (98%, Aldrich, used as received) and Mg turnings (Lancaster). MCM-41 mesoporous silica was supplied by the Laboratoire des Matériaux Minéraux, E.N.S. de Chimie Mulhouse, 3 rue Alfred Werner, 68093 Mulhouse Cédex, France. It was prepared according to literature method.^[159] Its BET surface area, determined by nitrogen adsorption at 77K, is 1060 m^2/g with a mean pore diameter of 28 Å (BJH method). The wall thickness was found to be 14 Å by subtraction of the pore diameter from the unit cell parameter deduced from X-ray powder diffraction data. MCM-41 supported tantalum hydrides $[(\equiv\text{SiO})_2\text{TaH}]$, **1a**, and $[(\equiv\text{SiO})_2\text{TaH}_3]$, **1b**, were prepared by impregnation in pentane or by sublimation for *in situ* IR monitoring as previously reported by the reaction of $[\text{Ta}(\text{CH}_2t\text{Bu})_3(=\text{CH}t\text{Bu})]$ with MCM-41 previously dehydroxylated at 500°C, followed by hydrogenolysis (550 Torr, 12h, 150°C). Pentane was distilled on NaK alloy followed by degassing through freeze-pump-thaw cycles.

Gas-phase analysis of alkanes: Gas phase analysis was performed on a Hewlett-Packard 5890 series II gas chromatograph equipped with a flame ionisation detector and an $\text{Al}_2\text{O}_3/\text{KCl}$ on fused silica column (50m X 0.32 mm). Dihydrogen gas phase analysis was performed on a Intersmat-IGC 120-MB gas chromatograph equipped with a catharometer.

Infrared spectra were recorded on a Nicolet 550-FT spectrometer by using an infrared cell equipped with CaF_2 windows, allowing *in situ* monitoring under controlled atmosphere. Typically 36 scans were accumulated for each spectrum (resolution, 2 cm^{-1}).

NMR Spectroscopy. All the NMR spectra were obtained on a Bruker 500 MHz wide bore spectrometer using a double resonance 4 mm MAS probe at the Laboratoire de Chimie Organométallique de Surface in Ecole Supérieure de Chimie Physique Electronique de Lyon. The samples were introduced under Argon in a zirconia rotor, which was then tightly closed.

The spinning frequency was set to 10 kHz for all the NMR experiments. A pellet of 50 mg was prepared from the reaction of tantalum hydrides with excess of D₂ (500 Torr) for 1N at 150°C. in order to have enough quantity for NMR analysis. This complex was treated under labeled dinitrogen pressure (100 torr, 2.1 mmol, 45 equivalents per Ta) at room temperature for 1h. Vacuum was applied to the disk for 15 min. The analyses were done by in-situ IR for different steps of the reaction and the sample was sent to the ¹⁵ CP MAS NMR analysis.

Selected IR frequencies for the reaction with ¹⁵N₂ at room temperature: 3747 (ν_{OH}), 3270-2850 (ν_{CH}), 2205 (ν_{NN}), 2270 (ν_{SiH}), 2220 (ν_{SiH₂}), 2100-1600 (δ_{Si-O-Si}), 1890-1700 (ν_{TaH}) cm⁻¹.

Elemental analyses were performed at the CNRS Central Analysis Service of Solaize, France, at the LSEO of Dijon, France, and at the Mikroanalytisches Labor Pascher in Remagen-Bendorf, Germany.

Preparation and reactivity of surface complexes:

*Hydrogenolysis of [(≡SiO)Ta(CH₂C(CH₃)₃)₂(=CHC(CH₃)₃)]: Preparation of [(≡SiO)₂TaH] and [(≡SiO)₂TaH₃], **1**:*

Loose powder of [(≡SiO)₂Ta(=CH*t*Bu)(CH₂*t*Bu)₂] (500mg, 0.32 mmol Ta) was twice treated at 150°C with anhydrous hydrogen (600 torr, 16.4 mmol, 65 equivalent / Ta) for 15 h. Gas chromatography analysis indicated the formation of 13±2 CH₄ coming from the Hydrogenolysis of 2,2-dimethylpropane, CMe₄ (2.6±0.4 CMe₄/Ta, expected 3). The gas evolved during the reaction was removed under vacuum and the final hydrides [(≡SiO)₂TaH], **1a**, and [(≡SiO)₂TaH₃], **1b**, were recovered as a brown powder. As already reported, some surface alkyl groups (<0.1 C/Ta) resist hydrogenolysis. Elemental Analysis: Ta 15.91%wt C 0.67%wt. Solid state ¹H MAS NMR = 29.5, 26.8, 23.2, 18.0, 13.0 (Ta(**H**)_x), 4.3, 4.0 (Si**H** and Si**H**₂), 1.8 (Si**OH**), 0.8 (CH_n) ppm. IR spectra were recorded at each step of the preparation. IR: 3747 (ν_{OH}), 3270-2850 (ν_{CH}), 2270 (ν_{SiH}), 2220 (ν_{SiH₂}), 2100-1600 (δ_{Si-O-Si}), 1890-1700 (ν_{TaH}), 1467 w, 1362 (δ_{CH}) cm⁻¹.

*In-situ IR study of the reaction of [(≡SiO)₂TaH_x(x=1,3)], **1** with dinitrogen:*

A disk of [(≡SiO)₂TaH_x(x=1,3)], **1**, (20 mg, 0.02 mmol Ta), prepared as previously reported, was treated under partial dinitrogen pressure (550 torr, 7.5 mmol, 300 equivalents per Ta) first at room temperature for 1h and then at 250°C for 4 h. The gas phase was then removed and IR spectra were recorded at each step of the preparation.

Selected IR frequencies for the reaction with N₂ at room temperature: 3747 (ν_{OH}), 3270-2850 (ν_{CH}), 2280 (ν_{NN}), 2270 (ν_{SiH}), 2220 (ν_{SiH₂}), 2100-1600 (δ_{Si-O-Si}), 1890-1700 (ν_{TaH}) cm⁻¹.

Selected IR frequencies for the reaction with N₂ at 250 °C: 3747 (ν_{OH}), 3502 (ν_{TaN-H}), 3461 (ν_{N-H}), 3400 (ν_{TaN₂H}), 3377 (ν_{TaN-H}), 3270-2850 (ν_{CH}), 2270 (ν_{SiH}), 2220 (ν_{SiH₂}), 2100-1600 (δ_{Si-O-Si}), 1890-1700 (ν_{TaH}), 1550 (δ_{SiNH₂}), 1520 (δ_{TaNH₂}) cm⁻¹.

The same experiment was also done with tantalum monohydride enriched complex **1** with N₂ at room temperature and gave exactly the same peaks in *in situ* IR spectroscopy at room temperature; however there were no peaks at 3400 cm⁻¹ corresponding (ν_{TaN₂H}) for these species upon heating at 250 °C but new peaks in NH region appeared.

Selected IR frequencies for the reaction with N₂ at 250 °C: 3747 (ν_{OH}), 3500 (ν_{TaN-H}), 3461 (ν_{N-H}), 3372 (ν_{TaN-H}), 3270-2850 (ν_{CH}), 2270 (ν_{SiH}), 2220 (ν_{SiH₂}), 2100-1600 (δ_{Si-O-Si}), 1890-1700 (ν_{TaH}), 1520 (δ_{TaNH₂}) cm⁻¹.

The experiment under labeled dinitrogen was done with a disk of [(≡SiO)₂TaH_x(x=1,3)], **1**, (40 mg, 0.05 mmol Ta), prepared as previously reported. It was treated under labeled dinitrogen pressure (150 torr, 2.1 mmol, 70 equivalents per Ta) at room temperature for 1h. Vacuum was applied to the disk for 20 min. The analyses were done by in-situ IR for different steps of the reaction and the sample was sent to the SS NMR analysis.

Selected IR frequencies for the reaction with ¹⁵N₂ at room temperature: 3747 (ν_{OH}), 3270-2850 (ν_{CH}), 2205 (ν_{NN}), 2270 (ν_{SiH}), 2220 (ν_{SiH₂}), 2100-1600 (δ_{Si-O-Si}), 1890-1700 (ν_{TaH}) cm⁻¹.

Selected NMR frequencies:

In-situ IR study of the reaction of [(≡SiO)₂TaD_x], 1-d with dinitrogen:

Similar experiments were carried out with [(≡SiO)₂TaD_x] with dinitrogen. A disk of [(≡SiO)₂TaH_x(x=1,3)], **1**, (18 mg, 0.013 mmol Ta), prepared as previously reported, and treated under D₂ (600 Torr) for one night at 150 °C in order to form the deuterated complex, **1-d**. Next day, the sample was reacted under dinitrogen pressure (550 torr, 7.5 mmol, 280 equivalents per Ta) at room temperature for 1h and then treated under vacuum in order to remove the coordinated dinitrogen. Addition and removing of N₂ steps were repeated several

times. The gas phase was then removed and IR spectra were recorded at each step of the preparation.

Selected IR frequencies for the reaction of $[(\equiv\text{SiO})_2\text{TaD}_x]$ with N_2 : 3747 (ν_{OH}), 3270-2850 (ν_{CH}), 2760 (ν_{OD}), 2280 (ν_{NN}), 2270 (ν_{SiH}), 2220 (ν_{SiH_2}), 2100-1600 ($\delta_{\text{Si-O-Si}}$), 1890-1700 (ν_{TaH}), cm^{-1} .

The same reaction was repeated with labelled dinitrogen but the red shift of 75 cm^{-1} on deuterated tantalum complex didn't give reliable results for this experiment (ν_{NN} was observed at 2205 cm^{-1}) with $^{15}\text{N}_2$.

In-situ IR study of the reaction of $[(\equiv\text{SiO})_2\text{TaH}_x]$, 1 with hydrazine:

Hydrazine was prepared by the reaction of KOH with hydrazine monohydrate 64-65 %, reagent grade, 98 % (Sigma Aldrich) according to literature procedure.^[100]

Addition of N_2H_4 (14.4 Torr at $25 \text{ }^\circ\text{C}$) on $[(\equiv\text{SiO})_2\text{TaH}_x]$, 1, (25 mg, 0.031 mmol) was done at room temperature and gave the following IR peaks.

Selected IR frequencies for the reaction of physisorbed N_2H_4 : 3368 (ν_{NH}), 3290 (ν_{NH}), 3197 (ν_{NH}), 1612 (δ_{NH_2}) cm^{-1} .

Selected IR frequencies for the reaction of $[(\equiv\text{SiO})_2\text{TaH}_x]$ with N_2H_4 : 3747 (ν_{OH}), 3359 (ν_{NH}), 3285 (ν_{NH}), 3190 (ν_{NH}), 3270-2850 (ν_{CH}), 2270 (ν_{SiH}), 2220 (ν_{SiH_2}), 2100-1600 ($\delta_{\text{Si-O-Si}}$), 1890-1700 (ν_{TaH}), 1605 (δ_{NH_2}) cm^{-1} .

Excess of the hydrazine was needed to consume the total TaH peaks and new peaks in NH region appeared from $100 \text{ }^\circ\text{C}$.

Selected IR frequencies for the reaction of $[(\equiv\text{SiO})_2\text{TaH}_x]$ with N_2H_4 at $100 \text{ }^\circ\text{C}$: 3747 (ν_{OH}), 3494 (ν_{NH}), 3358 (ν_{NH}), 3374 (ν_{NH}), 3294 (ν_{NH}), 3270-2850 (ν_{CH}), 2270 (ν_{SiH}), 2220 (ν_{SiH_2}), 2100-1600 ($\delta_{\text{Si-O-Si}}$), 1613 (δ_{NH_2}) cm^{-1} .

The same experiment was also done with $[(\equiv\text{SiO})_2\text{TaH}_1]$, 1, (15 mg, 0.02 mmol) with N_2H_4 which didn't lead to the complete consumption of TaH peaks at room temperature. Heating at $250 \text{ }^\circ\text{C}$ but new peaks in NH region appeared.

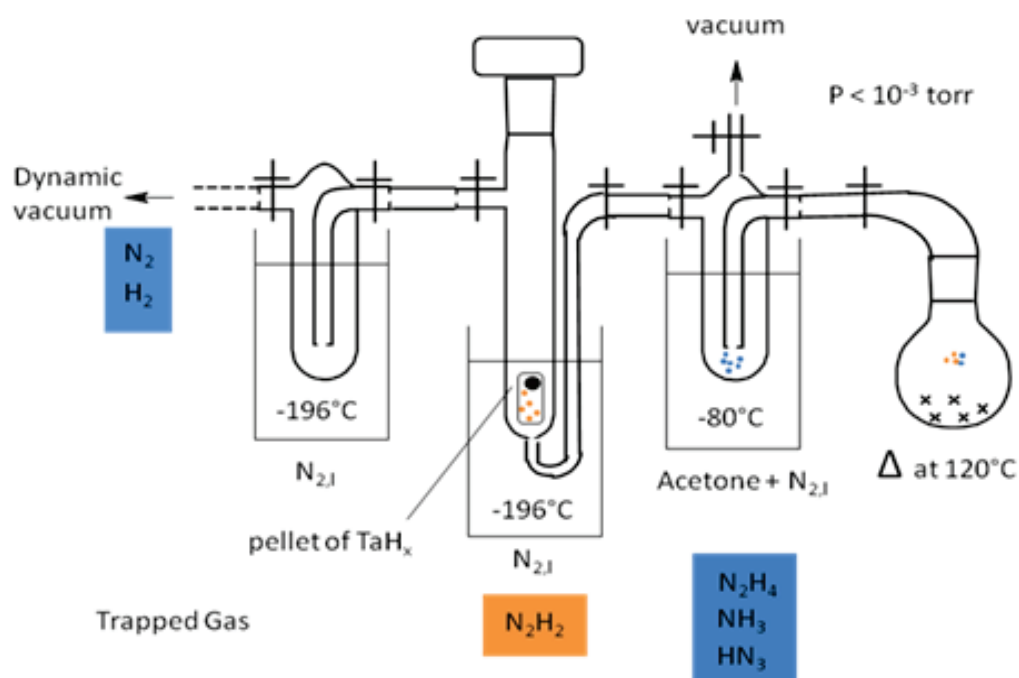
Selected IR frequencies for the reaction with N_2H_4 at $250 \text{ }^\circ\text{C}$: 3747 (ν_{OH}), 3500 ($\nu_{\text{Ta-N-H}}$), 3461 ($\nu_{\text{N-H}}$), 3372 ($\nu_{\text{Ta-N-H}}$), 3270-2850 (ν_{CH}), 2270 (ν_{SiH}), 2220 (ν_{SiH_2}), 2100-1600 ($\delta_{\text{Si-O-Si}}$), 1890-1700 (ν_{TaH}), 1520 (δ_{TaNH_2}) cm^{-1} .

Both samples were sent to elemental analysis after heating at 250°C.

Elemental analysis: Ta 15,7 %_{wt}; N 1,34 %_{wt}. (N/Ta by e.a. = ca.0.96 and 0.95).

In-situ IR study of the reaction of $[(\equiv\text{SiO})_2\text{TaH}_x]$, 1 with diazene:

Diazene synthesis has been described by thermal decomposition (100 °C) under a partial vacuum salt *p*-Toluenesulfonyl hydrazide (tosylhydrazine) particular the potassium salt (Sigma Aldrich 97 %). Diazene molecules are released in the gas phase in mixture with ammonia, hydrazine, nitride, nitrogen and hydrogen. Characterization of the presence of the diazene is made by infrared spectroscopy. Therefore, we have developed a system based on the method described in the article^[160] to trap vapors of ammonia and hydrazine leaving only diazene interacting with tantalum hydrides (see scheme 24). For this, a trap cooled intermediate at -80 °C (acetone and liquid nitrogen) is arranged between the flask containing the precursor diazene and the reactor containing the disk of TaH_x (18mg, 0.02 mmol), all under partial vacuum ($P < 10^{-3}$ Torr). Diazene vapors are condensed and purified in the immediate vicinity of the sample through a trap cooled with liquid nitrogen. The reactor containing the sample is then isolated and then allowed to warm up slowly to room temperature. From this phase, the reaction was monitored by *in-situ* infrared spectroscopy.



Scheme 24: Schematic illustration of diazene preparation and addition to a disk of silica supported tantalum hydrides.

Selected IR frequencies for the reaction of $[(\equiv\text{SiO})_2\text{TaH}_x]$ with N_2H_2 : 3415 (ν_{NH}), 3400 (ν_{NH}), 3320 (ν_{NH}) cm^{-1} .

Models and Computational details

Model.

The grafted complex is modeled using the cluster approach (Figure 32). The surface oxygen atoms covalently bonded to the tantalum centre have been assumed to be vicinal and the surface is represented by including the first SiO_4 shell. This model is similar to most of those used previously for representing silica supported transition metal hydrides¹⁰⁵ and also supported Schrock type olefin metathesis catalysts.^[161-164] Moreover, this model has been shown to correctly reproduce the spectroscopic properties of $[(\equiv\text{SiO})_2\text{Ta}(\text{NH})(\text{NH}_2)]$ as well as its reactivity with H_2 and NH_3 .^[165-167] Finally, this cluster model gives results that are similar to those obtained with calculations using periodic boundaries conditions.^[162, 165, 166]

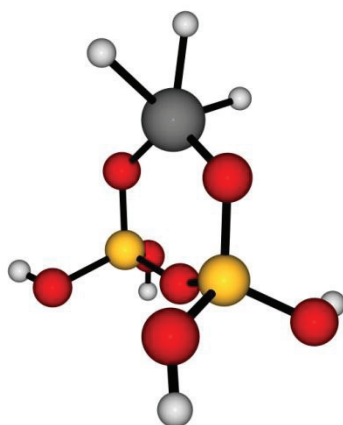


Figure 32: Cluster model representing the tantalum trihydride supported on silica.

Computational method.

Calculations have been carried out with the B3PW91^[168, 169] density functional and the Gaussian03 package.^[170] Silicon and tantalum atoms have been represented with the quasi-relativistic effective core pseudopotentials (RECP) of the Stuttgart-Bonn group, and the

associated basis sets augmented with a polarization function.^[171-174] All other atoms (O, N and H) have been represented by the Dunning's correlation consistent aug-cc-pVDZ basis sets.^[175] All optimizations were performed without any geometry constraint and the nature of the extrema has been checked by analytical frequency calculations. The Intrinsic Reaction Coordinate (IRC) has been calculated to ensure the nature of the two minima interconnected through the transition states. Three sets of energies are used to discuss the obtained results: i) electronic energies E without ZPE corrections; ii) Gibbs energies (G) computed with Gaussian03 at 1 atm and 523.15 K (experimental temperature used) and iii) when needed Gibbs energies (G) at 1 atm and 298.15 K. Gibbs energies are computed assuming an ideal gas, unscaled harmonic vibrational frequencies and the rigid rotor approximation. This is an approximative way of evaluating the entropic contributions but no simple procedure applicable to the experimental conditions is available.

VI. REFERENCES:

- [1] S. A. Lawrence, Amine: Synthesis, Properties and Applications, *Cambridge University Press*, **2004**, ISBN : 0 5221 78284 8.
- [2] S. Gambarotta, J. Scott, *Angew. Chem. Int. Ed.* **2004**, *43*, 5298.
- [3] T. A. Bazhenova, A. E. Shilov, *Coord. Chem. Rev.* **1995**, *144*, 69.
- [4] B. K. Burgess, D. J. Lowe, *Chem. Rev.* **1996**, *96*, 2983.
- [5] B. M. Barney, H. I. Lee, P. C. Dos Santos, B. M. Hoffman, D. R. Dean, L. C. Seefeldt, *Dalt. Tran.,* **2006**, 2277.
- [6] J. B. Howard, D. C. Rees, *Chem.Rev.* **1996**, *96*, 2965.
- [7] D. C. Rees, J. B. Howard, *Curr. Op. Chem. Biol.* **2000**, *4*, 559.
- [8] J. B. Howard, D. C. Rees, *Proc. of Nat. Acad. Sci. USA* **2006**, *103*, 17088.
- [9] B. E. Smith, in *Advan. Inorg. Chem.* **1999**, *47*, 159.
- [10] F. Barriere, *Coord. Chem. Rev.* **2003**, *236*, 71.
- [11] I. Dance, *Dalt. Trans.* **2010**, *39*, 2972.
- [12] B. Hinnemann, J. K. Nørskov, *J. Am. Chem. Soc.* **2004**, *126*, 3920.
- [13] R. Schlögl, *Angew. Chem. Int. Ed.* **2003**, *42*, 2004.
- [14] a) A. J. Harding, Ammonia manufacture and uses, *Oxford University Press*, **1959**; b) R. Imbihl, R. J. Behm, G. Ertl, W. Moritz, *Surface Science* **1982**, *123*, 129; c) O. Hinrichsen, F. Rosowski, A. Hornung, M. Muhler, G. Ertl, *J. Catal.* **1997**, *165*, 33; d) S. Harinipriya, M. Sangaranarayanan, *J. Mol. Catal.* **2004**, *207*, 107.
- [15] G. Ertl, Catalytic Ammonia Synthesis, Vol. 1, *Plenum*, **1991**.
- [16] B. A. MacKay, M. D. Fryzuk, *Chem. Rev.* **2004**, *104*, 385.
- [17] R. R. Schrock, *Proc. Nat. Acad. Sci. USA* **2006**, *103*, 17087.
- [18] N. Hazari, *Chem. Soc. Rev.* **2010**, *39*, 4044.
- [19] A. D. Allen, C. V. Senoff, *Chem. Commun.* **1965**, 621.

- [20] D. Pun, E. Lobkovsky, P. J. Chirik, *J. Am. Chem. Soc.* **2008**, *130*, 6047.
- [21] E. A. MacLachlan, M. D. Fryzuk, *Organometallics* **2006**, *25*, 1530.
- [22] D. V. Yandulov, R. R. Schrock, *J. Am. Chem. Soc.* **2002**, *124*, 6252.
- [23] D. V. Yandulov, R. R. Schrock, *Science* **2003**, *301*, 76.
- [24] M. D. Fryzuk, J. B. Love, S. J. Rettig, V. G. Young, *Science* **1997**, *275*, 1445.
- [25] W. H. Bernskoetter, A. V. Olmos, E. Lobkovsky, P. J. Chirik, *Organometallics* **2005**, *25*, 1021.
- [26] J. D. Cohen, M. Mylvaganam, M. D. Fryzuk, T. M. Loehr, *J. Am. Chem. Soc.* **1994**, *116*, 9529.
- [27] J. D. Cohen, M. D. Fryzuk, T. M. Loehr, M. Mylvaganam, S. J. Rettig, *Inor. Chem.* **1998**, *37*, 112.
- [28] J. A. Pool, E. Lobkovsky, P. J. Chirik, *Nature* **2004**, *427*, 527.
- [29] J. Chatt, A. J. Pearman, R. L. Richards, *Nature* **1975**, *253*, 39.
- [30] M. Hidai, Y. Mizobe, *Chem. Rev.* **1995**, *95*, 1115.
- [31] C. J. Pickett, *J. Bio. Inor. Chem.* **1996**, *1*, 601.
- [32] V. Ritleng, D. V. Yandulov, W. W. Weare, R. R. Schrock, A. S. Hock, W. M. Davis, *J. Am. Chem. Soc.* **2004**, *126*, 6150.
- [33] D. V. Yandulov, R. R. Schrock, *Inor. Chem.* **2005**, *44*, 5542.
- [34] R. R. Schrock, *Acc. Chem. Res.* **2005**, *38*, 955.
- [35] W. W. Weare, X. L. Dai, M. J. Byrnes, J. M. Chin, R. R. Schrock, P. Müller, *Proc. Nat. Acad. Sci. USA* **2006**, *103*, 17099.
- [36] C. J. Pickett, J. Talarmin, *Nature* **1985**, *317*, 652.
- [37] T. Murakami, T. Nishikiori, T. Nohira, Y. Ito, *J. Am. Chem. Soc.* **2003**, *125*, 334.
- [38] G. Marnellos, M. Stoukides, *Science* **1998**, *282*, 98.

- [39] L. Pospíšil, J. Bulíčková, M. Hromadová, M. Gál, S. Civiš, J. Cihelka, J. Tarábek, *Chem. Commun.* **2007**, 2270.
- [40] N. N. Rao, S. Dube, Manjubala, P. Natarajan, *App. Catal. B-Environmental* **1994**, *5*, 33.
- [41] K. Arashiba, Y. Miyake, Y. Nishibayashi, *Nature* **2011**, *3*, 120.
- [42] a) Y. Nishibayashi, S. Takemoto, S. Iwai, M. Hidai, *Inor. Chem.* **2000**, *39*, 5946; b) Y. Nishibayashi, S. Iwai, M. Hidai, *Science* **1998**, *276*, 5330, 540-542.
- [43] Y. Nishibayashi, *Dalton Trans.* **2012**, *41*, 7447.
- [44] H. J. Himmel, O. Hübner, W. Klopfer, L. Manceron, *Angew. Chem. Int. Ed.* **2006**, *45*, 2799.
- [45] H. J. Himmel, M. Reiher, *Angew. Chem. Int. Ed.* **2006**, *45*, 6264.
- [46] Z. H. Lu, L. Jiang, Q. Xu, *J. Phys. Chem. A* **2010**, *114*, 6837.
- [47] E. Solari, C. Da Silva, B. Iacono, J. Hesschenbrouck, C. Rizzoli, R. Scopelliti, C. Floriani, *Angew. Chem. Int. Ed.* **2001**, *40*, 3907.
- [48] G. K. B. Clentsmith, V. M. E. Bates, P. B. Hitchcock, F. G. N. Cloke, *J. Am. Chem. Soc.* **1999**, *121*, 10444.
- [49] I. Korobkov, S. Gambarotta, G. P. A. Yap, *Angew. Chem. Int. Ed.* **2002**, *41*, 3433.
- [50] I. Korobkov, S. Gambarotta, G. P. A. Yap, *Angew. Chem. Int. Ed.* **2003**, *42*, 4958.
- [51] G. B. Nikiforov, I. Vidyaratne, S. Gambarotta, I. Korobkov, *Angew. Chem. Int. Ed.* **2009**, *48*, 7415.
- [52] I. Vidyaratne, J. Scott, S. Gambarotta, P. H. M. Budzelaar, *Inor. Chem.* **2007**, *46*, 7040.
- [53] C. E. Laplaza, C. C. Cummins, *Science* **1995**, *268*, 861.
- [54] C. E. Laplaza, M. J. A. Johnson, J. C. Peters, A. L. Odom, E. Kim, C. C. Cummins, G. N. George, I. J. Pickering, *J. Am. Chem. Soc.* **1996**, *118*, 8623.

- [55] M. D. Fryzuk, C. M. Kozak, M. R. Bowdridge, B. O. Patrick, S. J. Rettig, *J. Am. Chem. Soc.* **2002**, *124*, 8389.
- [56] F. Akagi, T. Matsuo, H. Kawaguchi, *Angew. Chem. Int. Ed.* **2007**, *46*, 8778.
- [57] J. D. Gilbertson, N. K. Szymczak, D. R. Tyler, *J. Am. Chem. Soc.* **2005**, *127*, 10184.
- [58] J. L. Crossland, D. R. Tyler, *Coor. Chem. Rev.* **2010**, *254*, 1883.
- [59] K. Komori, H. Oshita, Y. Mizobe, M. Hidai, *J. Am. Chem. Soc.* **1989**, *111*, 1939.
- [60] M. D. Fryzuk, B. A. MacKay, S. A. Johnson, B. O. Patrick, *Angew. Chem. Int. Ed.* **2002**, *41*, 3709.
- [61] B. A. MacKay, R. F. Munha, M. D. Fryzuk, *J. Am. Chem. Soc.* **2006**, *128*, 9472.
- [62] Y. Ohki, M. D. Fryzuk, *Angew. Chem. Int. Ed.* **2007**, *46*, 3180.
- [63] M. D. Fryzuk, *Acc. Chem. Res.* **2009**, *42*, 127.
- [64] L. P. Spencer, B. A. MacKay, B. O. Patrick, M. D. Fryzuk, *Proc. Nat. Acad. Sci. USA* **2006**, *103*, 17094.
- [65] J. J. Curley, T. R. Cook, S. Y. Reece, P. Müller, C. C. Cummins, *J. Am. Chem. Soc.* **2008**, *130*, 9394.
- [66] D. J. Knobloch, E. Lobkovsky, P. J. Chirik, *Nature Chem.* **2010**, *2*, 30.
- [67] P. Avenier, M. Taoufik, A. Lesage, X. Solans-Monfort, A. Baudouin, A. de Mallmann, L. Veyre, J. M. Basset, O. Eisenstein, L. Emsley, E. A. Quadrelli, *Science* **2007**, *317*, 1056.
- [68] X. Solans-Monfort, C. Chow, E. Gouré, Y. Kaya, J.-M. Basset, M. Taoufik, E. A. Quadrelli, O. Eisenstein, *Inor. Chem.* **2012**, *51*, 7237.
- [69] K. Honkala, A. Hellman, I. N. Remediakis, A. Logadottir, A. Carlsson, S. Dahl, C. H. Christensen, J. K. Nørskov, *Science* **2005**, *307*, 555.
- [70] A. Hellman, E. J. Baerends, M. Biczysko, T. Bligaard, C. H. Christensen, D. C. Clary, S. Dahl, R. van Harrevelt, K. Honkala, H. Jonsson, G. J. Kroes, M. Luppi, U. Manthe,

- J. K. Nørskov, R. A. Olsen, J. Rossmeisl, E. Skúlason, C. S. Tautermann, A. J. C. Varandas, J. K. Vincent, *J. Phys. Chem. B* **2006**, *110*, 17719.
- [71] J. J. Mortensen, L. B. Hansen, B. Hammer, J. K. Nørskov, *J. Catal.* **1999**, *182*, 479.
- [72] S. Shetty, R. A. van Santen, *Top. in Catal.* **2010**, *53*, 969.
- [73] R. R. Schrock, *Angew. Chem. Int. Ed.* **2008**, *47*, 5512.
- [74] B. Le Guennic, B. Kirchner, M. Reiher, *Chemistry-a European Journal* **2005**, *11*, 7448.
- [75] D. V. Khoroshun, D. G. Musaev, K. Morokuma, *Molecular Physics* **2002**, *100*, 523.
- [76] Z. Cao, Z. Zhou, H. Wan, Q. Zhang, *Int. J. Quan. Chem.* **2005**, *103*, 344.
- [77] F. Studt, F. Tuczek, *Angew. Chem. Int. Ed.* **2005**, *44*, 5639.
- [78] A. Magistrato, A. Robertazzi, P. Carloni, *J. Chem. Theory- Comput.* **2007**, *3*, 1708.
- [79] S. Schenk, M. Reiher, *Inor. Chem.* **2009**, *48*, 1638.
- [80] F. Neese, *Angew. Chem. Int. Ed.* **2006**, *45*, 196.
- [81] H. Vázquez-Lima, P. Guadarrama, E. Ramos, S. Fomine, *J. Mol. Catal.* **2009**, *310*, 75.
- [82] R. L. McNaughton, M. Roemelt, J. M. Chin, R. R. Schrock, F. Neese, B. M. Hoffman, *J. Am. Chem. Soc.* **2010**, *132*, 8645.
- [83] H. Basch, D. G. Musaev, K. Morokuma, M. D. Fryzuk, J. B. Love, W. W. Seidel, A. Albinati, T. F. Koetzle, W. T. Klooster, S. A. Mason, J. Eckert, *J. Am. Chem. Soc.* **1999**, *121*, 523.
- [84] Q. Cui, D. G. Musaev, M. Svensson, S. Sieber, K. Morokuma, *J. Am. Chem. Soc.* **1995**, *117*, 12366.
- [85] F. Studt, F. Tuczek, *J. Comput. Chem.* **2006**, *27*, 1278.
- [86] F. Studt, B. A. MacKay, M. D. Fryzuk, F. Tuczek, *Dalt. Trans.* **2006**, 1137.
- [87] G. Christian, R. Stranger, B. F. Yates, C. C. Cummins, *Dalt. Trans.* **2007**, 1939.

- [88] G. J. Christian, R. N. L. Terrett, R. Stranger, G. Cavigliasso, B. F. Yates, *Chem. Eur. J.* **2009**, *15*, 11373.
- [89] G. Christian, R. Stranger, B. F. Yates, *Chem. Eur. J.* **2009**, *15*, 646.
- [90] A. Ariaifard, N. J. Brookes, R. Stranger, B. F. Yates, *Chem. Eur. J.* **2008**, *14*, 6119.
- [91] V. M. E. Bates, G. K. B. Clentsmith, F. G. N. Cloke, J. C. Green, H. D. L. Jenkin, *Chem. Commun.* **2000**, 927.
- [92] H. Tanaka, Y. Shiota, T. Matsuo, H. Kawaguchi, K. Yoshizawa, *Inorg. Chem.* **2009**, *48*, 3875.
- [93] H. Tanaka, F. Ohsako, H. Seino, Y. Mizobe, K. Yoshizawa, *Inorg. Chem.* **2010**, *49*, 2464.
- [94] H. Tanaka, H. Mori, H. Seino, M. Hidai, Y. Mizobe, K. Yoshizawa, *J. Am. Chem. Soc.* **2008**, *130*, 9037.
- [95] X. H. Zhang, B. Butschke, H. Schwarz, *Chem. Eur. J.* **2010**, *16*, 12564.
- [96] S. Baskaran, C. Sivasankar, *Eur. J. Inorg. Chem.* **2010**, 4716.
- [97] D. Roy, A. Navarro-Vazquez, P. V. R. Schleyer, *J. Am. Chem. Soc.* **2009**, *131*, 13045.
- [98] R. B. Yelle, J. L. Crossland, N. K. Szymczak, D. R. Tyler, *Inorg. Chem.* **2009**, *48*, 861.
- [99] J. Li, S. Li, *Angew. Chem. Int. Ed.* **2008**, *47*, 8040.
- [100] C. F. Hale, F. F. Shetterly, *J. Am. Chem. Soc.* **1911**, *33*, 1071.
- [101] M. Hidai, *Coord. Chem. Rev.* **1999**, *185-186*, 99.
- [102] G. J. Leigh, M. Jimenez-Tenorio, *J. Am. Chem. Soc.* **1991**, *113*, 5862.
- [103] R. A. Henderson, G. J. Leigh, C. J. Pickett, *Adv. Inorg. Chem. Radiochem.* **1983**, *27*, 197.
- [104] M. D. Fryzuk, S. A. Johnson, *Coord. Chem. Rev.* **2000**, *200-202*, 379.
- [105] T. Yamabe, K. Hori, T. Minato, K. Fukui, *Inorg. Chem.* **1980**, *19*, 2154.
- [106] D. J. Knobloch, E. Lobkovsky, P. J. Chirik, *J. Am. Chem. Soc.* **2010**, *132*, 10553.

- [107] S. M. Mansell, N. Kaltsoyannis, P. L. Arnold, *J. Am. Chem. Soc.* **2011**, *133*, 9036.
- [108] M. Hirotsu, P. P. Fontaine, A. Epshteyn, P. Y. Zavalij, L. R. Sita, *J. Am. Chem. Soc.* **2007**, *129*, 9284.
- [109] M. J. S. Gynane, J. Jeffery, M. F. Lappert, *J. Chem. Soc., Chem. Commun.* **1978**, 34.
- [110] W. J. Evans, L. R. Chamberlain, T. A. Ulibarri, J. W. Ziller, *J. Am. Chem. Soc.* **1988**, *110*, 6423.
- [111] P. Roussel, P. Scott, *J. Am. Chem. Soc.* **1998**, *120*, 1070.
- [112] M. D. Fryzuk, *Chem. Rec.* **2003**, *3*, 2.
- [113] W. H. Bernskoetter, E. Lobkovsky, P. J. Chirik, *J. Am. Chem. Soc.* **2005**, *127*, 14051.
- [114] T. E. Hanna, W. H. Bernskoetter, M. W. Bouwkamp, E. Lobkovsky, P. J. Chirik, *Organometallics* **2007**, *26*, 2431.
- [115] M. Hirotsu, P. P. Fontaine, P. Y. Zavalij, L. R. Sita, *J. Am. Chem. Soc.* **2007**, *129*, 12690.
- [116] D. Benito-Garagorri, W. H. Bernskoetter, E. Lobkovsky, P. J. Chirik, *Organometallics* **2009**, *28*, 4807.
- [117] S. P. Semproni, C. Milsmann, P. J. Chirik, *Organometallics* **2012**, *31*, 3672.
- [118] G. J. Kubas, R. R. Ryan, B. I. Swanson, P. J. Vergamini, H. J. Wasserman, *J. Am. Chem. Soc.* **1984**, *106*, 451.
- [119] P. G. Jessop, R. H. Morris, *Coord. Chem. Rev.* **1992**, *121*, 155.
- [120] R. H. Morris, *Can. J. Chem.* **1996**, *74*, 1907.
- [121] A. J. Lough, S. Park, R. Ramachandran, R. H. Morris, *J. Am. Chem. Soc.* **1994**, *116*, 8356.
- [122] G. J. Kubas, *Adv. Inorg. Chem.* **2004**, *56*, 127.
- [123] M. D. Fryzuk, P. A. MacNeil, *Organometallics* **1983**, *2*, 682.
- [124] M. D. Fryzuk, P. A. MacNeil, S. J. Rettig, *J. Am. Chem. Soc.* **1987**, *109*, 2803.

- [125] R. H. Morris, *Coord. Chem. Rev.* **2008**, *252*, 2381.
- [126] S. E. Clapham, A. Hadzovic, R. H. Morris, *Coord. Chem. Rev.* **2004**, *248*, 2201.
- [127] R. H. Morris, Review, Elsevier Science B.V., **2001**, 1-38.
- [128] R. Noyori, T. Okhuma, *Angew. Chem., Int. Ed.* **2001**, *40*, 40.
- [129] R. Noyori, *Angew. Chem., Int. Ed.* **2002**, *41*, 2008.
- [130] M. J. Palmer, M. Wills, *Tetrahedron: Asymmetry* **1999**, *10*, 2045.
- [131] C. A. Sandoval, T. Ohkuma, K. Muniz, R. Noyori, *J. Am. Chem. Soc.* **2003**, *125*, 13490.
- [132] K. Abdur-Rashid, S. E. Clapham, A. Hadzovic, J. N. Harvey, A. J. Lough, R. H. Morris, *J. Am. Chem. Soc.* **2002**, *124*, 15104.
- [133] R. Dorta, D. Broggini, R. Kissner, A. Togni, *Chem.--Eur. J.* **2004**, *10*, 4546.
- [134] C. C. Y. Ng, J. A. Osborn, *J. Am. Chem. Soc.* **1990**, *112*, 9400.
- [135] G. C. Welch, R. R. S. Juan, J. D. Masuda, D. W. Stephan, *Science* **2006**, *314*, 1124.
- [136] G. C. Welch, D. W. Stephan, *J. Am. Chem. Soc.* **2007**, *129*, 1880.
- [137] D. W. Stephan, *Org. & Biomol. Chem.* **2008**, *6*, 1535.
- [138] D. Coucouvanis, *Acc. Chem. Res.* **1991**, *24*, 1.
- [139] E. J. Corey, D. J. Pasto, W. L. Mock, *J. Am. Chem. Soc.* **1961**, *83*, 2957.
- [140] D. J. Pasto, D. M. Chipman, *J. Am. Chem. Soc.* **1979**, *101*, 2290.
- [141] D. Sutton, *Chem. Rev.* **1993**, *93*, 995.
- [142] H. Kisch, P. Holzmeier, *Adv. Organomet. Chem.* **1992**, *34*, 67.
- [143] G. Albertin, S. Antoniutti, A. Bacchi, M. F. De, G. Pelizzi, *Inorg. Chem.* **2005**, *44*, 8947.
- [144] G. Albertin, S. Antoniutti, A. Bacchi, B. Fregolent, G. Pelizzi, *Eur. J. Inorg. Chem.* **2004**, 1922.
- [145] G. Albertin, S. Antoniutti, M. T. Giorgi, *Eur. J. Inorg. Chem.* **2003**, 2855.

- [146] G. Albertin, S. Antoniutti, A. Bacchi, M. Boato, G. Pelizzi, *J. Chem. Soc., Dalton Trans.* **2002**, 3313.
- [147] D. Sellmann, A. Hennige, *Angew. Chem., Int. Ed.* **1997**, *36*, 276.
- [148] D. Sellmann, E. Boehlen, M. Waeber, G. Huttner, L. Zsolnai, *Angew. Chem. Int. Ed.* **1985**, *97*, 984.
- [149] D. Sellmann, K. Joedden, *Angew. Chem. Int. Ed.* **1977**, *89*, 480.
- [150] D. Sellmann, J. Kaepler, M. Moll, F. Knoch, *Inorg. Chem.* **1993**, *32*, 960.
- [151] T. Y. Cheng, J. C. Peters, G. L. Hillhouse, *J. Am. Chem. Soc.* **1994**, *116*, 204.
- [152] T. Y. Cheng, A. Ponce, A. L. Rheingold, G. L. Hillhouse, *Angew. Chem. Int. Ed.* **1994**, *33*, 703.
- [153] T. E. Glassman, M. G. Vale, R. R. Schrock, *Organometallics* **1991**, *10*, 4046.
- [154] G. Huttner, W. Gartzke, K. Allinger, *Angew. Chem.* **1974**, *86*, 860.
- [155] G. Maxwell, Editor, *Synthetic Nitrogen Products: A Practical Guide to the products and Processes*, *Kluwer Academic*, **2004**.
- [156] K.-i. Aika, K. Tamaru, Ammonia synthesis over non-iron catalysts and related phenomena, *Springer*, **1995**, 1- 103.
- [157] J. Li, S. Li, *Angew. Chem. Int. Ed.* **2008**, *47*, 8040.
- [158] R. R. Schrock, J. D. Fellmann, *J. Am. Chem. Soc.* **1978**, *100*, 3359.
- [159] C. Y. Chen, H. X. Li, M. E. Davis, *Micro. Mater.* **1993**, *2*, 17.
- [160] D. Lemal, F. Menger, E. Coats, *Dep. Chem. Univ. Wisconsin* **1963**, 86.
- [161] X. Solans-Monfort, E. Clot, C. Copéret, O. Eisenstein, *J. Am. Chem. Soc.* **2005**, *127*, 14015.
- [162] X. Solans-Monfort, J. S. Filhol, C. Copéret, O. Eisenstein, *New Jour. Chem.* **2006**, *30*, 842.

- [163] A. Poater, X. Solans-Monfort, E. Clot, C. Copéret, O. Eisenstein, *J. Am. Chem. Soc.* **2007**, *129*, 8207.
- [164] F. Blanc, J. M. Basset, C. Copéret, A. Sinha, Z. J. Tonzetich, R. R. Schrock, X. Solans-Monfort, E. Clot, O. Eisenstein, A. Lesage, L. Emsley, *J. Am. Chem. Soc.* **2008**, *130*, 5886.
- [165] P. Avenier, M. Taoufik, A. Lesage, X. Solans-Monfort, A. Baudouin, A. de Mallmann, L. Veyre, J. M. Basset, O. Eisenstein, L. Emsley, E. A. Quadrelli, *Science* **2007**, *317*, 1056.
- [166] P. Avenier, X. Solans-Monfort, L. Veyre, F. Renili, J. M. Basset, O. Eisenstein, M. Taoufik, E. A. Quadrelli, *Top. in Catal.* **2009**, *52*, 1482.
- [167] E. Gouré, P. Avenier, X. Solans-Monfort, L. Veyre, A. Baudouin, Y. Kaya, M. Taoufik, J. M. Basset, O. Eisenstein, E. A. Quadrelli, *New Jour. Chem.* **2011**, *35*, 1011.
- [168] A. D. Becke, *J. Chem. Phys.* **1993**, *98*, 5648.
- [169] J. P. Perdew, Y. Wang, *Phys. Rev.* **1992**, *45*, 13244.
- [170] M. J. Frisch, G. W. Trucks, H. B. Schlegel, G. E. Scuseria, M. A. Robb, J. R. Cheeseman, J. A. Montgomery, K. N. Kudin, J. C. Burant, J. M. Millam, S. S. Iyengar, J. Tomasi, V. Barone, B. Mennucci, M. Cossi, G. Scalmani, N. Rega, G. A. Petersson, H. Nakatsuji, M. Hada, M. Ehara, K. Toyota, R. Fukuda, J. Hasegawa, M. Ishida, T. Nakajima, Y. Honda, O. Kitao, H. Nakai, M. Klene, X. Li, J. E. Knox, H. P. Hratchian, J. B. Cross, C. Adamo, J. Jaramillo, R. Gomperts, R. E. Stratmann, O. Yazyev, A. J. Austin, R. Cammi, C. Pomelli, J. W. Ochterski, P. Y. Ayala, K. Morokuma, G. A. Voth, P. Salvador, J. J. Dannenberg, V. G. Zakrzewski, S. Dapprich, A. D. Daniels, M. C. Strain, O. Farkas, D. K. Malick, A. D. Rabuck, K. Raghavachari, J. B. Foresman, J. V. Ortiz, Q. Cui, A. G. Baboul, S. Clifford, J.

- Cioslowski, B. B. Stefanov, G. Liu, A. Liashenko, P. Piskorz, I. Komaromi, R. L. Martin, D. J. Fox, T. Keith, M. A. Al-Laham, C. Y. Peng, A. Nanayakkara, M. Challacombe, P. M. W. Gill, B. Johnson, W. Chen, M. W. Wong, C. Gonzalez, J. A. Pople, *Rev. B.04 ed., Gaussian Inc, 2003*.
- [171] A. Höllwarth, M. Böhme, S. Dapprich, A. W. Ehlers, A. Gobbi, V. Jonas, K. F. Köhler, R. Stegmann, A. Veldkamp, G. Frenking, *Chem. Phys. Lett.* **1993**, *208*, 237.
- [172] A. W. Ehlers, M. Böhme, S. Dapprich, A. Gobbi, A. Höllwarth, V. Jonas, K. F. Köhler, R. Stegmann, A. Veldkamp, G. Frenking, *Chem. Phys. Lett.* **1993**, *208*, 111.
- [173] D. Andrae, U. Häussermann, M. Dolg, H. Stoll, H. Preuss, *Theo. Chim. Act.* **1990**, *77*, 123.
- [174] A. Bergner, M. Dolg, W. Kuchle, H. Stoll, H. Preuss, *Mol. Phys.* **1993**, *80*, 1431.
- [175] R. A. Kendall, T. H. Dunning, R. J. Harrison, *J. Chem. Phy.* **1992**, *96*, 6796.
- [176] R. L. Miller, R. Toreki, R. E. LaPointe, P. T. Wolczanski, G. D. Van Duyne, D. C. Roe, *J. Am. Chem. Soc.* **1993**, *115*, 5570.

CHAPTER IV.

Attempts to use well-defined silica supported tantalum imido amido complex for C-H activation reactions

I. INTRODUCTION

Amines are an important and ubiquitous class of organic compounds in fine chemistry since their industrial applications in the 19th century. Their role as a building block particularly for the pharmaceutical applications is immense that amine drugs are designed to mimic or to interfere with the action of neurotransmitters (dopamine, serotonin, epinephrine, acetylcholine), analgesics (acetaminophen, demerol, morphine, phenacetin), anesthetics (novocaine, benzidrine, barbital) and decongestants (ephedra, diphenhydramine). In addition, they are present in a large class of biologically active products such as herbicides (metolachlor, triclopyr), nutrients (choline, histamine, putrescine, dimethylamine), surfactants and cleaning systems (amine oxide, ether amine/ diamine, quarternary amine).^[1-4]

Considering their numerous applications in different fields, there has been tremendous interest in synthesis of amines as useful intermediates. Nevertheless; various preparation methods requires intermediates such as glutamine, alkylamine, hexylamine, acrylonitrile, nitrates which are neither atom efficient nor ideal for a catalytic processes.^[5-12] One of the blue sky objectives can be therefore the direct synthesis of organic N-containing compounds from NH₃ or even more ambitiously from N₂.

Direct mild transformation of ammonia into useful amido compounds by a transition metal for catalyst is therefore one of the current challenges in organic chemistry. As already mentioned in the introduction of Chapter II, there are few crucial examples that are reported in the literature.^[13-22] Meanwhile, in 2007 our group described the activation of NH₃ and N₂ from the reaction of silica-supported tantalum hydrides, **1** leading well-defined tantalum imido amido complex as given in previous chapters.^[23, 24] The surface tantalum hydrides are found unique not only in their ability to cleave N₂ on a heterogeneous monometallic center with H₂ but also to activate NH₃ at room temperature via surface organometallic chemistry. Further studies on the reactivity of well-defined [(≡SiO)₂Ta(=NH)(-NH₂)], **2** showed the capacity of this complex to react with the H-H bond of H₂ molecule in addition to the N-H bond of ammonia explaining the nature of the reaction as a heterolytic bond cleavage.^[25, 26] In addition to these recent developments by our group, prior investigations in the laboratory had already showed that [(≡SiO)₂TaH_x (x: 1, 3)] complex can activate C-H bonds in alkanes to form tantalum(V)

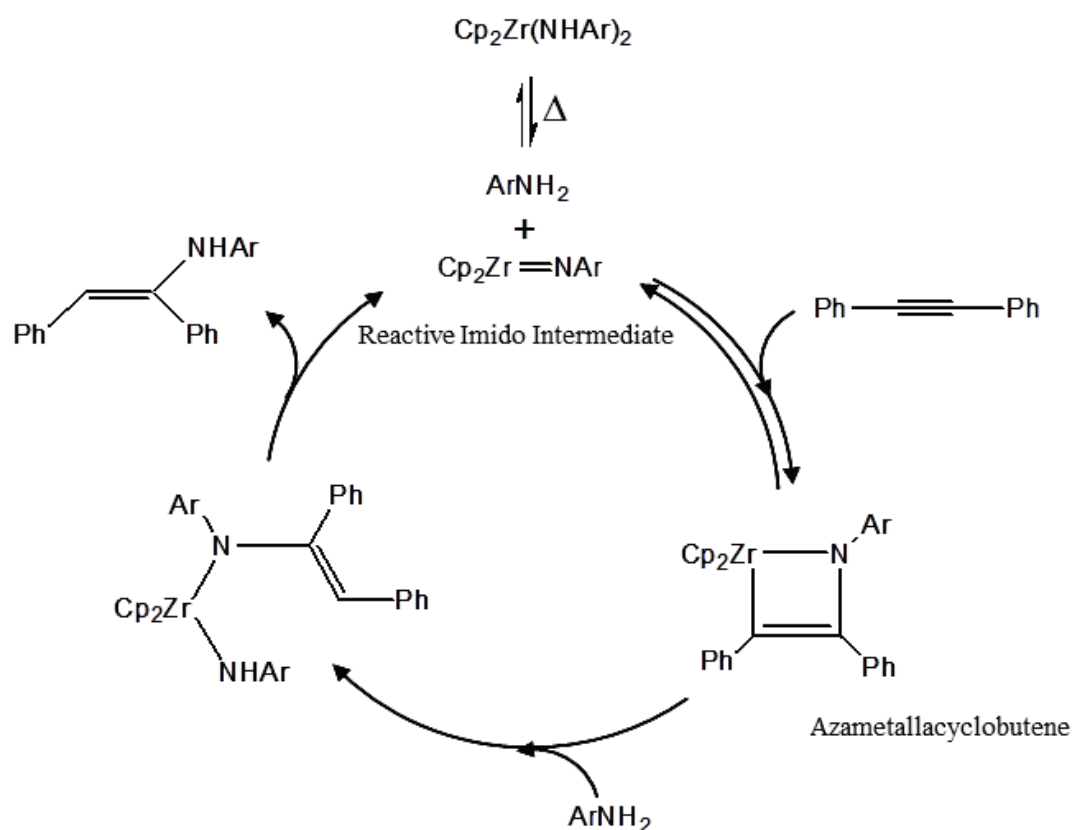
alkyl, alkylidene, and alkylidyne surface species.^[27, 28] This reactivity is tightly linked to the catalytic activity of **1** towards CH₄ and other alkanes for reactions such as H/ D exchange, hydrogenolysis, metathesis, and methaneolysis.^[29-32]

It was therefore reasonable for us to bring together these two reactivities (towards N and C-H activation) on well-defined tantalum imido amido and tantalum hydride complexes in order to study the blue sky objective: N₂ → NH₃ → N- containing organic compounds. The goal of this chapter is therefore to give our preliminary results of the reactions in this field. The tantalum imido amido species has been already shown to perform H/D exchange under pressure of H₂ or D₂ gas. In order to extend this reactivity, studies on the C-H activating capabilities of the imido amido species will be presented in the following part.

II. RESULTS AND DISCUSSION

II.1. Reactivity of silica-supported $[(\equiv\text{SiO})_2\text{Ta}(=\text{NH})(\text{NH}_2)]$ and $[(\equiv\text{SiO})_2\text{TaH}_x (x:1, 3)]$ complexes with alkynes:

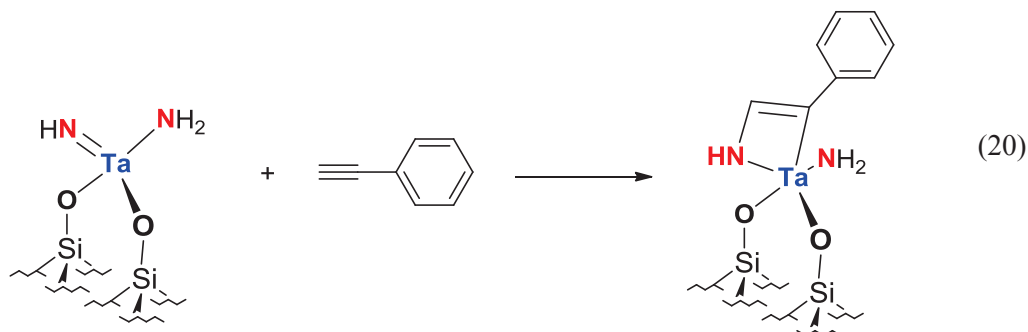
In 2007, Avenier studied the stoichiometric reactivity of $[(\equiv\text{SiO})_2\text{Ta}(=\text{NH})(\text{NH}_2)]$ complex by hydrogenolysis, hydroamination as well as hydrosilylation. The formation of N-C bond by hydroamination was catalyzed by tantalum imido amido complex especially reviewed. Scheme 25 represents an example of such catalysis diphenylacetylene hydroamination by 2,6-Dimethylaniline catalyzed by imidozirconocene $[\text{Cp}_2\text{Zr}(\text{NHAr})_2]$ (Ar= 2,6-Me₂C₆H₃) complex.^[33]



Scheme 25

The ability of complex **2** to its Ta-N and Ta=N bonds to form N-C bonds by addition of unsaturated hydrocarbons has been investigated within the framework of study on the

hydroamination of alkyne by Avenier. It was postulated that the stoichiometric anti-Markovnikov phenylacetylene addition occurred to yield new N-C bond by formation of an azatantalacyclobutene $[(\equiv\text{SiO})_2\text{Ta}(\text{NHCHCPh})(\text{NH}_2)]$ complex suggested by *in situ* IR and ^{13}C MAS NMR preliminary data (Figure 32 and 33).



I carried out further experiments on the reaction of tantalum imido amido complex and/ or tantalum hydrides with phenylacetylene and showed that the formation of azacyclobutene did not occur. The observed reactivity was the trimerization of phenylacetylene.

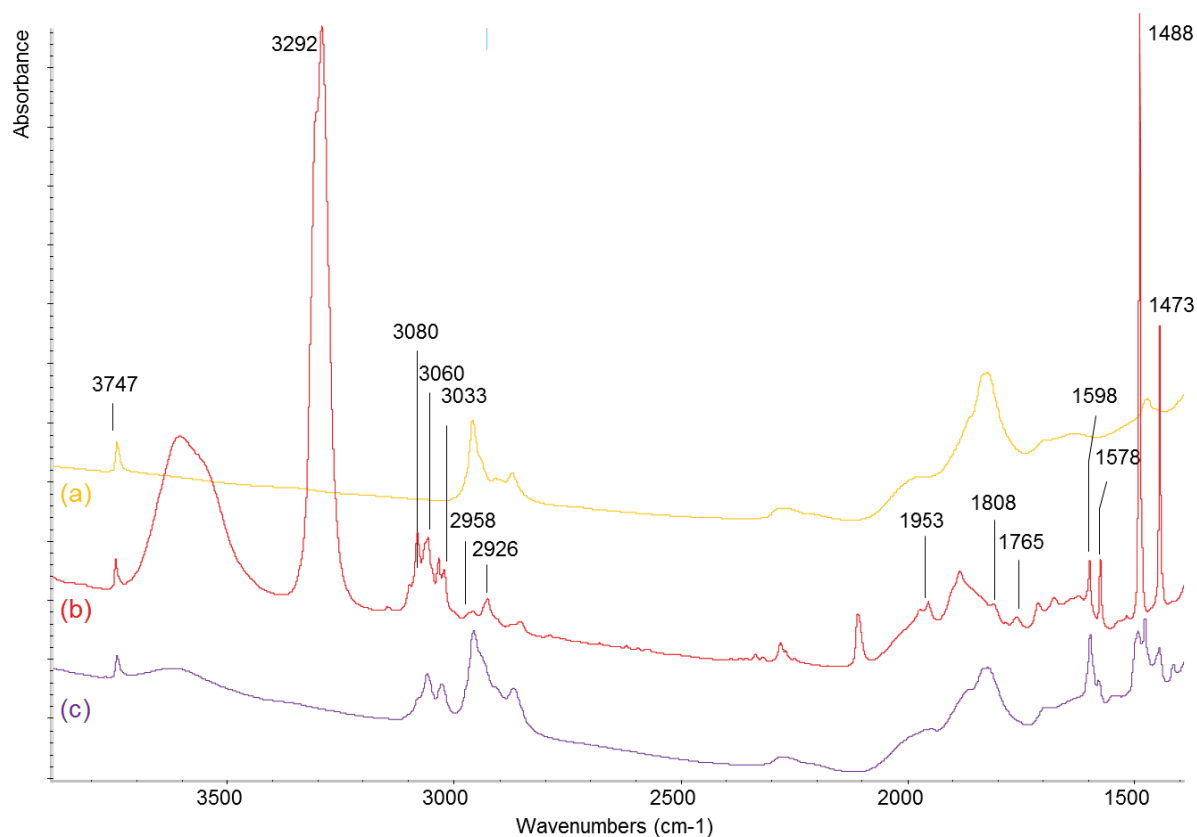


Figure 32: *In situ* IR spectra of (a) starting tantalum hydrides; (b) addition of phenylacetylene in excess; (c) collection of the gas phase in liquid nitrogen.

New peaks *in situ* IR spectroscopy in Figure 32 after phenylacetylene addition to the complex **1** leads mainly at 3080, 3057, 3033, 2958, 2926, 1956, 1808, 1765, 1598, 1578, 1488 and 1473 cm^{-1} which corresponded well to the peaks of triphenylbenzene in the literature at 3081, 3055, 3032, 2954, 2928, 1950, 1945, 1807, 1768, 1595, 1577, 1498, 1466 and 1460 cm^{-1} .

^{13}C NMR analyses confirm also this product from the reaction (Figure 33).

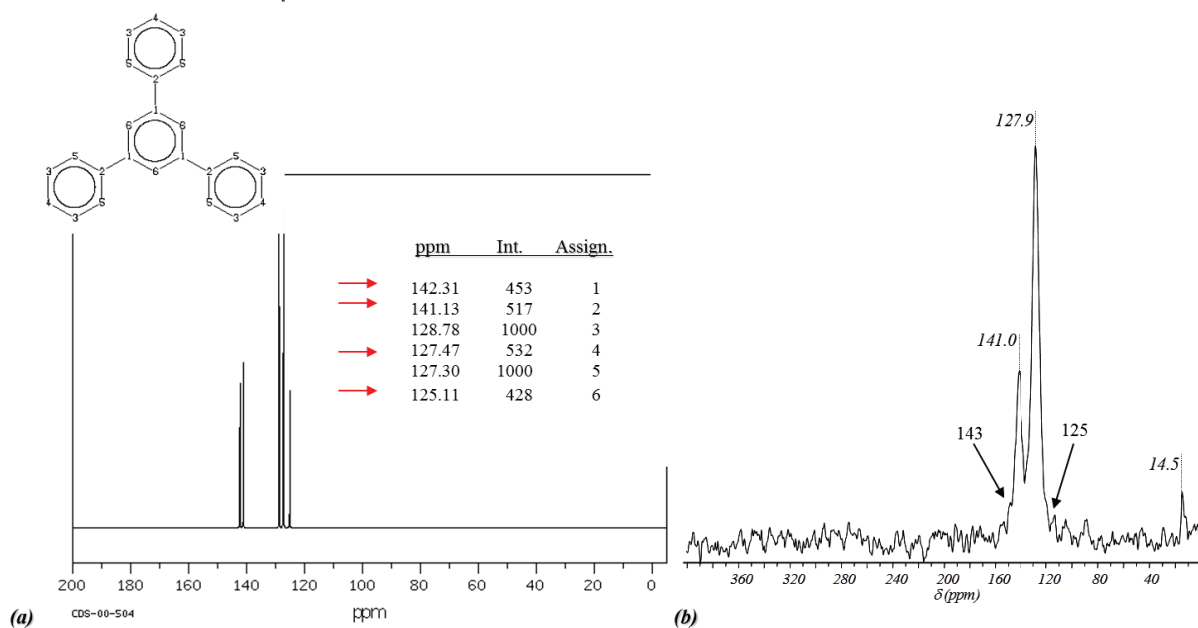


Figure 33: ^{13}C NMR spectra of (a) triphenylbenzene in the literature; (b) the product of the reaction of phenylacetylene with tantalum hydrides.

Figure 33 shows the comparison of the ^{13}C NMR spectra of the triphenylbenzene in the literature to the result of our reaction of $\text{PhC}\equiv\text{CH}$ with complex **1**.

It is therefore clear after our studies that we do not obtain the formation of N-C bond from the reaction of silica supported tantalum complexes with phenylacetylene. The analyses by *in situ* IR and NMR spectroscopies confirmed the presence of a cyclotrimerization compound which is triphenylbenzene for our reaction.

II.2. Well-defined $[(\equiv\text{SiO})_2\text{Ta}(=\text{NH})(\text{NH}_2)]$ complex in C-H activation reactions:

Reaction of silica supported $[(\equiv\text{SiO})_2\text{Ta}(=\text{NH})(\text{NH}_2)]$ complex at 150 °C under a vapor pressure of C_6D_6 (75 torr in 10 mL glass T; 0.4 mmol) induces complete exchange of the protons to deuterium on the imido amido species $[(\equiv\text{SiO})_2\text{Ta}(=\text{ND})(\text{ND}_2)]$ given in Table 6.

Table 6: Comparison of N-H and N-D IR bands observed for $[(\equiv\text{SiO})_2\text{Ta}(=\text{NH})(\text{NH}_2)]$

	N-H stretch (cm^{-1})	N-D stretch (cm^{-1})
$\nu(\text{SiO-H})$	3747	2761 (2731)
$\nu(\text{N-H})$	3495	2573 (2552)
$\nu(\text{N-H})$	3447	2521 (2517)
$\nu(\text{N-H})$	3376	2479 (2465)
$\delta(\text{NH}_2)$	1550	Not observed (1132)
$\delta(\text{NH}_2)$	1520	Not observed (1110)

Calculated shifts (which appear in parentheses) are based on the reduced-mass spring approximation. The shifts of the NH_2 deformation bands could not be observed because these bands appear in the opaque region of silica.

The N-H band intensity rapidly decreases and the new bands having the same overall shape as the $\nu(\text{NH}_x)$ are observed in the N-D region.

IR monitoring of H/ D exchange corresponds the following frequencies: 2760 $\nu(\text{OD})$, 2600 $\nu(\text{SiND}_2)$, 2580 $\nu(\text{TaND}_2)$, 2520 $\nu(\text{TaND}_2)+ \nu(\text{SiND}_2)$, 2474 $\nu(\text{TaND}_2)$, 2393 $\nu(\text{TaND}_3)$ cm^{-1} which are coherent with the data in the literature. Further experiments show that H/D exchange could occur at temperatures as low as 70 °C (Figure 34).

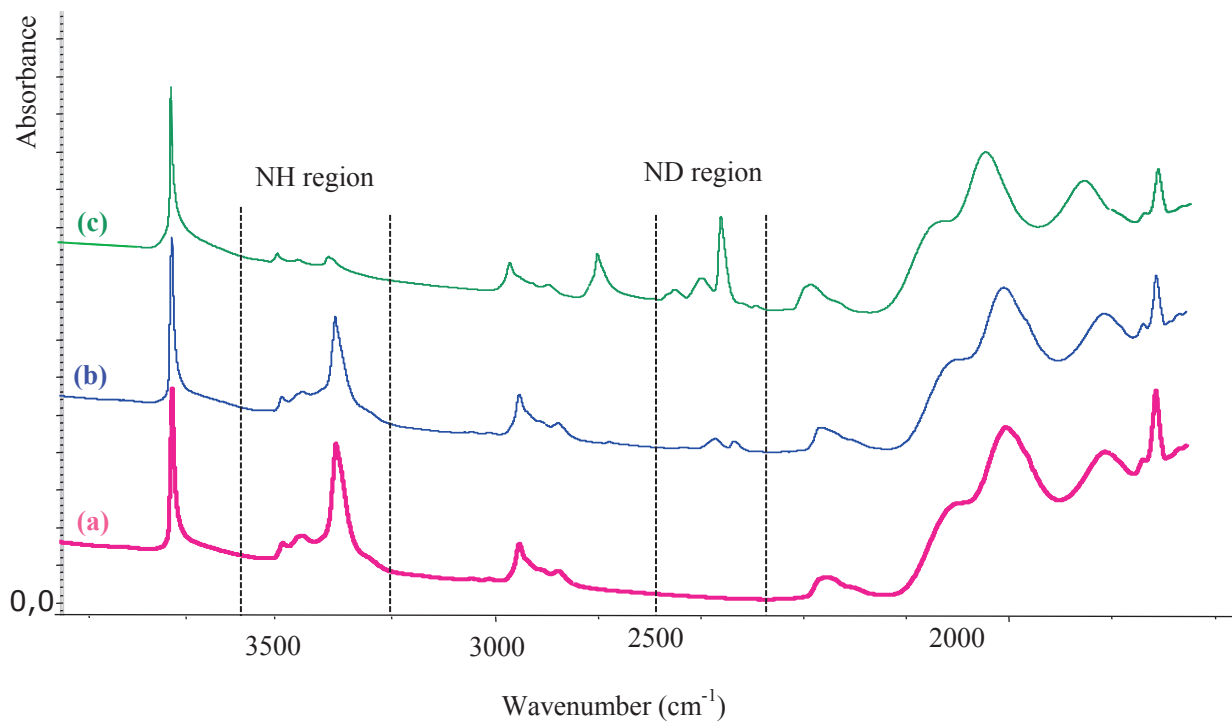


Figure 34: IR spectra of (a) complex **2**; (b) under C_6D_6 (excess C_6D_6 condensed in cold finger) at $70\text{ }^\circ\text{C}$ for 20 h; (c) after heating at $150\text{ }^\circ\text{C}$ overnight.

Moreover, the gas phase spectra of the sample after heating at $150\text{ }^\circ\text{C}$ clearly showed the presence of new C-H bonds at 3065 , 3055 and 2960 cm^{-1} corresponding to $\nu(C_{sp^2}H)$ and $\nu(C_{sp^3}H)$ peaks which were not present before (Figure 35).

While most of the peaks in the gas phase are assigned to C_6D_6 and C_6D_5H resulting from H/ D scrambling with $[(\equiv SiO)_2Ta(=NH)(NH_2)]$, the presence of aliphatic $\nu(CH_2)$ bands in the gas phase is not rationalized as of yet (see Annex/ Chapter IV for the reaction of complex **2** with C_6D_6 in the presence of H_2).

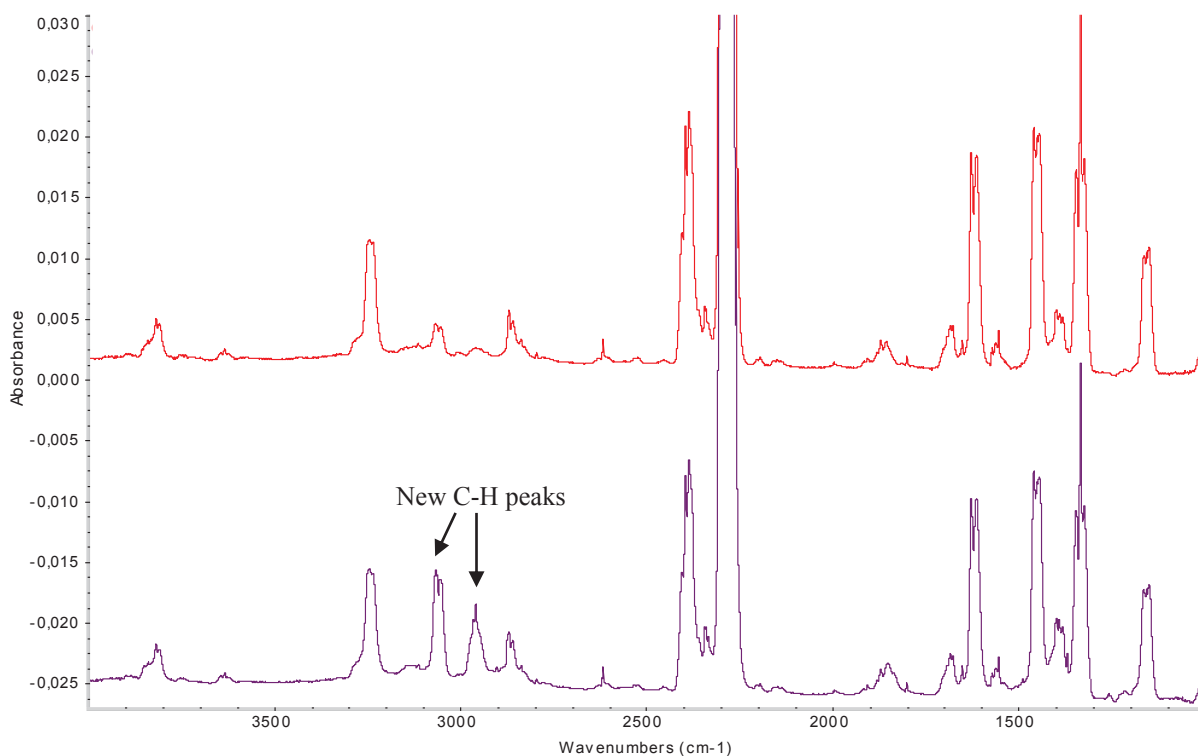


Figure 35: Gas phase IR spectra of reaction of C_6D_6 on complex **2**, $[(\equiv SiO)_2Ta(=NH)(NH_2)]$: (a) immediately after addition; (b) after heating at 150 °C overnight.

Complex **2** prepared from anhydrous ammonia is also reacted with the vapour pressure of $C_6D_5-CD_3$ (28 Torr, 15 μ mol) at different temperatures (see experimental section for details). The result of *in situ* IR spectroscopy outlines that the full H/ D exchange occur at 150 °C which is in a good agreement with the complete H/D exchange.

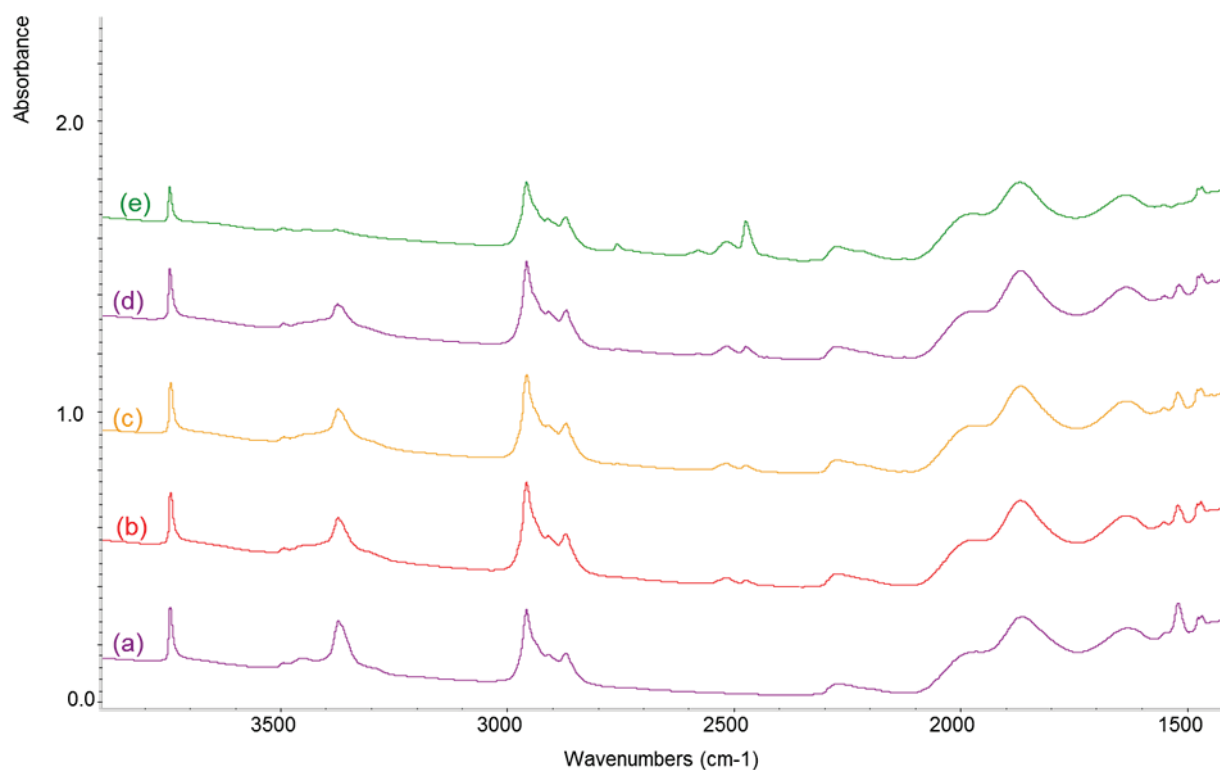


Figure 36: IR spectra of (a) silica-supported $[(\equiv\text{SiO})_2\text{Ta}(=\text{NH})(-\text{NH}_2)]$; (b) after the treatment under the vapour pressure of $\text{C}_6\text{D}_5\text{-CD}_3$ at 80°C overnight to previous sample, (excess $\text{C}_6\text{D}_5\text{-CD}_3$ condensed in cold finger); (c) after further heating of **2** at 100°C for 2h; (d) at 120°C for 2h and (e) last spectrum at 150°C for 2h.

Figure 36 presents the reaction of tantalum (V) imido amido species with $\text{C}_6\text{D}_5\text{-CD}_3$ at different temperatures. The traces of $\text{C}_6\text{D}_5\text{H-CD}_3$ and $\text{C}_6\text{D}_5\text{-CD}_2\text{H}$ are observed in the gas phase.

H/D exchange is also observed with the bulky olefin tBu-Ethylene after heating $[(\equiv\text{SiO})_2\text{Ta}(=\text{ND})(\text{ND}_2)]$ complex at 150°C under a vapor pressure (350 torr in 10 mL) of t-Bu-ethylene, IR spectroscopic analysis of the gas phase revealed that a band at 2290 cm^{-1} attributed to an olefinic C-D stretching. Because the ratio of deuterium to protons was so small in this system (t-Bu-ethylene was added in about ten-fold excess to the pellet), tracking the deuteration of the alkene substrate indicated that sp^2 C-H bonds are activated before sp^3 ones.

Finally methane was exposed to the complex $[(\equiv\text{SiO})_2\text{Ta}(=\text{NH})(-\text{NH}_2)]$. As known, the C-H bond in methane is one of the strongest C-H bonds; its bond dissociation energy is $103 \text{ kcal mol}^{-1}$.^[33] Accordingly, only a small amount of H/D exchange was observed on the tantalum imido amido species with CD_4 , even after prolonged heating at $200 \text{ }^\circ\text{C}$ (Figure 37).

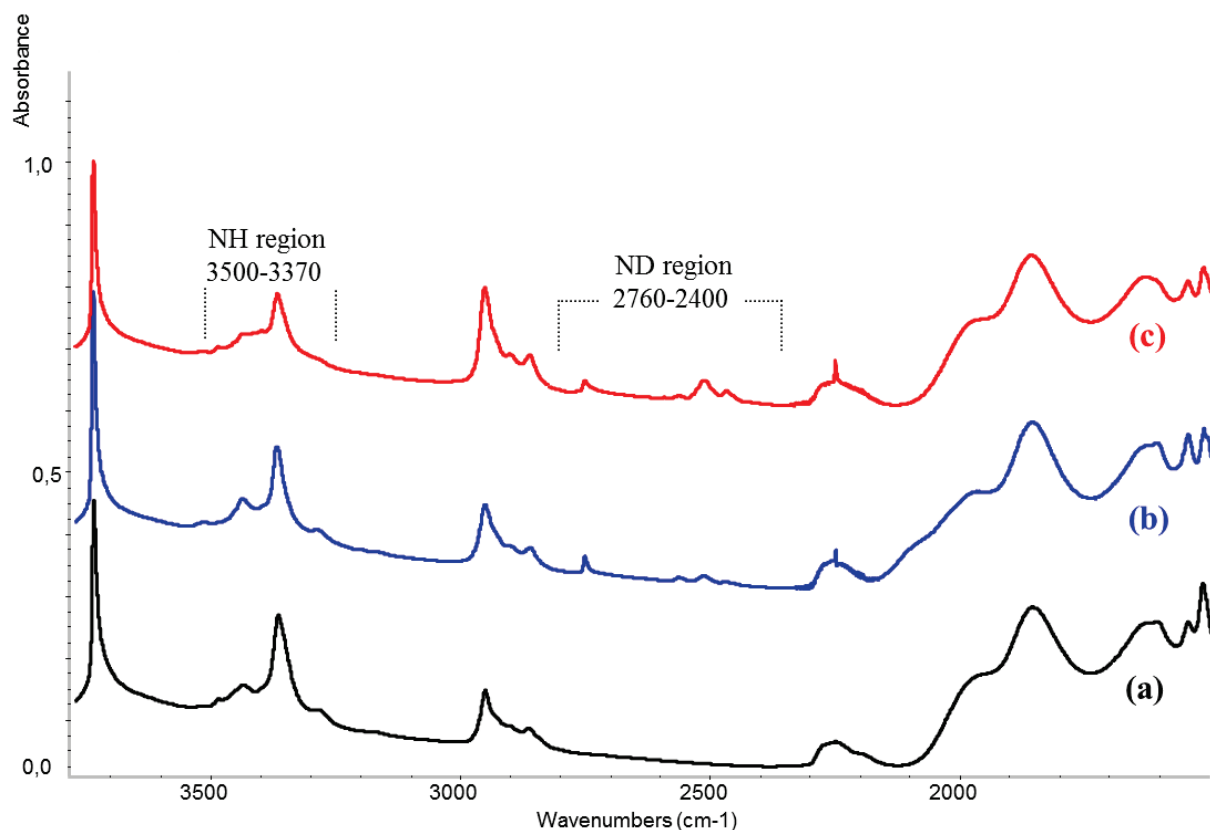


Figure 37: *In-situ* IR spectra of : (a) starting tantalum imido amido complex; (b) CD_4 addition at $150 \text{ }^\circ\text{C}$; (c) at $200 \text{ }^\circ\text{C}$ (Gas phase was collected in a cold finger during the experiment).

After heating the sample at $150 \text{ }^\circ\text{C}$ overnight, new bands are observed at 2760 , 2597 , 2572 , 2519 , and 2476 cm^{-1} . Some hydrogen atoms on the silanols, as well as on the imido amido species, has been exchanged whereas the exchange is not complete at that temperature. Although the $\delta\text{Ta}(\text{NH}_2)$ shift could not be observed, a decrease in the intensity of the peak at 1520 cm^{-1} is seen. The new major ND bands are at 2519 and 2476 cm^{-1} corresponding $\nu\text{Si}(\text{NH}_2)$ and $\nu\text{Ta}(\text{NH}_2)$, respectively.

The NH bands are still visible in the IR spectrum even after further heating at 200 °C for the entire weekend. Thus there seems to be a thermodynamic, rather than a kinetic barrier which precludes complete H/D exchange on $[(\equiv\text{SiO})_2\text{Ta}(=\text{NH})(\text{NH}_2)]$ by CD_4 .

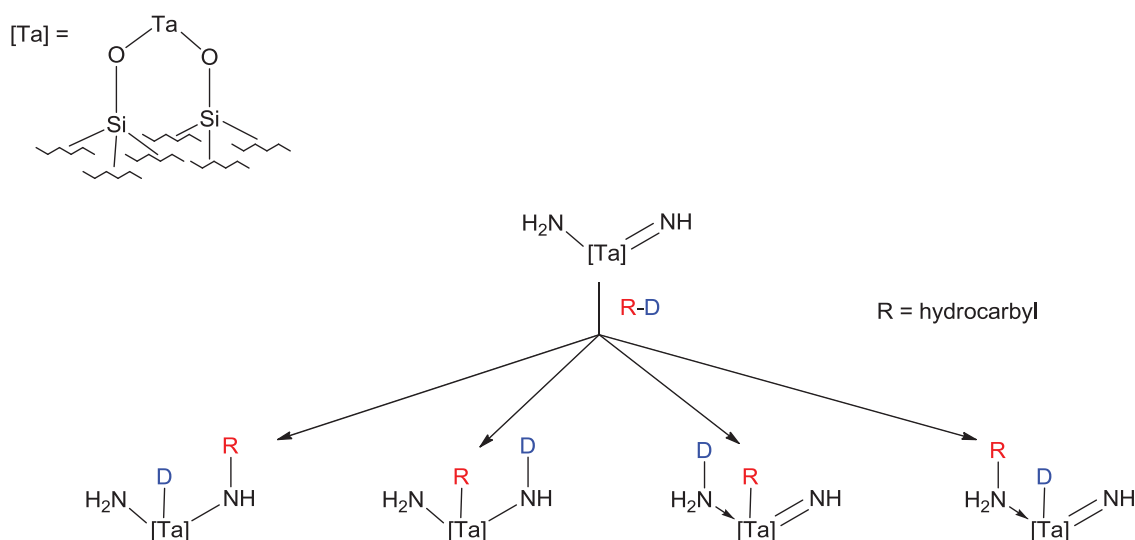
Taken together, these results indicate that the C-H bond displays interesting reactivity towards $[(\equiv\text{SiO})_2\text{Ta}(=\text{NH})(\text{NH}_2)]$. Previous data suggested that silica supported tantalum imido amido complex might be a catalyst for alkyne hydroamination by hypothesizing the formation of an azatantalacyclobutene from the addition of phenylacetylene over Ta=NH bond of **2**. We disproved such hypothesis by our experiments showing that no novel C-N bond is formed.

III. CONCLUSION AND PERSPECTIVES

We continued exploring the possibility of C-H activation over $[(\equiv\text{SiO})_2\text{Ta}(=\text{NH})(\text{NH}_2)]$ complex, exposing **2** to a vapour pressure of C_6D_6 and $\text{C}_6\text{D}_5\text{-CD}_3$ at 150 °C. IR observation showed the complete exchange of hydrogen to deuterium on the complex, while the treatment under t-Bu-Ethylene and CD_4 even at higher temperatures (150 – 200 °C) demonstrated a small amount of H/ D scrambling, probably due to the steric hindrance of the first and the strong bond dissociation energy of the second molecule.

These results indicate that the C-H bond displays interesting reactivity towards the well-defined $[(\equiv\text{SiO})_2\text{Ta}(=\text{NH})(\text{NH}_2)]$ species. It also appears that bonds between sp^2 C-H bonds are more easily activated than sp^3 ones.

It is possible that the H/D exchange observed with deuterated hydrocarbons occurs through the same mechanism as with H_2 or D_2 , *i.e.*, through heterolytic cleavage. Unlike hydrogen, the case with a C-H bond is more complex; heterolytic cleavage could formally occur through a variety of pathways described in Scheme 26, although the energies of the transition states are expected to be substantially different (and not studied yet). These very preliminary results are evolving from the development of organic nitrogen-containing complex through SOMC.



Scheme 26

IV. EXPERIMENTAL PART

General Procedure:

All experiments were carried out by using standard air-free methodology in an argon-filled Vacuum Atmospheres glovebox, on a Schlenk line, or in a Schlenk-type apparatus interfaced to a high-vacuum line (10^{-5} Torr). $[\text{Ta}(\text{CH}_2\text{C}(\text{CH}_3)_3)_3(=\text{CHC}(\text{CH}_3)_3)]$ was prepared by the reaction of TaCl_5 (Strem) with $t\text{Bu-CH}_2\text{MgCl}$ according to literature procedure. $\text{Bu-CH}_2\text{MgCl}$ was prepared from $t\text{BuCH}_2\text{MgCl}$ (98%, Aldrich, used as received) and Mg turnings (Lancaster). MCM-41 mesoporous silica was supplied by the Laboratoire des Matériaux Minéraux, E.N.S. de Chimie Mulhouse, 3 rue Alfred Werner, 68093 Mulhouse Cédex, France. It was prepared according to literature method. Its BET surface area, determined by nitrogen adsorption at 77K, is $1060 \text{ m}^2/\text{g}$ with a mean pore diameter of 28 \AA (BJH method). The wall thickness was found to be 14 \AA by subtraction of the pore diameter from the unit cell parameter deduced from X-ray powder diffraction data. MCM-41 supported tantalum hydrides $[(\equiv\text{SiO})_2\text{TaH}]$, **1a**, and $[(\equiv\text{SiO})_2\text{TaH}_3]$, **1b**, were prepared by impregnation in pentane or by sublimation for *in situ* IR monitoring as previously reported by the reaction of $[\text{Ta}(\text{CH}_2t\text{Bu})_3(=\text{CH}t\text{Bu})]$ with MCM-41 previously dehydroxylated at 500°C , followed by hydrogenolysis (550 Torr, 12h, 150°C). Pentane was distilled on NaK alloy followed by degassing through freeze-pump-thaw cycles.

Gas-phase analysis of alkanes: Gas phase analysis was performed on a Hewlett-Packard 5890 series II gas chromatograph equipped with a flame ionisation detector and an $\text{Al}_2\text{O}_3/\text{KCl}$ on fused silica column (50m X 0.32 mm). Dihydrogen gas phase analysis was performed on a Intersmat-IGC 120-MB gas chromatograph equipped with a catharometer.

Infrared spectra were recorded on a Nicolet 550-FT spectrometer by using an infrared cell equipped with CaF_2 windows, allowing *in situ* monitoring under controlled atmosphere. Typically 36 scans were accumulated for each spectrum (resolution, 2 cm^{-1}).

Preparation and studying the reactivity of surface complexes $[(\equiv\text{SiO})\text{Ta}(=\text{NH})(\text{NH}_2)]$:

Reaction of $[(\equiv\text{SiO})\text{TaH}_x (x: 1, 3)]$ with NH_3 for in-situ IR monitoring experiment:

A disk of $[(\equiv\text{SiO})_2\text{TaH}]$, **1a**, and $[(\equiv\text{SiO})_2\text{TaH}_3]$, **1b**, (30 mg, 23 mmol Ta) was treated under an excess of anhydrous ammonia (15 Torr, $6.1 \mu\text{mol}$) at room temperature for 2h to obtain

$[(\equiv\text{SiO})_2\text{Ta}(=\text{NH})(-\text{NH}_2)]$, **2**. The excess ammonia in the gas phase was removed under vacuum for 4h at 150 °C.

Selected IR frequencies (cm^{-1}): 3502 ($\nu_{\text{Ta-N-H}}$), 3461 ($\nu_{=\text{N-H}}$), 3377 ($\nu_{\text{Ta-N-H}}$), 3290 (ν_{NH_3}), 2587 (ν_{ND}), 2473 (ν_{ND}), 2424 (ν_{ND}), 2398 (ν_{ND_3}), 1605 (δ_{NH_3}), 1550 (δ_{SiNH_2}), 1520 (δ_{TaNH_2}) cm^{-1} .

*IR Monitoring of the H/D Exchange on $[(\equiv\text{SiO})_2\text{Ta}(=\text{NH})(-\text{NH}_2)]$, **2**, $2.\text{NH}_3$, and $[\equiv\text{Si-NH}_2]$.*
A disk of **2** and $2.\text{NH}_3$ was prepared as described above. The vapour pressure of C_6D_6 (100 Torr; 7 Equiv./ Ta) is added to the cell with complex **2** at room temperature then heated at 70 °C for 20 h and later at 150 °C for overnight. The same conditions are applied for the experiments with the vapour pressure of $\text{C}_6\text{D}_5\text{-CD}_3$ (28 Torr, 5 Equiv./ Ta), t-Bu-Ethylene (350 Torr, 15 Equiv./ Ta) and CD_4 (500 Torr, 13 Equiv./ Ta).

In the case of C_6D_6 and $\text{C}_6\text{D}_5\text{-CD}_3$, the temperature effect was investigated at room temperature, 70°C for overnight, 120 °C for 2h and 150 °C for overnight for H/D exchange. For the experiment with CD_4 , even at high temperatures such as 180°C and 200°C, the H/ D exchange was not complete.

Selected IR frequencies (cm^{-1}): 2760 (ν_{OD}), 2600(ν_{SiND_2}), 2580(ν_{TaND_2}), 2520 ($\nu_{\text{TaND}_2} + \nu_{\text{SiND}_2}$), 2474 (ν_{TaND_2}), 2393 (ν_{TaND_3}).

V. REFERENCES

- [1] S. A. Lawrence, Amine: Synthesis, Properties and Applications, *Cambridge University Press* **2004**, ISBN : 0 5221 78284 8.
- [2] B. R. Brown, The Organic Chemistry of Aliphatic Nitrogen Compounds, *Oxford Univ. Press*, **1994**, 800.
- [3] Z. Szakacs, S. Beni, Z. Varga, L. Oerfi, G. Keri, B. Noszal, *J. Med. Chem.* **2005**, *48*, 249.
- [4] M. H. S. Santos, *Int. J. Food Micro.* **1996**, *29*, 213.
- [5] C. A. Buehler, D. E. Pearson, Survey of Organic Syntheses, *Interscience*, **1970**, 1104.
- [6] K. Ohta, O. Mitsunobu, *Tetrahedron Lett.* **1991**, *32*, 517.
- [7] D. L. Romero, M. Busso, C. K. Tan, F. Reusser, J. R. Palmer, S. M. Poppe, P. A. Aristoff, K. M. Downey, A. G. So, *Proc. Nat. Acad. Sci. USA* **1991**, *88*, 8806.
- [8] K. Andersen, T. Liljefors, K. Gundertofte, J. Perregaard, K. P. Bogeso, *J. Med. Chem.* **1994**, *37*, 950.
- [9] M. Leopoldo, F. Berardi, N. A. Colabufo, G. P. De, E. Lacivita, R. Perrone, V. Tortorella, *J. Med. Chem.* **2002**, *45*, 5727.
- [10] J. D. Venable, H. Cai, W. Chai, C. A. Dvorak, C. A. Grice, J. A. Jablonowski, C. R. Shah, A. K. Kwok, K. S. Ly, B. Pio, J. Wei, P. J. Desai, W. Jiang, S. Nguyen, P. Ling, S. J. Wilson, P. J. Dunford, R. L. Thurmond, T. W. Lovenberg, L. Karlsson, N. I. Carruthers, J. P. Edwards, *J. Med. Chem.* **2005**, *48*, 8289.
- [11] C. Enguehard-Gueiffier, H. Huebner, H. A. El, H. Allouchi, P. Gmeiner, A. Argiolas, M. R. Melis, A. Gueiffier, *J. Med. Chem.* **2006**, *49*, 3938.
- [12] J. Ignatovich, K. Gusak, V. Kovalyov, N. Kozlov, E. Koroleva, *Arkivoc* **2008**, *9*, 42.
- [13] E. G. Bryan, B. F. G. Johnson, J. Lewis, *J. Chem. Soc.*, **1977**, 1328.
- [14] T. R. Cundari, *Organometallics* **1993**, *12*, 1998.
- [15] T. Braun, *Angew. Chem. Int. Ed.* **2005**, *44*, 5012.
- [16] J. Zhao, A. S. Goldman, J. F. Hartwig, *Science* **2005**, *307*, 1080.
- [17] M. Kanzelberger, X. Zhang, T. J. Emge, A. S. Goldman, J. Zhao, C. Incarvito, J. F. Hartwig, *J. Am. Chem. Soc.* **2003**, *125*, 13644.
- [18] G. D. Frey, V. Lavallo, B. Donnadiu, W. W. Schoeller, G. Bertrand, *Science* **2007**, *316*, 439.
- [19] C. M. Fafard, D. Adhikari, B. M. Foxman, D. J. Mindiola, O. V. Ozerov, *J. Am. Chem. Soc.* **2007**, *129*, 10318.

- [20] M. A. Salomon, A.-K. Jungton, T. Braun, *Dalton Trans.* **2009**, 7669.
- [21] H. M. Hoyt, R. G. Bergman, *Angew. Chem., Int. Ed.* **2007**, *46*, 5580.
- [22] N. Ochi, Y. Nakao, H. Sato, S. Sakaki, *J. Am. Chem. Soc.* **2007**, *129*, 8615.
- [23] P. Avenier, M. Taoufik, A. Lesage, X. Solans-Monfort, A. Baudouin, A. de Mallmann, L. Veyre, J. M. Basset, O. Eisenstein, L. Emsley, E. A. Quadrelli, *Science* **2007**, *317*, 1056.
- [24] P. Avenier, A. Lesage, M. Taoufik, A. Baudouin, A. De Mallmann, S. Fiddy, M. Vautier, L. Veyre, J.-M. Basset, L. Emsley, E. A. Quadrelli, *J. Am. Chem. Soc.* **2007**, *129*, 176.
- [25] P. Avenier, X. Solans-Monfort, L. Veyre, F. Renili, J.-M. Basset, O. Eisenstein, M. Taoufik, E. A. Quadrelli, *Top. Catal.* **2009**, *52*, 1482.
- [26] E. Gouré, P. Avenier, X. Solans-Monfort, L. Veyre, A. Baudouin, Y. Kaya, M. Taoufik, J. M. Basset, O. Eisenstein, E. A. Quadrelli, *New Jour. Chem.* **2011**, *35*, 1011.
- [27] S. Soignier, M. Taoufik, E. Le Roux, G. Saggio, C. Dablemont, A. Baudouin, F. Lefebvre, A. De Mallmann, J. Thivolle-Cazat, J.-M. Basset, G. Sunley, B. M. Maunders, *Organometallics* **2006**, *25*, 1569.
- [28] V. Vidal, A. Theolier, J. Thivolle-Cazat, J.-M. Basset, J. Corker, *J. Am. Chem. Soc.* **1996**, *118*, 4595.
- [29] L. Lefort, C. Coperet, M. Taoufik, J. Thivolle-Cazat, J.-M. Basset, *Chem. Commun.* **2000**, 663.
- [30] M. Chabanas, V. Vidal, C. Copéret, J. Thivolle-Cazat, J.-M. Basset, *Angew. Chem., Int. Ed.* **2000**, *39*, 1962.
- [31] V. Vidal, A. Theolier, J. Thivolle-Cazat, J.-M. Basset, *Science* **1997**, *276*, 99.
- [32] D. Soulivong, C. Coperet, J. Thivolle-Cazat, J.-M. Basset, B. M. Maunders, R. B. A. Pardy, G. J. Sunley, *Angew. Chem. Int. Ed.* **2004**, *43*, 5366.
- [33] R. G. Bergman, *Science* **1984**, *223*, 902.
- [38] R. J. Duchovic, W. L. Hase, H. B. Schlegel, M. J. Frisch, K. Raghavachari, *Chem. Phys. Lett.* **1982**, *89*, 120.
- [39] H. A. Smith, H. T. Meriwether, *J. Am. Chem. Soc.* **1949**, *71*, 413.
- [40] M. S. Eisen, T. J. Marks, *J. Am. Chem. Soc.* **1992**, *114*, 10358.
- [41] S. B. Halligudi, H. C. Bajaj, K. N. Bhatt, M. Krishnaratnam, *React. Kinet. Catal. Lett.* **1992**, *48*, 547.
- [42] R. D. Profilet, A. P. Rothwell, I. P. Rothwell, *J. Am. Chem. Soc.* **1993**, *42*.

- [43] I. P. Rothwell, *Chem. Commun.* **1997**, 1331.
- [44] V. M. Visciglio, J. R. Clark, M. T. Nguyen, D. R. Mulford, P. E. Fanwick, I. P. Rothwell, *J. Am. Chem. Soc.* **1997**, *119*, 3490.
- [45] E. T. Silveira, A. P. Umpierre, L. M. Rossi, G. Machado, J. Morais, G. V. Soares, I. J. R. Baumvol, S. R. Teixeira, P. F. P. Fichtner, J. Dupont, *Chem. Eur. J.* **2004**, *10*, 3734.

CHAPTER V.
General Conclusions

The objective of this thesis focused on surface organometallic chemistry approach through N_2 and NH_3 activation including the preparation of well-defined silica supported tantalum surface complexes, their characterization by various spectroscopic techniques, studying their reactivity and possible elementary reaction steps of the mechanism. Silica supported tantalum hydrides have already proven their reactivity in the catalytic transformation of alkanes by the C-H and C-C bond; in addition to the N-H bond cleavage of NH_3 and $N\equiv N$ cleavage of N_2 more recently forming the well-defined imido amido species.

In this context, we have acquired experimental and computational studies on the reactivity of $[(\equiv SiO)_2Ta(=NH)(NH_2)]$, **2** with H_2 and NH_3 . The complex **2** splits H-H and N-H bonds heterolytically through the Ta=NH and Ta-NH₂ ligands. Besides the developments of new applications of H_2 heterolytic splitting in the organometallic chemistry, the principles of Lewis acidity–basicity also extend to surface science and solid state chemistry, accounting for the assembly of complex arrays of electron donor and acceptors for the formation simple Lewis acid/ base adducts firstly reported by Stephan in 2006.^[1-3] The metal- free activation of small molecules has been reported by “Frustrated Lewis Pairs (FLPs)” which has been extended to demonstrate new reactivity, ultimately leading to new approaches in catalysis.

It has been also showed the importance of additional ammonia molecule to the outer-sphere of the system which made the proton transfer easier through the imido and amido ligands and decreased the energy barriers of the transition states. In addition, the latest investigations on the mechanistic insight on the ammonia N-H bond activation at room temperature by tantalum hydrides has been reported based on *in situ* infrared spectroscopy and DFT calculations. Heterolytic cleavage and bifunctional activation of hydrogen molecule and N-H bond is already described in the literature.^[4] This cleavage through the Lewis acid/ base couple formed by a metal center and a ligated nitrogen atom has been the key to substrate activation reactions with the eventual possibility of catalytic applications such as asymmetric hydrogenation of ketones and can possibly be of inspiration for SOMC based approach to heterogenous mild catalytic systems with ammonia^[5-7]

After understanding the mechanism of NH_3 activation, further studies were done with N_2 / N_2H_4 / N_2H_2 to find out the possible intermediates of the stoichiometric $N\equiv N$ bond cleavage over complex **1**. We reported our experimental results for the reactions of tantalum hydride mixture and monohydride enriched **1** with N-based compounds at room temperature and at

250 °C in the absence/ presence of the dihydrogen molecule. The different reactivities of these complexes through dinitrogen coordination/ activation were monitored mainly by *in situ* IR spectroscopy. SS NMR and elemental analysis have also been used for certain experiments to characterize the type of different bonding modes of dinitrogen to the samples.

Based on these experimental results and computational model calculations, we propose an alternative pathway for this reaction with respect to the one proposed by another group right after our N₂ cleavage results in 2008. The new pathway avoids the highest transition states where a hydride is added to a formally strongly negatively charged ligand by the possibility of dihydrogen coordination through Ta-N bond in the system. This behavior of dihydrogen is made possible by the electropositive tantalum, which makes a coordinated H₂ a reasonable proton donor and the presence of strongly polar Ta-N bonds that favor the heterolytic cleavage of H₂. Therefore, molecular dihydrogen has been used as the source of protons and electrons. In this reaction, the tantalum stays most of the time on the preferred high oxidation state (d⁰) and avoids redox type reaction which could be energy demanding.

Although surface science studies on model catalysts for dinitrogen reduction to ammonia in the literature have investigated the reaction of ammonia with metal surfaces,^[8-10] the capacity of isolated Ta atoms to fully cleave the N≡N bond is original in this context due to the single-site metallic activation through reduction the imido amido species. The surface organometallic approach of our group has yielded isolated Ta^{III/V} centers protected against bimetallic decomposition by the strong and inert siloxy bonds to the rigid silica surface. In addition, the characteristic chemistry displayed by tantalum hydrides toward dinitrogen was likely due to the capacity of SOMC to synthesize highly uncoordinated, electronically unsaturated, highly thermally stable, isolated metal atoms. No solution or surface molecular system has so far achieved all these properties simultaneously (i.e., well-defined isolated Ta^{III/V} atoms, three or five coordinate, stable up to 250 °C), which probably contributes to the capacity reported for cleaving the N≡N bond on an isolated metal atom with dihydrogen [rather than with the judicious alternate additions of protons and electron sources in solution applied in the Schrock system]. The singularity of this process is not only due to the role of tantalum hydrides as monometallic species to split N₂ but also the presence of molecular dihydrogen as the reducing agent (catalyst) in the system.

Overall, the observed surface reactivity of tantalum N-containing complexes has been discussed in terms of the elementary steps of molecular organometallic chemistry and surface-related properties. It is thus conceivable that this advancement might be effective for the emergence of N-based chemistry and catalysis from ammonia, as the discovery of the reactivity of tantalum hydrides toward methane has been for the emergence of alkane-based reactions catalysed by complex **1**.

As repeated in the last part of this thesis, various studies have been done in order to couple the reactivities of the well-defined tantalum complexes towards N and C-H bond activation to form N-C bond. These results indicate that the C-H bond displays interesting reactivity towards the Ta(=NH)(NH₂) species. It has been shown that tantalum imido amido species can activate the C-H bond of aromatics such as benzene and toluene at moderate (to high temperatures) as well as very weakly aliphatics such as methane and t-Bu-Ethylene at temperatures between 150-200 °C; It also appears that bonds between sp² C-H bonds are more easily activated than sp³ ones.

The main objective of surface organometallic chemistry is to prepare well-defined single site heterogeneous catalysts whose mechanism is also well understood in order to achieve the development of desired catalytic systems. As of now we have just obtained the foundation of such understanding by studying the very fundamental mechanisms of “simple bond” activation such as H-H, N-H and N≡N. All the work on applying this novel knowledge to the large scale synthesis of N-containing products still lays ahead.

REFERENCES:

- [1] G. C. Welch, R. R. S. Juan, J. P. Mascuda, D.W. Stephan, *Science* **2006**, 314, 112.
- [2] G. C. Welch, D.W. Stephan, *J. Am. Chem. Soc.* **2007**, 129, 1880.
- [3] D. W. Stephan, *Org.-Biomol. Chem.* **2008**, 6, 1535.
- [4] C. Gunanathan, B. Gnanaprakasam, M. A. Iron, L. J. W. Shiman, D. Mistein, *J. Am. Chem. Soc.* **2010**, 132, 14763.
- [5] P. Avenier, X. Solans- Monfort, L.Veyre, F. Renili, J. -M. Basset, O. Eisenstein, M. Taoufik, E. A. Quadrelli, *Top. Catal.* **2009**, 52, 1482.
- [6] C. Coperet, A. Grouiller, J.- M. Basset, H. Chermette, *Chem. Phys. Chem.* **2003**, 4, 608.
- [7] A. Poater, X. Solans-Monfort, E. Clot, C. Coperet, O. Eisenstein, *Dalton Trans.* **2006**, 3077.
- [8] T. Braun, *Angew. Chem. Int. Ed.* **2005**, 44, 5012.
- [9] N. Ochi, Y. Nakao, H. Sato, S. Sakaki, *J. Am. Chem. Soc.* **2007**, 129, 8615.
- [10] M.A. Salomon, A.K. Jungton, T. Braun, *Dalt. Trans.* **2009**, 7669.

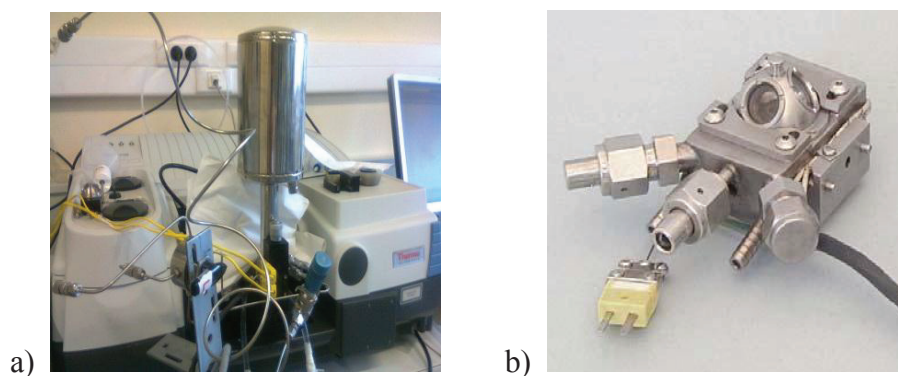
ANNEX

CHAPTER II

High pressure reaction chamber IR DRIFT:

- Reaction of $[(\equiv\text{SiO})_2\text{Ta}(=\text{NH})(\text{NH}_2)]$ with H_2

The reaction of $[(\equiv\text{SiO})_2\text{Ta}(=\text{NH})(\text{NH}_2)]$, **2**, was carried out by reaction chambers for praying mantis under partial pressure of dihydrogen in the presence and absence of the cooling conduit connected to a dewar. The results were monitored by IR spectroscopy.



CII- Annex- Figure 1: High Pressure Reaction Chamber IR DRIFT with Low/ High Temperature with its equipments: a) Thermocouples (yellow cables), vacuum connection (blue van), metal part for liquid nitrogen to cool the sample and gas connection (black van with its metal part); b) the praying mantis part with its reaction chamber with ZnSe high pressure windows.

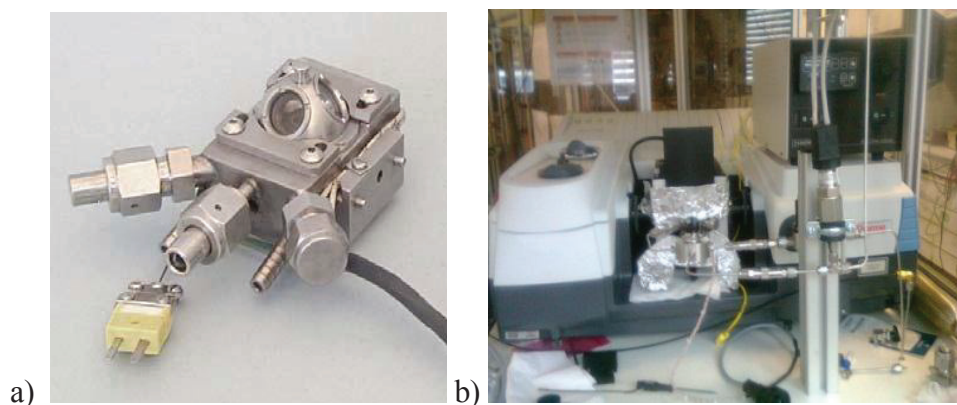
This method called “Diffuse reflection spectroscopy” is very sensitive for detecting changes at the surfaces of rough materials and is particularly effective for powders that have high surface areas. In our study we used the powder of tantalum imido amido complex prepared from MCM-41(see experimental part for the details of the preparation) to increase the grafted surface area to $1000 \text{ m}^2/\text{g}$ (28\AA pore size).

The High/ Low Temperature Reaction Chamber is well suited for performing studies under carefully controlled temperatures and pressures; using high pressure stainless steel dome with optical ZnSe windows (4 mm thick) (Fig.1b). A temperature controller provides accurate

regulation over a wide range of temperature (between -150 and +1250 °C) with thermocouples and a dewar is connected to the system in order to cool the sample stage below room temperature.

- The Survival of $[(\equiv\text{SiO})_2\text{Ta}(=\text{NH})(\text{NH}_2)]$ in High Temperature Reaction Chamber and the study under H_2 pressure :

Figure 2 below represents the equipments used for the reaction of complex **2** under partial pressure of dihydrogen.



CII- Annex- Figure 2: High Temperature and Pressure Reaction Chamber; a) the praying mantis part with its reaction chamber with ZnSe high pressure windows; b) the whole system connected to the gas line.

This system seemed to have more advantages comparing to the other reaction chamber as it can connect directly to the gas line therefore can avoid the leaks during the gas addition. However in case of our experiments with very sensible tantalum imido amido complex, it was not able to have continuous/ successful results for this reaction, because of very small leaks effecting the system during gas addition (coming from the general gas line) thus leading to the sample not able to survive after H_2 addition.

CHAPTER III

Hydride Characterization:

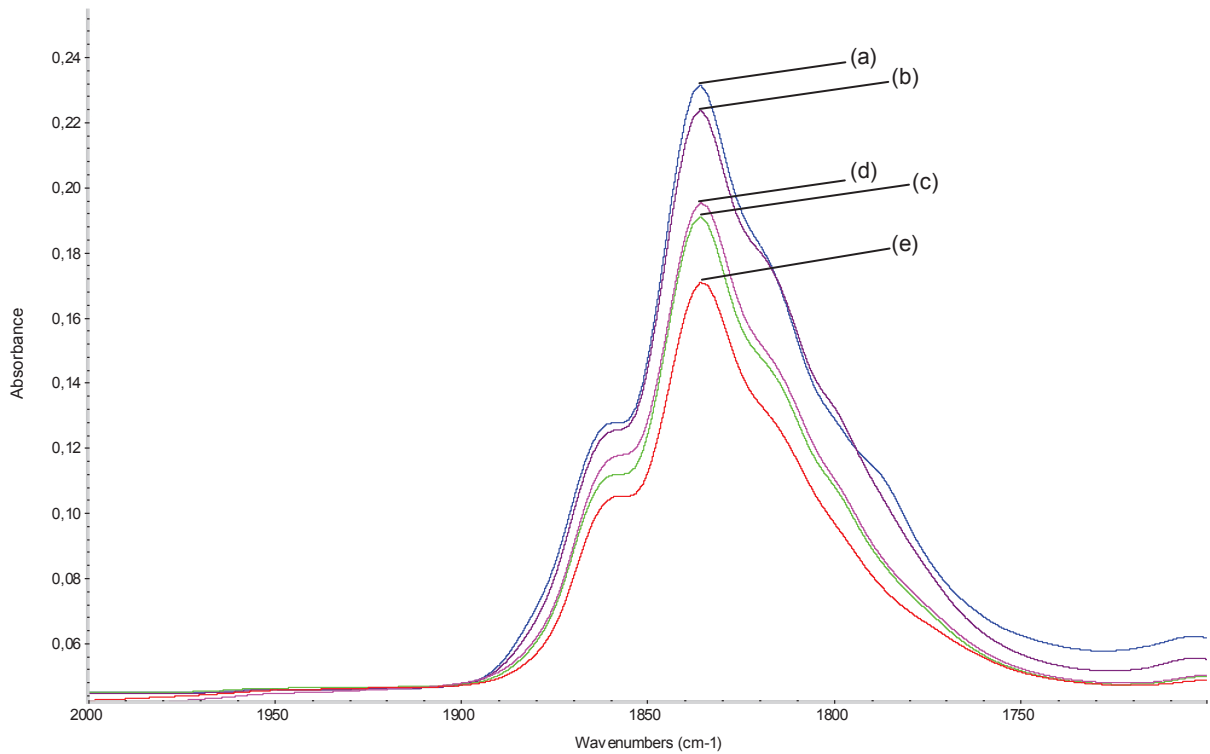
The surface tantalum hydrides, **1** are known to evolve 0.3 equivalents of H₂ upon heating to 150 °C. This suggests the presence of mono- ($[(\equiv\text{SiO})_2\text{TaH}_1$, **1a**) and trishydrides ($[(\equiv\text{SiO})_2\text{TaH}_1\text{H}_3$, **1b**), as well as the possibility of dihydrogen adducts acting as intermediates between the two states. To this end, a variety of characterization methods were used in an attempt to fully characterize the surface species present.

DRIFT

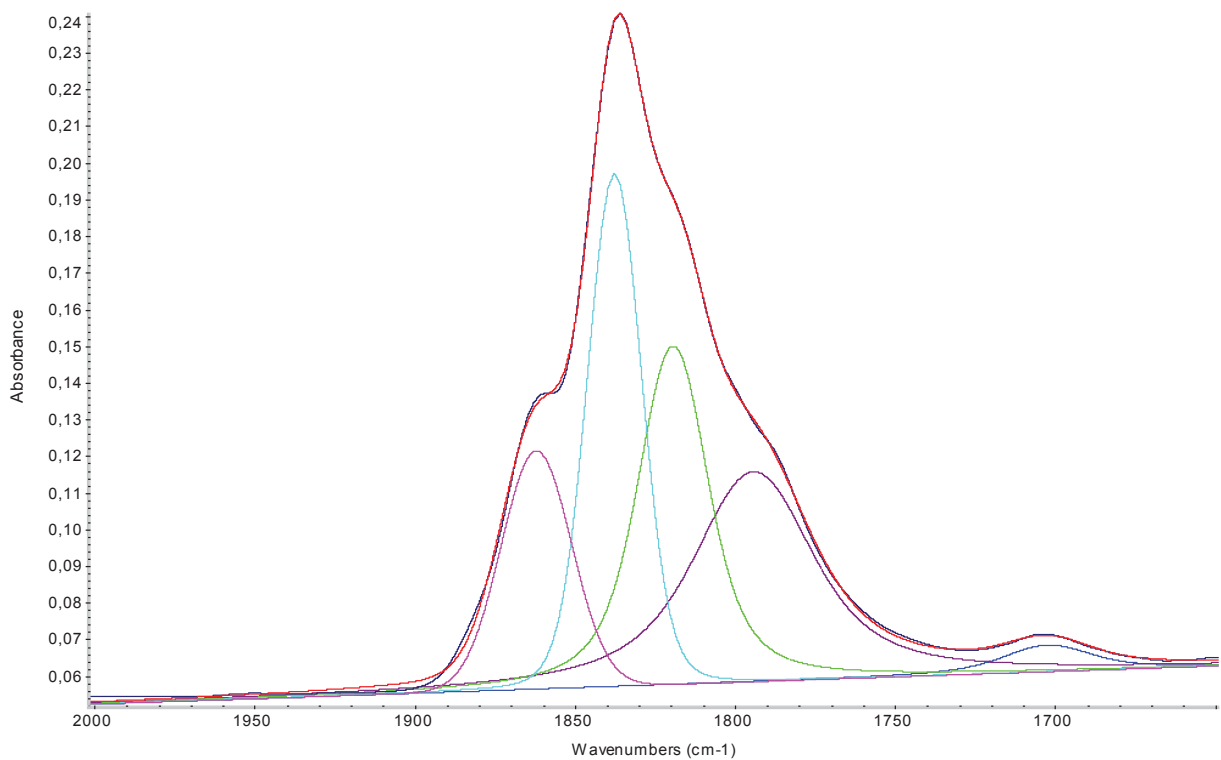
DRIFT was used to analyze powdered samples of the surface tantalum hydrides, in order to more accurately assign the complex IR band centered on 1830 cm⁻¹ that arises from the Ta hydrides. The cells were equipped with valves to permit the application of vacuum and the addition of gases onto the sample. Unfortunately, the air tightness of the cell was insufficient to permit proper analysis. The samples were observed to decompose—sharp decreases in hydride bands were observed—under application of vacuum, under a static Ar atmosphere, as well as under 10 bar H₂.

In situ IR

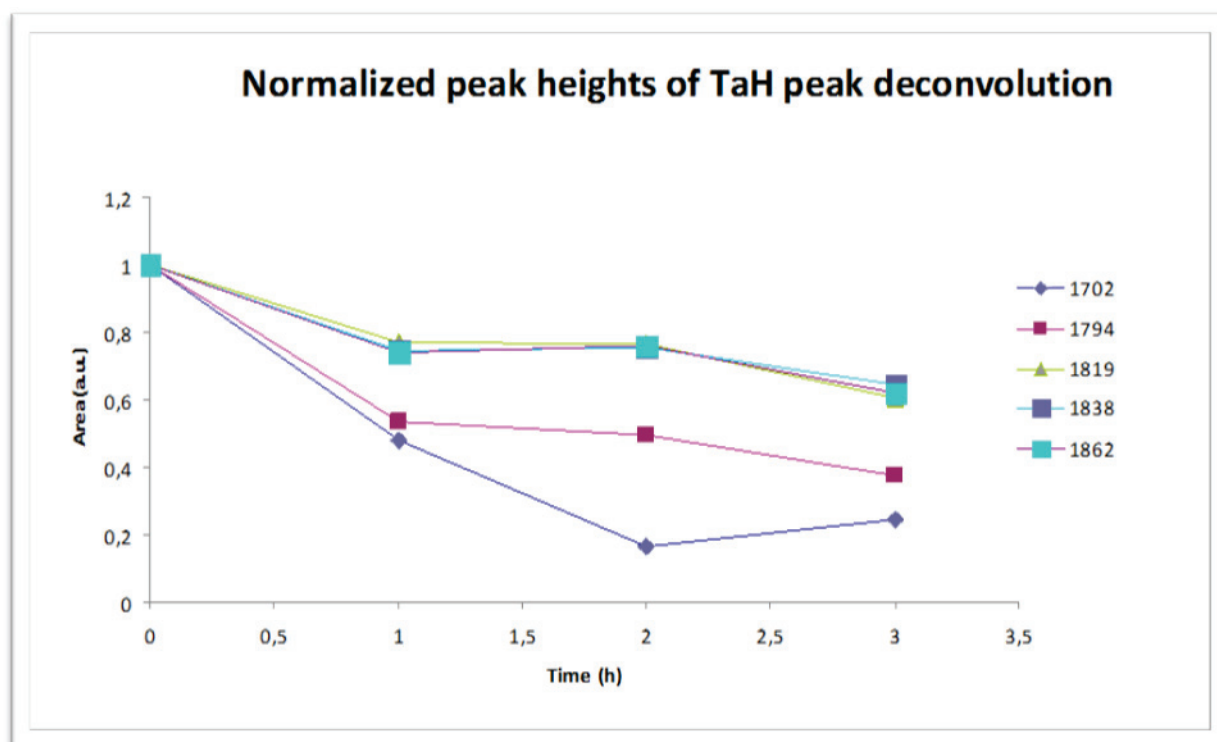
The conversion of TaH_x into TaH₁ was monitored by *in situ* IR spectroscopy on a pellet of TaH_x. Heating the native hydrides at 150 °C under dynamic vacuum (thus precluding monitoring of the H₂ loss) causes the IR band centered at 1830 cm⁻¹ to decrease in intensity to 67% of its initial value (Figure 1), consistent with the loss of Ta-H bonds and possibly the conversion of TaH₃ into TaH₁. A spectrum was taken hourly and a deconvolution (Figure 2) of the hydride peak was performed; the results are summarized in Figure 3. While the peak at 1837 cm⁻¹ remains relatively unchanged, the heights and areas of the peaks at 1794 cm⁻¹ and 1862 cm⁻¹ drop more precipitously. We may therefore tentatively assign the peak at 1837 cm⁻¹ to the monohydride species, TaH₁, while the other peaks could be indicative of species with multiple hydride ligands.



CIII- Annex- Figure 1: Monitoring the decrease in the intensity of $\nu(\text{Ta-H})$. (a): starting hydrides; (b): after application of vacuum at room temperature; (c): after heating at 150 °C under dynamic vacuum for 1 h; (d): after heating at 150 °C under dynamic vacuum for 2 h; (e): after heating at 150 °C under dynamic vacuum for 3 h.



CIII- Annex- Figure 2: Deconvolution of the peak of the starting Ta hydrides.

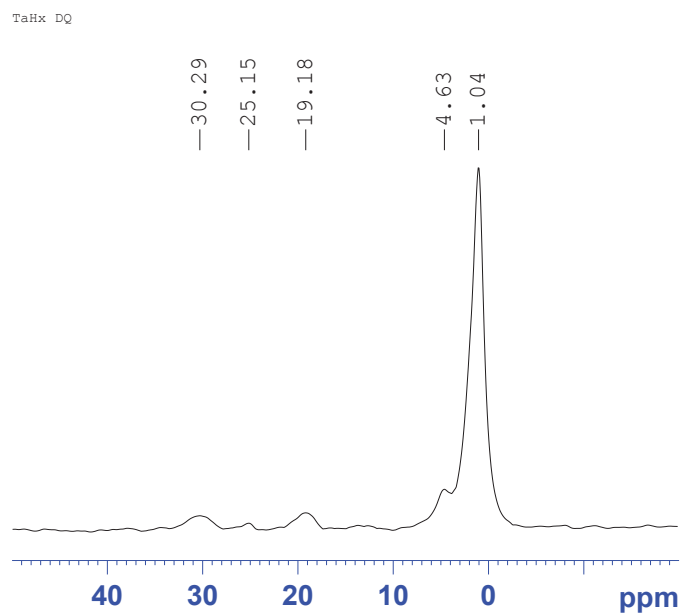


CIII- Annex- Figure 3: Traces of the decrease in peak heights (normalized) relative to the starting hydrides.

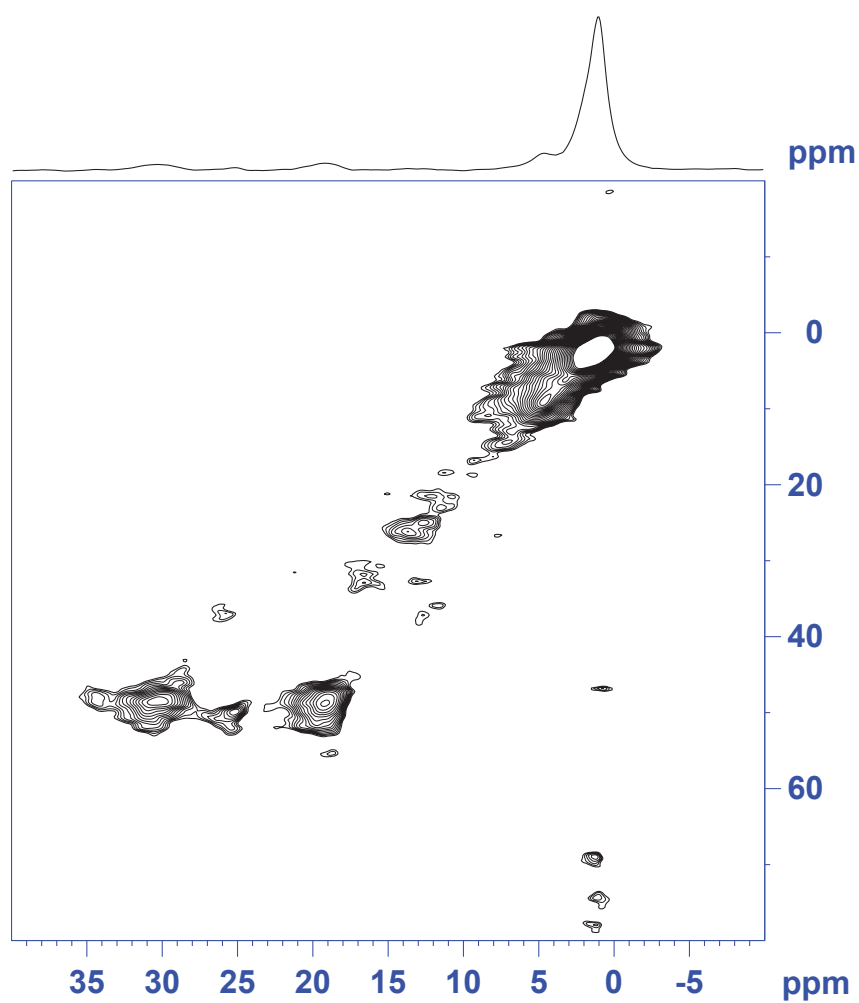
Analysis of the peak areas was also performed, but the data were less well-behaved.

Solid-state NMR

Double and triple quanta experiments were attempted on the Ta hydrides, TaH_x in order to get an idea of the species present on the surface. A high speed (rotation speed 60 kHz, probe diameter 1.3 mm) 1H SS NMR analysis was carried out by *Anne Lesage* at *CRMN Lyon*. The double quantum experiment (Figures 4 and 5) gave surprising results, implying the existence of multiple spin systems: an AX system (19.2 ppm and 30.3 ppm), an AA'XX' system (12.7 ppm and 25.7 ppm; each peak also autocorrelates), and one AA' system (16 ppm). The major peaks in the corresponding 1D spectrum are the peaks at 19.2 and 30.3 ppm, as shown in Figure 4. Integration of these peaks yields a 1:1 ratio. The triple quantum experiment did not yield any useful data.



CIII- Annex- Figure 4: 1D ¹H SS NMR spectrum of TaH_x on MCM-41.



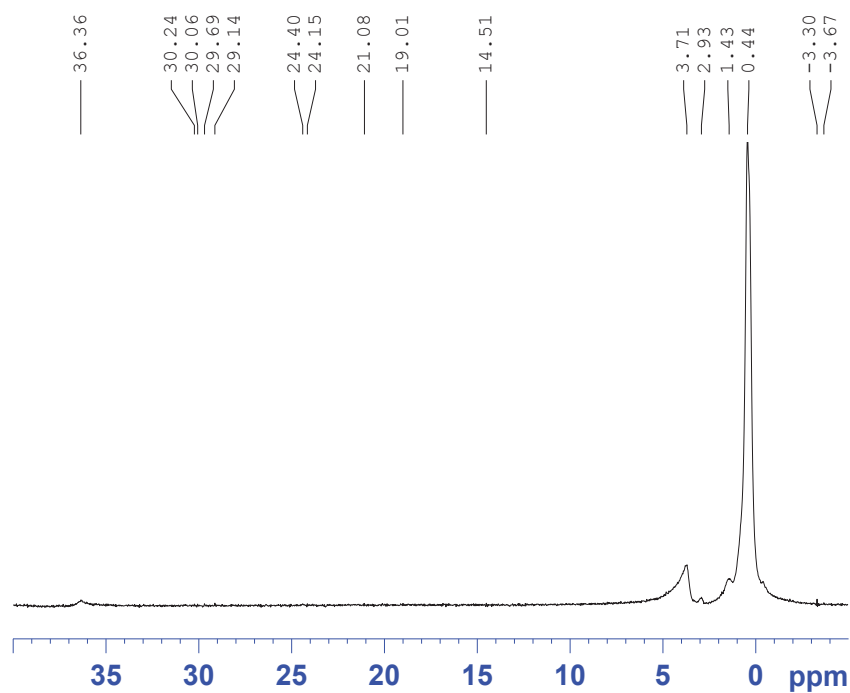
CIII- Annex- Figure 5: 2D ¹H DQ SS NMR spectrum of TaH_x on MCM-41.

The literature shifts of terminal (rather than bridging) Ta hydrides vary from about -3 to +23 ppm. Shifts close to 13 ppm were observed in $\text{Cp}^*\text{Ta}(\text{OAr})_2(\text{H})_2$ (Ar = 2,6-diMe-C₆H₃ or 2,4,6-triMe-C₆H₂). A slight change of the ligand set (replacing the Me groups by iPr groups on the aryloxy ligand) shifts the hydride further downfield to 16 ppm.

There are very few literature precedents for Ta hydride shifts further downfield than 20 ppm. The ppm values recorded for this sample imply a very deshielded environment; indeed, one of the most downfield values reported for a molecular Ta hydride is that of $(\text{SiOx})_3\text{TaH}_2$ (SiOx = t-Bu₃Si-O),^[176] which has some resemblance to our surface species.

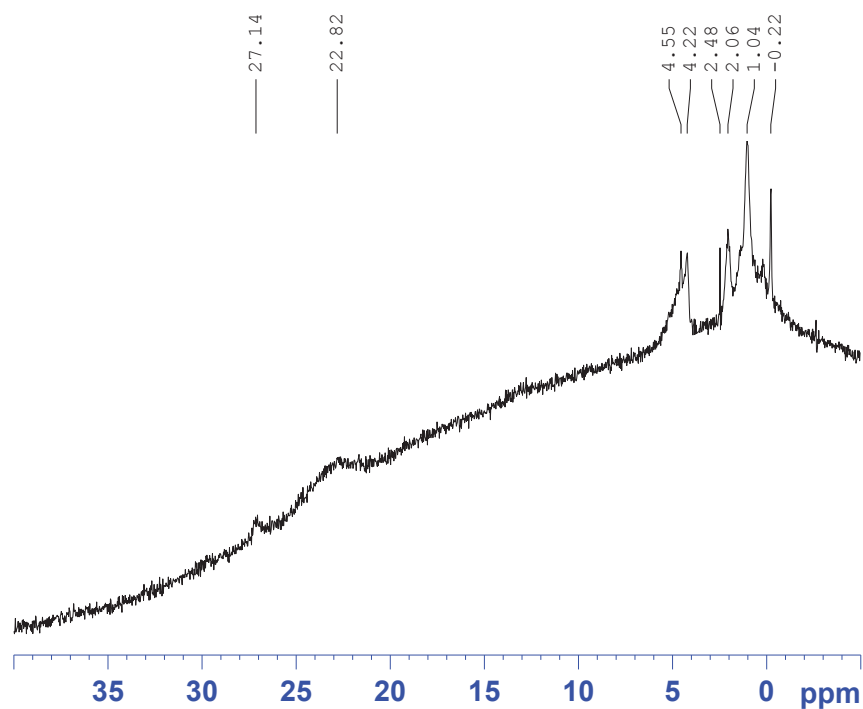
At the same time, the coupling between hydrogen ligands of such diverse chemical shifts is perhaps a little puzzling; how can these hydrides occupy such different chemical environments and yet still be close enough to couple. The DQ spectrum does not necessarily reflect through-bond coupling, but rather through-space coupling. While it is believed that the starting surface density of the silanol groups on the silica precludes such through-space coupling, the possibility that these correlations arise from interactions between hydrogen atoms on different Ta atoms cannot be excluded.

Contrary to previous experiments on samples synthesized by Priscilla Avenier and Laurent Veyre, no hydride peak was observed at 23 ppm. In an attempt to reproduce this finding, a sample of TaH_x on silica-700 (**1'**) was prepared to ascertain that the change in support did not lead to a change in the NMR spectrum. The results of this analysis appear in Figure Annex-6; again, no peak at 23 ppm is present.



CIII- Annex- Figure 6: ^1H SS NMR spectrum of recently-synthesized TaH_x on $\text{SiO}_2(700)$.

However, this peak at 23 ppm is present in a recent acquisition of an “old” sample of GIB07 which had been sealed and stored and the glovebox for 2 years (Figure 7).



CIII- Annex- Figure 7: ^1H SS NMR spectrum of TaH_x on $\text{SiO}_2(700)$ (GIB 07).

XPS

As the mono- and trishydride forms have formal different oxidation states (Ta(III) and Ta(V) respectively), analysis by XPS (at IRCELYON, Pierre Delichère and Swamy Prakash) could permit quantification of the amounts of Ta(III) and Ta(V) present in samples of TaH₁ and TaH_x. (The necessity of ultra-high-vacuum conditions prevents meaningful analysis of TaH₃ samples.) Samples were loaded into a tripartite sample holder (TaH₁: CC14, TaH_x: CC23) in the glovebox, and the chamber evacuated to ultra-high-vacuum (10⁻⁹ torr) and partially purged with N₂ before the sample holder was opened to the instrument. The analyses were unsuccessful due to the inadequacy of the sample holder; the tantalum hydride samples had oxidized before analysis could take place. As a result, the two samples had very similar spectra.

Outlook of Annex

IR remains a promising route for the characterization of the different hydrides, as evidenced by the results obtained on silica pellets *in situ*.

A triple quantum SS NMR experiment could definitively assign the resonances exclusively due to trishydrides (these peaks also correlate in a double quantum spectrum).

Finally, EPR on samples of Ta hydrides performed the existence of Ta(IV) (formally a d¹ species) present in the mixture of Ta hydrides. This oxidation state is possible if (SiO)₂TaH₂, (SiO)₃TaH, or (SiO)₄Ta are present in the sample. The presence of Ta(IV) on the surface would be an additional complication to a full understanding of the silica-supported Ta hydrides.

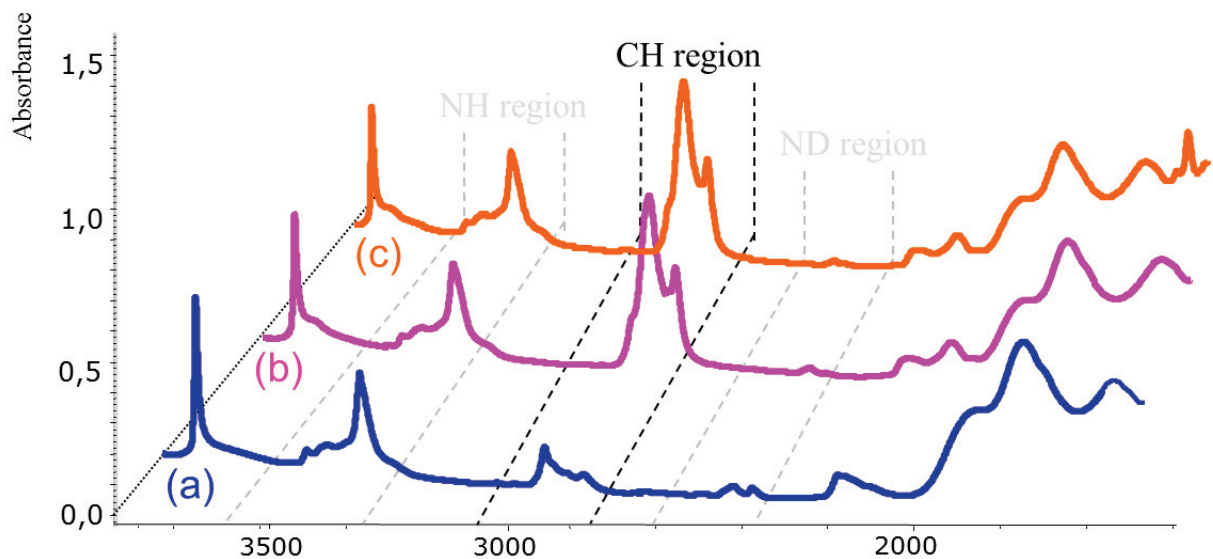
CHAPTER IV

-Reaction of $[(\equiv\text{SiO})_2\text{Ta}(=\text{NH})(\text{NH}_2)]$ with C_6D_6

Besides the reaction of complex **2** with benzene gave significant results by leading an H/D exchange and surprisingly the appearance of new peaks between $3100\text{-}2950\text{ cm}^{-1}$ in the gas phase assigned to aliphatic $-\text{CH}_2$ bands which might be occurring due to the hydrogenation of the substrate. Although various studies have been done on benzene hydrogenation over a decade,^[39-45] formation of cyclohexane (a precursor to adipic acid used to produce nylon) from this reaction is an industrially important problem which necessitated to develop new catalyst systems based on transition metal complexes, which have been proved to be effective catalysts giving selective products in many reactions under milder conditions.

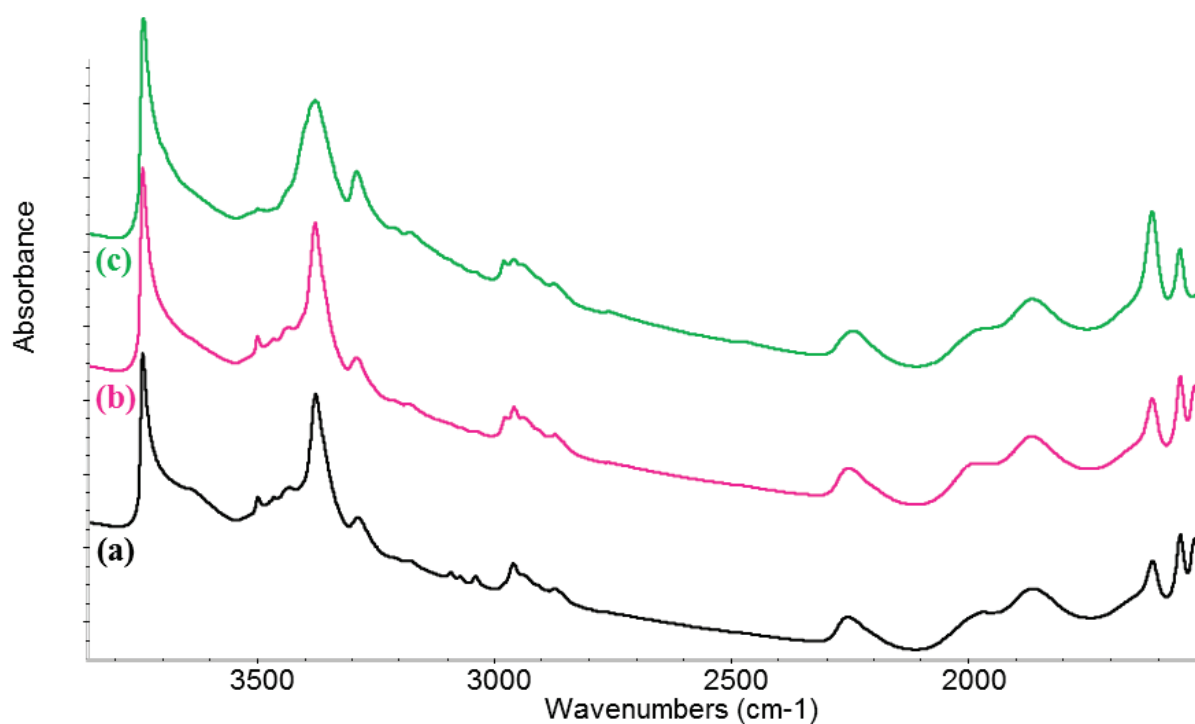
Therefore, we had preliminary studies on the reaction of complex **2** with C_6D_6 under hydrogen to test if the process was catalytic under H_2 atmosphere (i.e., if the hydrogen could regenerate the unlabelled imido amido species) by observing an effect on the H/D exchange. This was combined with stepwise heating of the sample in order to determine the lowest temperature at which H/D exchange occurred.

The reaction was monitored by *in-situ* IR spectroscopy (static conditions), figure below represents the addition of H_2 to the tantalum imido amido species under vapour pressure of C_6D_6 (75 torr in 10 mL glass T; 0.4 mmol) at $70\text{ }^\circ\text{C}$.



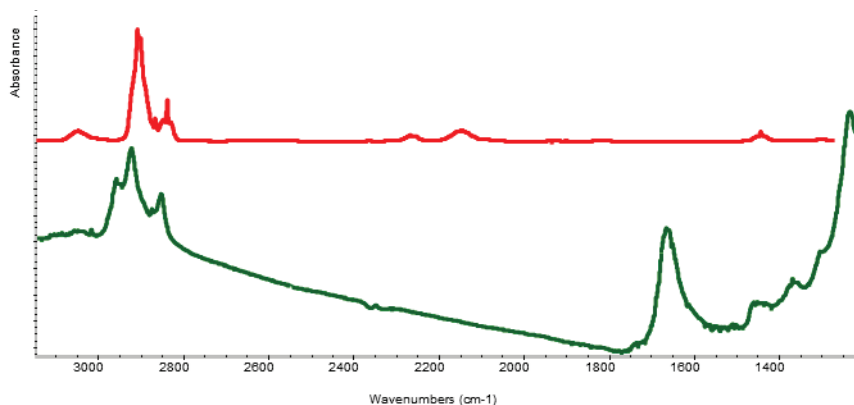
CIV- Annex- Figure 1: Reaction of (a) $[(\equiv\text{SiO})_2\text{Ta}(=\text{NH})(\text{NH}_2)]$ with C_6D_6 at 70°C ; (b) H_2 addition to the previous sample; (c) treatment under vacuum at 70°C .

Same reaction was done in the presence of C_6H_6 under H_2 with well-defined complex **2** at 70°C .



CIV- Annex- Figure 2: *in situ* IR spectra of: (a) the reaction of starting tantalum imido amido species with C_6H_6 ; (b) H_2 addition to the sample; (c) heating at 80°C .

Comparison of the gas phases of these two experiments showed the difference in the C-H region as given below:



CIV- Annex- Figure 3: IR spectra of the gas phases of the reaction of **2** with $C_6D_6 + H_2$ at 70 °C (red line) and with $C_6H_6 + H_2$ at 70 °C (green line).

According to the results, peaks in C-H region were changed after H_2 addition at 70 °C for both experiments which gave the activation of C-H bonds of the substrate. In addition, new peaks in $\nu(C_{sp^3}H)$ region were observed corresponding to the hydrogenation of benzene.